On the Histopathological Growth Patterns of Colorectal Liver Metastasis

a Study of Histology, Immunology, Genetics, and Prognosis

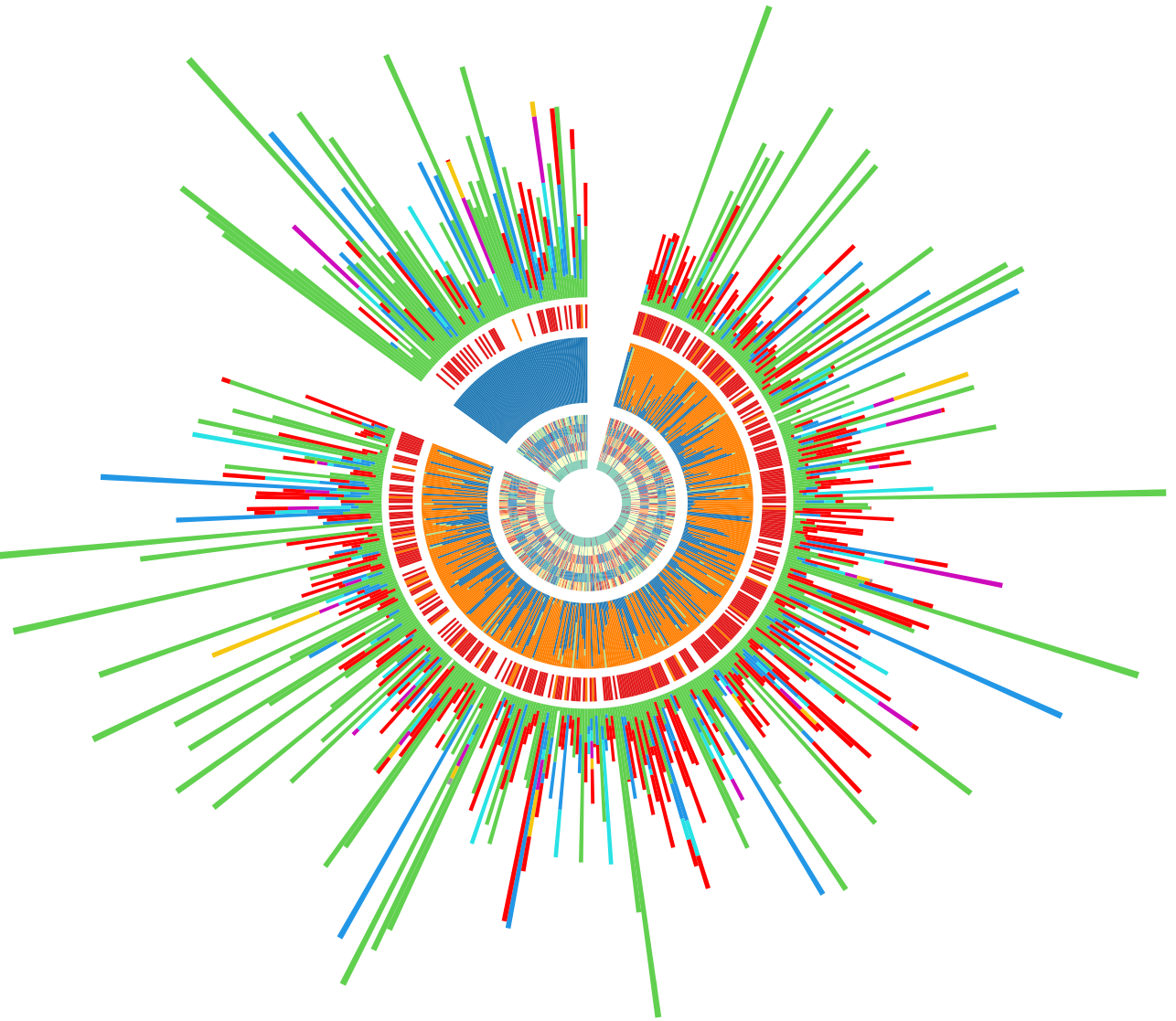

D.J. Höppener

–

2022

On the Histopathological Growth Patterns of Colorectal Liver Metastasis

-

a Study of Histology, Immunology, Genetics, and Prognosis

D.J. Höppener

Printing of this thesis was financially supported by the Erasmus University of Rotterdam, the Department of Surgery of the Erasmus MC, Erbe Nederland BV, Coloplast BV, ABN AMRO, ChipSoft, and Blaak & Partners.

ISBN: 978-94-6469-021-7

Design and layout: D.J. Höppener

On the Histopathological Growth Patterns of Colorectal Liver Metastasis

–

a Study of Histology, Immunology, Genetics, and Prognosis

Over de histopathologische groeipatronen van colorectale levermetastasen –
een studie naar histologie, immunologie, genetica, en prognose

Proefschrift

ter verkrijging van de graad van doctor aan de
Erasmus Universiteit Rotterdam
op gezag van de rector magnificus

Prof. dr. A.L. Bredenoord

en volgens besluit van het College voor Promoties.
De openbare verdediging zal plaatsvinden op

dinsdag 4 oktober 2022 om 15.30 uur

door

Diederik Jacobus Höppener
geboren te Deventer.

ERASMUS UNIVERSITEIT ROTTERDAM

Promotiecomissie

Promotor:	Prof. dr. C. Verhoef
Overige leden:	Prof. dr. P.J. Tanis
	Prof. dr. H.M. Verheul
	Prof. dr. I.D. Nagtegaal
	Prof. dr. J.H.W. de Wilt
	Dr. P.B. Vermeulen
	Dr. S.M. Wilting
Copromotor:	Dr. D.J. Grünhagen

Table of contents

Chapters

Appendices

```r
#Set working directory
setwd("V:/USERS/038931/Research/PhD")

#Loading packages
library(dplyr)
library(tidyr)
library(ggplot2)
library(cowplot)
library(DescTools)
library(gridExtra)
library(grid)
library(survival)
library(survminer)
library(rms)
library(tableone)
library(scales)
library(reshape2)
library(ggpubr)
library(RColorBrewer)
library(circlize)
library(ComplexHeatmap)

#---------------------- Data importation and mutation ----------------------
#Variable selection
cvar <- c("Gender", "ASA_cat", "Colonprim", "Left_right_sided", "pT_cat",
          "N_CRC", "Adj_CTx_CRC", "Syn_Meta", "Neo_CTx_CRLM", "Two_stage",
          "EHD", "Rec1", "R0_R1", "HGP", "TIS_CRLM", "TIS_Primary",
          "TIS_EHD")
dvar <- c("Date_res_CRLM", "Rec1_Date", "Date_death")
evar <- c("Event", "Event_DFS")
nvar <- c("Age_At_Resection_CRLM", "ASA", "pT_CRC", "pN_CRC",
          "Total_leasions_treated", "Diam_CRLM", "CEA_preop", "DFI_CRLM",
          "pHGP", "dHGP", "rHGP", "DFS", "OS")

#Load dataset
Data <- read.csv("PhD_final_v2.csv",
                 header = T, sep = ";", dec = ".",
                 na.strings = c("", " ", "NA", "999", 999, "Missing",
                 "missing"),
                 stringsAsFactors = TRUE)
data <- as_tibble(Data)

#Creating dataset
dat <- data[c(cvar, dvar, evar, nvar)]
```

Chapter I

General introduction and outline of this thesis

I

Histology – from “ἱστός” (histos) and “λόγος” (logos) – applies to the study (logos) of the microscopic anatomy of biological tissues (histos). Since the invention of the microscope, histology has greatly increased our comprehension of the fabric of tissue and disease. In medicine the histology of “diseased” tissue – histopathology, from “πάθος” (pathos), suffering – has formed our understanding of principal concepts such as pathogens, immunity, and cancer. Although science has technically evolved beyond the visual study of tissue at the cellular level through optical lenses, histopathology remains a cornerstone of modern medicine and continues to challenge our perception of disease to this day. This thesis, which is the subject of a single histopathological marker in colorectal cancer liver metastasis, is a testament to this.

Colorectal cancer

The colon and rectum constitute the final luminal parts of the gastrointestinal tract and the digestive system. Together they form the large intestine, or colorectum. The function of the colon is to absorb water and remaining nutrients and vitamins, compacting the indigestible matter for defecation as it is stored in the rectum. The gastrointestinal tract is environmentally exposed at the luminal surface. This sustained carcinogen exposure, together with the high cell proliferation rate of the glandular colorectal epithelium, leads to accumulative tissue and genomic damages throughout life, predisposing the colorectum for cancer formation, and making it the third most common type of cancer worldwide.[1] Given this aetiology, age (i.e., accumulative exposure) and lifestyle/diet (i.e., carcinogen content) are important risk factors that explain the increased colorectal cancer incidence seen in western countries, including the Netherlands.[2]

Most localised colorectal cancer can adequately be treated by surgical resection of the diseased part of the colorectum and, apart from obstructive bowel rupture and its sequelae, seldom causes death.[3] It is the dissemination of colorectal cancer to distant organs with subsequent loss of function that causes most colorectal cancer attributable deaths.[4] As such, colorectal cancer treatment is – in part – aimed at preventing and detecting metastasis through surgical resection with radio- & chemotherapeutic adjuncts and longitudinal surveillance, respectively.[5-8] Despite these therapeutic efforts, colorectal cancer still metastasises often. Almost half of all colorectal cancer patients experience disseminated disease throughout the course of their disease.[9] Topographically, the liver is the most common metastatic site, with somewhere between a quarter to one third of colorectal cancer patients affected in total.[10,11] Consequently colorectal cancer liver metastasis serves as a major actuator in colorectal cancer treatment, and the management of liver metastasis therefore determines colorectal cancer outcome to a considerable degree. Of all available treatments, local surgical management by resection or destructive ablation of colorectal liver metastasis is the only one that consistently achieves an appreciable proportion of cure.[12]

Surgical management of colorectal liver metastasis

Succinctly the liver detoxifies metabolites, synthesizes proteins, and produces necessary biochemicals for digestion and growth, making its absence incompatible with life. Complete surgical resection of the liver – hepatectomy – is therefore non-viable in the treatment of liver metastatic disease, at least not without replacement (i.e., transplantation).[13,14] Three intrinsic liver properties do however allow for far-reaching possibilities in the partial

surgical removal – partial hepatectomy – of the liver; an initial functional overcapacity, an anatomical organiation allowing partial removal, and an extraordinary regenerative capacity. It is these properties that form the principle of colorectal liver metastasis surgery: removal or destruction of the disease-affected liver can be permitted for as long as sufficient functional capacity remains.
Since the future functional liver remnant is inversely related to the extent of the surgical removal or destruction of its diseased parts, hepatic tumour load and anatomical location dictate patient eligibility. Consequently, not all patients with colorectal liver metastasis may (initially) be managed surgically. Patient eligibility can however be expanded by increasing the future liver capacity, either by reduction of hepatic tumour load with systemic or liver-directed therapies[15-18], minimizing loss of healthy functional tissue by parenchymal sparing and ablative modalities[19-21], maximizing future functional liver remnant through the in-situ induction of liver regeneration[22,23], or any combination thereof. These strategies have considerably expanded patient eligibility, and current estimates suggest that up to half of all patients who develop metachronous colorectal liver metastases are eligible for surgical treatment.[24]

While an appreciable proportion of colorectal liver metastasis patients can be cured by surgical management, a considerable part is not. Long-term cure is achieved in an approximate one-fifth of patients, with a great majority experiencing cancer recurrence within two years following treatment.[25,26] Although surgical resection of colorectal liver metastasis may also prolong life irrespective of cure[27], these outcomes still suggest room for improvement, but also the potential risk of futile surgeries. Considering the morbidity and at minimum a one percent mortality rate

associated with liver surgery, both warrant investigation.[28] To understand why some patients benefit from surgery and others do not is to understand underlying cancer biology. Hence there is a need for so called “biomarkers” in the surgical management of colorectal liver metastases; measurable indicators of some biological state or condition. In the search for colorectal liver metastasis biomarkers many have looked at patient clinicopathological characteristics, and indeed these correlate with outcome. Patient age and gender provide some composite risk of general health and life expectancy, the size and number of liver metastasis are related to outcome in the sense that they reflect tumour burden, and primary colorectal cancer histopathology risk factors such as lymph node involvement, transmural invasion depth, and anatomical localisation along the length of the colorectum carry over into the liver metastatic state.[26,29] Colorectal cancer genetic risk factors related to the MAPK pathway (i.e., RAS&RAF genetic mutations) have also been identified and provide additional prognostication and help select patients for specific chemotherapy regimens.[30,31] In clinical practice these factors combined are useful in that they provide clinicians and their patients a general sense of prognosis, but besides choice of chemotherapeutic agent, they hardly ever decisively guide treatment.[26] A better understanding therefore seems required, and identifying colorectal liver metastasis specific markers seems instrumental given the clear lack thereof.

Histopathological growth patterns of colorectal liver metastasis

A candidate colorectal liver metastasis specific biomarker may be found in the histopathological growth patterns. This histology marker was put forward in 2001 by Vermeulen et al.[32], although analogous classifications have been

described by others[33]. Through light microscopic evaluation different histomorphological expansion patterns of liver metastatic tumours in the surrounding host liver parenchyma can be identified; the desmoplastic, replacement, and pushing growth patterns. As the name implies desmoplastic or encapsulated liver metastases are morphologically recognised by a band of desmoplastic stroma separating tumour and liver parenchyma. Additional histologic features associated with the desmoplastic pattern include a dense lymphocytic infiltrate and a good glandular differentiation. Contrastingly the replacement growth pattern is characterised by mimicking the pre-existing liver architecture and invasion of cancer cells in the liver cell plates with direct contact between hepatocytes, whereby the metastasis appears to “replace” the host liver. Replacement metastases are often associated with negligible infiltration and a moderate to poor glandular differentiation. Together the replacement and desmoplastic patterns account for more than 95% of the growth patterns in colorectal cancer liver metastasis. The rare pushing type exhibits elements of both, but the defining features of neither. Pushing metastases are often well differentiated tumours sharply demarcated from the liver parenchyma with compression (i.e., “pushing”) of the surrounding liver cell plates, but without a desmoplastic capsule or direct hepatocyte cancer-cell contact.

As these patterns are expressed at the tumour-liver interface, assessment entails the systematic evaluation of the entire metastatic border using light microscopy or digital equivalents, estimating the relative percentage of each visually.[34] Patients are subsequently classified according to the extent of each individual growth pattern observed. Early studies discovered that patients with a predominantly desmoplastic pattern had better prognosis following colorectal liver metastasis surgery compared to

patients with either a predominant replacement, pushing, or mixed pattern.[34-36] With the publication of the first large retrospective series into their prognostic value however came a remarkable observation: prolonged survival was exclusive to the patients with a completely desmoplastic growth pattern, and any non-desmoplastic phenotype observed irrespective of its quantity was associated with worse outcome.[37] This distinction identifies a one-fifth minority of patients with remarkably good prognosis for liver metastatic colorectal cancer, even equalling that of non-metastatic cases. It is imperative for the development of the growth patterns as a biomarker to confirm that this observation is true. Subsequently it warrants investigation as to how morphologically a clear continuum exists suggesting plasticity, but that prognostically a binary division is evident, implying an absolute state. By identifying underlying mechanisms we may ultimately find ways to induce such states therapeutically to better treat or even cure these patients. Early immunohistochemical analyses revealed differences in endothelial- and tumour-cell proliferation rates, micro-vessel densities, and the co-option of sinusoidal blood vessels between the desmoplastic and replacement patterns, prompting the hypothesis that replacement metastases do not rely on sprouting angiogenesis but instead co-opt the pre-existing sinusoidal vasculature.[32,34,38] But other than that, the mechanisms of the different growth pattern phenotypes remain largely unknown.

Aim and outline

This thesis aims to validate and establish the histopathological growth patterns of colorectal cancer liver metastasis as a relevant biomarker (*chapters 2*, *3*, *4*, *5* & *8*), and to evaluate immunity and genetics as potential underlying biological mechanisms (*chapters 6* & *7*).

References

1. Bray F, Ferlay J, Soerjomataram I, Siegel RL, Torre LA, Jemal A. Global cancer statistics 2018: GLOBOCAN estimates of incidence and mortality worldwide for 36 cancers in 185 countries. *CA Cancer J Clin.* Nov 2018;68(6):394-424.
2. Safiri S, Sepanlou SG, Ikuta KS, et al. The global, regional, and national burden of colorectal cancer and its attributable risk factors in 195 countries and territories, 1990-2017: a systematic analysis for the Global Burden of Disease Study 2017. *The Lancet Gastroenterology & Hepatology.* 2019/12/01/ 2019;4(12):913-933.
3. McArdle CS, Hole DJ. Emergency presentation of colorectal cancer is associated with poor 5-year survival. *British Journal of Surgery.* 2004;91(5):605-609.
4. Afifi AM, Elmehrath AO, Ruhban IA, et al. Causes of Death Following Nonmetastatic Colorectal Cancer Diagnosis in the U.S.: A Population-Based Analysis. *Oncologist.* Sep 2021;26(9):733-739.
5. Thierry A, Corrado B, Matilde N, et al. Improved Overall Survival With Oxaliplatin, Fluorouracil, and Leucovorin As Adjuvant Treatment in Stage II or III Colon Cancer in the MOSAIC Trial. *Journal of Clinical Oncology.* 2009;27(19):3109-3116.
6. Bahadoer RR, Dijkstra EA, van Etten B, et al. Short-course radiotherapy followed by chemotherapy before total mesorectal excision (TME) versus preoperative chemoradiotherapy, TME, and optional adjuvant chemotherapy in locally advanced rectal cancer (RAPIDO): a randomised, open-label, phase 3 trial. *The Lancet Oncology.* 2021;22(1):29-42.
7. Wille-Jorgensen P, Syk I, Smedh K, et al. Effect of More vs Less Frequent Follow-up Testing on Overall and Colorectal Cancer-Specific Mortality in Patients With Stage II or III Colorectal Cancer: The COLOFOL Randomized Clinical Trial. *JAMA.* May 22 2018;319(20):2095-2103.
8. Primrose JN, Perera R, Gray A, et al. Effect of 3 to 5 years of scheduled CEA and CT follow-up to detect recurrence of colorectal cancer: the FACS randomized clinical trial. *JAMA.* Jan 15 2014;311(3):263-270.
9. Van Cutsem E, Oliveira J. Advanced colorectal cancer: ESMO Clinical Recommendations for diagnosis, treatment and follow-up. *Annals of Oncology.* 2009/05/01/ 2009;20:iv61-iv63.
10. Manfredi S, Lepage C, Hatem C, Coatmeur O, Faivre J, Bouvier AM. Epidemiology and management of liver metastases from colorectal cancer. *Ann Surg.* Aug 2006;244(2):254-259.
11. Engstrand J, Nilsson H, Strömberg C, Jonas E, Freedman J. Colorectal cancer liver metastases - a population-based study on incidence, management and survival. *BMC Cancer.* 2018/01/15 2018;18(1):78.
12. Hackl C, Neumann P, Gerken M, Loss M, Klinkhammer-Schalke M, Schlitt HJ. Treatment of colorectal liver metastases in Germany: a ten-year population-based analysis of 5772 cases of primary colorectal adenocarcinoma. *BMC Cancer.* Nov 4 2014;14:810.
13. Hagness M, Foss A, Line P-D, et al. Liver Transplantation for Nonresectable Liver Metastases From Colorectal Cancer. *Annals of Surgery.* 2013;257(5).
14. Dueland S, Syversveen T, Solheim JM, et al. Survival Following Liver Transplantation for Patients With Nonresectable Liver-only Colorectal Metastases. *Annals of Surgery.* 2020;271(2).
15. Bismuth H, Adam R, Lévi F, et al. Resection of nonresectable liver metastases from colorectal cancer after neoadjuvant chemotherapy. *Ann Surg.* Oct 1996;224(4):509-520; discussion 520-502.
16. Huiskens J, van Gulik TM, van Lienden KP, et al. Treatment strategies in colorectal cancer patients with initially unresectable liver-only metastases, a study protocol of the randomised phase 3 CAIRO5 study of the Dutch Colorectal Cancer Group (DCCG). *BMC Cancer.* May 6 2015;15:365.
17. Garlipp B, Gibbs P, Van Hazel GA, et al. Secondary technical resectability of colorectal cancer liver metastases after chemotherapy with or without selective internal radiotherapy in the randomized SIRFLOX trial. *Br J Surg.* Dec 2019;106(13):1837-1846.
18. Kingham TP, D'Angelica M, Kemeny NE. Role of intra-arterial hepatic chemotherapy in the treatment of colorectal cancer metastases. *J Surg Oncol.* Dec 15 2010;102(8):988-995.

19. Moris D, Ronnekleiv-Kelly S, Rahnemai-Azar AA, et al. Parenchymal-Sparing Versus Anatomic Liver Resection for Colorectal Liver Metastases: a Systematic Review. *Journal of Gastrointestinal Surgery.* 2017/06/01 2017;21(6):1076-1085.
20. Stang A, Fischbach R, Teichmann W, Bokemeyer C, Braumann D. A systematic review on the clinical benefit and role of radiofrequency ablation as treatment of colorectal liver metastases. *Eur J Cancer.* Jul 2009;45(10):1748-1756.
21. Mahadevan A, Blanck O, Lanciano R, et al. Stereotactic Body Radiotherapy (SBRT) for liver metastasis - clinical outcomes from the international multi-institutional RSSearch® Patient Registry. *Radiat Oncol.* Feb 13 2018;13(1):26.
22. Capussotti L, Muratore A, Baracchi F, et al. Portal vein ligation as an efficient method of increasing the future liver remnant volume in the surgical treatment of colorectal metastases. *Arch Surg.* Oct 2008;143(10):978-982; discussion 982.
23. Sandström P, Røsok BI, Sparrelid E, et al. ALPPS Improves Resectability Compared With Conventional Two-stage Hepatectomy in Patients With Advanced Colorectal Liver Metastasis: Results From a Scandinavian Multicenter Randomized Controlled Trial (LIGRO Trial). *Ann Surg.* May 2018;267(5):833-840.
24. Meyer Y, Olthof PB, Grünhagen DJ, et al. Treatment of metachronous colorectal cancer metastases in the Netherlands: A population-based study. *Eur J Surg Oncol.* Dec 4 2021.
25. Tomlinson JS, Jarnagin WR, DeMatteo RP, et al. Actual 10-year survival after resection of colorectal liver metastases defines cure. *J Clin Oncol.* Oct 10 2007;25(29):4575-4580.
26. Buisman FE, Giardiello D, Kemeny NE, et al. Predicting 10-year survival after resection of colorectal liver metastases; an international study including biomarkers and perioperative treatment. *Eur J Cancer.* Jun 2022;168:25-33.
27. Ruers T, Van Coevorden F, Punt CJA, et al. Local Treatment of Unresectable Colorectal Liver Metastases: Results of a Randomized Phase II Trial. *Journal of the National Cancer Institute.* 2017;109(9):djx015.
28. van der Werf LR, Kok NFM, Buis CI, et al. Implementation and first results of a mandatory, nationwide audit on liver surgery. *HPB (Oxford).* Oct 2019;21(10):1400-1410.
29. Kanas GP, Taylor A, Primrose JN, et al. Survival after liver resection in metastatic colorectal cancer: review and meta-analysis of prognostic factors. *Clin Epidemiol.* 2012;4:283-301.
30. Douillard JY, Oliner KS, Siena S, et al. Panitumumab-FOLFOX4 treatment and RAS mutations in colorectal cancer. *N Engl J Med.* Sep 12 2013;369(11):1023-1034.
31. Kopetz S, Grothey A, Yaeger R, et al. Encorafenib, Binimetinib, and Cetuximab in BRAF V600E-Mutated Colorectal Cancer. *N Engl J Med.* Oct 24 2019;381(17):1632-1643.
32. Vermeulen PB, Colpaert C, Salgado R, et al. Liver metastases from colorectal adenocarcinomas grow in three patterns with different angiogenesis and desmoplasia. *J Pathol.* Oct 2001;195(3):336-342.
33. Nagashima I, Oka T, Hamada C, Naruse K, Osada T, Muto T. Histopathological prognostic factors influencing long-term prognosis after surgical resection for hepatic metastases from colorectal cancer. *Am J Gastroenterol.* Mar 1999;94(3):739-743.
34. van Dam PJ, van der Stok EP, Teuwen LA, et al. International consensus guidelines for scoring the histopathological growth patterns of liver metastasis. *Br J Cancer.* Nov 7 2017;117(10):1427-1441.
35. Eefsen RL, Vermeulen PB, Christensen IJ, et al. Growth pattern of colorectal liver metastasis as a marker of recurrence risk. *Clin Exp Metastasis.* Apr 2015;32(4):369-381.
36. Van den Eynden GG, Bird NC, Majeed AW, Van Laere S, Dirix LY, Vermeulen PB. The histological growth pattern of colorectal cancer liver metastases has prognostic value. *Clin Exp Metastasis.* Aug 2012;29(6):541-549.
37. Galjart B, Nierop PMH, van der Stok EP, et al. Angiogenic desmoplastic histopathological growth pattern as a prognostic marker of good outcome in patients with colorectal liver metastases. *Angiogenesis.* May 2019;22(2):355-368.
38. Frentzas S, Simoneau E, Bridgeman VL, et al. Vessel co-option mediates resistance to anti-angiogenic therapy in liver metastases. *Nat Med.* Nov 2016;22(11):1294-1302.

```
#---------------------------- Concordance figures -------------------------
#EMC IC
pEMC_IC <- ggplot(res_EMC_IC, aes(x=No_Slides_Cat, y=mean)) +
  geom_errorbar(aes(ymin=LB, ymax=UB), width=0.1, color="black", size=0.75) +
  geom_point(shape=23, fill="black", color="black", size=3) +
  theme(panel.grid.major=element_blank(), panel.grid.minor=element_blank(),
        panel.background=element_blank(),
        axis.line=element_line(colour="black", size=0.75),
        axis.ticks=element_line(colour="black", size=0.75)) +
  scale_y_continuous(expand=c(0,0), limits=c(0.6,1.01),
                     breaks=c(0.6, 0.7, 0.8, 0.9, 1.0)) +
  labs(title="Within metastasis\n", x="\nNumber of blocks",
       y="\nMean concordance\n") +
  annotate("text", x=0.51, y=0.615,
           label=ifelse(pval_EMC_IC<0.001, "p < 0.001",
                        paste("p = ", sprintf("%.3f", pval_EMC_IC))),
           hjust=0, vjust=0,
           size=4.2) +
  geom_hline(yintercept=avg_EMC_IC,
             color="black",
             linetype="dashed") +
  annotate("text", x=0.50, y=avg_EMC_IC,
           label="mu",
           parse=TRUE,
           color="black",
           hjust=0, vjust=-0.5,
           size=3.5)

#EMC IP
res_EMC_IP <- rbind(res_EMC_cn, res_EMC_pt)
res_EMC_IP <- res_EMC_IP %>% mutate(CTx = factor(c("CTx-", "CTx-", "CTx-",
                                    "CTx+", "CTx+" , "CTx+")))
t.test(EMC_IP_cn$Concordance, EMC_IP_pt$Concordance)

dodge <- position_dodge(width = 0.3)
pEMC_IP <- ggplot(res_EMC_IP, aes(x=No_CRLM_Cat, y=mean, colour=CTx,
                  fill=CTx)) +
  scale_colour_manual(values=c("darkblue", "darkred"),
                      labels=c("CTx-     p = 0.678", "CTx+     p = 0.004")) +
  scale_fill_manual(values=c("darkblue", "darkred"),
                    labels=c("CTx-     p = 0.678", "CTx+     p = 0.004")) +
  geom_hline(yintercept=avg_EMC_cn,
             color="darkblue",
             linetype="dashed") +
  geom_hline(yintercept=avg_EMC_pt,
             color="darkred",
             linetype="dashed") +
  geom_errorbar(aes(ymin=LB, ymax=UB), width=0.15, size=0.75,
                position=dodge) +
  geom_point(shape=23, size=3, position=dodge) +
  theme(panel.grid.major=element_blank(), panel.grid.minor=element_blank(),
        panel.background=element_blank(),
        axis.line=element_line(colour="black", size=0.75),
        axis.ticks=element_line(colour="black", size=0.75),
        legend.title=element_blank(), legend.position=c(0, 0),
```

Chapter II

Histopathological growth patterns of colorectal liver metastasis exhibit little heterogeneity and can be determined with a high diagnostic accuracy

-

Clinical & experimental metastasis 2019

D.J. Höppener*, P.M.H. Nierop*, E. Herpel, N.N. Rahbari, M. Doukas, P.B. Vermeulen, D.J. Grünhagen, C. Verhoef.

*These authors contributed equally

Abstract

Introduction: Colorectal liver metastases (CRLM) exhibit distinct histopathological growth patterns (HGPs) that are indicative of prognosis following surgical treatment. This study aims to assess the reliability and replicability of this histological biomarker.

Methods: Within and between metastasis HGP concordance was analysed in patients who underwent surgery for CRLM. An independent cohort was used for external validation. Within metastasis concordance was assessed in CRLM with ≥2 tissue blocks. Similarly, concordance amongst multiple metastases was determined in patients with ≥2 resected CRLM. Diagnostic accuracy (area under the curve [AUC]) was compared by number of blocks and number of metastases scored. Interobserver agreement (Cohen's k) to the gold standard was determined for a pathologist and a PhD candidate without experience in HGP assessment after one and two training sessions.

Results: Both the within (95%, n=825) and the between metastasis (90%, n=363) HGP concordance was high. These results could be replicated in the external validation cohort with a within and between metastasis concordance of 97% and 94%, respectively. Diagnostic accuracy improved when scoring 2 vs. 1 blocks(s) or CRLM (AUC=95.9 vs. 97.7 [p=0.039] and AUC=96.5 vs. 93.3 [p=0.026], respectively), but not when scoring 3 vs. 2 blocks or CRLM (both p>0.2). After two training sessions the interobserver agreement for both the pathologist and the PhD candidate were excellent (k=0.953 and k=0.951, respectively).

Discussion: The histopathological growth patterns of colorectal liver metastasis exhibit little heterogeneity and can be determined with a high diagnostic accuracy, making them a reliable and replicable histological biomarker.

Introduction

Colorectal cancer (CRC) is one of the most prevalent solid malignancies in the world with approximately one third of patients developing hepatic metastases.[1-5] Even though surgical treatment is seen as the only potentially curative treatment option, reported 5-year survival rates vary widely (from 20% to 70%).[6-13]

Recently, a new potential histological biomarker has been described.[14, 15] Colorectal liver metastases (CRLM) grow in three distinct histopathological growth patterns (HGP), the desmoplastic, the replacement and the pushing type, each with unique morphological and biological features (*figure 1 a-f*). These distinct features have previously been described in detail.[16-18] In short: HGP assessment is performed by assessing the proportion (expressed as percentage) of each distinct HGP observed at the tumour-liver interface on H&E stained tissue sections.[14] Previous studies suggest that a high relative proportion of the replacement type is prognostic for an impaired overall survival.[19-22] The largest and most recent study analysed a cohort of 732 patients and found that it is the presence rather than the relative proportion of any non-desmoplastic type HGP (i.e. pushing and/or replacement type) that dictates poor prognosis.[15] In terms of clinical relevance, HGPs can therefore be classified into two categories: either pure desmoplastic (dHGP) or any observed non-desmoplastic type HGP (non-dHGP).[15]

While interesting from a biological point of view, this new classification raises methodological concerns. For if classification is based on either 100% dHGP or <100% dHGP, assessment could be more susceptible to sampling and reading error. In order to validate HGPs as a histological biomarker, knowledge on HGP concordance within a single

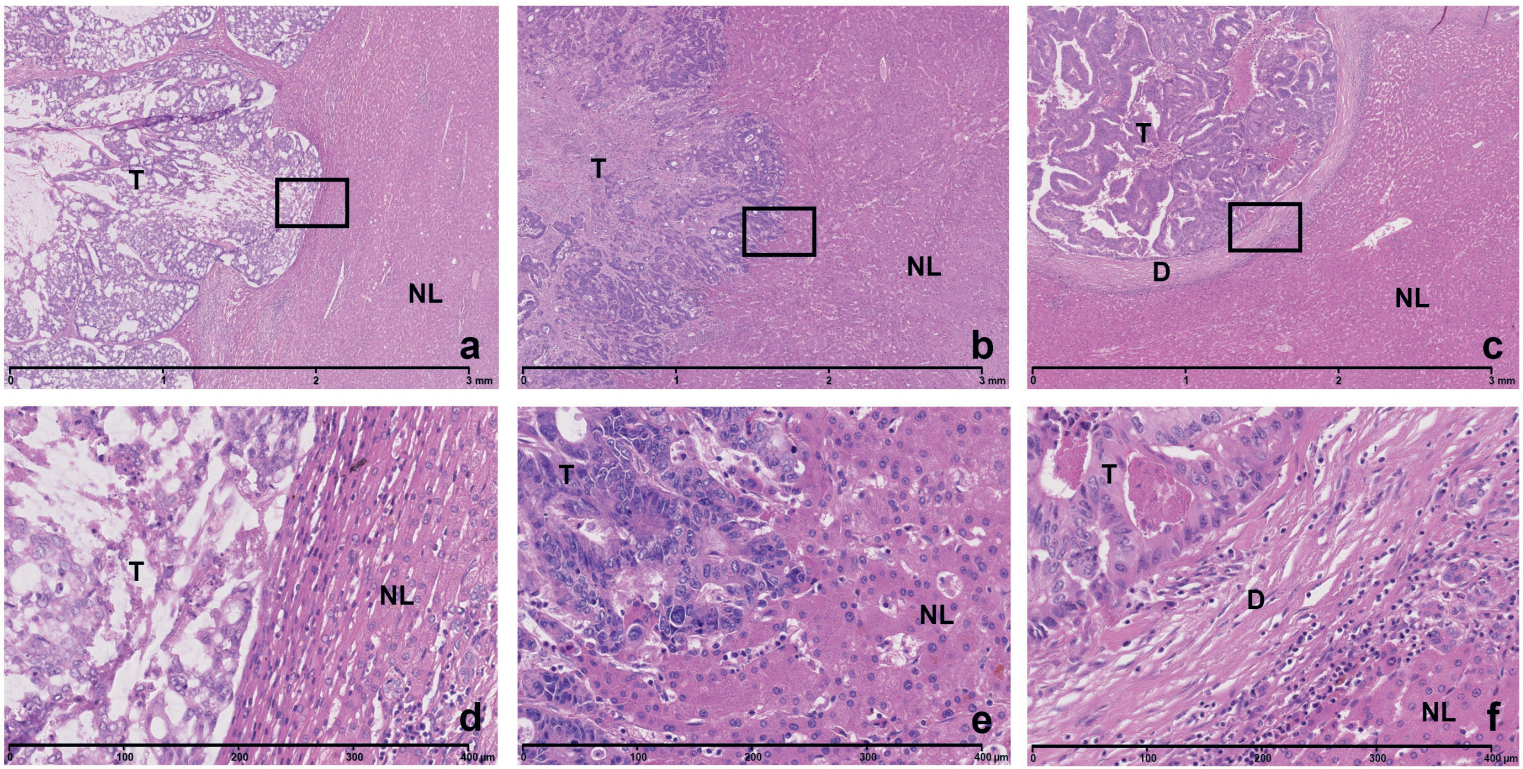

Figure 1. Three distinct types of histopathological growth patterns (HGPs) can be identified on H&E stained tissue blocks. (a, b & c) 2.5x magnification. (d, e & f) 20x magnification. (a&d) Pushing type HGP. (b&e) Replacement type HGP. (c&f) Desmoplastic type HGP. T: tumour, NL: normal liver & D: desmoplastic stroma.

and amongst multiple metastases within the same patient is essential, especially considering the growing evidence of (non-)genetic intra-tumoural heterogeneity in CRC.[23] Knowledge on diagnostic accuracy and learnability of HGP assessment is also necessitated to determine the reliability and replicability of this histological biomarker. This study therefore analyses within and between metastasis HGP concordance within the same cohort as described by Galjart et al.[15], as well as an external validation cohort[24]. In addition, diagnostic accuracy is determined for scoring a single or multiple Formalin-Fixed Paraffin-Embedded (FFPE) tissue blocks per CRLM and for scoring a single or multiple CRLM per patient. Lastly, the learning curve associated with HGP assessment is determined in two observers (pathologist and PhD candidate) without prior experience in HGP assessment.

Methods

The current study was approved by the medical ethics committee of the Erasmus University Medical Center (MEC-2018-1743). The need for informed consent was waived by the ethics committee due to the retrospective and non-invasive nature of the study. Drafting of the manuscript was performed in accordance with the REMARK guidelines.[25]

Patient selection

The patient selection for the current study was performed in the same cohort as described by Galjart et al.[15]. Patients undergoing resection of CRLM at the Erasmus MC Cancer Institute, the Netherlands, between January 2000 and March 2015 were eligible for inclusion.

Routine pathological assessment

During macroscopic pathological assessment of the surgical

specimens of CRLM, representative sections (e.g. tumour, tumour with relation to the surgical margin(s), capsule, background liver, non-tumorous liver in distance) were considered for preparation of FFPE tissue blocks. A 5µm section per block was cut and stained with Haematoxylin and Eosin (H&E) for pathological interpretation. If needed, deeper levels of the block were cut and stained with H&E.

Assessment of HGPs

H&E stained slides retrieved from the archive of the Pathology Department of the Erasmus MC were retrospectively reviewed by light microscopy (figure 1 a-f). Scoring of the HGPs was performed in accordance with international consensus guidelines.[14] For each block subjected to review the relative presence (in percentage %) at the tumour-liver interface of the distinct HGP's (pushing, desmoplastic and replacement type) was estimated. The metastasis HGP was defined as the pooled estimate (average with equal weights per block) of all blocks of a single CRLM. Concordantly, the patient HGP was defined as the pooled estimate (average with equal weights per CRLM) of all resected CRLM within a single patient. Given recent findings[15], block, metastasis, and patient HGP were classified as dHGP if only the desmoplastic type was observed (i.e. 100% dHGP), and as non-dHGP if any percentage of pushing and/or replacement type was observed (i.e. <100% dHGP). Due to this on/off classification, if non-dHGP is observed on a single block, corresponding metastasis and patient HGP is classified as non-dHGP, regardless of the HGP of other blocks within the same metastasis or other CRLM within the same patient.

For the within metastasis analysis, concordance (yes/no) of block HGP to metastasis HGP was recorded for all resected CRLM with ≥2 tissue blocks. Within metastasis concordance was defined as the proportion of concordant tissue blocks.

Since a lesion represents a three dimensional structure, consecutive slides from a single block (i.e. deeper levels) do not adequately represent its three dimensional nature. As such, consecutive slides from a single block were excluded from the within metastasis analysis. For the between metastasis analysis, concordance (yes/no) of metastasis HGP to patient HGP was determined in all patients with ≥2 CRLM resected in a single time-frame (e.g. no recurrent CRLM). Between metastasis concordance was defined as within patient proportion of concordant CRLM. Patient information and data on primary CRC and CRLM were extracted from a prospectively maintained database. Regarding systemic treatment status, patients were considered chemo-naive if they did not receive any form of chemotherapy within the six months prior to resection. Multivariable logistic regression analysis was performed for within metastasis discordance (yes/no) with primary tumour characteristics, known clinical risk factors, systemic treatment status, and number of blocks scored as predictors. Significant predictor(s) found for within metastasis discordance were used as stratification factor(s) for between metastasis analysis. Identical models were fitted within each stratum (if applicable) to predict discordance (yes/no) amongst multiple metastases. Mean within metastasis concordance was compared across number of blocks scored. Similarly, mean between metastasis concordance was compared within strata (if applicable) and by number of CRLM resected.

External validation

External validation of mean within and mean between metastasis concordance was performed by retrospective HGP assessment as described previously. The external validation cohort comprised of chemo-naive patients treated surgically for CRLM at the University Hospital of Heidelberg, Germany, between October 2001 and June 2009.[24] H&E stained sections of the validation cohort were provided by the tissue bank

of the National Center for Tumor Diseases (NCT). As the external validation cohort consisted of chemo-naive patients, comparisons to the original cohort were performed in (tissues from) chemo-naive patients only.

Diagnostic accuracy

Diagnostic accuracy for scoring a single FFPE block was determined in all CRLM with ≥2 blocks. Of these ≥2 blocks, one individual block was selected at random. The HGP of this randomly selected block was considered the predictor (i.e. test result), while the metastasis HGP – as determined by HGP assessment of all ≥2 blocks of the metastasis in question – was considered the response (i.e. true HGP status). This was done similarly for 2 blocks in all CRLM with ≥3 blocks. Identically, the diagnostic accuracy of scoring a single resected CRLM was determined within patients with ≥2 CRLM resected etc. The area under the curve [AUC] of the corresponding receiver operating characteristic (ROC) curves were compared for 2 vs. 1 block(s) or CRLM scored, and for 3 vs. 2 blocks or CRLM scored, respectively.

Learning curve

A gastro-intestinal pathologist (MD) and a PhD-candidate (DH) without prior pathology experience were recruited for learning curve analysis. Both observers had no prior experience in HGP assessment. The raters received a joint training session by a pathologist with over 10 years of experience in HGP assessment (PV). During this training session, 50 tissue sections were assessed collaboratively. Hereafter, both observers independently scored a test-set of an additional 50 tissue sections. Individual scores of the test-set were reviewed in a joint session with the trainer, followed by a second training session of 50 tissue sections. Subsequently a second test-set of 50 tissue sections was scored independently. After completion scores were again

collaboratively reviewed. For both test-sets, interobserver agreement of both observers compared to the gold standard was determined for the dHGP/non-dHGP classification. The scores of the experienced trainer were considered the gold standard.

Statistical analysis

Dichotomous or categorical data are reported as percentage, parametric continuous data are reported as mean (standard deviation [SD]) and non-parametric continuous data are reported as median (inter-quartile range [IQR]). Mean concordances were compared by an independent samples T-test or a one-way analysis of variance (ANOVA), depending on the number of strata. AUC values were compared as described by DeLong.[26] Interobserver agreement was determined using Cohen's kappa. All statistical analyses were performed using R version 3.5.3 (http://www.r-project.org). The R-package 'pROC' was used for comparison of AUC values. A p-value <0.05 was considered statistically significant.

Results

Patient characteristics

In total 785 patients underwent resection of one or more CRLM at the Erasmus MC Cancer Institute in the study period and were consequently scored for HGP. In total 1625 CRLM were resected. Of these, 835 CRLM had two or more H&E stained slides available for review (2135 slides in total) and were considered for within metastasis analysis. Of these, 31 slides of 10 individual CRLM were identified as consecutively cut from single FFPE blocks, and were excluded from within metastasis analysis. Resection of two or more CRLM was performed in 382 patients. Nineteen were excluded for between metastasis analysis due to missing data required to link individual tissue samples to individual CRLM. Within the remaining 363 patients a total of 1118 CRLM were resected.

Table 1. Characteristics of patients included for between metastasis concordance analysis

		n=363 (%)
Gender	Female	233 (64)
	Male	130 (36)
Age at resection CRLM - *(median [IQR])*		63.0 [57.0, 70.0]
Primary tumour location	Right-sided	61 (17)
	Left-sided	152 (42)
	Rectal	145 (40)
	Missing	5 (1)
T-stage	pT 0-2	70 (19)
	pT 3-4	265 (73)
	Missing	28 (8)
N-stage	N0	118 (33)
	N+	216 (60)
	Missing	29 (8)
Disease-free interval - months *(median [IQR])*		0.0 [0.0, 9.0]
Diameter of largest CRLM - cm *(median [IQR])*		3.1 [2.0, 4.8]
Preoperative CEA - µg/L *(median [IQR])*		20.0 [5.4, 70.1]
Preoperative CTx status	Chemo-naive	121 (33)
	Pre-treated	242 (67)
Two-staged resection	No	347 (96)
	Yes	16 (4)
Use of RFA or MWA	No	252 (69)
	Yes	111 (31)
Number of CRLM resected	2	175 (48)
	3	87 (24)
	4	58 (16)
	≥5	43 (12)
Histopathological growth pattern	dHGP	72 (20)
	non-dHGP	291 (80)

CRLM: colorectal liver metastasis, IQR: interquartile range, CEA: carcinoembryonic antigen, CTx: chemotherapy, RFA: radiofrequency ablation, MWA: microwave ablation, (non-)dHGP: (non-)desmoplastic type histopathological growth pattern

Patient characteristics are reported in *table 1*.

Within metastasis concordance

Non-dHGP was observed in 72% of reviewed tissue blocks. Results of the multivariable logistic regression model on within metastasis discordance are reported in *table 2*.

Table 2. Multivariable binary logistic regression models on discordance *(yes/no)* in histopathological growth pattern

		Within metastasis (n = 702)		*Between metastasis (n = 308)*			
				Chemo-naive (n = 111)		*Pre-treated (n = 197)*	
Variable		OR [95% CI]	*p-value*	OR [95% CI]	*p-value*	OR [95% CI]	*p-value*
Location of primary	*left vs right*	1.51 [0.72-3.49]	0.30	0.61 [0.09-5.24]	0.62	0.66 [0.26-1.66]	0.37
	rectal vs right	1.89 [0.88-4.40]	0.12	3.17 [0.67-23.79]	0.19	0.60 [0.22-1.66]	0.32
pT3-4 vs pT0-2		1.26 [0.65-2.55]	0.51	1.16 [0.26-6.01]	0.85	1.19 [0.46-3.27]	0.72
Node-positive primary		0.65 [0.39-1.10]	0.11	0.52 [0.12-2.13]	0.35	0.70 [0.33-1.46]	0.33
Disease-free interval - months [a]		1.00 [0.98-1.01]	0.85	1.00 [0.95-1.03]	0.83	1.02 [0.97-1.06]	0.43
Diameter of largest CRLM - cm [a]		-	-	1.46 [1.07-2.15]	0.03*	1.14 [0.98-1.32]	0.08
Preoperative CEA - µg/L [a]		1.00 [1.00-1.00]	0.15	1.00 [0.99-1.00]	0.28	1.00 [1.00-1.00]	0.56
Pre-treated vs chemonaive		2.12 [1.23-3.68]	0.007*	-	-	-	-
Number of blocks scored	*3 vs 2*	1.99 [1.14-3.44]	0.01*	-	-	-	-
	4 vs 2	2.08 [0.79-4.87]	0.11	-	-	-	-
	≥5 vs 2	1.42 [0.32-4.41]	0.59	-	-	-	-
Number of CRLM resected	*3 vs 2*	-	-	0.87 [0.19-3.44]	0.85	3.60 [1.41-9.55]	0.008*
	≥4 vs 2	-	-	1.62 [0.29-7.39]	0.55	5.89 [2.59-14.36]	<0.001*

OR: odds ratio, CI: confidence interval, CRLM: colorectal liver metastases and CEA: carcinoembryonic antigen

[a] = continuous data entered into the model

* = $\alpha < 0.05$

Systemic treatment status proved to be a significant predictor for HGP discordance (yes/no) amongst multiple blocks, with an odds ratio (OR) (95%CI) of 2.12 (1.23;3.68) and p=0.007 for pre-treated versus chemo-naive CRLM. Mean within metastasis concordance was 95%. *Figure 2a* shows the mean within metastasis concordance stratified by number of blocks scored. Mean within metastasis concordance (95%CI) for 2, 3, 4, or ≥5 blocks scored was 96% (95;97), 94% (92;96), 93% (88;98) and 94% (86;100) respectively, and was independent of the number of blocks scored (p=0.32).

Between metastasis concordance

Mean between metastasis concordance of all 363 patients was 90%. Since systemic treatment status was a significant predictor for within

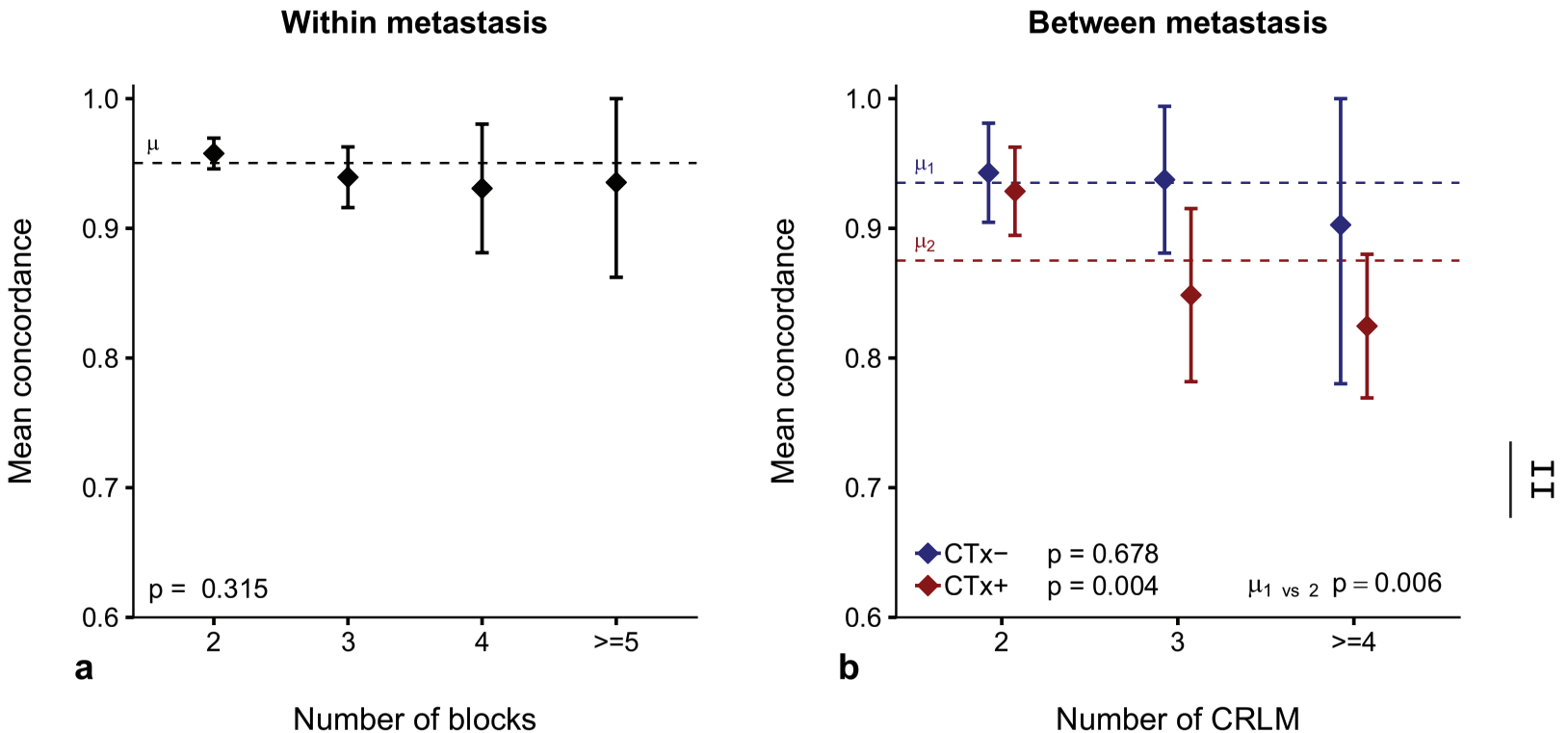

Figure 2. (a) Within metastasis histopathological growth pattern (HGP) concordance within the original cohort stratified by number of blocks scored. Overall mean within metastasis concordance (μ) was 95%. (b) Mean between metastasis HGP concordance within the original cohort stratified by preoperative chemotherapy status and number of colorectal liver metastasis (CRLM) resected. Mean between metastasis concordance in chemo-naive (CTx-) patients was 94% (μ1), and in pre-treated (CTx+) patients 88% (μ2). Error-bars represent the 95% confidence interval of the estimate.

metastasis discordance, between metastasis analysis was performed in chemo-naive and pre-treated patients separately. Non-dHGP was found in 85% of chemo-naive patients versus 78% in pre-treated patients (p=0.09). Results of the fitted multivariable logistic regression models on presence of HGP discordance (yes/no) amongst multiple resected CRLM are reported in *table 2*. Within chemo-naive patients, the size of the largest hepatic tumour on preoperative imaging proved a significant predictor for between metastasis discordance with OR (95%CI) 1.46 (1.07;2.15) and p=0.03 for every cm increase in size. The only significant predictor found for between metastasis discordance in pre-treated patients was number of CRLM resected. Corresponding OR (95%CI) were 3.60 (1.41-9.55) for 3 vs. 2 CRLM resected and 5.89 (2.59;14.36) for ≥4 vs. 2 CRLM resected (p=0.008 and p<0.001). Mean between metastasis concordance (figure 2b) was significantly lower in pre-treated vs. chemo-naive patients (88% vs. 94%, p=0.006). *Figure 2b* shows the mean between metastasis concordance for chemo-naive and pre-treated patients stratified by number of CRLM resected. In chemo-naive patients, mean between metastasis concordance [95%CI] did not differ amongst 2 (94% [91;98]), 3 (94% [88;99]) or ≥4 (90% [78;100]) CRLM resected (p=0.68). In pre-treated patients mean between metastasis concordance [95%CI] was significantly different amongst 2 (93% [90;96]), 3 (85% [78;92]) and ≥4 (83% [77;88]) CRLM resected (p=0.004).

External validation

The external cohort comprised of 276 patients of whom the HGP could be determined in 251 (91%). In total 168 patients had resection performed of two or more CRLM and could be included for between metastasis analysis. Within metastasis analysis was performed in 270 CRLM with two or more blocks. Baseline characteristics were comparable between the external validation cohort and the chemo-naive patients of the original cohort (*supplementary table 1*).

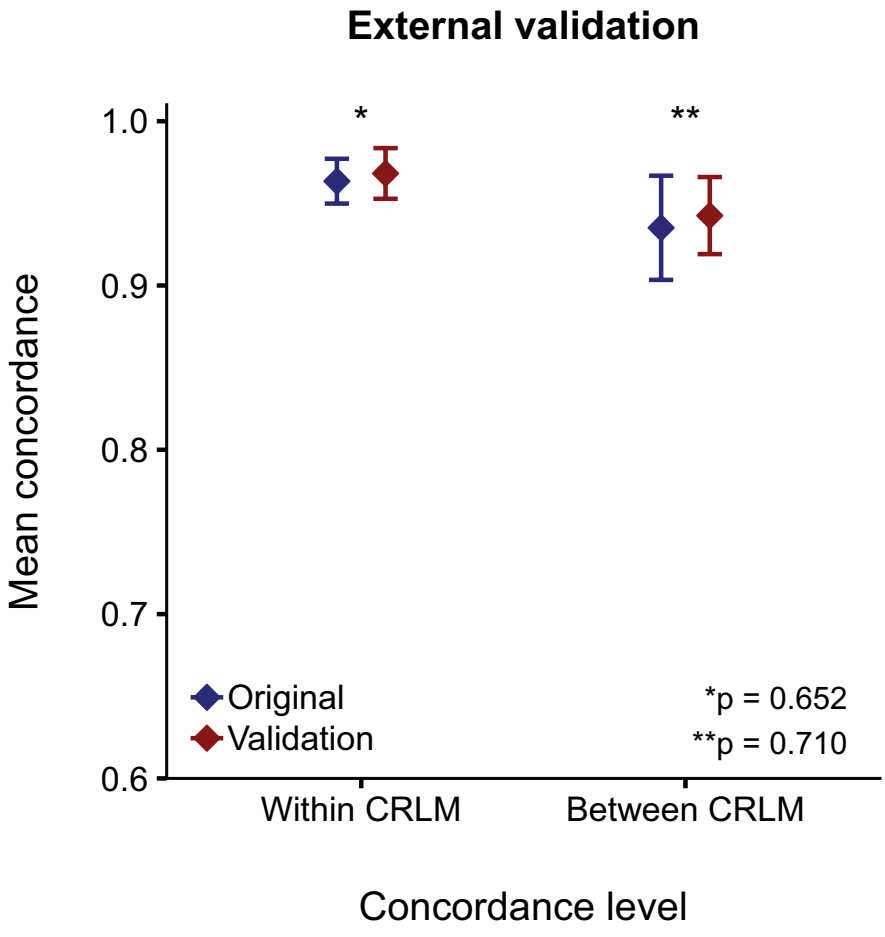

Figure 3. External validation of within and between colorectal liver metastasis (CRLM) concordance of histopathological growth pattern. Comparison was performed between the external validation cohort and chemonaive subjects from the original cohort.

Mean within (96% vs. 97%, p=0.652) and between (94% vs. 94%, p=0.710) metastasis concordance did not differ between the original (chemo-naive patients only) and validation cohort (*figure 3*).

Diagnostic accuracy

Supplementary figure 1a displays the AUC for scoring a single (95.9%), two (97.7%) or three blocks (98.8%) per metastasis.

A significant increase in diagnostic accuracy was observed for scoring 2 vs. 1 block(s) (p=0.04), but not for scoring 3 vs. 2 blocks (p=0.34). The AUC for scoring a single (93.3%), two (96.5%) or three (98.2%) resected CRLM per patient are reported in *supplementary figure 1b*. A significant increase in diagnostic accuracy was found for scoring 2 vs. 1 resected CRLM (p=0.03), but not for scoring 3 vs. 2 resected CRLM (p=0.24).

Learning curve

The results of both test-sets as scored by the gold standard, the pathologist and the PhD candidate are graphically displayed in *figure 4 a-f*. Interobserver agreement was higher in the second test-set for both the pathologist (k=0.95 vs. k=0.84) and the PhD candidate (k=0.95 vs. k=0.75). In the first test-set a difference in performance was seen between the pathologist and the PhD candidate (k=0.84 vs. k=0.75), whereas performance in the second test-set did not differ (both k=0.95).

Discussion

The current study found within metastasis concordance to be high (95%) when classifying the HGP as dHGP or non-dHGP. Furthermore, mean within metastasis concordance was independent of number of FFPE blocks scored. Overall between metastasis concordance was also high (90%), but differed for chemo-naive versus pre-treated patients (94% vs 88%). In chemo-naive patients, mean between metastasis concordance was independent of number of CRLM resected and the only predictor found in multivariable analysis for discordance was size of largest hepatic tumour on preoperative imaging. For pre-treated patients, the number of CRLM resected proved predictive for between metastasis discordance. This finding was supported by a significant difference in mean concordance

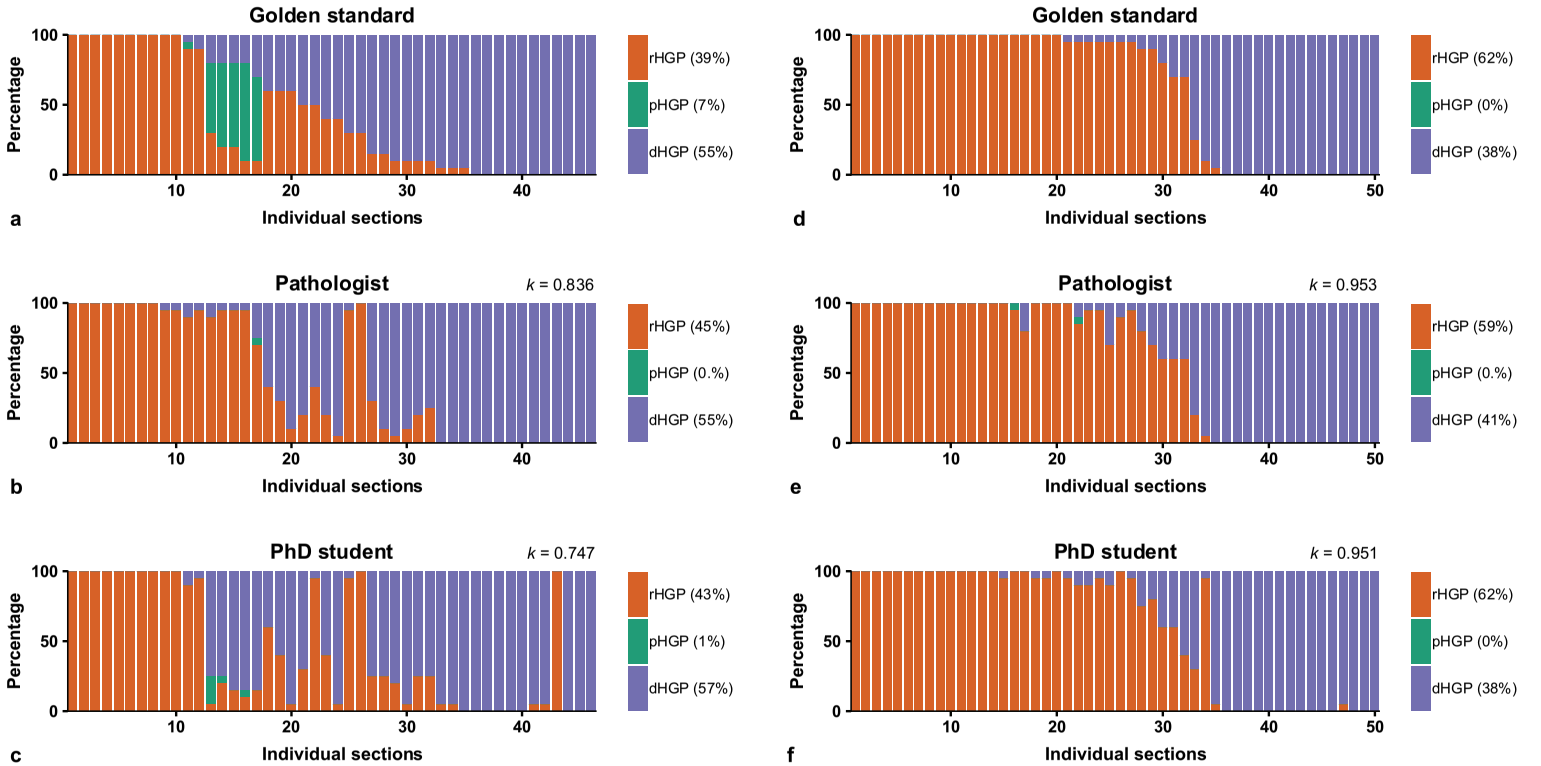

Figure 4. (a&d) Results of the first and second test-set as scored by the experienced trainer (gold standard). (b&e) Results of the first and second test-set as scored by the pathologist. (c&f) Results of the first and second test-set as scored by the PhD candidate. rHGP: replacement type histopathological growth pattern (HGP), pHGP: pushing type HGP & dHGP: desmoplastic type HGP.

for 2, 3 or ≥4 resected CRLM within pre-treated patients. External validation in a large cohort of chemo-naive patients found similarly high numbers of mean within (97%) and between (94%) metastasis concordance. Unfortunately, the external validation cohort comprised of chemo-naive patients only, as such external validation within pre-treated CRLM and patients could not be performed.

The current study suggests that systemic chemotherapy treatment prior to hepatic resection might affect the reliability of HGP assessment. In the same patient cohort, Galjart et al. reported a significant increase in dHGP within pre-treated patients.[15] It is as of yet unclear if this difference is due to chemotherapy directly changing HGP morphology, or due to selection bias in that patients with dHGP have improved prognosis and are thus more likely to complete their pre-operative chemotherapy and subsequent liver resection. Although inconclusive, the current study did find a higher heterogeneity amongst the HGP of slides and CRLM of pre-treated patients. This could be the result of chemotherapy having a direct effect on HGP morphology.

Two studies have previously reported on HGP concordance. Van Dam et al analysed within metastasis agreement of ≥4 sections in a small sample of 50 CRLM[14] and Eefsen et al. reported on between metastases agreement in a small group of 24 patients with multiple resected CRLM[17]. As both studies applied different cut-off values to determine the HGP (50% and 75% respectively), interpretation of its results in light of the current study is difficult. Considering recent developments, it seems logical that future HGP classification will be based on the dHGP/non-dHGP cut-off.

When determining the diagnostic accuracy of HGP assessment, the current study found high AUC values for scoring a single,

two, or three blocks (all >95%) or CRLM (all >92%). The currently obtained results show that scoring two instead of one FFPE block(s) per CRLM increased diagnostic accuracy significantly. This increase was not significant when scoring three versus two blocks. As such, scoring two blocks per CRLM seems preferable and little accuracy is gained by further increasing the number of blocks assessed. This could significantly decrease workload, especially considering when non-dHGP is observed in a single block, the other blocks of the same or different CRLM do not have to be assessed, for non-dHGP has already been established. Similar results were seen when looking at the diagnostic accuracy for scoring two versus one and three versus two CRLM resected in patients with multiple metastases. These findings suggest that CRLM treated by other modalities (e.g. ablative techniques) can accurately be diagnosed by CRLM resected within the same timeframe, especially in the case of two or more resected metastases.

Analysis of the learning curve showed that after a single training session by an experienced trainer good to excellent (k >0.7) interobserver agreement for dHGP/non-dHGP was reached by two unexperienced observers. As expected, an observer with prior experience in liver pathology had a superior initial performance. After two training sessions however, the interobserver agreement was near perfect (k >0.9) for both raters. These results suggest that HGP classification into dHGP or non-dHGP can be taught with relative ease and that interobserver agreement is high. In comparison, Chetty et al. reported on the interobserver agreement of tumour regression grade (TRG), a histopathological assessment within the field of colorectal cancer.[27] The overall agreement (expressed in k) was determined for three separate scoring systems: the Mandard[28], Dworak[29], and the modified rectal cancer

regression grading system (m-RCRG)[30]. Seventeen experienced rectal cancer pathologists were asked to score 10 slides of 10 separate cases of rectal cancer treated with long-course preoperative chemoradiation. Reported overall agreement for the Mandard, Dworak and m-RCRG were k=0.28, k=0.35 and k=0.38, respectively.[27] Furthermore, these results are also promising for automated HGP determination using digital image slides and 'pathomics', as it has shown great promise in other histological phenotypes.[31] Especially considering the new on/off phenomenon as described by Galjart et al.[15], automated HGP determination on digital sections is something worth investigating and seems feasible.

Common biomarkers used in clinical practice for the treatment of colorectal cancer include K-RAS and B-RAF mutational status. Richman et al. reported on within tumour heterogeneity of K-RAS and B-RAF in 69 primary CRC cases.[32] Intra-tumoural heterogeneity was found in 5/69 (7.2%) for K-RAS and 2/69 (2.9%) for B-RAF status.[32] When comparing multiple tumour sites, a recent meta-analysis by Bhullar et al. reported on the concordance of, amongst others, K-RAS and B-RAF between the primary tumour and its corresponding metastases.[33] Median biomarker concordance (range) for K-RAS and B-RAF were 93.7% (67-100) and 99.4% (80-100), respectively.[33]

It appears that little within and between metastasis heterogeneity exists in the HGP of CRLM when classified as dHGP and non-dHGP. In addition, the observed heterogeneity seems comparable to that observed for biomarkers currently used in clinical practice. Furthermore, the diagnostic accuracy and learnability of HGP assessment by light microscopy seems high. These findings suggest that the HGPs of CRLM are a reliable and replicable histological biomarker.

References

1. Torre LA, Bray F, Siegel RL, Ferlay J, Lortet-Tieulent J, Jemal A. Global cancer statistics, 2012. *CA Cancer J Clin.* 2015; 65: 87-108.
2. Manfredi S, Lepage C, Hatem C, Coatmeur O, Faivre J, Bouvier AM. Epidemiology and Management of Liver Metastases From Colorectal Cancer. *Ann Surg.* 2006; 244: 254-9.
3. Elferink MA, de Jong KP, Klaase JM, Siemerink EJ, de Wilt JH. Metachronous metastases from colorectal cancer: a population-based study in North-East Netherlands. *Int J Colorectal Dis.* 2015; 30: 205-12.
4. van der Geest LG, Lam-Boer J, Koopman M, Verhoef C, Elferink MA, de Wilt JH. Nationwide trends in incidence, treatment and survival of colorectal cancer patients with synchronous metastases. *Clin Exp Metastasis.* 2015; 32: 457-65.
5. van der Stok EP, Spaander MCW, Grunhagen DJ, Verhoef C, Kuipers EJ. Surveillance after curative treatment for colorectal cancer. *Nat Rev Clin Oncol.* 2017; 14: 297-315.
6. Kanas GP, Taylor A, Primrose JN, Langeberg WJ, Kelsh MA, Mowat FS, et al. Survival after liver resection in metastatic colorectal cancer: review and meta-analysis of prognostic factors. *Clin Epidemiol.* 2012; 4: 283-301.
7. Galjart B, van der Stok EP, Rothbarth J, Grunhagen DJ, Verhoef C. Posttreatment Surveillance in Patients with Prolonged Disease-Free Survival After Resection of Colorectal Liver Metastasis. *Ann Surg Oncol.* 2016; 23: 3999-4007.
8. Ayez N, van der Stok EP, Grunhagen DJ, Rothbarth J, van Meerten E, Eggermont AM, et al. The use of neo-adjuvant chemotherapy in patients with resectable colorectal liver metastases: Clinical risk score as possible discriminator. *Eur J Surg Oncol.* 2015; 41: 859-67.
9. van der Pool AE, Lalmahomed ZS, Ozbay Y, de Wilt JH, Eggermont AM, Jzermans JN, et al. 'Staged' liver resection in synchronous and metachronous colorectal hepatic metastases: differences in clinicopathological features and outcome. *Colorectal Dis.* 2010; 12: e229-35.
10. Lalmahomed ZS, Ayez N, van der Pool AE, Verheij J, JN IJ, Verhoef C. Anatomical versus nonanatomical resection of colorectal liver metastases: is there a difference in surgical and oncological outcome? *World J Surg.* 2011; 35: 656-61.
11. Ayez N, Burger JW, van der Pool AE, Eggermont AM, Grunhagen DJ, de Wilt JH, et al. Long-term results of the "liver first" approach in patients with locally advanced rectal cancer and synchronous liver metastases. *Dis Colon Rectum.* 2013; 56: 281-7.
12. de Ridder JAM, van der Stok EP, Mekenkamp LJ, Wiering B, Koopman M, Punt CJA, et al. Management of liver metastases in colorectal cancer patients: A retrospective case-control study of systemic therapy versus liver resection. *Eur J Cancer.* 2016; 59: 13-21.
13. van Amerongen MJ, van der Stok EP, Futterer JJ, Jenniskens SF, Moelker A, Grunhagen DJ, et al. Short term and long term results of patients with colorectal liver metastases undergoing surgery with or without radiofrequency ablation. *Eur J Surg Oncol.* 2016; 42: 523-30.
14. van Dam PJ, van der Stok EP, Teuwen LA, Van den Eynden GG, Illemann M, Frentzas S, et al. International consensus guidelines for scoring the histopathological growth patterns of liver metastasis. *Br J Cancer.* 2017; 117: 1427-41.
15. Galjart B, Nierop PMH, van der Stok EP, van den Braak R, Hoppener DJ, Daelemans S, et al. Angiogenic desmoplastic histopathological growth pattern as a prognostic marker of good outcome in patients with colorectal liver metastases. *Angiogenesis.* 2019.
16. Vermeulen PB, Colpaert C, Salgado R, Royers R, Hellemans H, Van Den Heuvel E, et al. Liver metastases from colorectal adenocarcinomas grow in three patterns with different angiogenesis and desmoplasia. *J Pathol.* 2001; 195: 336-42.
17. Eefsen RL, Van den Eynden GG, Hoyer-Hansen G, Brodt P, Laerum OD, Vermeulen PB, et al. Histopathological growth pattern, proteolysis and angiogenesis in chemonaive patients resected for multiple colorectal liver metastases. *J Oncol.* 2012; 2012: 907971.
18. Frentzas S, Simoneau E, Bridgeman VL, Vermeulen PB, Foo S, Kostaras E, et al. Vessel co-option mediates resistance to anti-angiogenic therapy in liver metastases. *Nat Med.* 2016; 22: 1294-302.
19. Van den Eynden GG, Bird NC, Majeed AW, Van Laere S, Dirix LY, Vermeulen PB. The

histological growth pattern of colorectal cancer liver metastases has prognostic value. *Clin Exp Metastasis.* 2012; 29: 541-9.
20. Eefsen RL, Vermeulen PB, Christensen IJ, Laerum OD, Mogensen MB, Rolff HC, et al. Growth pattern of colorectal liver metastasis as a marker of recurrence risk. *Clin Exp Metastasis.* 2015; 32: 369-81.
21. Nielsen K, Rolff HC, Eefsen RL, Vainer B. The morphological growth patterns of colorectal liver metastases are prognostic for overall survival. *Mod Pathol.* 2014; 27: 1641-8.
22. Pinheiro RS, Herman P, Lupinacci RM, Lai Q, Mello ES, Coelho FF, et al. Tumor growth pattern as predictor of colorectal liver metastasis recurrence. *Am J Surg.* 2014; 207: 493-8.
23. Punt CJ, Koopman M, Vermeulen L. From tumour heterogeneity to advances in precision treatment of colorectal cancer. *Nat Rev Clin Oncol.* 2017; 14: 235-46.
24. Rahbari NN, Reissfelder C, Schulze-Bergkamen H, Jager D, Buchler MW, Weitz J, et al. Adjuvant therapy after resection of colorectal liver metastases: the predictive value of the MSKCC clinical risk score in the era of modern chemotherapy. *BMC Cancer.* 2014; 14: 174.
25. Sauerbrei W, Taube SE, McShane LM, Cavenagh MM, Altman DG. Reporting Recommendations for Tumor Marker Prognostic Studies (REMARK): An Abridged Explanation and Elaboration. *J Natl Cancer Inst.* 2018; 110: 803-11.
26. DeLong ER, DeLong DM, Clarke-Pearson DL. Comparing the areas under two or more correlated receiver operating characteristic curves: a nonparametric approach. *Biometrics.* 1988; 44: 837-45.
27. Chetty R, Gill P, Govender D, Bateman A, Chang HJ, Deshpande V, et al. International study group on rectal cancer regression grading: interobserver variability with commonly used regression grading systems. *Hum Pathol.* 2012; 43: 1917-23.
28. Mandard AM, Dalibard F, Mandard JC, Marnay J, Henry-Amar M, Petiot JF, et al. Pathologic assessment of tumor regression after preoperative chemoradiotherapy of esophageal carcinoma. Clinicopathologic correlations. *Cancer.* 1994; 73: 2680-6.
29. Dworak O, Keilholz L, Hoffmann A. Pathological features of rectal cancer after preoperative radiochemotherapy. *Int J Colorectal Dis.* 1997; 12: 19-23.
30. Ryan R, Gibbons D, Hyland JM, Treanor D, White A, Mulcahy HE, et al. Pathological response following long-course neoadjuvant chemoradiotherapy for locally advanced rectal cancer. *Histopathology.* 2005; 47: 141-6.
31. Ehteshami Bejnordi B, Veta M, Johannes van Diest P, van Ginneken B, Karssemeijer N, Litjens G, et al. Diagnostic Assessment of Deep Learning Algorithms for Detection of Lymph Node Metastases in Women With Breast Cancer. *Jama.* 2017; 318: 2199-210.
32. Richman SD, Chambers P, Seymour MT, Daly C, Grant S, Hemmings G, et al. Intra-tumoral heterogeneity of KRAS and BRAF mutation status in patients with advanced colorectal cancer (aCRC) and cost-effectiveness of multiple sample testing. *Anal Cell Pathol (Amst).* 2011; 34: 61-6.
33. Bhullar DS, Barriuso J, Mullamitha S, Saunders MP, O'Dwyer ST, Aziz O. Biomarker concordance between primary colorectal cancer and its metastases. *EBioMedicine.* 2019.

Supplementary materials

Table S1. Comparison of baseline characteristics of chemo-naive patients in the original and external validation cohort included for between metastasis concordance analysis

		Cohort		
		Original n=121 (%a)	Validation n=168 (%a)	p-value
Gender	Female	75 (62)	107 (64)	0.72
	Male	46 (38)	60 (36)	
	Missing	0 (0)	1 (1)	
Age at resection CRLM - *(median [IQR])*		63.0 [60.0, 73.0]	63.0 [56.0, 69.0]	0.03
Primary tumour location	Colon	69 (58)	88 (53)	0.44
	Rectum	50 (42)	77 (47)	
	Missing	2 (2)	3 (2)	
T-stage	pT 0-2	29 (24)	26 (16)	0.07
	pT 3-4	91 (76)	140 (84)	
	Missing	1 (1)	2 (1)	
N-stage	N0	43 (36)	56 (34)	0.71
	N+	77 (64)	110 (66)	
	Missing	1 (1)	2 (1)	
Disease-free interval	>1 year	49 (40)	67 (40)	0.98
	≤1 year	72 (60)	99 (60)	
	Missing	0 (0)	2 (1)	
Diameter of largest CRLM	≤5 cm	105 (88)	84 (50)	<0.001
	>5 cm	15 (12)	83 (50)	
	Missing	1 (1)	1 (1)	
Preoperative CEA	≤200 µg/L	108 (92)	151 (90)	0.58
	>200 µg/L	9 (8)	16 (10)	
	Missing	4 (3)	1 (1)	
Histopathological growth pattern	dHGP	18 (15)	22 (13)	0.67
	non-dHGP	103 (85)	146 (87)	

CRLM: colorectal liver metastasis, IQR: interquartile range, CEA: carcinoembryonic antigen and (non-)dHGP: (non-)desmoplastic type histopathological growth pattern.
a Percentages are expressed as proportions across each stratum (i.e. excluding missing). Percentages for missing are expressed as proportion of missing values within each stratum.

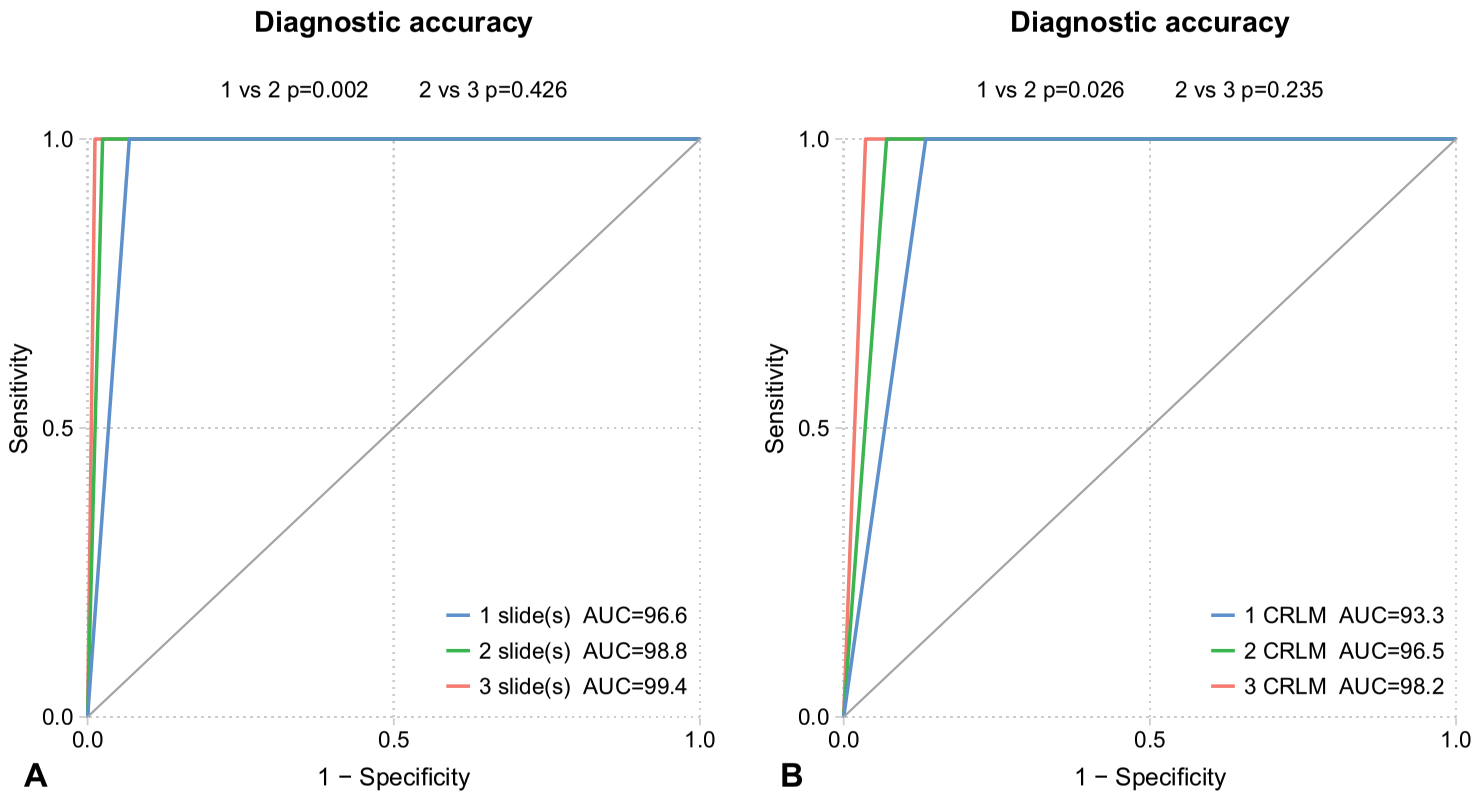

Figure S1. ROC curves for determining metastasis (a) and patient (b) HGP by scoring 1, 2, or 3 block(s)/ resected CRLM, respectively.

II

```r
#------------------------------ KM OS: HGP --------------------------------
#Variable selection
sdat <- AGV
tvar <- sdat$OS
evar <- sdat$Event
gvar <- sdat$HGP
svar <- sdat$Cohort
sdat <- tibble(tvar, evar, gvar, svar)

#Graph text
labs <- c("Desmoplastic", "Non-desmoplastic")
titl <- "Overall survival"
subt <- ""
xlab <- "Time in months"
ylab <- "Survival"

#survival fit
sfit <- survfit(Surv(tvar, evar) ~ gvar, data=sdat)
sdif <- survdiff(Surv(tvar, evar) ~ gvar + strata(svar), data = sdat)
pval <- pchisq(sdif$chisq, df=length(levels(sdat$gvar))-1, lower.tail=FALSE)

km <- ggsurvplot(sfit, data=sdat,
                 palette=c("#00bfc4","#f8766d"),
                 legend=c(0,0),
                 legend.title="",
                 legend.labs=labs,
                 title=titl,
                 xlab=xlab,
                 ylab=ylab,
                 size=0.75,
                 risk.table=TRUE,
                 censor.shape=73,
                 censor.size=2,
                 xlim=c(0,60),
                 break.x.by=12,
                 axes.offset=TRUE,
                 risk.table.title="",
                 risk.table.y.text=FALSE,
                 tables.height=0.2,
                 ggtheme=theme(legend.justification=c(0,0)),
                 tables.theme=theme_cleantable())

km$plot <- km$plot +
  ggplot2::annotate("text", x=60, y=0,
                    label=ifelse(pval<0.001, "p < .001",
                    paste("p = ", sprintf("%.3f", pval))),
                    size = 4.2, hjust=1, vjust=0) +
  ggplot2::annotate("text", x=30, y=1,
                    label=subt,
                    size = 4.2, hjust=0.5, vjust=0)

km$table <- km$table + theme(plot.title=element_blank())

#Save plot
km_OS_AGV <- km
```

Chapter III

Histopathological growth patterns and survival after resection of colorectal liver metastasis: an external validation study

-

JNCI Cancer Spectrum 2021

D.J. Höppener, B. Galjart, P.M.H. Nierop, F.E. Buisman, E.P. van der Stok, R.R.J. Coebergh van den Braak, M.J. van Amerongen, V.P. Balachandran, W.R. Jarnagin, T.P. Kingham, M. Doukas, J. Shia, I.D. Nagtegaal, P.B. Vermeulen, B. Groot Koerkamp, D.J. Grünhagen, J.H.W. de Wilt, M.I. D'Angelica, C. Verhoef.

Abstract

Background: After resection of colorectal cancer liver metastases (CRLM) two main histopathological growth patterns can be observed; a desmoplastic and a non-desmoplastic subtype. The desmoplastic subtype has been associated with superior survival. These findings require external validation.

Methods: A international multicentre retrospective cohort study was conducted in patients treated surgically for CRLM at three tertiary hospitals in the US and the Netherlands. Determination of histopathological growth patterns was performed on H&E-stained sections of resected CRLM according to guidelines. Patients displaying a desmoplastic histopathological phenotype (only desmoplastic growth observed) were compared to patients with a non-desmoplastic phenotype (any non-desmoplastic growth observed). Cut-off analyses on the extent of non-desmoplastic growth were performed. Overall (OS) and disease-free (DFS) survival were estimated using Kaplan-Meier and multivariable Cox analysis.

Results: In total 780 patients were eligible. A desmoplastic phenotype was observed in 19%. Desmoplastic patients had superior 5-year OS (73% versus 44%, $p<0.001$) and DFS (32% versus 15%, $p<0.001$) compared to their non-desmoplastic counterparts. A desmoplastic phenotype was associated with an adjusted hazard ratio for death (95%CI) of 0.36 (0.23-0.58), and 0.50 (0.37-0.66) for cancer recurrence. Cut-off analysis found no prognostic relationship between either OS or DFS and the extent of non-desmoplastic growth observed (all $p>0.1$).

Conclusions: This external validation study confirms the remarkably good prognosis after surgery for CRLM in patients with a desmoplastic phenotype. The extent of non-desmoplastic growth does not impact prognosis.

Introduction

During the course of their disease, up to 30% of patients with colorectal cancer (CRC) present with or develop liver metastases.[1] Surgical removal or ablation of colorectal cancer liver metastases (CRLM) remains the only potentially curative treatment in these patients, resulting in a 5 years overall survival (OS) of 40 to 60 percent.[2]

At pathological examination of CRLM two clinically relevant histopathological subtypes can be observed, namely a desmoplastic histopathological growth pattern (HGP) and a non-desmoplastic HGP. Considerable biological differences between both subtypes have been demonstrated.[3]
The desmoplastic HGP has been associated with increased angiogenic capacity and increased infiltration of cytotoxic T cells, while non-desmoplastic HGP tumours mostly establish vascularisation by means of co-option of pre-existing hepatic sinusoidal vessels. In addition, a reduced infiltration of immune cells and increased cancer motility is observed in these tumours.[4-6]

Over the years the HGP subtypes have gained interest and a potential impact on prognosis and the effectiveness of chemotherapy has been demonstrated.[7,8] The largest patient cohort to date was published by our group, showing substantial differences in 5 years OS outcomes between patients expressing a desmoplastic HGP (78%) and patients expressing any non-desmoplastic HGP (37%).[7] HGPs can easily be assessed on hematoxylin & eosin (H&E) stained tissue sections, and evaluation of HGPs results in low inter- and intra-observer variability.[9] Importantly, centers should be able to assess HGPs with minimal additional costs. In view of their potential clinical implications, HGPs could be an interesting biomarker to further incorporate into the clinical practice of patients with CRLM.

Prior to the implementation of HGPs in the clinic, external validation is required. This study therefore aims to evaluate the prognostic impact of HGPs after resection of CRLM in an international multicentre external validation cohort. Secondly, we sought to validate the optimal cut-off for HGP classification.

Methods

Patient selection and data

Patients who underwent complete surgical treatment for CRLM at either the Erasmus MC Cancer Institute (Rotterdam, the Netherlands), Memorial Sloan Kettering Cancer Center (New York, NY, USA), or Radboud University Medical Center (Nijmegen, the Netherlands) from 2000 till 2019 were potentially eligible for inclusion. Complete surgical treatment was defined as resection (with or without ablation) of all known CRLM and extrahepatic metastases if present. Patients had to have had their primary colorectal malignancy resected as well. Patients receiving adjuvant therapies (systemic chemotherapy and/or hepatic arterial infusion pump (HAIP) chemotherapy) were excluded for two reasons. Firstly, the current study entails an external validation of a previously described cohort which only included patients who did not receive adjuvant therapy.[7] In this external validation study a comparable but independent cohort of patients was selected. Secondly, a recent paper suggested modification of the effect of postoperative systemic chemotherapy by HGP, resulting in a survival benefit for the adjuvantly treated non-desmoplastic patients only.[8] Exclusion of these patients ensures unbiased evaluation of the prognostic effect unaltered by postoperative therapies. Patient demographics, clinicopathological disease characteristics and survival data were extracted from the respective centre’s prospectively maintained databases.

The study adheres to the REMARK guidelines for tumour marker prognostic studies.[10] Institutional ethical review and approval was obtained from the medical ethics committee of the Erasmus University Medical Center Rotterdam (MEC-2018-1743).

Treatment strategy and postoperative course

The Erasmus MC Cancer Institute, Memorial Sloan Kettering Cancer Center, and the Radboud University Medical Center are tertiary referral centers for liver surgery. All patients with suspected CRLM were discussed by a multidisciplinary team of surgical oncologists, medical oncologists, radiation oncologists, and radiologists. Presence of limited extrahepatic disease amenable to local treatment did not preclude complete surgical treatment. Noticeable practice differences between centres exist in use of perioperative chemotherapeutic therapies. HAIP chemotherapy is commonly used at the Memorial Sloan Kettering Cancer Center and is administered frequently in selected patients[11], whereas in the Netherlands HAIP chemotherapy is only administered within the context of randomised controlled clinical trials.[12,13] Moreover, perioperative systemic chemotherapy is considered standard of care throughout the United States. In the Netherlands, guidelines advocate to only administer preoperative chemotherapy to increase resectability in patients with unresectable disease, or to facilitate a parenchymal sparing approach. Postoperative systemic chemotherapy is not advocated. Practice variation regarding perioperative systemic chemotherapy does however exist in the Netherlands.[14]

Postoperative surveillance in all three centres consists of outpatient visits, serial blood serum carcinoembryonic antigen (CEA) assessments and medical imaging by computed tomography and/or magnetic resonance imaging.

Postoperative surveillance is generally scheduled every three to six months for the duration of five years, or longer at the patients' discretion. In the case of recurrent disease, optimal treatment strategy is again determined by each centre's multidisciplinary team.

Pathological assessment

Pathological assessment of HGP was performed retrospectively on H&E sections by at least two trained observers simultaneously and blinded for patient characteristics and outcome. Dedicated liver pathologists were consulted when necessary. All available H&E tissue sections of all resected CRLM of each individual patient were assessed for HGP phenotype by light microscopy or digital evaluation of digitalised sections.

In accordance with international consensus guidelines, the tumour-liver interface was evaluated for pathological phenotype. The three previously described HGP phenotypes are discussed in depth in these guidelines.[15] In summation, the desmoplastic phenotype is characterised by separation of tumour and liver parenchyma by a band of desmoplastic stroma (*figure 1A*). This band of desmoplastic stroma separating cancer cells from the liver parenchyma is absent in the non-desmoplastic phenotypes (*figure 1B*). As multiple phenotypes can appear in conjunction, the relative proportion of each phenotype is estimated on each H&E section and expressed as percentage. The final patient-level score is the average of each metastasis with equal weights assigned to discrete metastases and to individual slides within metastases. There is no minimum section requirement for HGP assessment. Sections are considered unsuitable if only a small fraction of the tumour-liver interface (less than 20%) is assessable, if tissue preservation quality is deemed unsuitable (e.g. tear of tissue at the transition zone) or when viable tumour

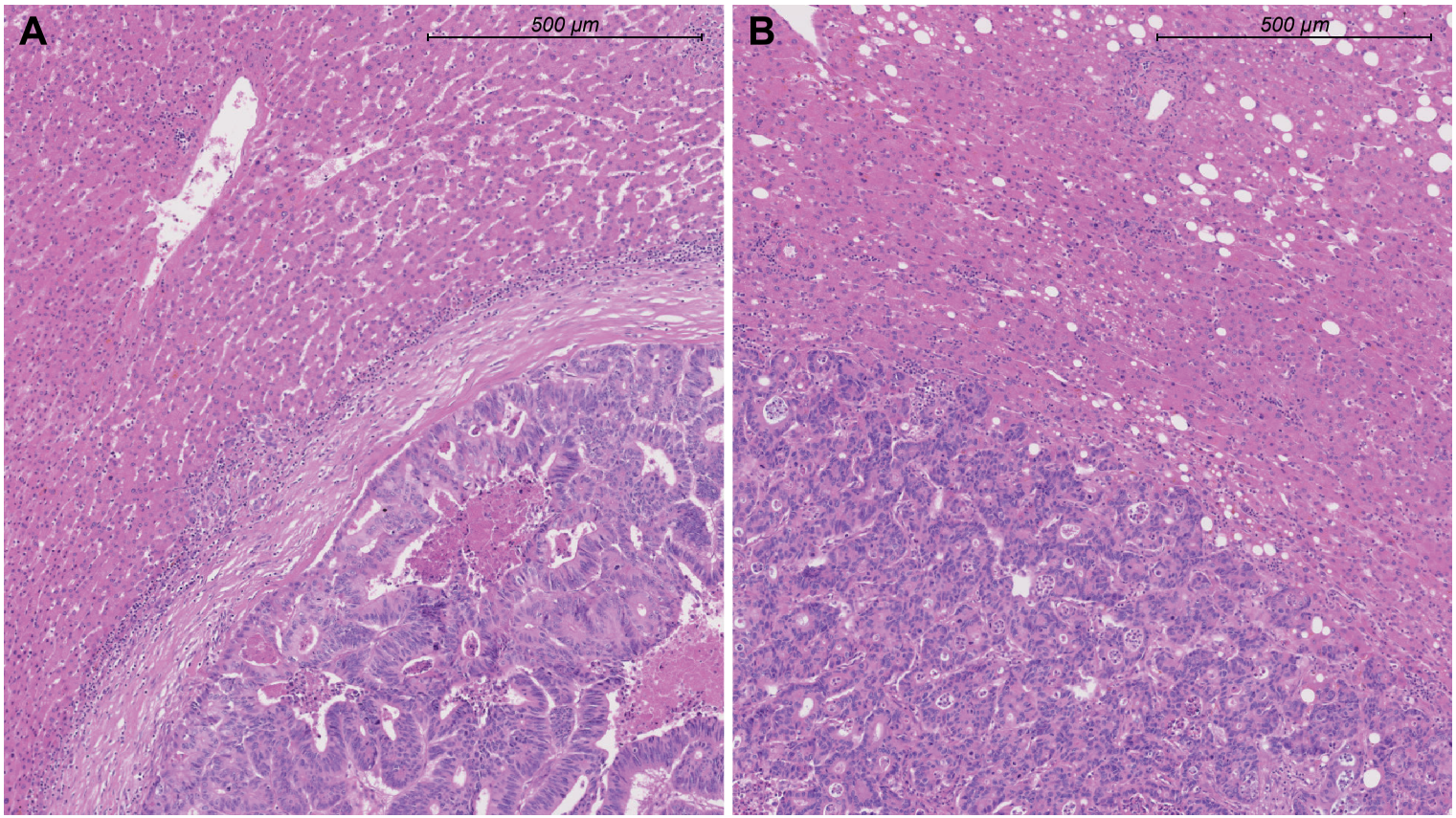

Figure 1. Hematoxylin & eosin stained tissue sections of resected CRLM viewed at 5 times magnification displaying a desmoplastic (A) and a non-desmoplastic (B) phenotype.

III

tissue is absent (i.e. complete pathological response). Patients were classified as desmoplastic if all slides of all resected CRLM uniformly displayed a desmoplastic phenotype (i.e. 100% desmoplastic, *figure 1a*), and as non-desmoplastic if any non-desmoplastic phenotype was observed in any slide of any resected CRLM (i.e. <100% desmoplastic, *figure 1B*). [7] For cut-off analyses patients were classified in subgroups according to the extent of non-desmoplastic phenotypes observed: 100% desmoplastic versus 0.1-33%, 33.1-67% and 67.1-100% non-desmoplastic, respectively.

Outcomes

Overall (OS) and disease-free survival (DFS) were evaluated. OS was defined as time from surgical resection to death. DFS was defined as the time from surgical resection to cancer recurrence or death, whichever came first. Patients were censored if alive with no evidence of disease. Outcomes were additionally evaluated stratified for preoperative chemotherapy status.

Statistical analyses

Categorical data are reported as absolute count with corresponding percentage. Non-parametric continuous data are reported as median with corresponding interquartile range (IQR). Differences in proportions were evaluated by means of the Chi-squared test. Medians were compared by the Kruskall-Wallis test. Survival curves were estimated according to Kaplan-Meier analysis and compared by means of the log-rank test. Five year survival estimates with corresponding 95% confidence interval (CI) are reported. Median follow-up for survivors was determined using the reverse Kaplan-Meier method. Uni- and multivariable Cox proportional hazards regression survival analyses were performed and reported as hazard ratios (HR) with corresponding 95% CI. All known clinicopathological risk factors were added to the

regression models. With regards to missing data, full case analyses were performed. The proportional hazards assumption was visually assessed by plotting Schoenfeld residuals and Kaplan-Meier curves. Since data on KRAS and BRAF mutational status was only available for less than half of the patients, separate Cox regression models were computed with additional correction for these genetic risk factors. Cox regression models with interaction terms were created to evaluate effect modification of HGP by preoperative chemotherapy.[7] All log-rank tests and Cox regression analyses were performed with centre as stratification factor. The statistical significance level was set at an α of 0.05. All statistical analyses were performed using the R Project for Statistical Computing version 4.0.3 (https://www.r-project.org/) with the packages ggplot2 (v3.3.2), rms (6.0-1), survival (v3.2-7), survminer (v0.4.8), and tableone (v0.12.0).

Results

Between 2000 and 2019 a total of 2.708 consecutive patients underwent resection of CRLM at either the Erasmus MC Cancer Institute (n=1.044), Memorial Sloan Kettering Cancer Center (n=1.352) or Radboud University Medical Center (n=312) and had resection specimens suitable for pathological HGP assessment. Of these, 732 patients treated at the Erasmus MC Cancer Institute are described in our previous paper[7], 582 received perioperative HAIP chemotherapy, 446 were treated with postoperative systemic chemotherapy, and 168 did not undergo complete surgical treatment, resulting in a total of 780 patients included in the current external validation study. Baseline characteristics stratified by centre are reported in *supplementary table 1*. A total of 213 patients were treated at the Erasmus MC Cancer Institute, 338 at the Memorial Sloan Kettering Cancer Center, and 229 at the Radboud University Medical Center.

Of the 213 newly described patients treated at the Erasmus MC Cancer Institute, 163 (76%) underwent surgery outside (i.e. after march 2015) the inclusion period of the previous study, 10 (5%) were additionally identified through data requests at the IT department, and for the remaining 40 (19%) H&E resection specimens were previously missing but have since been recovered.[7] Primary tumour and CRLM clinicopathological characteristics were comparable between centres, with the exception of the number of CRLM, presence of extrahepatic disease, and the disease-free interval between primary tumour resection and CRLM detection, all being more favourable in patients treated at the Radboud University Medical Center (*supplementary table 1*).

A desmoplastic histopathological phenotype was observed in 149 (19%) patients and was equally distributed across centres (*table 1*). About half (n=373, 48%, *table 1*) of all patients were treated with preoperative systemic chemotherapy, although this did differ between treatment centres (*supplementary table 1*). A desmoplastic phenotype was more often found in the pre-treated subpopulation: 23% (n=85/373) versus 16% (n=64/407) (p=0.01). Patients with a non-desmoplastic phenotype had slightly larger CRLM (median 3.0 cm versus 2.2 cm, p<0.001), a longer disease-free interval (median 2 vs 0 months, p=0.03), higher preoperative serum CEA levels (median 11.2 versus 5.3 µg/L, p<0.001), and more often had extrahepatic disease (12% versus 6%, p=0.04) (*table 1*). Data on KRAS, BRAF, and microsatellite stability status was available for 42%, 37%, and 23% of patients. The mutation rate of KRAS (50% versus 43%, p=0.33) and BRAF (4% versus 3%, p=0.82) did not differ between patients with a desmoplastic and a non-desmoplastic phenotype, respectively (*table 1*). Microsatellite instability (MSI) was more often seen in the desmoplastic phenotype (15% versus 4%, p=0.01, *table 1*).

Overall and disease-free survival

The median follow-up for survivors was 42 months (IQR: 21-66 months). During follow-up 501 (64%) patients experienced recurrence and 294 (38%) died. Patients with a desmoplastic phenotype had significantly longer OS compared to their non-desmoplastic counterparts, with 5-year (95%CI) OS estimates of 73% (64-84%) for desmoplastic versus 44% (39-50%) for non-desmoplastic (*figure 2A*, p<0.001). Similar differences were observed for DFS, with 5-year (95%CI) estimates of

Table 1. Baseline characteristics stratified by histopathological phenotype

		Missing (%)	Desmoplastic n = 149 (%)	Non-desmoplastic n = 631 (%)	p-value
Treatment centre	Erasmus MC		45 (30)	168 (27)	0.66
	MSKCC		63 (42)	275 (44)	
	Radboud UMC		41 (28)	188 (30)	
Age at resection - *(median [IQR])*			65 [52, 72]	65 [56, 72]	0.31
Gender	Male		92 (62)	374 (59)	0.58
	Female		57 (38)	257 (41)	
ASA classification	ASA I-II	*4 (1)*	87 (59)	377 (60)	0.87
	ASA >II		60 (41)	252 (40)	
Primary tumour location	Left-sided	*24 (3)*	49 (35)	254 (41)	0.35
	Right-sided		41 (29)	166 (27)	
	Rectal		51 (36)	195 (32)	
T-stage	pT 0-2	*56 (7)*	21 (16)	76 (13)	0.39
	pT 3-4		113 (84)	514 (87)	
N-stage	N0	*10 (1)*	64 (44)	220 (35)	0.06
	N+		83 (56)	403 (65)	
Number of CRLM - *(median [IQR])*		*2 (0)*	2.0 [1.0, 3.0]	2.0 [1.0, 3.0]	0.12
Largest CRLM in cm - *(median [IQR])*		*3 (0)*	2.2 [1.3, 3.3]	3.0 [2.0, 4.6]	<0.001
DFI in months* - *(median [IQR])*		*11 (1)*	0.0 [0.0, 11.8]	2.0 [0.0, 16.0]	0.03
Preop. CEA in µg/L - *(median [IQR])*		*65 (8)*	5.3 [2.7, 16.4]	11.2 [4.2, 32.5]	<0.001
Neoadjuvant chemotherapy	No		64 (43)	343 (54)	0.01
	Yes		85 (57)	288 (46)	
Resection margin involved	No	*1 (0)*	136 (91)	541 (86)	0.08
	Yes		13 (9)	89 (14)	
Extrahepatic disease	No		140 (94)	556 (88)	0.04
	Yes		9 (6)	75 (12)	
KRAS mutational status	Wildtype	*450 (58)*	29 (50)	155 (57)	0.33
	Mutant		29 (50)	117 (43)	
BRAF mutational status	Wildtype	*491 (63)*	48 (96)	231 (97)	0.82
	Mutant		2 (4)	8 (3)	
MSI status	MSS	*600 (77)*	35 (85)	134 (96)	0.01
	MSI		6 (15)	5 (4)	

*Between resection of primary tumour and detection of CRLM
Abbreviations in alphabetical order: ASA: American Society of Anesthesiologists; CEA: carcinoembryonic antigen; CRLM: colorectal liver metastasis; DFI: disease-free interval; Erasmus MC: Erasmus MC Cancer Institute; IQR: interquartile range; MSI: microsatellite instable; MSKCC: Memorial Sloan Kettering Cancer Center; MSS: microsatellite stable; Radboud UMC: Radboud University Medical Center.

32% (23-45%) for desmoplastic versus 15% (12-19%) for non-desmoplastic (*figure 2B*, p<0.001). The overall recurrence rate was significantly lower for the patients with a desmoplastic HGP (46% versus 69%, p<0.001). In the full case multivariable analysis of 625 (80%) patients, a desmoplastic phenotype resulted in an adjusted HR (95%CI) of 0.36 (0.23-0.58) for OS and 0.50 (0.37-0.66) for DFS (*tables 2A&B*).

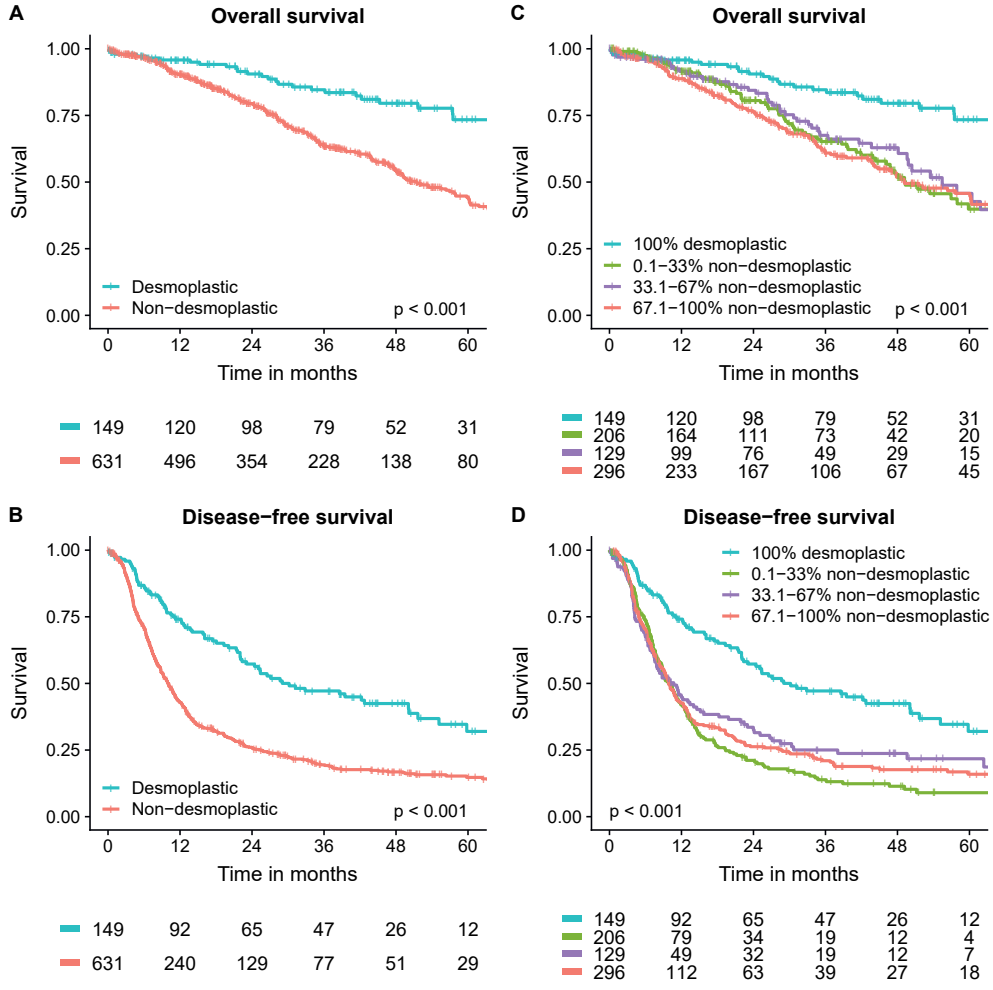

Figure 2. A&B: Kaplan-Meier overall (A) and disease-free (B) survival estimates of patients with a desmoplastic versus a non-desmoplastic phenotype. C&D: Kaplan-Meier overall (C) and disease-free (D) survival estimates according to the extent of non-desmoplastic growth.

Table 2. Uni- and multivariable Cox regression analyses for overall (A) and disease-free survival (B)

	Table 2A. Overall survival						Table 2B. Disease-free survival					
	Univariable			Multivariable (n=625)			Univariable			Multivariable (n=625)		
	HR	[95%CI]	p-value	HR	[95%CI]	p-value	HR	[95%CI]	p-value	HR	[95%CI]	p-value
Age at resection (cont.) - *years*	1.01	[1.00-1.02]	0.01	1.01	[1.00-1.02]	0.13	1.00	[0.99-1.00]	0.34	1.00	[0.99-1.01]	0.95
ASA classification - *>II vs I-II*	1.26	[0.94-1.71]	0.13	1.29	[0.90-1.87]	0.17	1.14	[0.91-1.41]	0.25	1.22	[0.95-1.57]	0.12
Right-sided primary - *yes vs no*	1.46	[1.13-1.88]	0.004	1.36	[1.00-1.86]	0.05	1.05	[0.86-1.27]	0.65	1.03	[0.82-1.29]	0.81
T-stage - *pT3-4 vs pT0-2*	1.36	[0.92-2.00]	0.12	1.28	[0.82-2.01]	0.28	1.24	[0.95-1.61]	0.11	1.09	[0.81-1.46]	0.57
N-stage - *N+ vs N0*	1.18	[0.93-1.51]	0.18	1.23	[0.91-1.66]	0.18	1.29	[1.08-1.55]	0.005	1.24	[1.01-1.53]	0.04
DFI* (cont.) - *months*	1.00	[0.99-1.01]	0.65	1.00	[0.99-1.01]	0.67	0.99	[0.99-1.00]	0.01	0.99	[0.98-1.00]	0.01
Number of CRLM (cont.)	1.10	[1.06-1.15]	<0.001	1.09	[1.04-1.14]	<0.001	1.11	[1.08-1.15]	<0.001	1.08	[1.04-1.12]	<0.001
Largest CRLM (cont.) - *cm*	1.06	[1.03-1.10]	<0.001	1.06	[1.02-1.11]	0.006	1.06	[1.03-1.09]	<0.001	1.05	[1.01-1.09]	0.009
Preoperative CEA (cont.) - *100 µg/L*	1.01	[1.00-1.02]	0.006	1.01	[1.00-1.02]	0.03	1.01	[1.00-1.02]	0.09	1.01	[1.00-1.02]	0.24
Resection margin - *R1 vs R0*	1.83	[1.36-2.47]	<0.001	1.22	[0.84-1.76]	0.30	1.84	[1.47-2.31]	<0.001	1.46	[1.11-1.92]	0.007
Extrahepatic disease - *yes vs no*	1.63	[1.15-2.29]	0.005	1.59	[1.05-2.41]	0.03	1.85	[1.44-2.38]	<0.001	2.21	[1.64-2.98]	<0.001
Neoadjuvant chemotherapy - *yes vs no*	1.25	[0.96-1.62]	0.10	1.26	[0.93-1.71]	0.13	1.45	[1.20-1.74]	<0.001	1.26	[1.01-1.56]	0.04
Desmoplastic phenotype - *yes vs no*	0.39	[0.27-0.56]	<0.001	0.36	[0.23-0.58]	<0.001	0.44	[0.35-0.56]	<0.001	0.50	[0.37-0.66]	<0.001

*Between resection of primary tumour and detection of CRLM

Abbreviations in alphabetical order: ASA: American Society of Anesthesiologists; Cont.: entered as continuous variable; CEA: carcinoembryonic antigen; CRLM: colorectal liver metastasis; DFI: disease-free interval.

Considering KRAS and BRAF mutation status, 227 (29%) full cases were available for multivariable analysis and a desmoplastic phenotype remained independently (adjusted HR [95%CI]) associated with both OS (0.43 [0.20-0.92]) and DFS (0.42 [0.25-0.70]) (*tables 3A*&*B*).

When evaluating the optimal cut-off for HGP determination, no statistically significant differences in either OS or DFS were observed between patients with a 0.1-33%, 33.1-67% and 67.1-100% relative presence of non-desmoplastic HGP (all p>0.1). Patients with a desmoplastic phenotype displayed superior survival compared to all other subgroups (all p<0.001, *figures 2C*&*D*). For both OS and DFS similar results were obtained in multivariable analysis (n=625 full cases, all p<0.01, *supplementary tables 2A*&*B*).

Table 3. Uni- and multivariable Cox regression analyses for overall (A) and disease-free survival (B) including KRAS and BRAF status

	Table 3A. Overall survival					Table 3B. Disease-free survival				
	Univariable		Multivariable (n=227)			Univariable		Multivariable (n=227)		
	HR [95%CI]	p-value	HR [95%CI]	p-value		HR [95%CI]	p-value	HR [95%CI]	p-value	
Age at resection (cont.) - *years*	1.01 [1.00-1.02]	0.01	1.02 [1.00-1.04]	0.05		1.00 [0.99-1.00]	0.34	1.00 [0.99-1.01]	0.99	
ASA classification - *>II vs I-II*	1.26 [0.94-1.71]	0.13	0.91 [0.52-1.61]	0.75		1.14 [0.91-1.41]	0.25	1.02 [0.71-1.48]	0.91	
Right-sided primary - *yes vs no*	1.46 [1.13-1.88]	0.004	1.01 [0.59-1.71]	0.98		1.05 [0.86-1.27]	0.65	0.83 [0.58-1.19]	0.32	
T-stage - *pT3-4 vs pT0-2*	1.36 [0.92-2.00]	0.12	1.74 [0.73-4.11]	0.21		1.24 [0.95-1.61]	0.11	1.48 [0.86-2.56]	0.16	
N-stage - *N+ vs N0*	1.18 [0.93-1.51]	0.18	0.98 [0.58-1.66]	0.95		1.29 [1.08-1.55]	0.005	1.15 [0.80-1.67]	0.45	
DFI* (cont.) - *months*	1.00 [0.99-1.01]	0.65	0.97 [0.95-0.99]	0.003		0.99 [0.99-1.00]	0.01	0.99 [0.97-1.00]	0.01	
Number of CRLM (cont.)	1.10 [1.06-1.15]	<0.001	1.03 [0.95-1.11]	0.46		1.11 [1.08-1.15]	<0.001	1.06 [1.00-1.12]	0.04	
Largest CRLM (cont.) - *cm*	1.06 [1.03-1.10]	<0.001	1.02 [0.94-1.11]	0.56		1.06 [1.03-1.09]	<0.001	0.99 [0.93-1.06]	0.81	
Preoperative CEA (cont.) - *100 µg/L*	1.01 [1.00-1.02]	0.006	0.95 [0.83-1.10]	0.53		1.01 [1.00-1.02]	0.09	1.02 [0.91-1.15]	0.71	
Resection margin - *R1 vs R0*	1.83 [1.36-2.47]	<0.001	1.87 [1.01-3.47]	0.05		1.84 [1.47-2.31]	<0.001	1.63 [1.07-2.46]	0.02	
Extrahepatic disease - *yes vs no*	1.63 [1.15-2.29]	0.005	1.49 [0.81-2.76]	0.20		1.85 [1.44-2.38]	<0.001	2.16 [1.41-3.29]	<0.001	
Neoadjuvant chemotherapy - *yes vs no*	1.25 [0.96-1.62]	0.10	1.44 [0.82-2.51]	0.20		1.45 [1.20-1.74]	<0.001	0.98 [0.68-1.41]	0.91	
KRAS status - *mutant vs wildtype*	1.55 [1.11-2.18]	0.01	2.21 [1.33-3.65]	0.002		1.33 [1.04-1.70]	0.03	1.43 [1.03-1.98]	0.03	
BRAF status - *mutant vs wildtype*	1.59 [0.58-4.37]	0.37	3.42 [1.00-11.71]	0.05		1.08 [0.53-2.23]	0.83	1.03 [0.39-2.72]	0.95	
Desmoplastic phenotype - *yes vs no*	0.39 [0.27-0.56]	<0.001	0.43 [0.20-0.92]	0.03		0.44 [0.35-0.56]	<0.001	0.42 [0.25-0.70]	<0.001	

*Between resection of primary tumour and detection of CRLM

Abbreviations in alphabetical order: ASA: American Society of Anesthesiologists; Cont.: entered as continuous variable; CEA: carcinoembryonic antigen; CRLM: colorectal liver metastasis; DFI: disease-free interval.

Effect of preoperative chemotherapy

No significant interaction between preoperative chemotherapy and HGP was observed (OS p=0.61, DFS p=0.64). OS and DFS differed significantly between desmoplastic and non-desmoplastic HGP patients in both the chemo-naive and pre-treated subpopulations.

In chemo-naive patients the 5-year (95%CI) OS estimate for a desmoplastic phenotype was 82% (69-97%) compared to 52% (44-60%) for a non-desmoplastic phenotype (*figure 3A*, p<0.001). Again, similar differences were observed for DFS, with 5-year (95%CI) DFS estimates of 36% (23-59%) for desmoplastic versus 20% (15-26%) for non-desmoplastic (*figure 3B*, p<0.001). For pre-treated patients

the 5-year (95%CI) OS for a desmoplastic phenotype was 67% (55-82%) compared to 37% (30-46%) for a non-desmoplastic phenotype (*figure 3C*, p<0.001). Subsequently, the 5-year (95%CI) DFS was 29% (18-46%) for pre-treated desmoplastic versus 9% (6-13%) for pre-treated non-desmoplastic (*figure 3D*, p<0.001). After correction for potential confounding, a desmoplastic phenotype was associated with superior survival outcomes in both the chemonaive (n=352 full cases, adjusted

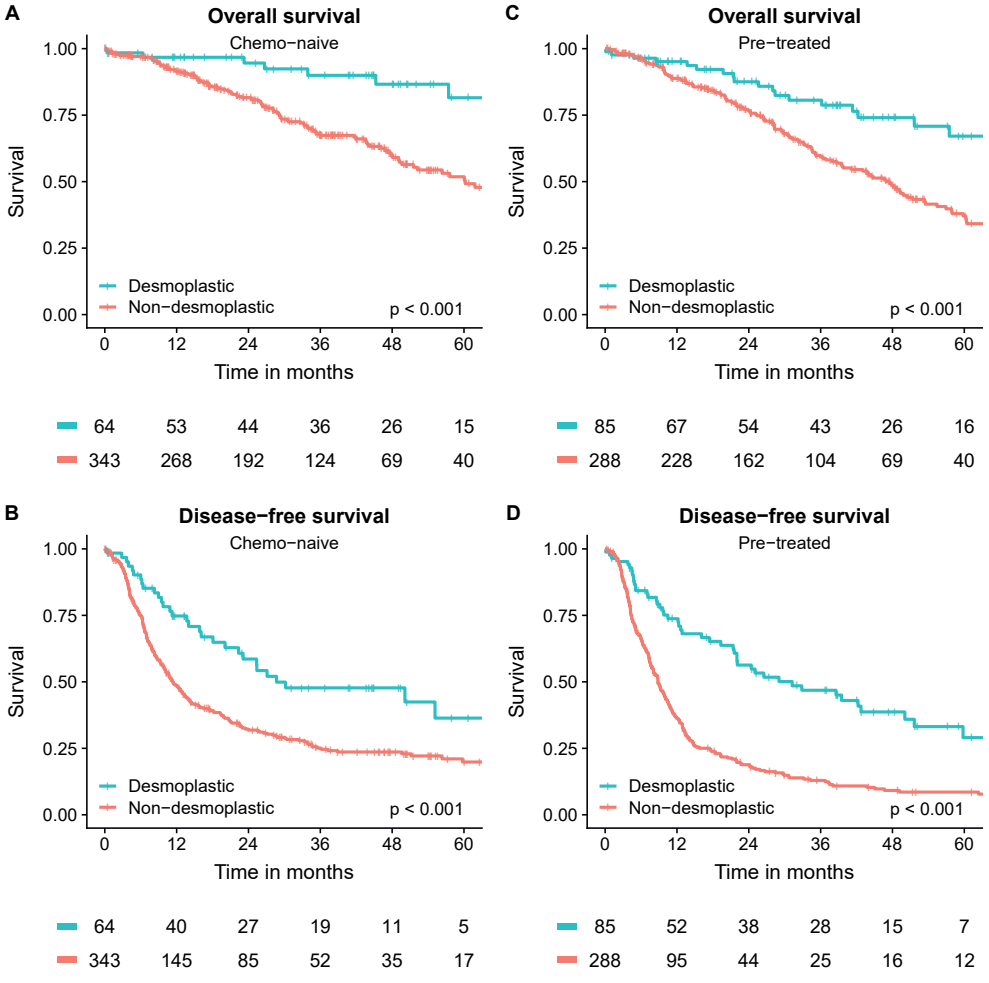

Figure 3. Kaplan-Meier overall (A&C) and disease-free (B&D) survival estimates for chemo-naive (A&B) and pre-treated (C&D) patients with a desmoplastic versus a non-desmoplastic phenotype.

HR [95%CI] OS 0.29 [0.13-0.65]; DFS 0.53 [0.34-0.82], *supplementary tables 3A&B*) and pre-treated subpopulations (n=273 full cases, adjusted HR [95%CI] OS 0.43 [0.23-0.79]; DFS 0.43 [0.29-0.64], *supplementary tables 3C&D*).

Discussion

In this study, we present the results of an international multicentre external validation study on the prognostic value of HGPs after complete surgical treatment of CRLM. A desmoplastic phenotype was independently associated with superior OS and DFS outcomes in both chemo-naive and pre-treated patients. As the extent of HGP phenotypes observed can vary both within the same tumour, as well as across multiple tumours in the same patient, external validation of the optimal cut-off for classification was also performed. In line with previous reports this external validation study confirms that it is the presence of any non-desmoplastic phenotype, rather than the relative quantity, that drives prognosis.

The first report of HGPs in CRLM was published in 1991 by Morino et al.[16], and since then several reports have followed.[15,17] Due to heterogeneity in histopathological assessment, cut-offs, and terminology, formal meta-analysis of the available data is not possible, but most studies demonstrate favourable outcomes in patients with a predominant desmoplastic phenotype.[17] The largest study to date was published by our group and reported a 5-years OS of 78% in chemo-naive patients with a desmoplastic HGP.[7] In the present study we observed a 5 year OS of 73% in all patients with a desmoplastic phenotype, and a comparable 5-year OS of 82% within the chemo-naive subpopulation. In line with these results, lower recurrence rates and superior DFS were seen in patients with a desmoplastic phenotype,

reflecting the remarkably good cancer-related outcomes in these patients with metastatic CRC. In addition our study is the first to investigate association and prognosis of HGPs in light of KRAS and BRAF mutational status. Although data on these genetic risk factors was only available for approximately 40% of patients, no association between the histopathological phenotype and mutations in either of these genes was observed, and after correction for these genetic risk factors a desmoplastic phenotype was still independently associated with good overall and cancer-free survival.

In order to standardise assessment of HGPs, international consensus guidelines have been established.[15] In these guidelines classification of HGP is based on predominance, with an advocated cut-off value of 50%. Both our previous paper and the current external validation study – which represent the two largest studies to date – demonstrate that predominance of a distinct HGP is irrelevant. Superior survival outcomes were only observed in patients with a uniform desmoplastic phenotype. In the patients with any observed non-desmoplastic growth, the extent of this observation does not seem to bear any prognostic consequences. We therefore deem reappraisal of the current guidelines for HGP assessment necessary; classification of HGPs in CRLM should be based on the presence or absence of non-desmoplastic growth.

Besides implications for HGP assessment and postoperative prognosis, this observation is also interesting from a cancer biology perspective as it suggests that HGPs can be regarded as a binary biological switch. While this paper does not provide a clear indication for the actual underlying process, in the 23% of patients with available data we did observe a significant association between MSI and a desmoplastic phenotype. Because of their genetic hypermutability MSI

tumours express more mutational neoantigens which can become targets for T cells.[18,19] The more potential immune targets are present, the more likely an effective antitumour response can be elicited.[19] This is why MSI tumours are thought to form metastases less often and why MSI represents the only indication for systemic immunotherapy in metastatic CRC so far.[20,21] Since MSI tumours only accounted for 15% of patients with a desmoplastic phenotype in our study, a desmoplastic HGP could reflect more a state of (hepatic) anticancer immunity. This is supported by several other studies which demonstrate that a desmoplastic phenotype was associated with an enrichment of immune cells in the tumour microenvironment, specifically CD8+ T cells.[5,6] One could therefore hypothesise that a non-desmoplastic histopathological phenotype, observed in however small a quantity, may be a reflection of the tumour's intrinsic or obtained ability to evade the anticancer immune response. Our study is however at serious risk of selection bias regarding availability of MSI status and validation should therefore be pursued, as well as research into the other biological and immunological aspects of these histopathological phenotypes.

Preoperative chemotherapy was administered in approximately half of the patients in this validation cohort. It has been suggested that response to chemotherapy might induce misclassification of HGP type, which could limit the applicability of HGPs in patients receiving preoperative chemotherapy.[7] In our previous study, no significant impact of HGPs in pre-treated patients was found in multivariable OS analysis. Although this study also found a diminished adjusted HR for OS in pre-treated patients, a desmoplastic phenotype remained associated with superior survival after correction for confounders. The results of this external validation study are promising to increase the applicability of this biomarker, as administration of preoperative

chemotherapy is standard of care in many countries.

Many reports evaluating HGPs are now available, most of which demonstrate relevant prognostic and clinical implications.[6,7,9,15,17,22-30] In addition, the effect of HGPs on survival (adjusted HR 0.36) is considerable, underlining its importance. We therefore feel that application in clinical practice should be pursued. An important step would be incorporation of the desmoplastic and non-desmoplastic phenotypes in the standard pathological report after resection of CRLM. This can be done on standard H&E slides with excellent intra-observer agreement[9], limited resources, and minimal additional time or medical costs required. If included, this prognostic information becomes readily available for clinicians and could be incorporated in individual counseling of patients. Herein a desmoplastic phenotype could be considered a marker for good prospects regarding survivorship. In addition, efforts should be made to determine whether the effectiveness of postoperative chemotherapy can be predicted by the HGP phenotype. Buisman et al. showed no benefit of postoperative chemotherapy in patients with a desmoplastic HGP, but validation of these results is needed.[8] Being a postoperative pathology-based biomarker, the impact on preoperative decision making is absent for now. Cheng et al. showed that preoperative assessment of HGPs can however be done on imaging with an area under curve of over 0.9.[31] When validated and optimised for use in clinical practice, HGPs could also be assessed and used in preoperative medical decision making.

This study presents the largest cohort investigating the prognostic impact of HGPs after resection of CRLM currently available and validates findings from previous studies. Nevertheless, the study has its limitations which are mostly related to its retrospective nature. An important

limitation also remains the limited data on established genetic risk factors, since KRAS and BRAF mutation status were only available for less than half of patients.[32] Many of the patients in the current study were treated before the introduction of standard molecular testing, and in earlier years mutation status was only determined in patients with disease recurrence for choice of palliative systemic chemotherapy regimens, underscoring the risk of selection bias. Nevertheless, in those patients with data on KRAS and BRAF no association or impact on prognosis was seen. In addition, correction for sidedness of the primary tumour, which can be considered a weak proxy for mutational status[33-37], also did not diminish the prognostic value of a desmoplastic phenotype. Similar risk for selection bias exists regarding MSI status, which we found to be associated with a desmoplastic phenotype. While our study therefore does assess HGPs in light of KRAS, BRAF, and MSI status, in-depth genetic association studies on these histopathological phenotypes are needed to limit potential bias, confirm our findings, and also to investigate other CRC driver genes.

In conclusion, this study validates the prognostic impact of a desmoplastic phenotype in a large international multicentre cohort of surgically treated CRLM patients. We were able to confirm that patients with a desmoplastic phenotype have superior survival outcomes when compared to patients with any observed non-desmoplastic phenotype. The extent of non-desmoplastic growth does not impact prognosis. These data show that histopathological growth patterns harbour important prognostic value, warranting implementation in clinical practice.

References

1. Manfredi S, Lepage C, Hatem C, Coatmeur O, Faivre J, Bouvier AM. Epidemiology and management of liver metastases from colorectal cancer. *Ann Surg.* Aug 2006;244(2):254-259.
2. Kanas GP, Taylor A, Primrose JN, et al. Survival after liver resection in metastatic colorectal cancer: review and meta-analysis of prognostic factors. *Clin Epidemiol.* 2012;4:283-301.
3. Vermeulen PB, Colpaert C, Salgado R, et al. Liver metastases from colorectal adenocarcinomas grow in three patterns with different angiogenesis and desmoplasia. *J Pathol.* Oct 2001;195(3):336-342.
4. Frentzas S, Simoneau E, Bridgeman VL, et al. Vessel co-option mediates resistance to anti-angiogenic therapy in liver metastases. *Nat Med.* Nov 2016;22(11):1294-1302.
5. Hoppener DJ, Nierop PMH, Hof J, et al. Enrichment of the tumour immune microenvironment in patients with desmoplastic colorectal liver metastasis. *Br J Cancer.* Jul 2020;123(2):196-206.
6. Brunner SM, Kesselring R, Rubner C, et al. Prognosis according to histochemical analysis of liver metastases removed at liver resection. *Br J Surg.* Dec 2014;101(13):1681-1691.
7. Galjart B, Nierop PMH, van der Stok EP, et al. Angiogenic desmoplastic histopathological growth pattern as a prognostic marker of good outcome in patients with colorectal liver metastases. *Angiogenesis.* May 2019;22(2):355-368.
8. Buisman FE, Van der Stok EP, Galjart B, et al. Histopathological growth patterns as biomarker for adjuvant systemic chemotherapy in patients with resected colorectal liver metastases. *Clin Exp Metastasis.* 2020.
9. Hoppener DJ, Nierop PMH, Herpel E, et al. Histopathological growth patterns of colorectal liver metastasis exhibit little heterogeneity and can be determined with a high diagnostic accuracy. *Clin Exp Metastasis.* Aug 2019;36(4):311-319.
10. Sauerbrei W, Taube SE, McShane LM, Cavenagh MM, Altman DG. Reporting Recommendations for Tumor Marker Prognostic Studies (REMARK): An Abridged Explanation and Elaboration. *J Natl Cancer Inst.* Aug 1 2018;110(8):803-811.
11. Groot Koerkamp B, Sadot E, Kemeny NE, et al. Perioperative Hepatic Arterial Infusion Pump Chemotherapy Is Associated With Longer Survival After Resection of Colorectal Liver Metastases: A Propensity Score Analysis. *J Clin Oncol.* Jun 10 2017;35(17):1938-1944.
12. Buisman FE, Homs MYV, Grünhagen DJ, et al. Adjuvant hepatic arterial infusion pump chemotherapy and resection versus resection alone in patients with low-risk resectable colorectal liver metastases - the multicenter randomized controlled PUMP trial. *BMC Cancer.* Apr 5 2019;19(1):327.
13. Buisman FE, Grünhagen DJ, Homs MYV, et al. Adjuvant Hepatic Arterial Infusion Pump Chemotherapy After Resection of Colorectal Liver Metastases: Results of a Safety and Feasibility Study in The Netherlands. *Ann Surg Oncol.* Dec 2019;26(13):4599-4607.
14. Elfrink AKE, Kok NFM, van der Werf LR, et al. Population-based study on practice variation regarding preoperative systemic chemotherapy in patients with colorectal liver metastases and impact on short-term outcomes. *Eur J Surg Oncol.* Apr 5 2020.
15. van Dam PJ, van der Stok EP, Teuwen LA, et al. International consensus guidelines for scoring the histopathological growth patterns of liver metastasis. *Br J Cancer.* Nov 7 2017;117(10):1427-1441.
16. Morino T, Tanaka J, Tobe T. Clinico-pathological features of liver metastases from colorectal cancer in relation to prognosis. *Nihon Geka Hokan.* May 1 1991;60(3):154-164.
17. Fernandez Moro C, Bozoky B, Gerling M. Growth patterns of colorectal cancer liver metastases and their impact on prognosis: a systematic review. *BMJ Open Gastroenterol.* 2018;5(1):e000217.
18. Boland CR, Goel A. Microsatellite instability in colorectal cancer. *Gastroenterology.* Jun 2010;138(6):2073-2087 e2073.
19. Chen DS, Mellman I. Elements of cancer immunity and the cancer–immune set point. *Nature.* 2017/01/01 2017;541(7637):321-330.
20. Buckowitz A, Knaebel HP, Benner A, et al. Microsatellite instability in colorectal cancer is associated with local lymphocyte infiltration and low

frequency of distant metastases. *Br J Cancer.* May 9 2005;92(9):1746-1753.
21. André T, Shiu K-K, Kim TW, et al. Pembrolizumab in Microsatellite-Instability-High Advanced Colorectal Cancer. *New England Journal of Medicine.* 2020/12/03 2020;383(23):2207-2218.
22. Eefsen RL, Van den Eynden GG, Hoyer-Hansen G, et al. Histopathological growth pattern, proteolysis and angiogenesis in chemonaive patients resected for multiple colorectal liver metastases. *J Oncol.* 2012;2012:907971.
23. Eefsen RL, Vermeulen PB, Christensen IJ, et al. Growth pattern of colorectal liver metastasis as a marker of recurrence risk. *Clin Exp Metastasis.* Apr 2015;32(4):369-381.
24. Nielsen K, Rolff HC, Eefsen RL, Vainer B. The morphological growth patterns of colorectal liver metastases are prognostic for overall survival. *Mod Pathol.* Dec 2014;27(12):1641-1648.
25. Nierop PMH, Galjart B, Hoppener DJ, et al. Salvage treatment for recurrences after first resection of colorectal liver metastases: the impact of histopathological growth patterns. *Clin Exp Metastasis.* Apr 2019;36(2):109-118.
26. Pinheiro RS, Herman P, Lupinacci RM, et al. Tumor growth pattern as predictor of colorectal liver metastasis recurrence. *Am J Surg.* Apr 2014;207(4):493-498.
27. van Dam PJ, Daelemans S, Ross E, et al. Histopathological growth patterns as a candidate biomarker for immunomodulatory therapy. *Semin Cancer Biol.* Oct 2018;52(Pt 2):86-93.
28. Van den Eynden GG, Bird NC, Majeed AW, Van Laere S, Dirix LY, Vermeulen PB. The histological growth pattern of colorectal cancer liver metastases has prognostic value. *Clin Exp Metastasis.* Aug 2012;29(6):541-549.
29. Nierop PMH, Hoppener DJ, van der Stok EP, et al. Histopathological growth patterns and positive margins after resection of colorectal liver metastases. *HPB (Oxford).* Jun 2020;22(6):911-919.
30. Hof J, Visser L, Höppener DJ, et al. B Cells as Prognostic Biomarker After Surgery for Colorectal Liver Metastases. *Front Oncol.* 2020;10:249.
31. Cheng J, Wei J, Tong T, et al. Prediction of Histopathologic Growth Patterns of Colorectal Liver Metastases with a Noninvasive Imaging Method. *Ann Surg Oncol.* Dec 2019;26(13):4587-4598.
32. Kawaguchi Y, Kopetz S, Newhook TE, et al. Mutation Status of RAS, TP53, and SMAD4 is Superior to Mutation Status of RAS Alone for Predicting Prognosis after Resection of Colorectal Liver Metastases. *Clin Cancer Res.* Oct 1 2019;25(19):5843-5851.
33. Gonsalves WI, Mahoney MR, Sargent DJ, et al. Patient and tumor characteristics and BRAF and KRAS mutations in colon cancer, NCCTG/Alliance N0147. *J Natl Cancer Inst.* Jul 2014;106(7).
34. Margonis GA, Buettner S, Andreatos N, et al. Association of BRAF Mutations With Survival and Recurrence in Surgically Treated Patients With Metastatic Colorectal Liver Cancer. *JAMA Surg.* Jul 18 2018;153(7):e180996.
35. Smith CG, Fisher D, Claes B, et al. Somatic profiling of the epidermal growth factor receptor pathway in tumors from patients with advanced colorectal cancer treated with chemotherapy +/- cetuximab. *Clin Cancer Res.* Aug 01 2013;19(15):4104-4113.
36. Yaeger R, Cercek A, Chou JF, et al. BRAF mutation predicts for poor outcomes after metastasectomy in patients with metastatic colorectal cancer. *Cancer.* Aug 1 2014;120(15):2316-2324.
37. Buisman FE, Galjart B, Buettner S, Groot Koerkamp B, Grünhagen DJ, Verhoef C. Primary tumor location and the prognosis of patients after local treatment of colorectal liver metastases: a systematic review and meta-analysis. *HPB (Oxford).* Mar 2020;22(3):351-357.

Supplementary Table 1. Baseline characteristics stratified by treatment centre

		Missing (%)	Erasmus MC n = 213 (%)	MSKCC n = 338 (%)	Radboud UMC n = 229 (%)	p-value
Age at resection - *(median [IQR])*			65 [58, 71]	61 [52, 72]	67 [60, 73]	<0.001
Gender	Male		146 (69)	175 (52)	145 (63)	<0.001
	Female		67 (31)	163 (48)	84 (37)	
ASA classification	ASA I-II	4 (1)	187 (88)	93 (28)	184 (81)	<0.001
	ASA >II		25 (12)	244 (72)	43 (19)	
Primary tumour location	Left-sided	24 (3)	87 (42)	132 (41)	84 (38)	0.10
	Right-sided		48 (23)	101 (31)	58 (26)	
	Rectal		74 (35)	90 (28)	82 (37)	
T-stage	pT 0-2	56 (7)	28 (13)	31 (11)	38 (17)	0.15
	pT 3-4		182 (87)	256 (89)	189 (83)	
N-stage	N0	10 (1)	86 (41)	118 (35)	80 (35)	0.36
	N+		124 (59)	215 (65)	147 (65)	
Number of CRLM - *(median [IQR])*		2 (0)	2.0 [1.0, 4.0]	2.0 [1.0, 3.0]	1.0 [1.0, 3.0]	<0.001
Largest CRLM in cm - *(median [IQR])*		3 (0)	2.8 [1.9, 4.5]	2.8 [2.0, 4.5]	2.8 [1.9, 4.3]	0.67
DFI in months* - *(median [IQR])*		11 (1)	0.0 [0.0, 11.0]	0.0 [0.0, 19.0]	6.0 [0.0, 18.0]	0.004
Preop. CEA in µg/L - *(median [IQR])*		65 (8)	11.3 [4.5, 33.5]	8.6 [3.4, 25.9]	10.0 [3.8, 30.0]	0.28
Neoadjuvant chemotherapy	No		135 (63)	103 (30)	169 (74)	<0.001
	Yes		78 (37)	235 (70)	60 (26)	
Resection margin involved	No	1 (0)	179 (84)	294 (87)	204 (89)	0.35
	Yes		33 (16)	44 (13)	25 (11)	
Extrahepatic disease	No		190 (89)	283 (84)	223 (97)	<0.001
	Yes		23 (11)	55 (16)	6 (3)	
KRAS mutational status	Wildtype	450 (58)	24 (50)	131 (56)	29 (60)	0.59
	Mutant		24 (50)	103 (44)	19 (40)	
BRAF mutational status	Wildtype	491 (63)	43 (96)	198 (97)	38 (95)	0.75
	Mutant		2 (4)	6 (3)	2 (5)	
MSI status	MSS	600 (77)	54 (96)	60 (91)	55 (95)	0.42
	MSI		2 (4)	6 (9)	3 (5)	
Histopathological phenotype	Desmoplastic		45 (21)	63 (19)	41 (18)	0.66
	Non-desmoplastic		168 (79)	275 (81)	188 (82)	

*Between resection of primary tumour and detection of CRLM
Abbreviations in alphabetical order: ASA: American Society of Anesthesiologists; CEA: carcinoembryonic antigen; CRLM: colorectal liver metastasis; DFI: disease-free interval; Erasmus MC: Erasmus MC Cancer Institute; IQR: interquartile range; MSI: microsatellite instable; MSKCC: Memorial Sloan Kettering Cancer Center; MSS: microsatellite stable; Radboud UMC: Radboud University Medical Center.

Supplementary table 2. Uni- and multivariable Cox regression models of cut-off analyses for overall (A) and disease-free survival (B)

	Supplementary table 2A. Overall survival				Supplementary table 2B. Disease-free survival			
	Univariable		Multivariable (n=625)		Univariable		Multivariable (n=625)	
	HR [95%CI]	p-value	HR [95%CI]	p-value	HR [95%CI]	p-value	HR [95%CI]	p-value
Age at resection (cont.) - *years*	1.01 [1.00-1.02]	0.01	1.01 [1.00-1.02]	0.11	1.00 [0.99-1.00]	0.34	1.00 [0.99-1.01]	0.94
ASA classification - *>II vs I-II*	1.26 [0.94-1.71]	0.13	1.27 [0.88-1.84]	0.20	1.14 [0.91-1.41]	0.25	1.21 [0.94-1.56]	0.13
Right-sided primary - *yes vs no*	1.46 [1.13-1.88]	0.004	1.37 [1.00-1.88]	0.05	1.05 [0.86-1.27]	0.65	1.04 [0.82-1.31]	0.75
T-stage - *pT3-4 vs pT0-2*	1.36 [0.92-2.00]	0.12	1.28 [0.82-2.00]	0.28	1.24 [0.95-1.61]	0.11	1.09 [0.81-1.46]	0.57
N-stage - *N+ vs N0*	1.18 [0.93-1.51]	0.18	1.23 [0.91-1.66]	0.19	1.29 [1.08-1.55]	0.005	1.25 [1.01-1.54]	0.04
DFI* (cont.) - *months*	1.00 [0.99-1.01]	0.65	1.00 [0.99-1.01]	0.71	0.99 [0.99-1.00]	0.01	0.99 [0.98-1.00]	0.01
Number of CRLM (cont.)	1.10 [1.06-1.15]	<0.001	1.09 [1.04-1.14]	<0.001	1.11 [1.08-1.15]	<0.001	1.08 [1.04-1.12]	<0.001
Largest CRLM (cont.) - *cm*	1.06 [1.03-1.10]	<0.001	1.07 [1.02-1.11]	0.005	1.06 [1.03-1.09]	<0.001	1.05 [1.01-1.09]	0.008
Preoperative CEA (cont.) - *100 µg/L*	1.01 [1.00-1.02]	0.006	1.01 [1.00-1.02]	0.03	1.01 [1.00-1.02]	0.09	1.01 [1.00-1.02]	0.24
Resection margin - *R1 vs R0*	1.83 [1.36-2.47]	<0.001	1.23 [0.85-1.78]	0.27	1.84 [1.47-2.31]	<0.001	1.45 [1.10-1.91]	0.008
Extrahepatic disease - *yes vs no*	1.63 [1.15-2.29]	0.005	1.62 [1.07-2.45]	0.02	1.85 [1.44-2.38]	<0.001	2.19 [1.62-2.95]	<0.001
Neoadjuvant chemotherapy - *yes vs no*	1.25 [0.96-1.62]	0.10	1.27 [0.93-1.73]	0.13	1.45 [1.20-1.74]	<0.001	1.25 [1.00-1.55]	0.05
Desmoplastic phenotype	Reference		Reference		Reference		Reference	
0.1-33% non-desmoplastic	2.53 [1.68-3.82]	<0.001	2.90 [1.75-4.82]	<0.001	2.49 [1.89-3.27]	<0.001	2.07 [1.51-2.85]	<0.001
33.1-67% non-desmoplastic	2.15 [1.37-3.36]	<0.001	2.30 [1.33-3.97]	0.003	2.02 [1.48-2.74]	<0.001	1.82 [1.27-2.60]	0.001
67.1-100% non-desmoplastic	2.80 [1.91-4.11]	<0.001	2.89 [1.77-4.73]	<0.001	2.24 [1.72-2.91]	<0.001	2.07 [1.51-2.82]	<0.001

*Between resection of primary tumour and detection of CRLM

Abbreviations in alphabetical order: ASA: American Society of Anesthesiologists; Cont.: entered as continuous variable; CEA: carcinoembryonic antigen; CRLM: colorectal liver metastasis; DFI: disease-free interval.

Supplementary table 3. Uni- and multivariable Cox regression analyses for overall (A&C) and disease-free survival (B&D) within the chemo-naive (A&B) and pre-treated (C&D) subpopulations

	Supplementary table 3A&B. Overall and disease-free survival in chemo-naive patients					
	A. Overall survival			B. Disease-free survival		
	Univariable		Multivariable (n=352)	Univariable		Multivariable (n=352)
	HR [95%CI]	p-value	HR [95%CI]	p-value	HR [95%CI]	p-value	HR [95%CI]	p-value
Age at resection (cont.) - *years*	1.02 [1.00-1.04]	0.02	1.02 [1.00-1.05]	0.05	1.00 [0.99-1.01]	0.78	1.00 [0.99-1.02]	0.47
ASA classification - *>II vs I-II*	1.57 [0.97-2.55]	0.07	1.47 [0.87-2.48]	0.15	1.27 [0.92-1.76]	0.14	1.24 [0.88-1.75]	0.22
Right-sided primary - *yes vs no*	1.65 [1.12-2.44]	0.01	1.36 [0.86-2.15]	0.19	1.22 [0.93-1.59]	0.16	1.12 [0.82-1.53]	0.47
T-stage - *pT3-4 vs pT0-2*	2.07 [1.11-3.86]	0.02	1.75 [0.89-3.43]	0.11	1.58 [1.07-2.33]	0.02	1.41 [0.93-2.13]	0.10
N-stage - *N+ vs N0*	1.32 [0.92-1.89]	0.14	1.41 [0.92-2.16]	0.11	1.27 [0.99-1.63]	0.06	1.32 [1.00-1.76]	0.05
DFI* (cont.) - *months*	1.00 [0.99-1.01]	0.43	1.00 [0.99-1.02]	0.51	0.99 [0.99-1.00]	0.15	0.99 [0.98-1.00]	0.10
Number of CRLM (cont.)	1.08 [1.00-1.17]	0.06	1.08 [0.99-1.17]	0.09	1.16 [1.09-1.22]	<0.001	1.14 [1.07-1.22]	<0.001
Largest CRLM (cont.) - *cm*	1.07 [1.01-1.13]	0.02	1.08 [1.01-1.16]	0.03	1.04 [0.99-1.09]	0.11	1.06 [1.00-1.13]	0.05
Preoperative CEA (cont.) - *100 µg/L*	1.05 [1.01-1.11]	0.03	1.04 [0.98-1.10]	0.24	1.02 [0.97-1.07]	0.43	0.99 [0.93-1.06]	0.88
Resection margin - *R1 vs R0*	1.32 [0.76-2.27]	0.32	1.25 [0.67-2.34]	0.49	1.63 [1.12-2.38]	0.01	1.63 [1.07-2.48]	0.02
Extrahepatic disease - *yes vs no*	1.61 [0.85-3.04]	0.15	1.63 [0.76-3.49]	0.21	2.01 [1.34-3.03]	<0.001	1.69 [1.07-2.69]	0.03
Desmoplastic phenotype - *yes vs no*	0.34 [0.18-0.64]	<0.001	0.29 [0.13-0.65]	0.003	0.49 [0.33-0.72]	<0.001	0.53 [0.34-0.82]	0.005

	Supplementary table 3C&D. Overall and disease-free survival in pre-treated patients					
	C. Overall survival			D. Disease-free survival		
	Univariable		Multivariable (n=273)	Univariable		Multivariable (n=273)
	HR [95%CI]	p-value	HR [95%CI]	p-value	HR [95%CI]	p-value	HR [95%CI]	p-value
Age at resection (cont.) - *years*	1.01 [1.00-1.02]	0.06	1.01 [0.99-1.03]	0.22	1.00 [0.99-1.01]	0.49	1.00 [0.98-1.01]	0.70
ASA classification - *>II vs I-II*	1.17 [0.80-1.72]	0.42	1.01 [0.60-1.71]	0.97	1.05 [0.79-1.41]	0.73	1.16 [0.79-1.70]	0.45
Right-sided primary - *yes vs no*	1.54 [1.09-2.18]	0.01	1.46 [0.93-2.30]	0.10	0.95 [0.72-1.25]	0.69	0.92 [0.65-1.31]	0.65
T-stage - *pT3-4 vs pT0-2*	1.01 [0.60-1.71]	0.96	1.01 [0.52-1.95]	0.98	0.88 [0.61-1.27]	0.50	0.76 [0.48-1.19]	0.23
N-stage - *N+ vs N0*	1.06 [0.76-1.49]	0.73	1.14 [0.72-1.80]	0.59	1.19 [0.92-1.55]	0.18	1.18 [0.84-1.65]	0.34
DFI* (cont.) - *months*	1.00 [0.98-1.01]	0.38	0.98 [0.97-1.00]	0.07	1.00 [0.99-1.00]	0.23	0.99 [0.98-1.00]	0.09
Number of CRLM (cont.)	1.11 [1.06-1.16]	<0.001	1.09 [1.03-1.16]	0.004	1.09 [1.05-1.13]	<0.001	1.05 [1.00-1.10]	0.05
Largest CRLM (cont.) - *cm*	1.07 [1.02-1.12]	0.006	1.06 [0.99-1.13]	0.10	1.06 [1.03-1.10]	<0.001	1.05 [1.00-1.11]	0.05
Preoperative CEA (cont.) - *100 µg/L*	1.01 [1.00-1.02]	0.03	1.01 [1.00-1.02]	0.05	1.01 [1.00-1.01]	0.18	1.00 [0.99-1.01]	0.53
Resection margin - *R1 vs R0*	2.11 [1.45-3.09]	<0.001	1.31 [0.79-2.18]	0.29	1.89 [1.41-2.53]	<0.001	1.73 [1.17-2.55]	0.006
Extrahepatic disease - *yes vs no*	1.67 [1.11-2.52]	0.01	2.23 [1.31-3.81]	0.003	1.60 [1.16-2.20]	0.004	2.62 [1.73-3.98]	<0.001
Desmoplastic phenotype - *yes vs no*	0.41 [0.26-0.65]	<0.001	0.43 [0.23-0.79]	0.007	0.37 [0.27-0.52]	<0.001	0.43 [0.29-0.64]	<0.001

*Between resection of primary tumour and detection of CRLM

Abbreviations in alphabetical order: ASA: American Society of Anesthesiologists; Cont.: entered as continuous variable; CEA: carcinoembryonic antigen; CRLM: colorectal liver metastasis; DFI: disease-free interval.

III

```
#MV OS&DFS regression models for adjusted HR for all cut-offs
#Regression database (patient selection)
regdat <- CDB
regdat$HGP <- factor(regdat$HGP, levels=levels(CDB$HGP)[c(2,1)])
regdat$COA <- factor(regdat$COA, levels=levels(CDB$COA)[c(5,4,3,2,1)])
regdat$COAdrp <-
      factor(regdat$COAdrp, levels=levels(CDB$COAdrp)[c(2,3,4,1)])

#Regression variables
regvar <- c("Age_At_Resection_CRLM", "ASA_cat", "Left_right_sided_cat",
            "pT_cat", "N_CRC", "DFI_CRLM", "Total_leasions_treated",
            "Diam_CRLM_pat", "CEA_100", "EHD", "R0_R1", "Peri_SYS")
coavar <- c("HGP", "COA", "COAdrp")

#OS Survival variables (event and time)
srvevt <- c("Event")
srvtim <- c("OS")

#Multivariable cox model HGP OS
mvcoxf <- paste0("cph(Surv(", srvtim, ", ", srvevt, ") ~ ",
                 paste(c(regvar, coavar[1]), collapse=" + "),
                 ", data = regdat)")
mvcoxm <- eval(parse(text=mvcoxf))
mvhrci <- cbind(exp(coef(mvcoxm)), exp(confint(mvcoxm)),
                pnorm(abs(mvcoxm$coef/sqrt(diag(mvcoxm$var))),
                      lower.tail=F)*2)
mvhrci <- mvhrci[c(13:(length(mvhrci)/4)),]
OHhgp <- paste0(sprintf("%.2f", mvhrci[1]), " (",
                sprintf("%.2f", mvhrci[2]), "-",
                sprintf("%.2f", mvhrci[3]), ")")
OHhgp <- c("reference", OHhgp)

#Multivariable cox model HGP COA OS
mvcoxf <- paste0("cph(Surv(", srvtim, ", ", srvevt, ") ~ ",
                 paste(c(regvar, coavar[2]), collapse=" + "),
                 ", data = regdat)")
mvcoxm <- eval(parse(text=mvcoxf))
mvhrci <- cbind(exp(coef(mvcoxm)), exp(confint(mvcoxm)),
                pnorm(abs(mvcoxm$coef/sqrt(diag(mvcoxm$var))),
                      lower.tail=F)*2)
mvhrci <- mvhrci[c(13:(length(mvhrci)/4)),]
OHcoa <- paste0(sprintf("%.2f", mvhrci[,1]), " (",
               sprintf("%.2f", mvhrci[,2]), "-",
               sprintf("%.2f", mvhrci[,3]), ")")
OHcoa <- c("reference", OHcoa)

#Multivariable cox model HGP COAdrp OS
mvcoxf <- paste0("cph(Surv(", srvtim, ", ", srvevt, ") ~ ",
                 paste(c(regvar, coavar[3]), collapse=" + "),
                 ", data = regdat)")
mvcoxm <- eval(parse(text=mvcoxf))
mvhrci <- cbind(exp(coef(mvcoxm)), exp(confint(mvcoxm)),
                pnorm(abs(mvcoxm$coef/sqrt(diag(mvcoxm$var))),
                      lower.tail=F)*2)
mvhrci <- mvhrci[c(13:(length(mvhrci)/4)),]
```

Chapter IV

Histopathological growth patterns of liver metastasis: updated consensus guidelines for pattern scoring, perspectives, and recent mechanistic insights

–

British Journal of Cancer 2022

E. Latacz*, D.J. Höppener*, A. Bohlok*, S. Leduc, S. Tabariès, C. Fernández Moro, C. Lugassy, H. Nyström, B. Bozóky, G. Floris, N. Geyer, Pnina Brodt, L. Llado, L. van Mileghem, M. de Schepper, A.W. Majeed, A. Lazaris, P. Dirix, Q. Zhang, S.K. Petrillo, S. Vankerckhove, I. Joye, Y. Meyer, A. Gregorieff, N. Ruiz Roig, F. Vidal-Vanaclocha, L. Denis, R. Caetano Oliveira, P. Metrakos, D.J. Grünhagen, I.D. Nagtegaal, D.G. Mollevi, W.R. Jarnagin, M.I. D'Angelica, A.R. Reynolds, M. Doukas, C. Desmedt, L. Dirix, V. Donckier, P.M. Siegel, R. Barnhill, M. Gerling, C. Verhoef, P.B. Vermeulen.

*These authors contributed equally.

Abstract

The first consensus guidelines for scoring the histopathological growth patterns (HGPs) of liver metastases were established in 2017. Since then, numerous studies have applied these guidelines, have further substantiated the potential clinical value of the HGPs in patients with liver metastases from various tumour types and are starting to shed light on the biology of the distinct HGPs. In the present guidelines, we give an overview of these studies, discuss novel strategies for predicting the HGPs of liver metastases, such as deep learning algorithms for whole slide histopathology images and medical imaging, and highlight liver metastasis animal models that exhibit features of the different HGPs. Based on a pooled analysis of large cohorts of patients with liver-metastatic colorectal cancer, we propose a new cut-off to categorise patients according to the HGPs. An up-to-date standard method for HGP assessment within liver metastases is also presented with the aim of incorporating HGPs into the decision-making processes surrounding the treatment of patients with liver metastatic cancer. Finally, we propose hypotheses on the cellular and molecular mechanisms that drive the biology of the different HGPs, opening some exciting pre-clinical and clinical research perspectives.

Introduction

The histopathological growth patterns (HGPs) of liver metastases are a morphological reflection of the distinct ways in which cancer cells interact with the surrounding liver. These HGPs can be identified by light microscopy on tissue sections that include the metastasis-liver interface. In 2017, the first set of guidelines for scoring the growth patterns was published.[1] Since that time, numerous additional studies have utilised these consensus guidelines to score the HGPs of liver metastases. These studies, listed in *table 1*, have further substantiated the clinical value of HGPs in hepatic metastases from colorectal cancer and extended this concept to other tumour types, such as breast carcinoma, melanoma, and pancreatic cancer. Moreover, these publications have significantly increased our understanding of HGP biology by describing the molecular and cellular differences between growth patterns by, for example, looking at growth pattern-specific immune responses.[2-6] In addition, attempts have been made to develop technologies for predicting HGPs using medical imaging and machine-learning algorithms.[7-10] Novel animal models for liver metastasis exhibiting features of the different HGPs are a particularly valuable development.[11-17] These models will allow us to: 1) perform functional validation of HGP-specific signalling pathways described in the clinical samples of liver metastases, 2) identify non-invasive surrogate markers for the different HGPs, and 3) test the efficacy of new therapeutic strategies based on the HGPs.

Clinical and experimental studies have provided ample new information that warrants an updated, second version of the international guidelines for scoring the HGPs in the context of liver metastasis. The main goal of the guidelines is to incorporate these histological features into the clinical decision-making processes surrounding

the treatment of patients with liver metastatic cancer. We therefore provide a detailed histopathological description of the growth patterns of liver metastases and propose an updated standard method for HGP assessment within liver metastases, including immunohistochemical staining as an aid to scoring HGPs. One of the important features of the new guidelines is a modified and clinically applicable cut-off for considering a colorectal cancer (CRC) liver metastasis (CRLM) as desmoplastic or non-desmoplastic. This change in cut-off is supported by retrospective studies with large cohorts of patients with liver metastatic CRC.[18,19] In the new guidelines, we present a pooled analysis of previously published cohorts to demonstrate the improved prognostic value of this new cut-off recommendation. In addition, we propose hypotheses that could explain the transition from one HGP to another, based on comprehensive immunohistochemical analyses of both the tumour-liver interface and the centre of the metastases. We also speculate on molecular mechanisms that may underlie the biological differences of the growth patterns. Finally, we discuss exciting new research perspectives for the HGPs, including digital image processing techniques and deep learning methods for automated HGP scoring using digitised haematoxylin-and-eosin-stained (H&E-stained) tissue sections.[20-22]

Methods

Literature search

We performed a literature search for studies published since January 2015 that focused on the HGPs of liver metastases using the PubMedR resource of the U.S. National Library of Medicine. The search terms were designed to find studies on the evaluation of the interface between liver metastases and the surrounding liver tissue, independent of the primary tumour type and the host species. Additional studies were found by manual cross-referencing. Ultimately, manuscripts were selected by three reviewers (EL, DJH and PV). Only manuscripts that were not already presented in Table 1 of the first consensus guidelines publication[1] are discussed in the current overview table (*table 1*).

Evaluation of the HGP cut-off algorithms

To compare the prognostic value of different HGP cut-off algorithms, survival analyses were performed. The HGP and survival data used for these analyses have been previously published as separate cohorts and were pooled for the current analysis.[1,18,23-25] All available H&E-stained sections of all resected liver metastases for every patient included in this assessment were analysed according to the 2017 consensus guidelines.[1] The final HGP score per patient is the average of all metastases, independent of the size of the metastases or number of analysed tissue sections per metastasis. Data on overall and disease-free survival (OS, DFS, defined as the time between first liver metastasis resection and death or cancer recurrence, respectively) and HGP were available for 1931 patients: 903 patients underwent surgical resection (1998 - 2019) in the Erasmus MC Cancer Institute (Rotterdam, the Netherlands), 716 patients in the Memorial Sloan Kettering Cancer Center (New York, NY, USA), and 312 patients in the Radboud University Medical Centre (Nijmegen, the Netherlands). All patients treated with curative intent, who

did not receive hepatic arterial infusion pump chemotherapy, and for whom H&E-stained sections were available, were included. Approval by the institutional ethical review boards was obtained in each individual centre separately.

Immunohistochemistry

For immunohistochemistry with antibodies (clone; manufacturer's code) directed at CK7 (RN7; NCL-L-CK7-560), CK18 (DC-10; NCL-CK18), CK19 (b170; NCL-CK19), CK20 (PW31; NCL-L-CK20-561), Caldesmon (H-CD; Dako-M3557), CD34 (QBEnd/10; Dako-M7165), CD146 (UMAB154; Origene-UM800051), NGFR (polyclonal; Atlas-HPA004765) and alpha-SMA (1a4; DAKO-M0851), formalin-fixed paraffin-embedded (FFPE) tissue representing the respective areas were cut to 4 µm thickness. All immunohistochemical stains were done on a Leica (Germany) BOND-MAX automated stainer as part of clinical routine at Karolinska University Hospital, Huddinge, Sweden. Pretreatment was done using Bond Epitope Retrieval Solution 2 EDTA (Leica) for 20 minutes. Immunohistochemistry for antibodies directed at melan-A (A103; Dako-M7196) was done on a Leica BOND-RX automated stainer at Institut Curie, Paris, France. Pretreatment was done using Bond Epitope Retrieval Solution 2 EDTA (Leica) for 20 minutes.

Statistics

For the comparison of different cut-off algorithms, OS and DFS were estimated using the Kaplan-Meier method and reported as 5-year (%), 10-year (%) and median (months) survival including a corresponding 95% confidence interval (CI). Adjusted hazard ratios (HR) for OS and DFS are based on multivariable Cox proportional hazards regression models. All statistical analyses were performed with the R Project for Statistical Computing (version 4.0.2; https://www.r-project.org/).

Results - guidelines

Histopathological description of the growth patterns of liver metastases

Liver metastases can interact differently with the liver parenchyma as they colonise the liver, which is manifest histologically as one of several distinct growth patterns. These patterns can generally be identified by light microscopy in H&E-stained sections of FFPE tissue at the interface between the cancer cells and the liver parenchyma.[26-30] The key histopathological characteristics of the HGPs have been described in table 2 of the first international consensus guidelines[1] and remain valid in that form. An updated overview of the histology of the different HGPs is presented in *table 2* and in *figures 1A-K* of the current scoring guidelines.

Table 1. Studies published since January 2015 that focused on the HGPs of liver metastases

First author	Reference	Methodology	Tumour type	Main findings
Animal models				
Alzubi M.A.	Clin Exp Metastasis 2019[11]	Portal vein injection of cancer cells of PDX mammary tumours of 14 patients in NOD *scid gamma* mice.	Breast cancer	HGPs could be assessed in six PDX models: replacement, desmoplastic and pushing HGPs were identified.
Piquet L.	Cancers 2019[12]	Co-inoculation into the spleen of human primary hepatic stellate cells and 5 human uveal melanoma cell lines in NOD *scid gamma* or NOD CRISPR *Prkdc Il2r gamma* mice.	Uveal Melanoma	Desmoplastic, replacement and mixed liver metastases were observed. The HGP was not altered by co-inoculation of stellate cells (figure 5A and table 2 of the publication)
Vlachogiannis G.	Science 2018[13]	A biobank of patient-derived organoids and xenografts was constructed (110 fresh biopsies from 71 patients enrolled in four prospective phase 1/2 clinical trials were processed)	Colorectal and gastro-oesophageal cancer	A predominance of replacement HGP was observed in xenografts from resistant patient, whereas tumours established from sensitive patient showed a prevalence of desmoplastic and pushing HGPs.
Ibrahim N.S.	Cancers 2020[14]	Intra-splenic injection of MC-38 mouse CRC cell line in inducible Ang1 knock-out C57BL/6 mice.	Colorectal cancer	Replacement HGP liver metastases in control mice and desmoplastic HGP liver metastases in Ang1 knock-out condition.
Masaki S.	Int J Exp Pathol 2020[15]	Fatty liver conditions were induced in BALB/c mice. CT26 cells were injected into the liver.	Colorectal cancer	Tumours in control mice showed encapsulated growth patterns, while tumours in fatty livers showed invasive growth without encapsulation.
Tabariès S.	Commun Biol 2021[16]	Intrahepatic transplantation of patient liver metastasis tissue fragments in Scid-beige mice. Expression profiles of claudins were compared between dHGP and rHGP in PDXs and in liver metastases of patients.	Colorectal cancer	Liver metastases in mice express the HGP of the liver metastases of the patient-donor. Claudin-2 in patient-derived extracellular vesicles may be a marker of rHGP.
Bartlett A.	Cancers 2021[17]	Portal vein injection of D2OR, a low metastatic mouse mammary tumour cell line in nulliparous BALB/c immune competent mice and weaning-induced liver involution mice.	Breast cancer	The post-weaning liver is in an immune suppressed state with increased tumour incidence and multiplicity. A greater diversity of HGPs was noted in the post-weaning mice, consistent with the liver microenvironment dictating tumour histology.

Immune contexture (also: Watanabe K. in 'HGP scoring methodology' section)				
Stremitzer S.	Br J Cancer 2020[2]	The immune phenotype of liver metastases was scored based on the distribution of CD8-immunostained cytotoxic T-lymphocytes as 'desert', 'excluded' (together 'non-inflamed') and 'inflamed' (81 patients). Bevacizumab-based chemotherapy was administered to all patients before partial liver resection.	Colorectal cancer	The inflamed immune phenotype was associated with the desmoplastic HGP and was associated with improved RFS and OS in univariable, not multivariable analyses.
Liang J.	Cancer Immunol Immunother 2020[3]	The immunoscore was calculated according to the densities of immunostained CD3 + and CD8 + cells (166 patients). One immunoscore per patient was calculated based on assessments in the tumour centre and in the invasive margin.	Colorectal cancer	A high immunoscore was more often encountered in liver metastases with a desmoplastic HGP than with a replacement HGP. A combined risk score (HGP, immunoscore and clinical risk score) was developed and a 90% 5-year OS rate was observed for patients in the low-risk group (30% of the patients).
Höppener D.J.	Br J Cancer 2020[4]	The immune contexture of resected liver metastases was analysed in 3 cohort of chemo-naive patients (117, 34 and 79 patients, respectively) with immunohistochemistry (semi-quantitative grading, quantitative digital image analysis) and flow cytometry. The 100% desmoplastic HGP cut off was applied.	Colorectal cancer	An increased immune infiltrate is associated with the desmoplastic HGP, both surrounding and in the metastases. Intra-epithelial CD8+ cells were also increased in the desmoplastic HGP.
Messaoudi N.	Br J Cancer 2022[6]	Immunohistochemistry and automated quantitative analysis on tissue microarray (176 patients) of CD3, MHC-I and CD73. Liver metastases were categorized according to the dominant HGP and according to the 100% desmoplastic HGP cut off.	Colorectal cancer	Desmoplastic liver metastases were more infiltrated by CD3 + cells, expressed lower levels of MHC-I, and similar levels of CD73. Elevated CD73 expression was associated with a worse outcome of patients with desmoplastic HGP liver metastases. Low MHC-I expression in patients with replacement-type metastases improved outcome.
Garcia-Vicién G	Cancers 2022[89]	The spatial distribution of lymphocytic infiltrates in CRC liver metastases was explored in the context of the HGPs by multiplex immunofluorescence staining and digital image analysis in a cohort of 22 resected metastases without pre-surgery chemotherapy. HGPs were scored following the previous guidelines. The desmoplastic rim was excluded from the invasive margin for lymphocyte counting ('Measure B').	Colorectal cancer	The number of CD8-positive cells at the invasive margin was independent of the HGP. In non-desmoplastic metastases, the cytotoxic T cells did not enter the tumour cell nests and CD4-positive cells were more abundant at the invasive margin than in desmoplastic lesions.
HGP scoring methodology				
Höppener D.J.	Clin Exp Metastasis 2019[39]	Within and between metastasis HGP concordance was analysed in 363 patients with 2 or more resected liver metastases. The association of diagnostic accuracy with number of sections and number of metastases evaluated was determined. Interobserver agreement of HGP scoring was assessed after training. The 100% desmoplastic HGP cut off was applied.	Colorectal cancer	Within metastasis concordance ranged from 93% to 96%. Between metastasis concordance was 90%. Diagnostic accuracy peaked at two sections and two metastases. After two training sessions, interobserver agreement had a kappa-value of more than 0.9.
Watanabe K.	Cancer Med 2020[5]	Biopsies of liver metastases of 107 patients with pancreatic cancer (21- or 18-gauge needle) were used for HGP assessment. The dominant HGP was determined. If a HGP was present in more than 80% of the interface, the HGP was called 'homogenous' (analysis in 14 patients).	Pancreatic cancer	Of 279 patients, 107 patients had a biopsy that contained the tumour-liver interface. HGP had a homogenous expression in 13/14 patients. Disease control rate as well as overall survival rate were lower in the replacement HGP group. The replacement HGP biopsies showed less inflammation (H&E) and contained less CD8 + cells than the other biopsies.

Szczepanski J.	Am J Surg Pathol 2021[90]	The HGP was scored in biopsies of liver metastases of melanoma (n=30; 22 skin melanomas; 6 ocular melanomas; 2 unknown origin).	Melanoma	In 8/30 (4 ocular, 4 skin, 27%) melanoma liver metastases, a sinusoidal HGP was seen. In none of the 96 metastases of breast, colon, pancreaticobiliary cancer and neuroendocrine tumours this HGP was encountered.
Medical imaging				
Gulia S.	BMJ Case Rep 2016[7]	A case report of a radiographically occult liver metastasis leading to liver failure is presented.	Breast cancer	A biopsy established the diagnosis of a liver metastasis with intra-sinusoidal growth pattern.
Cheng J.	Ann Surg Oncol 2019[8]	A radiomic algorithm was developed to identify the dominant HGPs of liver metastases by computed tomography (CT) imaging. Pre- and post-contrast as well as arterial and portal venous phase images (ROI: tumour-liver interface) contributed to the algorithm (126 metastases of 94 chemo-naive patients - variety of scanners but standardized acquisition protocol and use of contrast agent).	Colorectal cancer	The dominant HGP of the liver metastases could be predicted with 65% sensitivity and 92% specificity (accuracy of 77%). A decisive feature used by the algorithm is the presence (desmoplastic) or absence (replacement) of peripheral rim enhancement in the portal-venous phase. No clinical or qualitative image data were used by the algorithm.
Han Y.	Front Oncol 2020[9]	A radiomic algorithm was developed to identify the dominant HGP of liver metastases by magnetic resonance imaging (MRI). (ROI: tumour-liver interface (TLI) - 182 liver metastases (107 chemo-naive patients))	Colorectal cancer	The radiomic algorithm that best predicted the dominant HGP was based on quantitative features extracted from the TLI combined with clinical data and a qualitative image feature ('lobular margin') (79% accuracy, 100% sensitivity, 35% specificity). The desmoplastic HGP had more heterogeneous radiomic features than the replacement HGP.
Starmans M.P.A.	Clin Exp Metastasis 2021[10]	A radiomic algorithm was developed to distinguish liver metastases with 100% desmoplastic HGP from liver metastases with 100% replacement HGP by CT imaging (76 chemo-naive patients with 93 metastases).	Colorectal cancer	Despite the use of only portal venous phase contrast-enhanced images, variations in lesion segmentation and acquisition protocols, accuracy was 65%, sensitivity 72% and specificity 58%.
Wei S.	Eur J Radiol 2021[67]	The CT image-based radiomics algorithm to identify the dominant HGP developed in Cheng et al. (2019) was used to predict response to bevacizumab-chemotherapy in 119 patients (346 lesions) with unresectable CRC liver metastases.	Colorectal cancer	AUC for predicting early response was 0.72. The radiomics algorithm-derived HGP was the only independent predictor of 1-year PFS.
Li W.H.	Quant Imaging Med Surg 2022[91]	MRI features were used to predict the dominant HGP in 53 chemo-naive patients.	Colorectal cancer	AUC for predicting the dominant HGP based on diameter difference between pre- and post-contrast images and rim enhancement was 0.83.
HGP as biomarker (HGP assessment not according to guidelines, according to guidelines with dominant HGP as categories and according to guidelines with 100% desmoplastic HGP versus any percentage of replacement as categories)				
de Ridder J.A.M.	Ann Surg Onc 2015[92]	The presence/absence of a fibrous capsule was scored on H&E sections of resected liver metastases of 124 chemo-naive patients with a solitary metastasis. The proportion of the tumour-liver interface with/without capsule was not reported.	Colorectal cancer	In univariable but not multivariable analysis, the presence of a fibrous capsule was associated with improved OS (109 months versus 57 months).
Serrablo A.	Eur J Surg Oncol 2016[93]	The presence/absence of a fibrous capsule with a thickness of at least 0,5mm in the entire tumour-liver interface was assessed on H&E sections (147 patients: 74/147 with pre-surgery systemic treatment)	Colorectal cancer	The capsule was present in 17% of the patients, independent of pre-surgery treatment status, and did not have an impact on survival.
Fonseca G.M.	J Surg Oncol 2018[94]	Tumour border pattern was scored according to the Jass classification (infiltrative, expansive). A fibrous capsule was scored as being absent or present. A single tissue block of the largest metastasis was selected for each patient (229 patients, all with peri-operative systemic treatment).	Colorectal cancer	Both absence of a fibrous capsule (75% of patients) and infiltrative growth (74% of patients) were associated with shorter OS and DFS in multivariable and/or univariable analyses. Both parameters were also associated with hepatic recurrence.

Cremolini C.	Br J Cancer 2018[95]	HGPs were scored according to the international guidelines. The effect of the HGPs on OS and DFS was investigated in a cohort of patients with liver metastases and with chemotherapy combined with either bevacizumab or cetuximab prior to surgery (159 patients).	Colorectal cancer	There was no effect of HGP on OS or DFS. An important remark is that the proportion of patients with liver metastases with a dominant pushing HGP was much higher than reported in most other studies (41%).
Falcao D.	Eur J Surg Oncol 2018[96]	HGPs of liver metastases were scored in 110 patients of which 52 patients received pre-surgery chemotherapy. A mixed HGP was identified when more than one HGP was expressed by the metastases and each HGP was present in at least 25% of the interface.	Colorectal cancer	The pushing HGP was independently associated with worse OS and DFS. An important remark is that the proportion of patients with liver metastases with a pushing HGP was much higher than reported in most other studies (30%).
Barnhill R.	J Pathol Clin Res 2018[44]	The dominant HGP was scored according to the international guidelines. Gene alterations were assessed by array CGH (41 liver metastases originating from 41 patients).	Uveal melanoma	Dominant replacement HGP metastases were present in 73% of patients (27%: desmoplastic HGP). On multivariate analysis, only HGP and resection status predicted OS (HR of 6.5 for replacement HGP).
Galjart B.	Angiogenesis 2019[18]	HGPs were scored according to the international guidelines but patients were categorized as having 100% desmoplastic (dHGP) liver metastases or not (non-dHGP) (732 patients of which 367 chemo-naive before surgery)	Colorectal cancer	About 20% of the patients with surgical resection of CRC liver metastases ended up in 100% dHGP group. This was associated with an outstanding outcome, especially in the chemo-naïve group (78% with at least 5 years OS)
Nierop P.M.H.	Clin Exp Metastasis 2019[23]	HGP was scored as 100% desmoplastic (dHGP) versus non-dHGP in 690 patients free of disease after first resection of liver metastases of which 492 developed recurrent disease.	Colorectal cancer	Patients with dHGP at first partial hepatectomy were more often treated with curative intent and more often had recurrences salvageable by local treatment modalities.
Ao T.	Virchows Arch 2019[97]	The desmoplastic reaction in and around liver metastases was scored as mature/intermediate (mature collagen fibers and keloid-like collagen) and immature (myxoid collagen present) in 204 patients with resected liver metastases of which 78 had received preoperative chemotherapy	Colorectal cancer	The type of desmoplastic reaction was independently associated with outcome with 65% 5-years OS in the mature /intermediate group versus 35% in the immature group.
Barnhill R.	J Pathol Clin Res 2020[45]	HGP was scored as 100% desmoplastic (dHGP) versus 'any % of replacement' (any rHGP) (43 liver metastases from 42 patients).	Cutaneous melanoma	Multivariate analysis demonstrated that only HGP was associated with OS after resection of the liver metastases (HR for 'any rHGP' of 3.8).
Zhang Y.L.	J Oncol 2020[98]	Encapsulation of hepatocellular carcinoma was assessed in 188 patients (method not specified).	Hepato-cellular carcinoma	In multivariate analyses, the presence of a capsule was associated with improved DFS and OS (HR of 0.60 and 0.51, respectively).
Buisman F.E.	Clin Exp Metastasis 2020[25]	HGP was scored as 100% desmoplastic (dHGP) versus non-dHGP in resected liver metastases of 1236 patients of whom 656 received pre-operative chemotherapy.	Colorectal cancer	Adjuvant chemotherapy improved OS and DFS only in patients with non-dHGP liver metastases who did not receive pre-operative chemotherapy (HR of 0.52 and 0.71, respectively)
Baldin P.	J Pathol Clin Res 2021[99]	A pathological score (combining 'more than 3 lesions', 'R1 positive margin', 'non-100% desmoplastic HGP', 'steatohepatitis') and the consensus Immunoscore were tested for effect on outcome in 221 patients (85% received pre-operative chemotherapy; 582 liver metastases). Remark: per patient HGP used for outcome analysis was determined by selecting the 'worst' metastasis: pure replacement or mixed HGP.	Colorectal cancer	Non-desmoplastic HGP predicted shorter time to relapse in univariate and multivariate analyses (HRs 1,84 en 1,75, respectively). Patients with a favourable pathological score and a high immunoscore had the lowest risk of relapse (about 60% 5 yrs survival).
Temido M.	Cancer Management and Research	HGP was scored as dHGP (100%) versus any % of non-desmoplastic growth (17 patients).	Gastric cancer	dHGP was independently associated with improved OS (HR=0.1, p=0.02).

Bohlok A.	NPJ Breast Cancer 2020[42]	HGP was scored as 100% replacement (rHGP) versus 'any % of desmoplastic (any dHGP) (36 patients (11 patients with multiple metastases)).	Breast cancer	Any dHGP was independently associated with better PFS after liver surgery when compared with rHGP (HR=0.24, p = 0.009). All patients with rHGP relapsed within 20 months after liver surgery.
Jayme V.R.	Ann Surg Oncol 2021[101]	Tumour growth pattern of CRC liver metastases was defined as 'infiltrative' or 'pushing', according to Jass J.R. in 182 patients who underwent partial hepatectomy.	Colorectal cancer	Patients with infiltrative liver metastases (68% of patients) had worse OS and DFS, independent of surgical margin width.
Zhang Y.L.	Zhonghua Bing Li Xue Za Zhi 2021[102]	The dominant HGP was scored according to the international guidelines in 80 patients with partial hepatectomy.	Colorectal cancer	The 3-year PFS of patients with dHGP liver metastases (54%) was significantly longer compared with rHGP (40%). HGP was an independent prognostic factor for survival.
Höppener D.J.	JNCI Cancer Spectr 2021[19]	HGP was scored as dHGP (100%) versus any % of non-desmoplastic growth in international multicentre retrospective validation study (780 patients treated by liver surgery).	Colorectal cancer	The association of dHGP and good outcome was confirmed, independent of *KRAS* and *BRAF* status. The presence, not the extent, of a non-desmoplastic component, negatively impacts outcome.
Meyer J.M.	HPB (Oxford) 2021[103]	In a cohort of 155 patients with resected non-cirrhotic hepatocellular carcinoma (HCC), HGP (100% desmoplastic versus any % of replacement) and microvascular invasion (MVI) were scored.	Hepato-cellular carcinoma	Both non-dHGP and MVI were associated with worse outcome (OS, DFS) in multivariate analyses. For OS, there was effect modification between HGP and MVI, with patients with MVI and non-dHGP having the shortest survival time.
Vles M-J	HPB (Oxford) 2022[104]	In a cohort of 221 patients who received simultaneous resection and ablation as a first treatment for liver metastases, HGP was scored in the resected metastases (100% desmoplastic versus any % of replacement (non-desmoplastic)).	Colorectal cancer	A non-desmoplastic HGP of the resected metastases independently predicted local tumour progression adjacent to the post-ablation zone (HR of 1.55 (p = 0.04)).
Meyer Y	Clin Exp Metastasis 2022[48]	In a cohort of 132 patients with liver metastases from 25 different tumour types, HGP was scored (100% desmoplastic versus any % of replacement (non-desmoplastic)).	Non-colorectal, non-neuro-endocrine tumours	The HGPs could be identified in all tumour types. A desmoplastic HGP was associated with favourable outcome (OS: HR of 0.51 (p = 0.04); RFS: HR of 0.38 (p < 0.01)) upon multivariable analysis.
HGP and tumour biology				
Grossniklaus H.E.	Hum Pathol 2016[46]	Post-mortem histological liver analysis of 15 patients who died from metastatic uveal melanoma. Immunofluorescence staining for MMP9 and VEGF.	Uveal melanoma	Cancer cells in the 'infiltrative' growth pattern (resembling replacement HGP) do not express VEGF and MMP9, while cancer cells in the 'nodular' growth pattern (resembling pushing & desmoplastic HGP) express VEGF and MMP9. Hypothesis: infiltrative metastases originate in the sinusoidal space while nodular metastases originate in the portal tracts.
Ceausu A.R.	Anticancer Res 2018[105]	Double immunostaining for keratin8/18-vimentin and for E-cadherin-vimentin. The mesenchymal/epithelial hybrid phenotype cells were quantified (25 patients).	Colorectal, pancreatic and gastric cancer	All the liver metastases of pancreatic cancer had a replacement HGP; all the liver metastasis of gastric cancer had a pushing HGP; CRC liver metastases exhibited all 3 HGPs. Replacement and pushing type metastases have a higher amount of cancer cells with EMT phenotype than desmoplastic metastases.
Lazaris A.	J Pathol Clin Res 2018[106]	Immunohistochemistry (CD31 and CD34/Ki67; VEGF) to quantify microvessel density and blood vessels with endothelial cell proliferation (50 liver metastases of 50 patients). The dominant HGP was determined.	Colorectal cancer	Metastases with a desmoplastic HGP have a lower microvessel density than metastases with a replacement HGP. Endothelial cell proliferation was much higher in desmoplastic liver metastases unless systemic treatment was given prior to surgery. In chemo-naïve patients, there was no difference in VEGF-expression levels between both HGPs.

Wu J.B.	World J Gastroenterol 2019[107]	HGP was scored in the liver metastases and in the primary tumours (liver metastases from 29 patients with matching primary tumours). Additional histological parameters were assessed in the primary tumours. Whole exome sequencing (WES) was performed on 5 cases.	Colorectal cancer	15 cases with desmoplastic HGP and 14 cases with replacement HGP. High tumour budding score, absence of Crohn's disease-like inflammatory response and infiltrating HGP of the primary tumour were associated with replacement HGP. Small cohort with WES results.
Nierop P.M.H.	HPB Oxford 2019[24]	All available H&E-stained sections of all resected CRC liver metastases from 1302 patients were used for HGP scoring (100% desmoplastic versus any% of replacement). Hepatic resection margins were evaluated as positive or negative.	Colorectal cancer	Upon multivariate analyses, a non-desmoplastic HGP and number of metastases was associated with increased risk of positive resection margins.
Blank A.	Front Med 2019[108]	Tissue microarray of 81 primary tumours and 139 corresponding liver metastases. Tumour budding was scored in primary CRCs and in liver metastases (intra- and peri-metastatic) on H&E and pan-cytokeratin-stained section. The association of budding in the primary tumour and HGP of the liver metastases was not analysed.	Colorectal cancer	Assessment of budding only reliable in desmoplastic liver metastases without extensive ductular reaction. No clear association of budding in primary CRC and metastases.
Palmieri V.	J Pathol 2020[109]	RNA sequencing (16 liver metastases from chemo-naive patients: 7 predominant replacement HGP and 9 desmoplastic) and immunohistochemistry (20 liver metastases from chemo-naive patients: 10 replacement and 10 desmoplastic cases).	Colorectal cancer	*CXCL6* and *LOXL4* upregulated in replacement HGP metastases. LOXL4 protein is expressed in neutrophils at the tumour-liver interface of these metastases.
Ao T.	Virchows Archiv 2020[110]	The association of the type of desmoplastic reaction (mature, intermediate, immature) in the primary tumour and the liver metastases was investigated in 45 patients with synchronous liver metastases.	Colorectal cancer	A significant association was reported ($r=0.40$, $P = 0.0069$).
Bohlok A.	J Surg Oncol 2021[79]	The metabolic Clinical Risk Score (mCRS), which includes FDG-PET as a metabolic parameter, was compared with the HGP of liver metastases and the prognostic value of combining mCRS and HGP was assessed in 108 patients.	Colorectal cancer	Liver metastases with a 100% desmoplastic HGP had a significantly lower glucose-uptake (metabolic activity) than non-desmoplastic liver metastases. A low mCRS was associated with improved outcome in patients with dHGP liver metastases.
Rada M.	Commun Biol 2021[111]	Gene expression analyses and subsequent validation by immunohistochemistry in clinical samples of CRC liver metastases. Functional validation by targeted knock-down in CRC cancer cell lines and by using animal models.	Colorectal cancer	RUNX1 overexpression was shown to play a central in vessel co-option during replacement growth by inducing cancer cell motility and EMT. TSP1 and TGFbeta1 are involved in this process.
Burren S.	Pathol Res Pract 2021[112]	In a cohort of 76 patients with mismatch repair proficient CRC liver metastases, HGP and peripheral and central budding were scored.	Colorectal cancer	Liver metastases with a replacement HGP more often show budding in their centre than desmoplastic metastases.
Nierop P.M.H.	J Pathol Clin Res 2021[61]	In 3 cohorts of patients (n=877, 1203 and 70) the effect on pre-surgery chemotherapy on the HGP was assessed. The cohort of 70 patients belongs to a randomized clinical study.	Colorectal cancer	On average, the presence of a desmoplastic HGP increased with a factor of 1.5 when chemotherapy was administered before surgery. This was confirmed in the randomized study. The biology of the 'converted' metastases remains unclear.
Review manuscripts				
van Dam P-J.	Semin Cancer Biol 2018[32]	Key differentiating histopathological characteristics of the HGPs and their impact on tumour biology are described. The review sums up arguments to support the hypothesis that the HGPs of liver metastasis have distinct cancer immune set-points and, thus, might affect clinical management strategies when immunomodulatory treatment is considered.		

Donnem T.	Nat Rev Cancer 2018[113]	The discovery of non-angiogenic, vessel co-opting tumour growth is described as well as the biology of this means of vascularization and the implications for cancer treatment. The replacement HGP of liver metastases is discussed as one of the examples of non-angiogenic growth described in human studies.
Fernández Moro C.	BMJ Open Gastro 2018[49]	This review has identified all studies up to December 2017 that reported the HGPs in patients with liver metastatic CRC, the relative frequencies of these HGPs, and the association with outcome. In 14 out of 17 cohorts, a significant favourable outcome was reported for patients with desmoplastic liver metastases. In 8 out of 12 cohorts, a significantly unfavourable outcome for patients with replacement-type liver metastases was found. The authors found no studies that reported an opposite association between HGP and outcome.
Baldin P.	Acta Gastroenterol Belg 2018[114]	The review summarizes prognostic/predictive histopathological and molecular parameters for patients with liver metastatic colorectal cancer, the HGPs being one of these parameters. The authors argue for the integration of HGP in the pathology report.
Kuczynski E.A.	Nat Rev Clin Oncol 2019[115]	Evidence that tumours located in numerous organs can use vessel co-option as a mechanism of tumour vascularization is described, the liver with the replacement HGP of metastases being one of the highlighted organs. Molecular mechanisms and implications for patients are also discussed.
Caetano Oliveira R.	J Oncol 2019[116]	The prognostic significance, the biology and the therapeutic implications of the HGPs of CRC liver metastases are discussed. The authors propose to include the HGPs in the pathology report of resection of hepatic metastases.
Kuczynski E.A.	Angiogenesis 2020[117]	The authors collected evidence linking vessel co-option with resistance to anti-angiogenic drugs in numerous tumour types. In human studies of both primary hepatocellular carcinoma and liver metastases the non-angiogenic replacement growth pattern has been described. The authors list the studies in animals and humans that associate this growth pattern with resistance to anti-VEGF and/or anti-angiogenic compounds.
Latacz E.	Angiogenesis 2020[31]	The authors of this review hypothesize that common biological themes may be responsible for the HGPs of tumours in different organs, for example brain, lungs and liver. They further stress that cancer cell motility may be one of the driving forces behind the vessel co-opting (replacement) HGP.
Blazquez R.	Semin Cancer Biol 2020; 60: 324-333	Nine patterns of the macro-metastasis/organ parenchyma interface (MMPI) divided over 3 groups are described. The 3 subgroups are: 'displacing' (non-infiltrative) and two infiltrative MMPI-groups: 'epithelial' and 'diffuse'. An organ-independent MMPI assessment protocol is proposed.
Latacz E.	Semin Cancer Biol 2021[66]	The authors argue that, based on the (retrospective) studies discussed in this review, we will be able to identify HGPs of liver metastases through medical imaging soon. This will significantly encourage medical oncologists to implement HGPs in clinical practice. The most promising results were achieved in studies that developed a radiomic algorithm.
Caetano Oliveira R.	Semin Cancer Biol 2021[118]	This review focusses on the possibilities to identify the HGPs when a surgical liver resection specimen is not available (pre-surgery, in patients not eligible for surgical resection of their liver metastases, during systemic treatment to detect a change of HGP as a marker of response/resistance).
Rigamonti A.	Cancers 2021[119]	Parameters that predict clinical behaviour of CRC liver metastases are discussed in this review, the HGP being one of these parameters.
Kurebayashi Y.	Hepatol Res 2021[78]	The immune microenvironment of hepatocellular carcinoma, intrahepatic cholangiocarcinoma and CRC liver metastases is discussed. Although there is a clear relationship between immune cell infiltration and HGP, the authors conclude that the knowledge of the interaction between cancer cells in the liver, immune cells and non-immune stromal cells is still incomplete and can be expanded by single cell RNA-sequencing.
Garcia-Vicién G.	Int J Mol Sci 2021[120]	Several aspects of the liver microenvironment, such as the sinusoidal vasculature, the arterial and venous blood supply, and the specific mesenchymal and immune cell component, are addressed in the context of the HGPs of CRC liver metastases. The authors conclude that we still do not know what causes one or the other HGP when cancer cells arrive in the liver and form a metastasis.
Haas G	Front Cell Dev Biol. 2021[121]	Vessel co-option and the HGPs of liver metastases but also of tumours growing in other organs are discussed. The idea of the distinct metabolic status of cancer cells in the replacement HGP being a potential therapeutic target is launched in this review.
Rompianesi G	World J Gastroenterol 2022[122]	Review of studies implementing artificial intelligence (machine learning and deep learning) in the diagnosis and management of patients with CRC liver metastases. The authors conclude that an accurate identification of the HGPs (by medical imaging) could significantly improve individualized treatment approaches.

Abbreviations: CGH = comparative genomic hybridization; CRC = colorectal cancer; CRISPR = clustered regularly interspaced short palindromic repeats; CT = computed tomography; DFS = disease-free survival; dHGP = desmoplastic histopathological growth pattern; EMT = epithelial-to-mesenchymal transition; H&E = haematoxylin-and-eosin stained; HGP = histopathological growth pattern; HR = hazard's ratio; MMP = matrix metalloprotease; MRI = magnetic resonance imaging; mCRS = metabolic clinical risk score; NOD scid = nonobese diabetic severe combined immunodeficiency; MMPI = macro-metastasis/organ parenchyma interface; OS = overall survival; PFS = progression-free survival; PDX = patient-derived xenograft; RFS = relapse free survival; rHGP = replacement histopathological growth pattern; ROI = region of interest; TLI = tumour-liver interface; VEGF = vascular endothelial growth factor; WES = whole exome sequencing.

The desmoplastic and the replacement HGPs are the most common patterns, based on recent studies that have used the 2017 consensus guidelines (*table 1*). For example, either the desmoplastic or the replacement HGP was evident in 97.5% of the tumour-liver interface of all CRC liver metastases of 732 patients[18], almost equally distributed between both HGPs. In the desmoplastic HGP, the cancer cells are separated from the surrounding liver parenchyma by a fibrotic rim. Often a dense infiltrate of immune cells is present at the transition between the liver parenchyma and the fibrous rim. Desmoplastic liver metastases frequently show glandular differentiation (when derived from an adenocarcinoma) and are vascularised by a process of angiogenesis (*figures 1A-C*).[31]

In replacement-type liver metastases, cancer cells are in contact with the hepatocytes, they replace the hepatocytes, and, in the process, they co-opt the sinusoidal blood vessels of the liver. As a result, the tissue architecture of the metastases with this HGP mimics the tissue architecture of the liver, such that the metastatic cancer cells arrangement recapitulates 'hepatic cell plates' in between co-opted hepatic sinusoidal blood vessels. Typically, and based on observations done in carcinoma liver metastases, only a few immune cells are present at the tumour-liver interface and in the tumour centre[32], although this is not a scoring criterion. Adenocarcinoma metastases with a replacement growth pattern do not usually show glandular differentiation at the tumour-liver interface (*figures 1D-F*). Angiotropic extravascular migration has been observed in replacement-type liver metastases of melanoma[33] (see section dedicated to angiotropic extravascular migration): single or small clusters of melanoma cells may extend along sinusoidal channels into the surrounding liver parenchyma with distances of several millimeters.

Table 2. Key histopathological characteristics of the growth patterns of liver metastases.

	Desmoplastic	Replacement	Pushing	Sinusoidal	Portal (including intrabiliar)
General architecture	A desmoplastic rim separates metastatic tissue from liver tissue.	Cancer cells are arranged in plates in continuity with the hepatocyte plates.	Metastatic tissue pushes the liver tissue aside (without recognizable desmoplastic rim).	Cancer cells grow in the sinusoidal vessel lumina or in the Disse space, adjacent to the hepatocyte plates.	Metastatic tissue grows within portal tracts and septa and/or within the lumen of biliary branches
Liver architecture mimicry	-	+	-	+	n.a.
Liver stroma preserved	-	+	-	+	+
Contact of cancer cells with liver epithelial cells	Not with hepatocytes Occasional contact with cholangiocytes of ductular reaction	+ (hepatocytes)	-	-	With cholangiocytes if intrabiliary growth
Desmoplastic reaction around the metastasis	+	-	-	-	n.a.
Compression of liver cell plates	+	-/+	+	-	n.a.
Contour	sharp	irregular	sharp	irregular	n.a.
Inflammatory cell infiltrate	++	+/-	+/-	+/-	n.a.
Proliferation of bile ducts (ductular reaction)	+/-	-	-	-	-/+
Glandular differentiation (if adenocarcinoma)	+	-	+	-	+
	Figures 1A-C	Figures 1D-F	Figures 1G & H	Figure 1I	Figures 1J & K

The pushing growth pattern is an uncommon pattern. For example, the pushing HGP was present in only 2.5% of the tumour-liver interface of all CRC liver metastases of 732 patients.[18] This growth pattern is characterised by cancer cells that appear to push away the liver parenchyma without an intervening fibrous rim. Cancer cells do not invade the hepatocyte plates, they do not replace the hepatocytes, and they do not co-opt the sinusoidal blood vessels. The surrounding liver is composed of hepatocytes that are arranged parallel to the tumour-liver interface and appear slender because they are atrophic or compressed by the growing metastases (*figures 1G* and *1H*).

Liver metastases with a sinusoidal HGP are characterised by cancer cells in the sinusoidal vascular spaces (*figure 1I*).

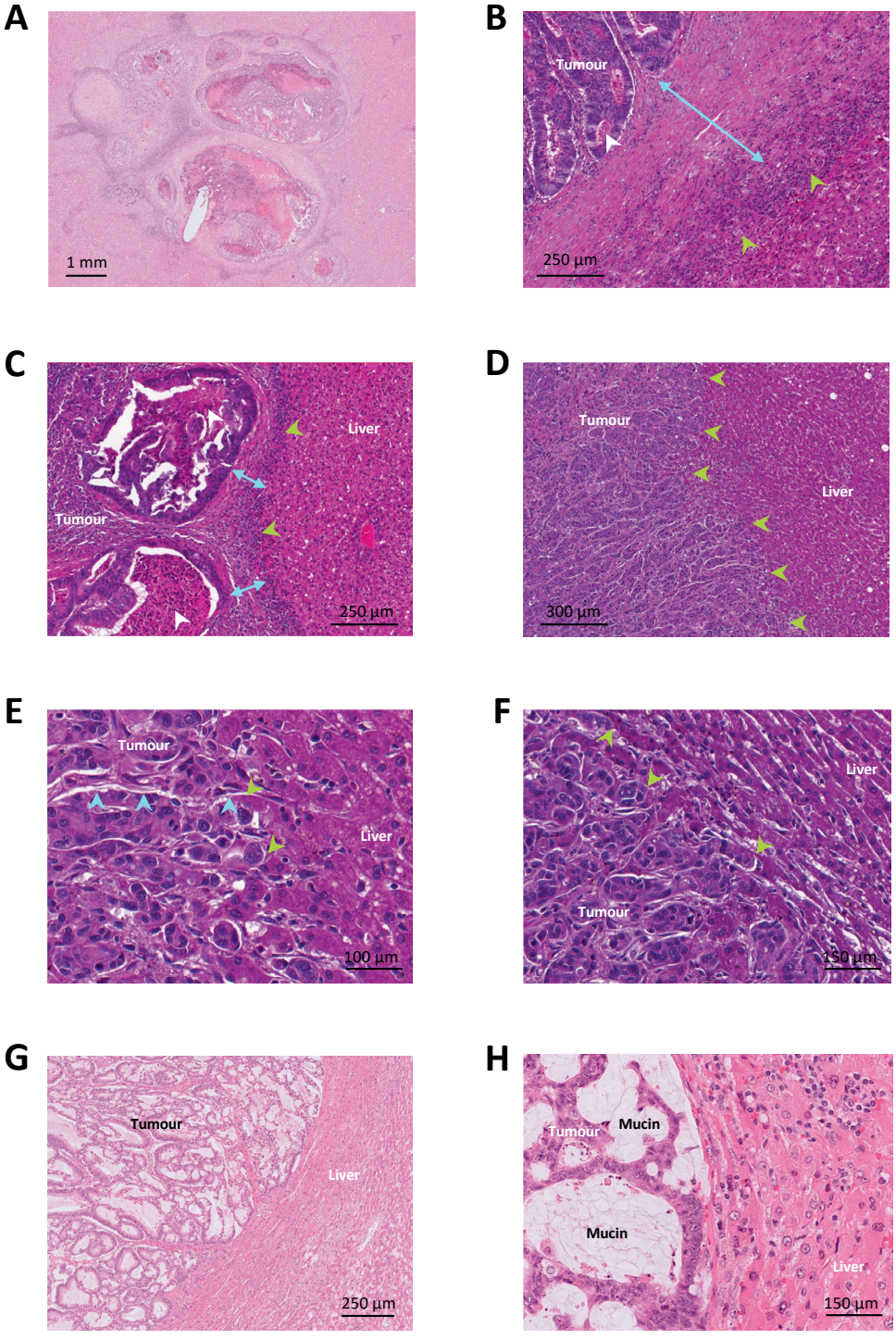
A
1 mm
B
Tumour
250 µm
C
Liver
Tumour
250 µm
D
Tumour
Liver
300 µm
E
Tumour
Liver
100 µm
F
Liver
Tumour
150 µm
G
Tumour
Liver
250 µm
H
Tumour
Mucin
Mucin
Liver
150 µm

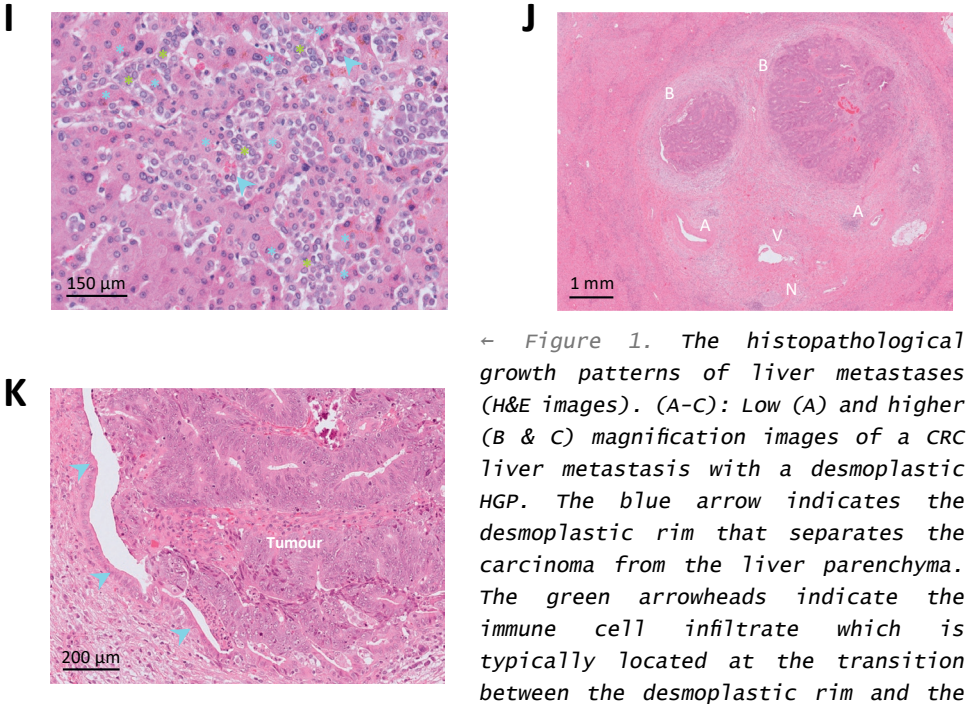

← *Figure 1. The histopathological growth patterns of liver metastases (H&E images). (A-C): Low (A) and higher (B & C) magnification images of a CRC liver metastasis with a desmoplastic HGP. The blue arrow indicates the desmoplastic rim that separates the carcinoma from the liver parenchyma. The green arrowheads indicate the immune cell infiltrate which is typically located at the transition between the desmoplastic rim and the liver parenchyma. The tumours show glandular differentiation and cell detritus in the lumina of these glandular structures, reminiscent of the histology of a primary CRC (white arrowheads). (D) Low magnification image of a CRC liver metastasis with a replacement HGP. The green arrowheads indicate the tumour-liver interface. There is no glandular differentiation: cancer cells from solid nests and trabeculae. (E) & (F) Higher magnification of the tumour-liver interface of CRC liver metastases with a replacement HGP. The green arrowheads indicate contact between cancer cells and hepatocytes. In (E), cancer cells form cell plates that are in continuity with the liver cell plates. A co-opted sinusoidal blood vessel is marked by the blue arrowheads. In (F), the liver cell plates are pushed aside but cancer cells are still in contact with hepatocytes while invading into these liver cell plates (green arrowheads). (G) Low magnification image of a CRC liver metastasis with a pushing HGP. (H) On higher magnification, a sharp tumour-liver interface is noticed without desmoplastic rim and without cancer cells invading into the liver parenchyma. Often metastases with a pushing HGP produce mucin, as shown in this example. (I) Lobular breast carcinoma liver metastasis with a sinusoidal HGP (autopsy case). Cancer cells are located within the lumen of sinusoidal blood vessels (green asterisks), in between liver cell plates (blue asterisks). Red blood cells are intermingled with the cancer cells (blue arrowheads). (J) Low magnification image of intrabiliary tumour growth (CRC) in a portal tract. The structures constituting a portal tract are present: artery branches (A), vein branch (V), nerve bundle (N), and branches of the bile duct (B), in this case filled with cancer cells. (K) Higher magnification of the left bile duct branch of image J. The normal bile duct epithelium (blue arrowheads) is still present but is replaced by cancer tissue that fills the lumen of the bile duct branch.*

The sinusoidal HGP appears limited to patients with aggressive disease and is more frequently encountered in autopsy specimens, which could imply that it is a feature of end-stage disease.[7,34-37] Liver metastases can also spread along the portal tracts. Cancer cells can invade the fibrous stroma of these tracts, fill the lumen of portal vein branches or the lymphatic vessels, or grow along nerves (neurotropism) and blood vessels (angiotropism). In addition, cancer cells can proliferate inside biliary ducts of the portal tracts by replacing the normal epithelial lining of these ducts (*figures 1J* and *1K*).

Tumour type-dependent differences in the growth patterns have been described. For example, when comparing the replacement HGP in breast cancer metastases and CRLM, the histological characteristics of replacement growth were often present from the tumour-liver interface and up to the centre of the metastases in the breast cancer cases, while they were limited to the interface in all CRLM.[38] Also, the presence of single cancer cells in the liver parenchyma at a distance from the tumour-liver interface in replacement-type liver metastases (so called angiotropic extravascular migration) appears to be more obvious in melanoma liver metastases than in liver metastases of CRC or other carcinomas (unpublished observations).

Update of the cut-off value to categorise patients with colorectal cancer according to the histopathological growth pattern of the liver metastases

Given that a single liver metastasis can be composed of regions with different growth patterns, this histological parameter is assessed by estimating the relative fraction of the total length of the interface for each growth pattern present in the metastasis. In cases of multiple sections per metastasis or multiple liver metastases per

patient, the mean percentage across sections and lesions, respectively, is calculated.[1] In the previous version of the scoring guidelines, a 50% cut-off was proposed to categorise patients, based on its prognostic value. This approach generated four distinct HGP classes: ‘predominant desmoplastic’, ‘predominant replacement’, ‘predominant pushing’ and a ‘mixed’ class in the absence of a predominant HGP. Multiple studies have demonstrated a favourable outcome in patients with CRC liver metastases with a predominant desmoplastic HGP (*table 1*).

However, the results of a study by Galjart and colleagues from the Erasmus Medical Centre in Rotterdam[18] provide a strong rationale for revising the cut-off value used to clinically categorise patients with CRC liver metastases according to the HGP. The study compared different cut-offs based on a large dataset of patients with CRLM. The results suggest that the prognosis of patients with resected CRC liver metastases is primarily determined by the presence of a replacement and/or a pushing growth pattern as opposed to a pure desmoplastic growth pattern (corresponding to 100% of the assessed tumour-liver interface). Favourable survival rates were demonstrated only for patients with liver metastases with complete desmoplastic growth, a condition present in 24% of all patients included in the study by Galjart et al (2019).[18] Remarkably, non-desmoplastic growth - of any fraction - reduced the 5-year OS rate from 78% to 37% in the cohort of patients who did not receive pre-surgery systemic treatment (adjusted HR 0.39; 95% CI: 0.23-0.67) and from 53% to 40% in the cohort of patients who did receive pre-surgery systemic treatment (adjusted HR 0.92; 95% CI: 0.64-1.30). This difference in outcome was recently confirmed in a large multicentre external validation study.[19]

We now present a comprehensive clinical evaluation of a large international multicentre cohort of 1931 patients with CRC in which we assessed the impact on outcome using the recent 'Rotterdam cut-off'[18,19] compared to the 'predominant HGP cut-off' described in the original international consensus guidelines[1]. The clinicopathological baseline and treatment characteristics are summarised in *table 3*.

Table 3. Clinicopathological baseline and treatment characteristics

		missing (%)	n = 1931 (%)
Cohort	Erasmus MC		903 (47)
	MSKCC		716 (37)
	Radboud UMC		312 (16)
Age at resection CRLM - *(median [IQR])*			64.0 [56.0, 71.0]
Gender	Male		1170 (61)
	Female		761 (39)
ASA classification	ASA I-II	*39 (2)*	1284 (68)
	ASA >II		609 (32)
Primary tumour location	Left-sided	*62 (3)*	458 (25)
	Right-sided		798 (43)
	Rectal		613 (33)
T-stage	pT 0-2	*87 (5)*	287 (16)
	pT 3-4		1557 (84)
N-stage	N0	*31 (2)*	729 (38)
	N+		1172 (62)
Number of CRLM - *(median [IQR])*		*12 (1)*	2.0 [1.0, 3.0]
Largest CRLM in cm - *(median [IQR])*		*35 (2)*	2.8 [1.9, 4.5]
DFI in months* - *(median [IQR])*		*14 (1)*	1.0 [0.0, 17.0]
Synchronous (DFI ≤3 months)	Synchronous		1023 (53)
	Metachronous		908 (47)
Preoperative CEA in µg/L - *(median [IQR])*		*143 (7)*	11.0 [4.0, 33.7]
Perioperative chemotherapy	No chemotherapy	*41 (2)*	773 (41)
	Neoadjuvant only		689 (36)
	Adjuvant only		232 (12)
	Perioperative		196 (10)
Resection margin involved	No	*10 (1)*	1675 (87)
	Yes		247 (13)
Extrahepatic disease**	No		1731 (90)
	Yes		200 (10)

**Between resection of primary tumour and detection of CRLM*
***Defined as any extrahepatic disease with the exception of the primary tumour present at the time of or prior to first CRLM surgery.*
Abbreviations in alphabetical order: ASA: American Society of Anaesthesiologists; CEA: carcinoembryonic antigen; CRLM: colorectal liver metastasis; DFI: disease-free interval; Erasmus MC: Erasmus MC Cancer Institute; IQR: interquartile range; MSKCC: Memorial Sloan Kettering Cancer Center; Radboud UMC: Radboud University Medical Center.

The median follow-up for survivors was 67 months (IQR: 34 – 112 months). When applying the Rotterdam cut-off, 1516 (79%) patients had non-desmoplastic liver metastases and 21% had pure desmoplastic liver metastases. Of the 1516 patients with a non-desmoplastic HGP, 201 (10%), 549 (28%), 305 (16%), and 461 (24%) patients had liver metastases with a 100%, 67.1-99%, 33.1-67%, and 0.1-33% non-desmoplastic HGP, respectively (*table 4*). When patients were classified according to the predominant HGP cut-off, 839 (43%) patients had liver metastases with a predominant replacement HGP, 19 (1%) with a predominant pushing HGP, 1031 (53%) with a predominant desmoplastic HGP, and 42 (2%) with a mixed HGP (*table 4*). The following findings support the 'Rotterdam cut-off':

1. Patients with resected CRC liver metastases that possess an exclusively desmoplastic growth pattern have a clear survival advantage over all other patients. Median OS (months (95% CI)) for desmoplastic versus non-desmoplastic patient cohorts is 88 (77-112) versus 53 (49-58) months, respectively. Median DFS for desmoplastic versus non-desmoplastic patient cohorts is 24 (20-33) versus 11 (11-12) months, respectively (*figures 2A* and *2B*, *table 4*). The adjusted HRs for OS and DFS (95% CI) are 0.64 (0.52-0.78) and 0.61 (0.52-0.71), respectively (*table 4*).
2. There is no difference in survival among patients belonging to the discrete non-desmoplastic classes (*figures 2C* and *2D*, *table 4*). This probably explains why the survival advantage of the favourable patient cohort over the unfavourable patient cohort is less pronounced when the predominant HGP cut-off algorithm is used (*figures 2E* and *2F*, *table 4*). For example, the adjusted HR for OS is 0.64 (95% CI: 0.52-0.78) versus 0.76 (95% CI: 0.65-0.88) respectively, when comparing the Rotterdam and the 'predominant HGP' cut-offs (*table 4*). A similar difference of 0.61 (95% CI: 0.52-0.71) versus 0.82 (95% CI: 0.73-0.93) can be observed for DFS (*table 4*).

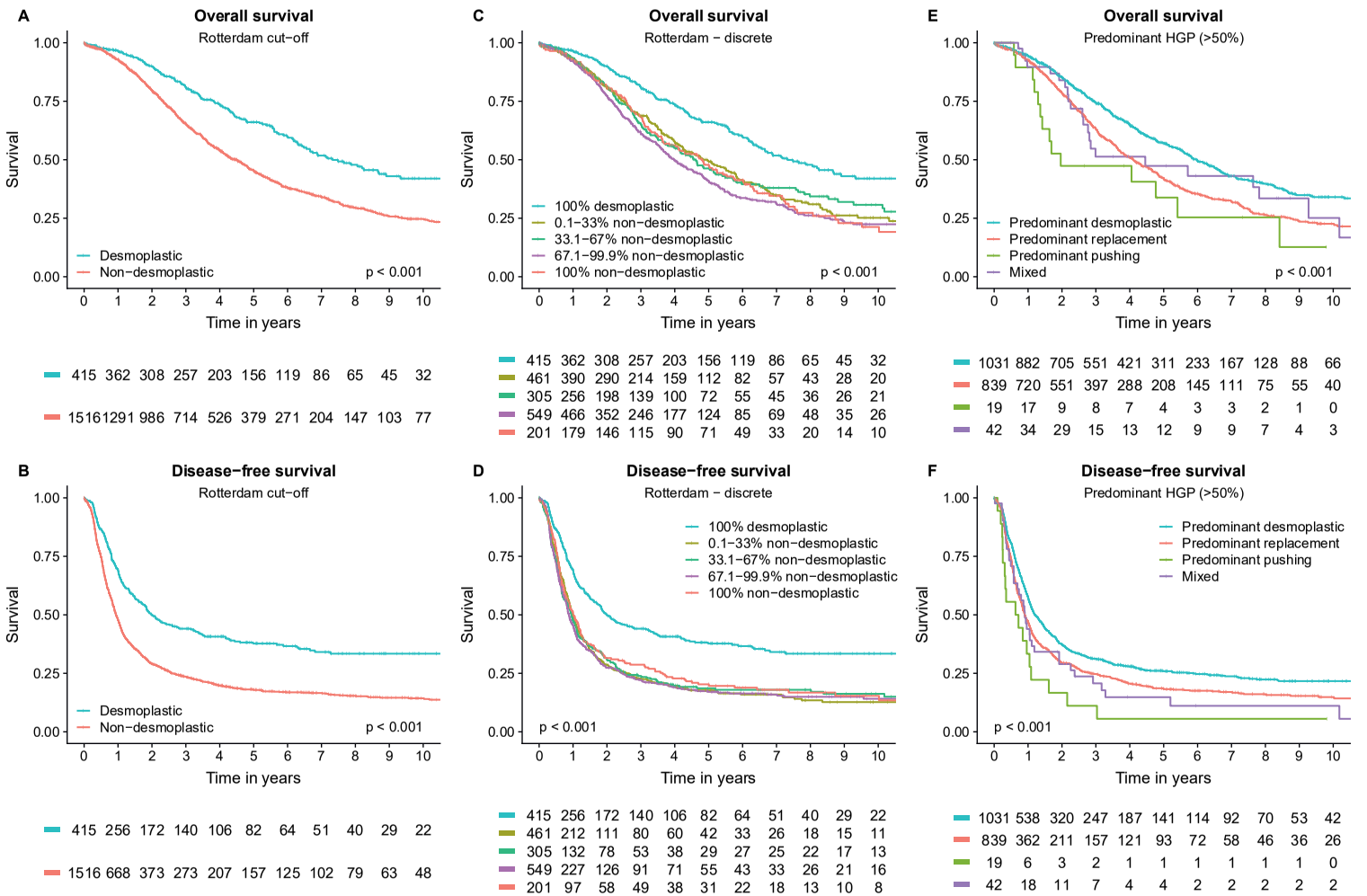

Figure 2. Kaplan-Meier curves depicting overall and disease-free survival of patients with colorectal liver metastases following resection, stratified by the new cut-off for HGP categorisation (A to D) and by the predominant HGP (E and F).

Table 4. Overall and disease-free survival estimates for different HGP cut-offs in 1931 patients treated with curative intent resection for CRLM

		Overall survival (95%CI)				Disease-free survival (95%CI)			
Cut-off	n (%)	5 year - %	10 year - %	Median - *months*	Adjusted HR*	5 year - %	10 year - %	Median - *months*	Adjusted HR*
Entire cohort	1931 (100)	50 (47-53)	28 (26-32)	60 (56-65)	-	22 (20-24)	18 (16-21)	13 (12-13)	-
Rotterdam cut-off									
Non-desmoplastic	1516 (79)	45 (42-48)	25 (22-28)	53 (49-58)	*reference*	18 (16-20)	14 (12-17)	11 (11-12)	*reference*
Desmoplastic	415 (21)	66 (61-72)	42 (35-50)	88 (77-112)	0.64 (0.52-0.78)	38 (33-43)	33 (28-39)	24 (20-33)	0.61 (0.52-0.71)
Rotterdam cut-off - discrete									
100% non-desmoplastic	201 (10)	48 (41-56)	21 (14-31)	57 (44-69)	*reference*	20 (15-27)	15 (10-23)	12 (10-15)	*reference*
67.1-99.9% non-desmoplastic	549 (28)	41 (36-46)	22 (18-28)	48 (44-55)	1.13 (0.89-1.45)	17 (14-21)	14 (11-18)	11 (10-12)	1.10 (0.89-1.35)
33.1-67% non-desmoplastic	305 (16)	46 (40-54)	31 (24-39)	55 (45-66)	0.95 (0.72-1.25)	19 (14-24)	16 (12-22)	11 (10-13)	0.99 (0.79-1.25)
0.1-33% non-desmoplastic	461 (24)	49 (44-55)	25 (20-32)	58 (51-70)	1.05 (0.81-1.36)	18 (14-22)	13 (9-17)	12 (11-13)	1.05 (0.85-1.31)
100% desmoplastic	415 (21)	66 (61-72)	42 (35-50)	88 (77-112)	0.67 (0.51-0.88)	38 (33-43)	33 (28-39)	24 (20-33)	0.64 (0.51-0.80)
Predominant HGP cut-off (>50%)									
Predominant replacement	839 (43)	42 (38-46)	23 (19-27)	49 (45-56)	*reference*	18 (16-22)	15 (12-18)	11 (10-12)	*reference*
Predominant pushing	19 (1)	34 (17-66)	*NA*	24 (17-*NA*)	1.03 (0.55-1.95)	6 (1-37)	*NA*	8 (4-19)	1.12 (0.64-1.95)
Mixed	42 (2)	47 (33-69)	25 (11-55)	53 (33-129)	1.04 (0.65-1.68)	15 (7-32)	11 (4-29)	11 (8-23)	1.23 (0.84-1.78)
Predominant desmoplastic	1031 (53)	57 (53-61)	34 (30-39)	72 (67-79)	0.76 (0.65-0.88)	26 (23-29)	22 (19-25)	14 (13-17)	0.82 (0.73-0.93)

**Multivariable regression model (n=1565 included in full-case analyses) corrected for age, gender, ASA class, primary tumour location, T-stage, nodal status, disease-free interval (continuous), number of CRLM (continuous), size of largest CRLM (continuous), preoperative CEA (continuous), extrahepatic disease, resection margin status, and perioperative systemic chemotherapy.*

Abbreviations in alphabetical order: ASA: American Society of Anaesthesiologists; CEA: carcinoembryonic antigen; CRLM: colorectal liver metastasis; HGP: histopathological growth pattern; HR: hazard ratio; NA: not available.

3. The learnability and accuracy of HGP-scoring according to the new cut-off have been shown to be high.[39] Moreover, this algorithm represents a simplified method of HGP scoring when considering prognostic impact. Indeed, when a non-desmoplastic component (replacement or pushing) is detected while analysing a series of H&E-stained sections from a patient, the result is clear, and no further scoring is required. However, for scientific research purposes, and to further validate the new cut-off, care should be taken not to compromise the acquisition of more detailed quantitative data and assessing the HGPs in all the available H&E-stained sections of all the resected liver metastases is still preferred.

The international group of authors of this second consensus guidelines for scoring HGPs of hepatic metastases therefore proposes to test this algorithm in prognostic studies with other primary tumour types as well. In studies that aim at deciphering the molecular underpinnings of the different growth patterns, a cut-off agnostic approach should probably be adopted, to not obscure lessons to be learned from inter-tumour heterogeneity of the HGPs.

Categorisation of the histopathological growth patterns of non-CRC liver metastases

Distinct HGPs have been identified in liver metastases from a broad range of primary solid tumours, mostly carcinomas. The replacement (also referred to sometimes as 'replacing', 'trabecular' or 'infiltrative') growth pattern, the desmoplastic growth pattern (also sometimes called 'encapsulated') and the pushing growth pattern (also sometimes called 'expansive') have been described in liver metastases from primary lung, pancreatic, stomach, gallbladder/bile duct and breast carcinoma.[5,38,40-42] The study of HGPs in liver metastases from these tumour types is relevant given that, for example, about 11% of patients with lung carcinomas, 36% of patients with pancreatic carcinoma, and 14% of patients with stomach cancer have liver metastases at diagnosis.[43] The sinusoidal growth pattern has been encountered in autopsy specimens of patients with non-small cell lung cancer (NSCLC) and breast cancer.[7,34-37] In addition to carcinomas, the desmoplastic, pushing, replacement and sinusoidal growth patterns have also been identified in hepatic metastases of both skin and uveal melanoma.[44-46] Additional types of HGP have also been described in uveal melanoma, however without evaluation of the interface between liver metastases and the surrounding liver tissue.[46,47] In these studies, the different results reported may be ascribed to the sources of material studied;

almost entirely derived from autopsies, and of partial biopsy samplings. The HGPs have recently also been identified in sarcoma-derived hepatic metastases, in a study describing the HGPs in a cohort of patients with non-colorectal, non-neuroendocrine liver metastases.[48]

Although the prognostic/predictive role of the HGPs has been studied mainly in patients with CRC[1,18,19,49], there are recent reports on the impact of the HGPs on outcome in patients with liver metastatic melanoma, breast carcinoma and pancreatic cancer.[5,42,44,45] In a study of 42 patients with skin melanoma, the presence of any replacement HGP (1% of the tumour-liver interface or more), present in 20 patients (48%), significantly predicted worse overall survival while the 100% desmoplastic HGP correlated with improved OS, an effect that continued to be significant upon multivariate analysis (HR = 3.79, p = 0.01).[45] In a study of 41 patients with liver metastatic uveal melanoma, the dominant HGP (>50% of tumour-liver interface) was used to categorise patients.[44] A dominant replacement HGP, present in 30 patients (73%), predicted diminished OS with a HR in multivariate analysis of 6.51 (p = 0.008). An updated analysis with extension of the patient cohort and categorisation according to the 100% desmoplastic HGP cut-off has recently been completed (Barnhill et al, manuscript in preparation).

The HGPs of breast cancer liver metastases have only been sporadically studied and have been mainly described in autopsy specimens.[34,35,38,41] In this context, and when compared with CRC liver metastases, the replacement HGP and even the sinusoidal HGP are more frequently encountered in breast cancer liver metastases. Surgical removal of breast cancer hepatic metastases is still rarely practiced. However, there is a subpopulation of patients with liver metastatic breast carcinoma for whom a favourable course

after resection has been documented, contradicting the common idea that breast cancer is always a systemic disease[50] and a rationale behind ongoing clinical trials, for example BreCLIM-2 (ClinicalTrials.gov Identifier: NCT04079049). With this in mind, Bohlok et al (2020)[42] have scored the HGPs in 36 patients who underwent surgical resection for breast cancer liver metastases. Given that only one patient presented with liver metastases with a pure desmoplastic HGP while 16 patients had liver metastases with a pure replacement HGP, a pragmatic approach was adopted to categorise patients as having liver metastases with '100% replacement' versus 'any desmoplastic' HGP. The study confirmed the association of replacement HGP liver metastases with poor outcome as observed with other tumour types. Indeed, all patients with a pure replacement HGP relapsed within 2 years after surgery. In addition, even in this small cohort of patients, improved OS was observed for patients with 'any desmoplastic' HGP liver metastases as compared to the other patients upon multivariate analysis (HR = 0.20, p = 0.023).[42] A large international study has recently been undertaken by several authors of the guidelines to further address the impact of the HGPs on outcome in patients with liver metastatic breast cancer.

More than one-third of patients with neuroendocrine tumours (NETs) present with distant disease, with the liver being the most common metastatic site. Although newer therapeutic options are becoming available, resection of NET liver metastases is still often performed.[51] Given the broad spectrum of NETs, from well-differentiated NETs to poorly differentiated neuroendocrine carcinomas, it would be interesting to study the HGPs of NET liver metastases. To the best of our knowledge, this has not been done yet.

In conclusion, the distinct HGPs can be identified independently of the primary solid tumour type and the desmoplastic HGP is invariably associated with better outcome than the replacement HGP, after surgical removal of liver metastases. This is consistent with the idea that common, tumour type-independent and liver-specific biological programs are activated in liver-metastatic cancer cells and shape growth pattern emergence in the liver.[52]

Clinical significance of the pushing growth pattern

The prognostic/predictive value of the pushing HGP is still unclear. Before the first international guidelines were published, there were no unequivocal instructions for distinguishing the pushing HGP from the replacement HGP where tumour cells appear to push away the liver parenchyma (so called pushing-type or type-2 replacement HGP).[1] As a result, the proportion of metastases with a pushing HGP has been overestimated in studies carried out prior to the publication of the first consensus guidelines.[49] For example, Nielsen et al. (2014)[53] and Eefsen et al. (2015)[54] reported that 45% of the patients with resected CRC liver metastases presented with a dominant pushing HGP. By applying the consensus guidelines of 2017, the proportion of metastases with a pushing HGP was found to be reproducibly smaller across more recent studies. In the study by Galjart et al. (2019)[18] for example, less than 1% of patients presented with a dominant pushing HGP in their CRC liver metastases. Determining the clinical value of the pushing HGP will therefore only be possible in large multi-centre studies.

The histopathological growth patterns and treatment response

Several observations suggest that systemic treatment can alter the HGP of liver metastases. In the study by Frentzas et al. (2016)[41], the growth pattern of recurrent CRLM,

defined as those metastases that were not detectable by imaging before systemic treatment but appeared during bevacizumab-chemotherapy, was compared with the growth pattern of metastases that were already visible before systemic treatment. The recurrent metastases more often demonstrated a replacement HGP when compared to the metastases that were already visible before systemic treatment (80% versus 50%). In support of these observations, several preclinical studies have demonstrated the switch from an angiogenic to a vessel co-opting growth pattern associated with resistance to treatment with anti-VEGF drugs in several malignancies. These include hepatocellular carcinoma[55], lung metastases of renal cell carcinoma[56], brain metastases of melanoma[57] and glioblastoma[58].

Other studies[59,60] found associations between systemic treatment of patients with CRLM and histological characteristics that are highly suggestive of replacement growth. The so-called ‘dangerous halo’ consists of an irregular tumour-liver interface in a CRLM that was seen selectively in patients that received chemotherapy before partial hepatectomy. Although beyond the scope of the Mentha et al. study, the histological images in their report show that the ‘dangerous halo’ consists of areas of replacement growth while the lesion without the ‘dangerous halo’ has a desmoplastic HGP (Figure 1 in Mentha et al. (2009)[59]). Taken together, the findings of Frentzas et al. (2016)[41] and the reports on the ‘dangerous halo’[59,60] link the replacement HGP to chemotherapy resistance with or without anti-VEGF treatment in patients with liver metastatic colorectal cancer.

There are, however, studies suggesting that chemotherapy induces the desmoplastic growth pattern in patients with replacement-type CRLM.[18,61] Nierop and colleagues (2021)

[61] have assessed the HGP of resected liver metastases in three cohorts of respectively 877, 1203 and 70 patients with CRC, respectively. The latter cohort was derived from a phase III clinical trial in which patients were randomised between either peri-operative chemotherapy and resection or resection only. In all three cohorts, the average presence of the desmoplastic HGP at the tumour-liver interface was significantly higher in patients with pre-operative chemotherapy compared to chemo-naïve patients (67% versus 43%, 63% versus 40%, and 61% versus 33%, respectively ($p<0.005$)). The fact that this shift in HGP was observed in a randomised study is consistent with a lack of selection in the association of pre-operative chemotherapy and the desmoplastic HGP. However, it remains to be determined whether chemotherapy induces a transformation of replacement-type liver metastases into lesions that form a desmoplastic rim or whether pre-existing desmoplastic lesions are more resistant to chemotherapy.

Taken together, it appears that a transition from one HGP to another could occur in patients with CRLM following systemic treatment. However, despite all the studies discussed above, a reliable assessment in individual patients of the effect of systemic treatment on the HGPs of liver metastases will only be possible when non-invasive imaging (as discussed below) or blood analyses will be available to identify the HGPs at several time points during treatment. One promising blood marker was recently proposed.[16] Circulating extracellular vesicles (EVs) derived from patients with replacement-type CRLM exhibited significantly higher protein expression of Claudin-2 relative to EVs isolated from patients with desmoplastic liver metastases. Thus, high protein levels of Claudin-2 in EVs isolated in the blood circulation of patients with liver metastatic CRC may predict the replacement HGP in CRLM.

Standard method for assessment of the histopathological growth patterns of liver metastases

The updated consensus guidelines for tissue sampling of surgical liver resections and for scoring and reporting of the HGPs of liver metastases are presented in *table 5*.

Table 5. Standard method for histopathological growth pattern assessment of liver metastases.

- Sampling of resection specimens:
  - ◇ Complete sampling (tumour-liver interface and centre) of metastases up to 2 cm.
  - ◇ Sampling of a complete central section (tumour-liver interface and centre) of metastases larger than 2 cm.
  - ◇ If an alternative sampling method is applied, for example a tumour-type specific approach, this should be reported.
- The growth pattern is a histological parameter assessed by light microscopic imaging of good quality H&E sections of FFPE tissue of resection specimens of liver metastases. Tissue cores from needle biopsy procedures are not suitable for HGP assessment. Resection specimen tissue sections with only a limited part of the tumour-liver interface are considered insufficient to assess the growth pattern of liver metastases. Also, if no viable tumour tissue is present in the metastasis, the growth pattern cannot be assessed. Delayed fixation (autopsy cases), surgical cautery or radiofrequency ablation artifacts may lead to insufficient quality of the tissue sections for scoring the growth patterns.
- The histological growth patterns of liver metastases can be evaluated by a pathologist or by any other investigator trained by a pathologist. The authors of the guidelines may be contacted for training sessions.
- The growth pattern is a characteristic of the tumour–liver interface, more specifically the interface with the adjacent non-tumorous hepatic lobular tissue. The centre of the metastasis does not contribute to the classification of a growth pattern.
- The three common growth patterns are: desmoplastic, pushing and replacement.
- The sinusoidal growth pattern is rare. In addition, metastases can grow in portal tracts and inside biliary ducts.
- When more than one growth pattern is present in a metastasis: estimate the relative fraction of each growth pattern as a percentage of the total length of the interface*.
- In case of multiple metastases/patient: assess the growth pattern(s) in every individual liver metastasis.
- Reporting of the HGPs per patient*:
  - ◇ For each metastasis (defined by its largest diameter), report the proportion of the interface with replacement, desmoplastic and pushing HGP (for example: ‘metastasis 1: 20% replacement, 80% desmoplastic, 0% pushing).
  - ◇ Small areas with a distinct HGP covering less than 5% of the

interface should still be reported.
  - ◇ The presence of intrabiliary, portal and sinusoidal growth should be reported as a separate remark.
  - ◇ ‘Escape’ should be reported as being absent or present in metastases resected after chemotherapy.
- The categorisation of a patient according to the growth pattern of a liver metastasis or of multiple metastases will depend on the primary tumour type and the aim of the growth pattern assessment.
- Caveats and practical tips:
  - ◇ Portal tracts at the tumour–liver interface and growth near the liver capsule (facing the peritoneal surface or soft tissue without intermediate liver parenchyma) should not be considered as part of the tumour–liver interface.
  - ◇ Metastatic growth inside portal tracts or biliary ducts should not be regarded as desmoplastic growth.
  - ◇ o The presence and extent of intrabiliary tumour growth can be underestimated, as the biliary epithelium is often replaced by cancer cells which eventually fill the lumen with accompanying necrosis.
  - ◇ o Reactive proliferation of bile ducts (ductular reaction) in the desmoplastic rim can simulate a replacement growth pattern. In addition, cancer cells can build common structures with the reactive bile ductuli.
  - ◇ In case of severe inflammation and associated tissue changes it may be difficult to identify the growth patterns. The presence of co-opted hepatocytes and tumour cell-hepatocyte contact in the periphery of the metastasis are indicative of the replacement growth pattern. Immunohistochemistry or silver impregnation staining of the sections (e.g., Gordon- Sweet’s reticulin staining) may be helpful to identify the growth patterns.
  - ◇ Pushing-type of growth should not be overestimated: only when there is no cancer cell-hepatocyte contact, the pushing HGP can be considered.

**Remark: Specific scoring and reporting rules may apply to certain tumour types and settings. For example, when the HGPs are assessed to obtain prognostic information in a patient with CRLM, it will be sufficient to look for areas of replacement HGP to distinguish a non-desmoplastic from a desmoplastic status.*

The proposed sampling guidelines are not based on published experimental evidence but are rather an empirical approach. [62] Given that the invasion front of liver metastases is often heterogeneous in respect to HGPs, a balance must be struck between accurate assessment of growth patterns and practical feasibility of sampling in a pathology laboratory. In addition, the sampling procedure may be tumour-type

dependent. For example, when dealing with CRLM, a two-step approach can be envisaged for clinical routine, given that the presence of any proportion of the interface with a non-desmoplastic HGP in any of the resected metastases has clear prognostic significance.[18,19] Initial sampling or scoring may consist of a limited number of paraffin blocks and in the event that a region with a non-desmoplastic growth is identified in the H&E-stained sections, the patient will be categorised into the corresponding HGP group. In accordance with our proposed updated guidelines, additional and more extensive sampling or scoring will only be necessary if no regions with non-desmoplastic growth are encountered at initial sampling or scoring.

In reporting the HGPs of liver metastases, several factors will need to be considered. The context of HGP assessment and the primary tumour type need to be considered because they will determine how a patient will be categorised based on the liver metastasis HGP. For example, for patients with CRLM, the HGP can provide prognostic information. For these patients, categorisation can, therefore, be based on the cut-off specified in the current guidelines. For other primary tumour types, large studies that have defined a clinically relevant cut-off value are still lacking and data reporting should be as precise as possible, in order for the HGP-score to be available for future data analyses because predictive and prognostic HGP cut-off values may be different for different primary tumour types.

There are essentially two ways to report HGPs when multiple metastases are resected. One approach simply averages the scores for each HGP (desmoplastic, replacement, pushing) across every available H&E-stained section for all the resected metastases. The other approach uses an average of the scores for each HGP of all the available H&E-stained

sections for each individual metastasis separately and reports a score for every metastasis that has been resected. The latter approach may be used when biological differences between metastases are expected, for example related to a difference in response to pre-surgery systemic treatment. With the aim of identifying the presumed treatment-induced transition towards the replacement HGP in future studies, we propose the following clinicopathological definition of an 'escape' phenotype: 'Liver metastases resected after pre-operative systemic treatment combining signs of pathological response in the centre of the metastases while also exhibiting at least a partly preserved desmoplastic rim and small peripheral areas of replacement-type outgrowth or a complete halo of replacement growth'. Typically, these areas of replacement growth do not show any of the characteristic signs of treatment response, as shown in examples in *figure 3*. Further information on the clinical value of this phenotype and its biological underpinning will be derived from future studies on the HGPs of liver metastases. We therefore propose to score the presence or absence of 'escape' in liver metastases that are resected after administration of systemic pre-operative treatment.

Immunohistochemical staining as an aid to scoring HGPs
In some liver metastases, the histology is more complex, and this can result in a less straightforward assessment of the HGPs. The 'caveats' are listed in the *table 5*. Although the assessment of HGPs of liver metastases is based exclusively on H&E-stained tissue sections, additional immunohistochemical analyses may provide clarity when these challenging conditions arise.

One example is the presence of an extensive immune cell infiltrate that obscures the tumour-liver interface. In this case, the presence or absence of contact between tumour cells

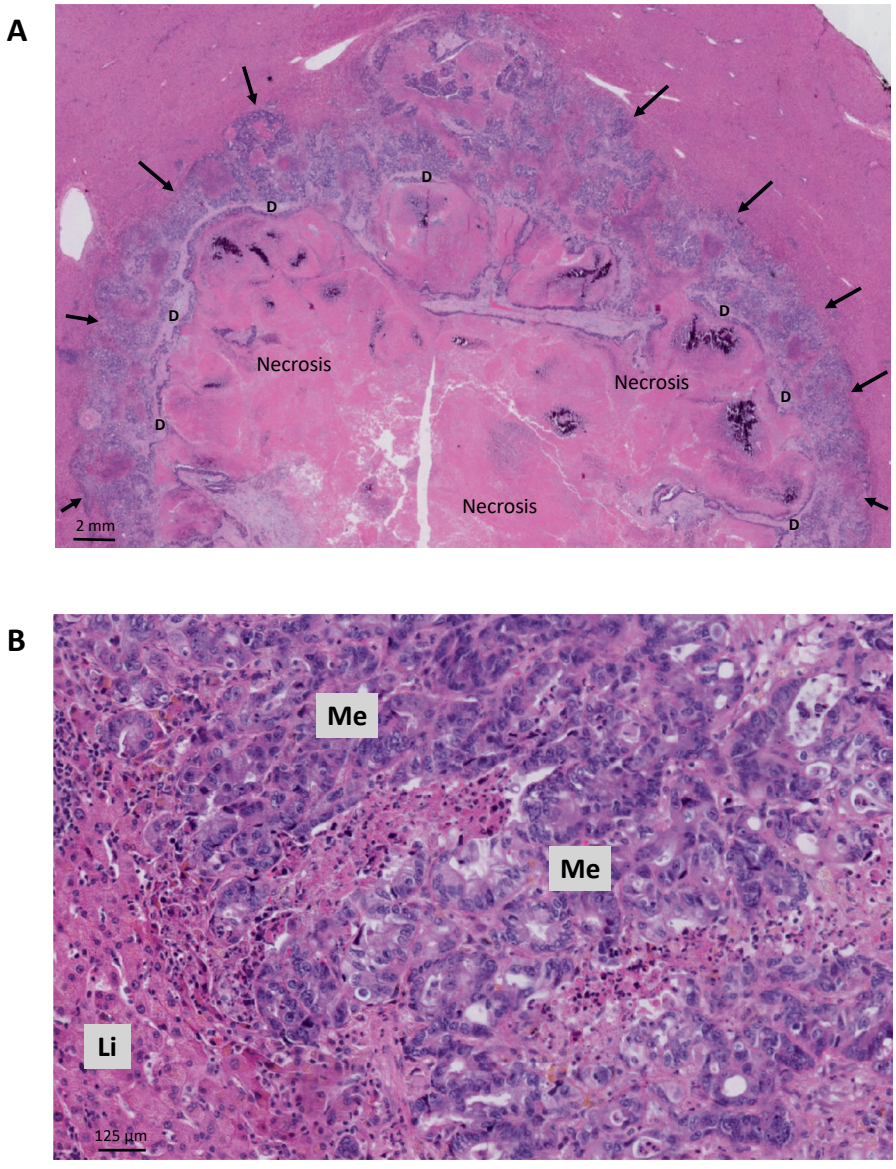

Figure 3. H&E image of the escape phenotype. (A) Low magnification image with large necrotic areas in the centre of the CRC liver metastasis, remnants of the desmoplastic rim (d) and vital replacement-type outgrowth at the tumour-liver interface (arrows). This is a 'halo' of vital cancer infiltrating the liver tissue for several millimetres at the periphery of the metastasis, with signs of response in its centre. (B) Higher magnification of the 'escape' area with replacement HGP. Li, liver; Me, metastatic tumour tissue.

and hepatocytes and the degree of hepatocyte co-option will determine whether the replacement HGP must be considered. A double immunostaining approach coupling a hepatocyte marker and a tumour cell marker can also be useful in such cases. For example, for liver metastases from a colorectal carcinoma, the combination of antibodies directed against caudal type homeobox 2 (CDX-2), cytokeratin (CK) 20 or CK19 (tumour cells) and Hepar-1, arginase1, or CK18 (hepatocytes) can be used (*figure 4A*). This immunostaining may also help to distinguish a replacement HGP in which the liver cell plates are pushed away from the rare pushing HGP (*figure 4B*).

A second example where a clear-cut assessment of the HGP may be challenging is the presence of a prominent ductular reaction at the tumour-liver interface. It can indeed be difficult to distinguish cancer cells from cholangiocytes in this ductular reaction, especially when nuclear pleomorphism of the cancer cells is limited and small aggregates or glandular structures of cancer cells are formed. In addition, cancer cells and cholangiocytes can be involved in common ductular structures. A possible solution is to combine cholangiocyte (CK7, CK19 or carbohydrate antigen 19-9 (CA19-9)) and cancer cell markers (for CRLM, for example CK20 or CDX-2) (*figure 4C*) as an added tool for the analysis. Double immunostaining for cancer cell and cholangiocyte markers can also be used to identify intrabiliary growth when only a few cholangiocytes remain that are difficult to detect on an H&E-stained section (*figure 4D*).

Results - perspectives

Patient-derived xenograft models to study the HGPs of liver metastases

The characterisation of the distinct growth patterns using protein-based and genomic approaches on surgically resected

A

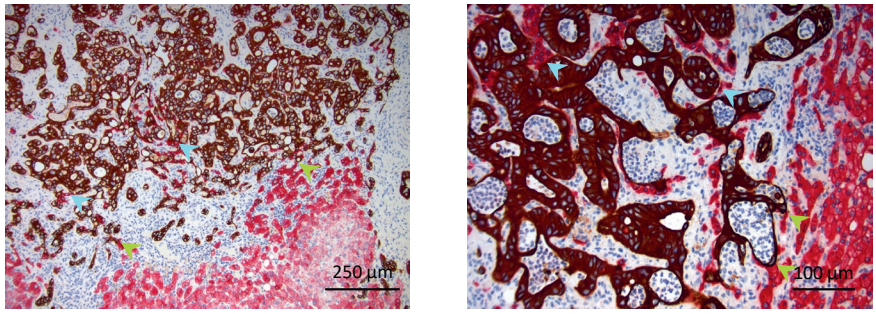

CK19-CK18

B

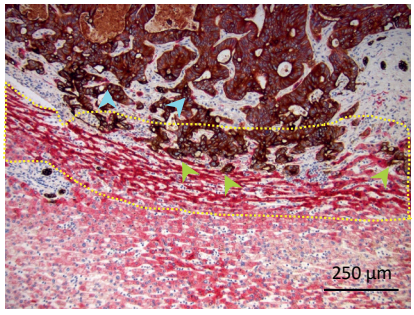

CK19-CK18

C

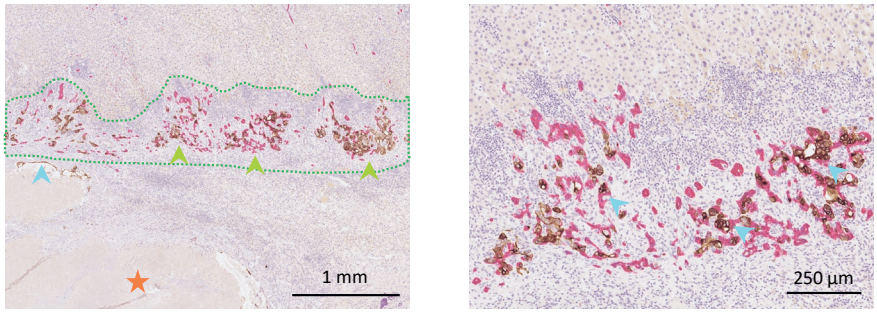

CK20-CK7

D

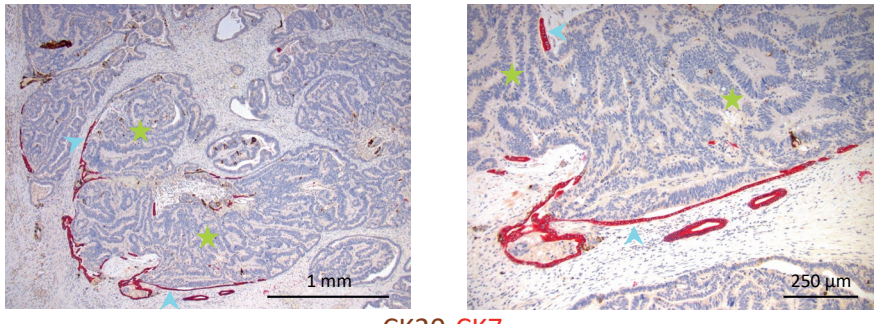

CK20-CK7

clinical specimens has begun to shed light on the underlying biological processes that might drive the formation and growth of these lesions (*table 1*). However, the field currently lacks animal models that faithfully recapitulate the specific histological features of these metastases (in particular desmoplastic metastases), necessary for functional dissection of the molecular mediators that are currently only associated with one type of lesion or the other.

← Figure 4. Immunohistochemical staining as an aid to HGP scoring
A. Detection of the replacement HGP in the presence of an extensive immune cell infiltrate that obscures the tumour-liver interface by identification of cancer cell-hepatocyte contact (green arrowheads) at the tumour-liver interface and co-option of hepatocytes (blue arrowheads) in liver lobules undergoing replacement by cancer cells. CK19 (DAB, brown) stains colorectal cancer cells. CK18 (AP, red) stains hepatocytes. Left: low magnification; Right: high magnification.

B. Detection of the pushing-type replacement (type 2) HGP in which the hepatocyte plates are slender (yellow dotted area) and arranged in parallel with the tumour-liver interface. Green arrowheads indicate cancer cell-hepatocyte contact and blue arrowheads hepatocyte co-option. CK19 (DAB, brown) stains colorectal cancer cells. CK18 (AP, red) stains hepatocytes.

C. Prominent ductular reaction at the tumour-liver interface in the desmoplastic HGP. Areas of ductular reaction (green arrowheads) are present in the outer region of the fibrous rim (green dotted region). Cancer cells are (blue arrow) identified in the metastasis centre, adjacent to necrotic areas (orange star). Right. Detail of the ductular reaction at the tumour-liver interface. Cholangiocytes (CK7+) form irregular, angulated, anastomosing ductuli. Note the presence of interspersed cancer cells (CK20+, blue arrows) within the ductuli, forming common ductular structures. CK20 (DAB, brown) stains colorectal cancer cells. CK7 (AP, red) stains cholangiocytes.

D. Detection of intrabiliary tumour growth. A discontinuous lining of biliary epithelial cells (blue arrows) can be identified surrounding colorectal cancer cells (sparsely positive for CK20 in this case) with focal contact between colorectal cancer cells and biliary epithelial cells (green stars). CK20 (DAB, brown) stains colorectal cancer cells. CK7 (AP, red) stains cholangiocytes. Left: low magnification; right: high magnification.

To better understand the underlying biology of desmoplastic and replacement liver metastases and to test therapeutic strategies tailored to these distinct lesions, it will be important to develop PDXs that faithfully recapitulate the histological features seen in patients. To this end, members of the Liver Metastasis Research Network at the Goodman Cancer Institute (McGill University) and the McGill University Health Centre have developed a patient-derived xenograft (PDX) pipeline where freshly resected CRLM, or biopsy samples, from the operating theatre are brought immediately to the laboratory and are directly implanted into the livers of SCID/beige mice.[16] The surgical specimen is divided into approximately 1mm^3 fragments, which are then carefully inserted into an incision made in the left cardiac liver lobe of recipient mice. This approach has led to the successful establishment of more than 30 PDX models that represent both replacement and desmoplastic lesions. Importantly, a high degree of concordance (over 95%) between the HGPs of the metastases that develop in the PDX models, when compared to the metastatic lesion in the patients from which they were derived, has been achieved. In addition, organoids from these PDX models have been generated (PDXOs) and propagated in culture (Tabariès S, Gregorieff A and Siegel P, unpublished observations). When re-injected into the livers of mice, these PDXOs generate desmoplastic or replacement lesions that recapitulate the HGP of the patient sample and PDX model (*figure 5*). While these models may provide useful information on the drivers underlying specific HGPs, the lack of an adaptive immune response in the recipient mice, may present a challenge to obtaining complete information on the associated immune microenvironments. Although several methods have been described to generate so-called ‘humanised mice’, a less challenging approach is represented by the patient-derived explants (PDE), ex vivo systems in which the in vivo tissue architecture and immune

microenvironment of human tumours can be maintained.[63] These PDE platforms have been shown to be able to predict clinical response to inhibitors of the PD-1-PD-L1 axis in patients with various types of cancer[64] and might thus be used to study the biology of liver metastases with distinct HGPs.

A

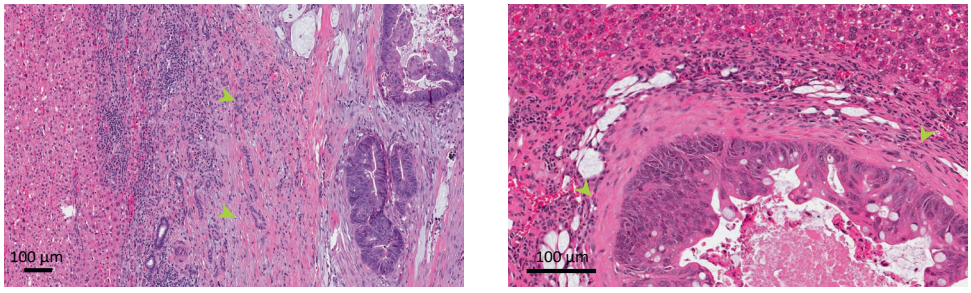

Patient PDX

B

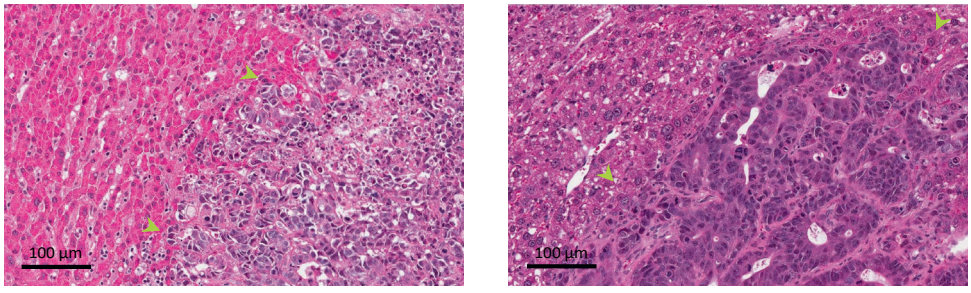

Patient PDX

Figure 5. Patient-derived xenograft (PDX) mice models for CRC liver metastases with a desmoplastic and a replacement HGP (H&E images). A. Resected liver metastasis with a desmoplastic HGP (Left) and corresponding xenograft PDX-model (Right). Green arrows indicate the desmoplastic rim in the patient and in the liver metastasis of the mouse (PDX#35, see Tabariès S, 2021).[16]

B. Resected liver metastasis with a replacement HGP (Left) and corresponding xenograft PDX-model (Right). Green arrows indicate some of the areas in which the cancer cells grow into the liver cell plates and contact the hepatocytes, both in the patient and in the liver metastasis of the mouse (PDX#30, see Tabariès S, 2021).[16]

Automated scoring of HGPs of liver metastasis

An increasing number of pathology laboratories are digitising glass slides into high-resolution whole slide images (WSIs). This creates an opportunity to develop algorithms based on machine learning and artificial intelligence that can extract clinically useful information from, for example, WSIs of H&E-stained tumour sections. At least two teams have implemented this approach to score the HGPs of liver metastases in an automated way.

The algorithm developed by Qianni Zhang and her team determines the relative contribution of the replacement and of the desmoplastic HGP in a CRC liver metastasis, including the proportion of the tumour-liver interface with 'uncertain' HGP.[20] By combining image processing and deep learning methods, they can achieve pixel level segmentation of the tumour-liver interface. The algorithm is based on the accurate identification and segmentation of the different tissue types at this interface by using deep neural networks and by taking both cell and tissue characteristics into account. The neural network is employed to identify the tissue type using patches of a certain size. The characterisation of cell types within these patches then adds sensitivity, especially at the transition of one tissue type to another. In addition, uncertain regions are classified by analysing the similarity of this region and its neighbour, a concept called 'context-aware tissue region classification'. To train the model at the tissue level, many patches were annotated by pathologists at the Karolinska University Hospital, as belonging to liver parenchyma, fibrosis, necrosis, tumour, or inflammation. At the cell level, the model was trained by pathologists to recognise hepatocytes, cells belonging to fibrotic tissue, tumour cells and inflammatory cells. Once the algorithm succeeded in accurately classifying the tissue types of an entire WSI,

rules were developed to detect the growth patterns based on the apposition of different types of tissue at the tumour-liver interface: ‘liver-fibrosis-tumour’ for the desmoplastic HGP and ‘liver-tumour’ for the replacement HGP. Extensive analytical and clinical validation is still ongoing.

The algorithm developed by Jeroen Van der Laak and his team was designed to distinguish CRLM with 100% desmoplastic HGP from liver metastases with any proportion of non-desmoplastic HGP by mimicking the visual feature extraction of an entire WSI at once, as done by pathologists.[21,22] Due to the extensive computational power required to process the gigapixel WSIs at once, reduction of dimensionality (or compression) was necessary. This was achieved by training an encoder in a supervised way to solve several representative tasks in computational pathology. This encoder then reduced both the size and the noise level of the WSIs. In a second step, a convolutional neural network was trained using the image-level labels of ‘100% desmoplastic HGP’ and ‘any % of non-desmoplastic HGP’. When the algorithm was applied to predict the HGP of CRLM, an AUC by ROC analysis of 0.895 was obtained. The algorithm was also able to divide a cohort of 337 patients into two risk categories that predicted OS (HR: 2.35, $p<0.001$). It appears therefore that the HGP of liver metastases can reliably be assessed through the compression and analysis of the WSIs of H&E-stained sections and that this assessment has prognostic power.

These methods[20,21] demonstrate the power of automated scoring algorithms to assist the pathologist in collecting prognostic information based on parameters reflecting tumour biology. Moreover, when these computer vision algorithms can directly learn from clinical data such as survival, they will also be useful as a biomarker discovery tool.[21]

Angiotropic extravascular migratory metastasis by pericytic mimicry

Migration of cancer cells along blood vessels at and distal to the advancing front of primary tumours and metastases has been extensively studied by the team of Lugassy and Barnhill, particularly in melanoma (for review:[33]). During this process of angiotropic extravascular migration, cancer cells are in contact with endothelial cells ('angiotropism') via an amorphous matrix that abundantly contains laminin and other constituents of the basement membrane, thereby replacing the pericytes ('pericyte mimicry'). This type of extravascular migration has been proposed as an alternative to the intravascular route of metastatic spread and seems to be driven by cancer cells re-activating embryogenesis-like programs.[31,65] In replacement-type but not in desmoplastic liver metastases of melanoma, individual cancer cells can be observed in the liver parenchyma disconnected and at a distance from the tumour-liver interface (*figure 6*). As such, growth of liver metastases in a replacement pattern and extravascular migration by angiotropism and pericytic mimicry can be regarded as complementary processes representing a continuum of cancer progression with likely common underlying biological mechanisms. To accurately detect extravascular migration of individual cancer cells in liver metastases with a replacement growth pattern, immunohistochemical staining with cancer cell-specific markers is necessary. Studies that quantify the extent of this angiotropic extravascular migration in liver metastases are ongoing. It will be important to determine whether the presence of angiotropic extravascular migration in liver metastases with a replacement HGP contributes to a poorer outcome.

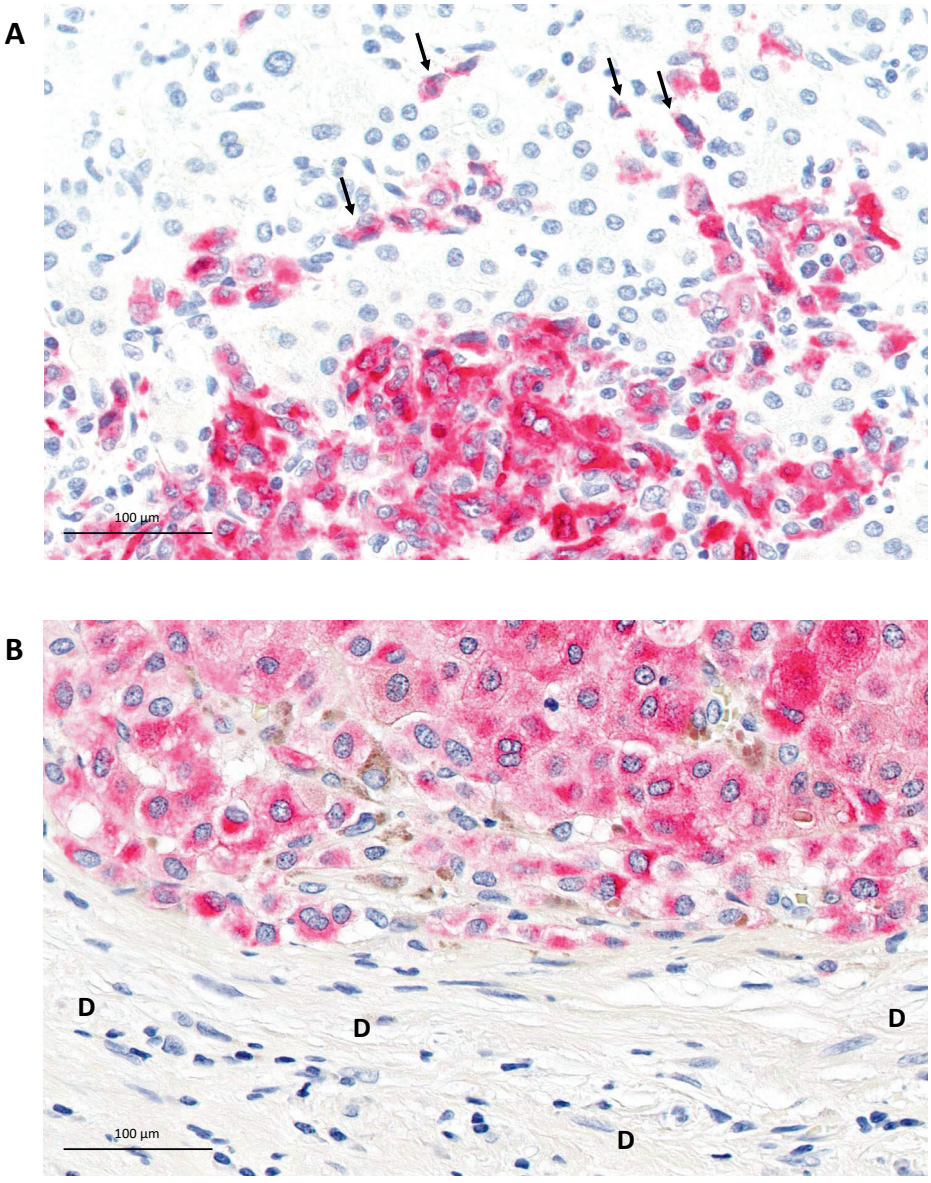

Figure 6. Images of melan-A immunostaining of melanoma liver metastases. (A) High magnification images of the tumour-liver interface of a melanoma liver metastasis with a replacement HGP. Small groups of melanoma cells and individual melanoma cells have migrated away from the tumour-liver interface (arrows). (B) High magnification images of the tumour-liver interface of a melanoma liver metastasis with a desmoplastic HGP. No migration of melanoma cells in the desmoplastic rim, marked by 'D'.

Medical imaging as a tool to identify the HGPs of liver metastases

The implementation of the HGPs in clinical practice will depend, in part, on creating the means for recognising the growth patterns without the need for surgical removal of the liver metastases and analysis by a pathologist. Medical imaging may be a promising approach to solve this challenge. Indeed, several smaller studies suggest that CT and MRI images contain information about the growth pattern (see Table 1 of previous guidelines manuscript by van Dam P et al (2017)[1] and of the current guidelines).[66] This is not surprising, given the major histological and biological differences between the desmoplastic and replacement growth pattern. It is, however, only during the last few years that two teams have attempted to identify growth patterns of liver metastases by medical imaging in a more systematic manner. In Erasmus MC, Rotterdam, Starmans and colleagues have extracted more than 500 radiomics features from CT-images of 76 patients with 93 CRC liver metastases with pure desmoplastic (48%) or pure replacement (52%) HGP.[10] Importantly, these features were extracted from entire metastases, not only from the lesion boundaries. A decision model based on the selection of relevant features and classification of these features by machine learning had a mean area under the curve of 0.69. Adding clinical information to the model did not improve the power to predict the HGPs. Obviously, future studies will have to include metastases with a mixed HGP. Nevertheless, this study is a valuable proof of concept for the utility of this approach.

A team at the Peking University People's Hospital has recently published three studies on the identification of HGPs of CRC liver metastases by medical imaging.[8,9,67] It is important to note that these studies attempt to identify the predominant growth pattern. Cheng and colleagues[8] analysed

contrast-enhanced CT-images of 126 CRC liver metastases, of which 68 had a predominant (>50%) desmoplastic HGP and 58 had a predominant replacement HGP. Pre-contrast and post-contrast CT-images (from both the arterial and portal venous phases) were used. Of each of these 3 phases, 20 radiomics features were selected by an algorithm based on minimal redundancy and maximal relevance. A fused decision-tree based signature of the three phases resulted in a predictive model with an area under the curve of 0.94. Adding clinical information or qualitative information provided by the radiologist did not improve the predictive power.

In a similar study, MRI-derived regions, both covering the whole tumour volume as well as the tumour-liver interface specifically, were subjected to radiomic feature extraction in a cohort of 182 CRC liver metastases, of which 59 had a predominant (>50%) desmoplastic HGP and 123 had a predominant replacement HGP.[9] The predictive model that combined clinical characteristics, qualitative imaging data generated by the radiologist and radiomic feature data from the tumour-liver interface had and area under the curve of 0.91.

In their most recent study, the team at the Peking University People's Hospital has used their CT-based radiomics HGP-signature to predict response and PFS in a cohort of 119 patients with liver metastatic CRC treated with a combination of chemotherapy and bevacizumab.[67] Among 346 metastases studied, 206 had a radiological predominant desmoplastic HGP and 140 had a radiological predominant replacement HGP. Patients with only metastases with a predominant desmoplastic HGP only as assessed by radiology had a significantly improved 1-year PFS (HR = 0.34; $p<0.001$).

Although the studies by Cheng J et al (2019)[8], Han Y et al (2020)[9], and Wei S et al (2021)[67] are very promising,

validation of the results in larger cohorts by independent research teams and with images acquired in different hospital is still necessary. In addition, at least for patients with CRLM, it will be necessary to select, by means of imaging, those patients who have metastases with a 100% desmoplastic growth pattern. So, even though considerable progres has been made to better determine the HGP prior to resection of the liver metastases, there might still be a need to develop computational tools to integrate as many parameters as feasible to stratify patients more accurately.

Results - biology

New biological insights into growth patterns through immunohistochemical analyses

Why does a liver metastasis in one patient develop a desmoplastic rim, while a metastasis in a different patient has a replacement-type growth pattern, even when the primary tumour type is the same? The full answer to this question and the biological mechanisms that underlie the different growth patterns remain elusive. There are reasons to assume that cancer cell motility and differentiation[41], angiocrine signals[68], and interactions of cancer cells with hepatocytes[16] and with stromal and inflammatory cells[32] are important factors regulating the emergence of a distinct growth pattern. However, the precise mechanisms and the order of events leading to the specific growth patterns remain unclear. There are compelling observations to suggest that systemic treatment can alter the growth pattern.[41,61] Also, given that some mouse PDX models can recapitulate the pattern observed in the donor patient, the growth pattern may be, at least in part, determined by cancer cell intrinsic properties.[16] However, this does not exclude epigenetic control and the influence of tumour microenvironment as important further mechanisms.[52]

Based on immunohistochemical stainings performed by the Karolinska team (Carlos Fernández Moro, Marco Gerling, Béla Bozóky) to map the spatial relationships and phenotypic states of epithelial and stromal cells, we propose two additional working hypotheses to explain the biology of the HGPs.

A first working hypothesis is that the replacement growth pattern is the default pattern of growth for cancer cells forming a tumour in the liver. This means that spontaneous or induced transition to the desmoplastic pattern regularly takes place as a second step. An intrinsic and important limitation of determining growth patterns by histological analysis of a resection specimen is that we only get information from a single time point. A non-invasive method to assess the HGPs, such as imaging, would allow longitudinal, repeated determination of HGPs. We may, however, be able to infer information about the history of a liver metastasis by comparing the centre of the tumour with its periphery. Surprisingly, after immunohistochemical analysis, we found remnants of portal triads (branches of the bile duct and of the hepatic artery) in the centre of both replacement and desmoplastic metastases. These portal elements are regularly found to be embedded in specialised portal-type stromal cells expressing Nerve Growth Factor Receptor (NGFR)- and alpha Smooth Muscle Actin (alpha-SMA, *figure 7A*). This observation supports a model in which the metastatic tumour co-opts the sinusoidal blood vessels and the portal tract architecture of the liver, a mode of growth that likely is advantageous, both for blood supply and structural support. While portal triad co-option is readily identifiable at the tumour-liver interface of replacement-type liver metastases, it may be more subtle in the fibrous rim of the desmoplastic type, where pre-existing liver structures appear atrophic and attenuated. Here, immunohistochemistry

can be used to identify atrophic remnants of the portal triad. Together, this leads us to propose the hypothesis that replacement growth, in most cases, precedes desmoplastic growth in metastases with the latter HGP. The time point at which the growth patterns may switch and the factors responsible for the proposed conversion remain unclear. There are other observations to support a model in which replacement growth is the default growth pattern of liver metastases. For example, when cancer cells spread within the bile ducts, the cancer cells rest on the basement membrane of the normal biliary epithelial lining and progress by replacing these normal cells and by co-opting the subepithelial stroma (figure 7B). In addition, we occasionally observe bile ducts as part of the ductular reaction in the desmoplastic rim, in which cancer cells create hybrid cancer cell-cholangiocytes ductular structures (*figure 7C*). Although these histological observations need further validation and quantification, they do support other observations consistent with growth pattern plasticity. Indeed, resistance to chemotherapy can coincide with a switch to the replacement HGP[41,59], while pre-operative chemotherapy converts metastases in some patients from replacement to desmoplastic HGP[61]. Also, during disease progression in patients with recurrent colorectal liver metastases, there is an evolution towards the more aggressive replacement HGP, as observed by analysing repeated resections.[18]

A second working hypothesis is that the fibrous rim surrounding desmoplastic liver metastases and the portal tract are biologically related. This hypothesis is supported by two observations. Firstly, the stromal cells of the desmoplastic rim, and especially of the outer portion of the rim neighbouring the surrounding liver parenchyma, strongly co-express NGFR and alpha-SMA, indicative of a “myofibroblast” or “activated fibroblast” phenotype (figure

7D). NGFR is expressed by progenitors of Ito/stellate cells and of portal fibroblasts in the foetal liver[69,70] and this receptor also plays a crucial role during pathological liver fibrosis by inducing fibrogenic gene expression, for example of the Transforming Growth Factor beta1-gene, in activated (myo)fibroblasts.[71-73] Secondly, by co-immunostaining for CK18, as a marker of hepatocytes, and CK19, as a marker of cholangiocytes, we often observe mosaic ductular structures in the desmoplastic rim composed of a mixture of cells with a hepatocyte-like and a cholangiocyte-like phenotype (figure 7E). Activated fibroblasts are known to induce cholangiocyte differentiation in hepatic stem-like cells (for example, via Jagged-1 and Hedgehog ligands) and this process partly relies on NGFR expression in the activated liver fibroblasts.[73,74] NGFR-expressing and activated, alpha-SMA-positive fibroblasts in the desmoplastic rim may therefore activate extracellular matrix production and induce a ductular reaction by engaging bipotent progenitors, resembling portal tract development as well as liver fibrosis in other pathological conditions involving liver injury.[75] In the metastasis context, destruction of liver cells by the invading tumour, inflammation, and damage of the peritumoural liver tissue are potential mechanisms of liver injury.

Hypotheses to explain the biology of the distinct histopathological growth patterns

There is currently no satisfactory explanation for the specific biology of each of the histopathological growth patterns. *Table 6* therefore summarises some hypotheses to explain the distinct phenotypes of the desmoplastic and replacement growth patterns. These hypotheses are derived from histopathological insights, pre-clinical animal models, and the comparison with organ development in the embryo. The hypotheses listed in *table 6* are not mutually exclusive and elements of each probably contribute to the specific growth

patterns of liver metastases. In addition, some hypotheses outlined only address individual growth patterns.

Taken together, cancer cells within a liver metastasis exhibiting a replacement growth pattern appear to adapt to the microenvironment of the liver parenchyma and may therefore be sensitive to a liver pro-metastatic reaction of the patient[76], while cancer cells of a desmoplastic metastasis create their own microenvironment. Against

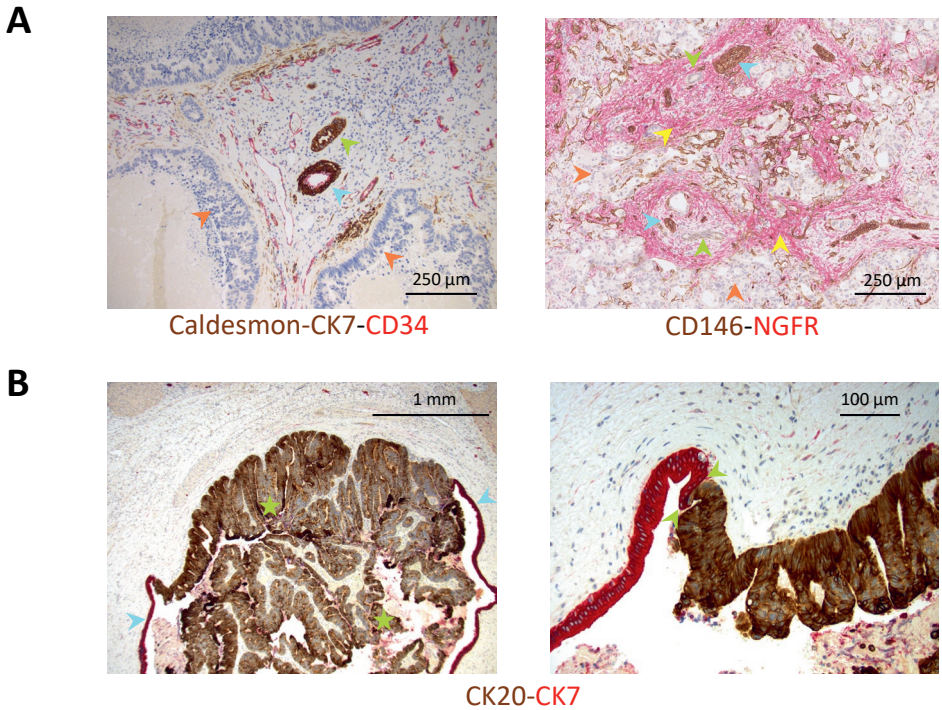

← *Figure 7 A-C. New biological insights into growth patterns through immunohistochemical analyses.*
A. Remnants of portal zones in the centre of colorectal liver metastases. Left. Detail of a tumour centre in a metastasis with a predominant replacement HGP showing remnant of a portal zone with bile duct (green arrowhead) and hepatic artery

this background, it could be argued that cancer cells in a replacement metastasis behave like hepatocytes or hepatocyte progenitor cells communicating with the liver niche (for example with the co-opted sinusoidal endothelial cells), whereas cancer cells in a desmoplastic metastasis more autonomously form a tumour that resembles the primary tumour. The plasticity of the growth patterns suggested by clinical observations appears to indicate that this divergent behaviour of cancer cells in the liver is not, or at least not entirely, the result of a different mutational gene profile, but rather of epigenetic events and the ability to respond to stimuli from the microenvironment, such as soluble factors elicited by the liver pro-metastatic reaction[76] and liver immune responses[77].

branch (blue arrowhead). Note colonisation by viable cancer cells of the periportal limiting plate region (orange arrowhead). Caldesmon (DAB, brown) stains smooth muscle cells, mainly in the media layer of the hepatic artery. CK7 (DAB, brown) stains bile duct epithelium. CD34 (AP, red) stains the endothelium of the hepatic artery and of the stromal capillary network. Right. Tumour centre in a metastasis with a desmoplastic HGP showing multiple remnants of portal zones between lobules that have undergone complete replacement by cancer cells (orange arrowheads). The bile ducts (green arrows) and branches of the hepatic artery (blue arrows) are embedded in NGFR+ portal stroma (yellow arrowheads). CD146 (DAB, brown) stains smooth muscle cells (mainly in the wall of hepatic arteries) and areas of ductular reaction. NGFR (AP, red) stains activated portal fibroblasts and stellate cells.

B. Intrabiliary tumour growth in a CRC liver metastasis. Left. Densely packed cancer cells (green stars) show exophytic growth and fill the bile duct lumen. Portions of preserved biliary epithelium (blue arrows) are still identified. Right. Detail illustrating the replacement-like growth of cancer cells, which progress by establishing direct contact with and replacing the cholangiocytes while co-opting their basal membrane. CK20 (DAB, brown) stains colorectal cancer cells. CK7 (AP, red) stains cholangiocytes.

C. Hybrid cancer cell-cholangiocyte ductular structures. Ductular reaction in the desmoplastic rim with cancer cells (CK20-positive, DAB, brown) forming hybrid structures with cholangiocytes (CK7-positive, AP, red).

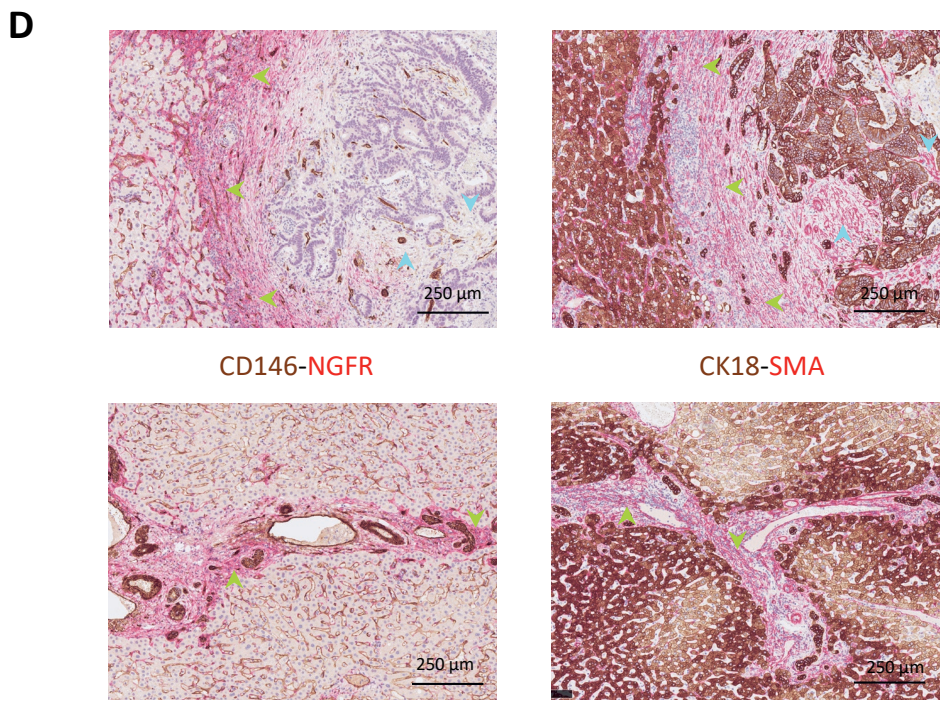

← *Figure 7 D-E. D. Stromal cell heterogeneity in a metastasis with a desmoplastic HGP. Top. The outer region of the desmoplastic rim stains strongly positively for NGFR (Left, green arrows) and α-smooth muscle actin (alpha-SMA) (Right, green arrowheads), consistent with activated portal/stellate cell stroma. In contrast, the stroma in the metastasis centre is positive for alpha-SMA but negative for NGFR, indicating a desmoplastic character (Left and right, blue arrows). Bottom. Reference illustrations of activated portal stroma in non-neoplastic liver, showing (Left) NGFR and (Right) alpha-SMA immunoreactivity (Left and right, green arrows). CD146 (DAB, brown) stains vascular and sinusoidal endothelium and smooth muscle in branches of the hepatic artery and portal vein. NGFR (AP, red) stains activated portal fibroblasts and stellate cells. CK18 (DAB, brown) stains hepatocytes and cholangiocytes. Alpha-SMA (AP, red) stains activated portal fibroblasts, stellate cells and desmoplasia-associated myofibroblasts.*

E. Ductular reaction in the desmoplastic rim with cells with a hepatocyte-like (CK18-positive, AP, red) and a cholangiocytes-like (CK18, DAB, brown) phenotype (green arrows).

Table 6. Hypotheses to explain the biology of the HGPs of liver metastases

Hypothesis	Supporting evidence and/or supporting argument
Site of implantation	
The site of cancer cell implantation in the liver determines the HGP	In animal models of liver metastasis (where cancer cells were introduced either via an arterial route or a portal route) the arterial route gave rise to a significantly higher proportion of desmoplastic metastases, originating from within portal tracts, than when cancer cells entered the liver via the vena portae, which more often resulted in a replacement-type liver metastases (Paku S & Lapis K, 1993[123]; Vidal-Vanaclocha F, 2008[124]).
Revertant in situ growth	
The replacement HGP is a reversion to *in situ* growth of cancer cells (growth within the boundaries of a basement membrane)	Cancer cells in replacement-type liver metastases take the place of hepatocytes and rest on the Space of Disse. The hybrid ductular structures (cancer cell-cholangiocyte) and growth within bile ducts are other examples of *in situ* growth of cancer cells in the liver. Revertant *in situ* growth has been described in lymph node metastases of cancer which adopt a similar growth pattern with cancer cells replacing lymphocytes and co-opting the vasculature (Barsky SH, 1997[125]).
Coagulation and inflammation	
The presence (desmoplastic) or absence (replacement) of coagulation and inflammation determine the HGPs	Angiogenesis, coagulation, inflammation, and fibrosis are interrelated processes during wound healing and may also be the driving force behind the desmoplastic HGP of liver metastases. When cancer cells can avoid activating any of these processes, liver metastases can adopt the replacement HGP. Only minimal fibrin deposits and hypoxia, one of the factors inducing angiogenesis, occur in liver metastases with a replacement HPG (Stessels F, 2004[38]) and replacement pattern liver metastases often show an 'immune desert' (Stremitzer S, 2020[2]).
Response to liver injury	
The HGPs reflect the response patterns of the liver to injury, with the desmoplastic HGP resembling biliary liver fibrosis and the replacement pattern resembling liver regeneration.	There are two responses to liver injury – the fibrotic response and the liver regeneration response (Ding B, 2014[82]). The desmoplastic rim contains a portal-type of stroma (this manuscript) and proliferating bile ducts (ductular reaction) which resembles the fibrotic response to liver injury (Schuppan D, 2013[126]). In replacement-type liver metastases, the cancer cells are arranged in cell plates and replace the parenchymal hepatocytes, thereby preserving the vascular architecture of the liver parenchyma, which resembles morphologically progenitor cell-driven liver regeneration (Deszo K, 2012[127]).
Transcriptional reprogramming	
The HGPs are the result of transcriptional reprogramming driven by an HGP-specific epigenetic landscape.	CRC cells have been shown to express liver-specific genes in liver metastases, thereby loosing expression of colon-specific genes. This reprogramming is driven by a change in enhancer-regions in the genome (Teng S, 2020[52]). In the replacement HGP, cancer tissue mimics liver tissue histologically, supporting the hypothesis that cancer cells switch on a liver organogenesis program that may be driven by the sinusoidal endothelial cells as in vascularizing organogenesis (Matsumoto K, 2001[80]; Crivellato E, 2007[81]; Ding B, 2014[82]; Daniel E, 2019[83]). Desmoplastic liver metastases histologically resemble the primary colorectal tumour and may also have a similar transcriptional profile.
Cancer cell motility	
The ability of cancer cells to move and migrate determines the HGPs because cancer cell motility is necessary for the replacement HGP.	Knocking down of *ARPC3*, a gene coding for a subunit of an actin nucleating complex necessary for cell motility, or *RUNX1*, coding for Runt Related Transcription Factor-1 (which is upstream of ARP2/3) changes the HGP from a replacement pattern to a desmoplastic pattern in an animal model of liver metastasis (Frentzas S, 2016[41]; Rada M, 2021[111]).
Replacement HGP is the default	
The replacement HGP is the default growth pattern.	Remnants of co-opted portal triads are present in the centre of liver metastases, independent of the HGP. This suggests that desmoplastic liver metastases originate from replacement-type metastases, given that co-option of portal triads is not observed at the interface with the liver in desmoplastic liver metastases. Cancer cells also replace normal epithelial cells when they spread within a bile duct or form hybrid structures with cholangiocytes of a ductular reaction (this manuscript), supporting the idea the cancer cells have a natural tendency to interact with normal cells. What induces the transition from replacement to desmoplastic growth is still unknown.
Angiotropic extravascular migration and pericyte mimicry	
The replacement HGP relies on these processes.	Both the growth along sinusoidal blood vessels via angiotropic migration and pericyte mimicry and the histological resemblance of replacement liver metastases to liver parenchyma suggest that programs of embryogenesis are active in this type of metastases (Lugassy C, 2020[33]).

Discussion

Since the publication of the first consensus guidelines[1], numerous studies have been conducted describing the impact of HGPs on the outcome of patients with liver metastases (*table 1*). These studies are not limited to liver metastases from colorectal carcinoma, but also include patients with liver metastases from breast carcinoma, melanoma, and pancreatic adenocarcinoma.[5,42,44,45] The association between replacement HGP and poorer patient outcome, independent of the primary tumour type, has been confirmed by these new studies. A new cut-off to categorise patients with CRLM according to the HGPs is presented in the current guidelines. This cut-off is derived from the observation in a large multi-centre cohort of patients that any proportion of non-desmoplastic HGP, however small, is associated with a worse prognosis. The extent of non-desmoplastic features within the metastases in itself does not seem to modulate outcome any further. We have therefore updated the guidelines for scoring the HGPs of CRLM for the purposes of prognostication of patients, and we propose herein some immunohistochemical assays that may help to identify the growth patterns in more challenging situations, such as in the presence of dense inflammation or systemic treatment effects.

The tumour-type independent prognostic value of the HGPs fuels the idea that the biology of the replacement HGP is fundamentally different from that of the desmoplastic growth pattern. Some of these differences have been well described. In the desmoplastic growth pattern, a dense immune-inflammatory cell infiltrate surrounds the fibrous rim, while the replacement growth pattern has the characteristics of an immune desert, especially when no chemotherapy is involved.[2-4,32,78] The desmoplastic pattern has angiogenic vascular hot spots in between cancer cell nests and hypoxic areas while the replacement growth pattern shows a uniformly

high vessel density and minimal hypoxia, probably because of efficient vessel co-option.[30,38,41] Consequently, replacement-type liver metastases are also metabolically more active than desmoplastic liver metastases, as demonstrated by FDG-PET analyses.[79]

A striking morphological difference between the growth patterns lies in the organisation of the cancer cells and the interaction with the host liver tissue. In replacement-type liver metastases, cancer cells mimic hepatocytes by an arrangement in solid cell plates in between the co-opted sinusoidal blood vessels. This type of growth clearly resembles the 'vascularizing organogenesis' that takes place when the liver develops in the embryo and may also be guided by instructive signals originating in the liver sinusoidal endothelial cells.[80-83] Accordingly, cancer cells belonging to replacement-type liver metastases seem to hijack the embryological program of liver development with the resulting tumour adopting the histological architecture of liver tissue. The work of Teng and team[52] supports this hypothesis. They have shown that CRLM, when compared with primary colorectal cancer, simultaneously gain liver-specific and lose colon-specific transcription programs. They also showed that this is the result of a reprogrammed enhancer landscape. Enhancers are regulatory elements in the genome that are influenced by the environment and, as such, play an important role in tissue-specific gene expression patterns and cell identity. However, whether differences in the enhancer landscape can also explain the morphological differences between the replacement and the desmoplastic growth pattern of liver metastases still needs to be investigated. During desmoplastic growth of liver metastases, the cancer cells arrange in more differentiated structures, not as cancer cell plates, and resemble the glandular structures of primary colorectal and breast cancer. In other words, desmoplastic

liver metastases morphologically mimic the primary tumour they originate from, where cancer cells typically induce a continuous wound-healing response with inflammation, fibrosis, coagulation, and angiogenesis. This probably involves tumour-host interactions that are active in the primary tumour and epithelial-stromal interactions of the normal tissue counterpart (e.g., colon, breast, etc.). These hypothetical and morphology-driven views on the divergent biological mechanisms of the liver metastasis growth patterns are now being investigated by bulk RNA-sequencing, single cell RNA-sequencing, in situ RNA-sequencing, and multiplex immunohistochemistry. PDX-models and co-organoids derived from patient liver metastases are used for functional validation. Alternative hypotheses to explain the distinct histopathological growth patterns are listed in *table 6*.

At a single time-point, patients often have liver metastases consisting of both desmoplastic and replacement HGP regions. This is, for example, true for about 60% of all patients with resected CRLM[18], independent of whether chemotherapy was administered before surgery. Co-occurrence of distinct HGPs thus seems to be part of the growth process of liver metastases and this may be the consequence of transitioning from one HGP to another. We now propose the working hypothesis, based on immunohistochemical analyses, that the replacement HGP is the default growth pattern of liver metastases. Although there are data to support the view that pre-surgery chemotherapy can induce desmoplastic growth in some metastases[18,61] and that a switch to replacement growth can occur upon resistance to systemic treatment[41], the cellular and molecular mechanisms responsible for these transitions from one growth pattern to another remain to be elucidated. What these and other findings do seem to suggest is that epigenetic processes drive the growth patterns rather than mutational hardwiring. Recently, the concept of

'histostasis', driven by cancer cell-autonomous properties, has been put forward to explain the morphological resemblance between metastatic tissue and the corresponding primary tumour.[84] As a complement, we propose here to introduce the concept of 'histokinesis', a process driven by cancer cell-responsiveness to instructive host tissue-derived signals, such as the pro-metastatic liver reaction[76], to explain the clear morphological differences between the primary tumour and, for example, replacement-type liver metastases. This is probably a more general biological concept, given the observations of similar growth patterns in, for example, lung metastases.[56,85-87]

The plasticity of the growth patterns might be exploited in future therapeutic strategies. A prerequisite to feasibility would be a continuous evaluation of the growth pattern in a pre-surgical setting of systemic treatment. This implies a reliable non-invasive method for repeatedly identifying the growth patterns during the patient treatment. *Table 1* highlights the initiatives of several teams worldwide to develop algorithms to assess the growth patterns of liver metastases by medical imaging.[8-10,66] In addition, several studies are still ongoing with results to be expected in the coming years. As an alternative, circulating markers in the blood of patients may be useful to identify the prevailing growth pattern at a certain moment in time. A study by Tabariès[16] proposes exosome-derived claudin-profiling as a tool to predict the growth pattern of CRLM.

The role of systemic treatment, either neo-adjuvant or adjuvant, for patients with a priori resectable metachronous CRLM remains unclear. In many countries, patients will receive standard post-operative chemotherapy, following metastasectomy performed with curative intent. Although the benefit of adjuvant treatment is still to be fully

appreciated, surgery alone is often not considered. To face the problem of potentially low accrual in a study that compares surgery alone with surgery combined with adjuvant chemotherapy, we suggest limiting the study population to those patients with liver metastases that exclusively have the desmoplastic growth pattern upon careful pathological evaluation of the resected metastases, as a first approach. Alternatively, and only when a non-invasive pre-operative marker of the HGPs becomes available (as liver biopsies to evaluate the HGP are not suitable), a window of opportunity study could be envisioned to examine the role of specific treatments for replacement and desmoplastic liver metastases in patients with (borderline) resectable liver metastases. For example, given the distinct immune contexture of each of the growth patterns, the choice of immunotherapy may need to be adapted to the growth pattern of the liver metastases. Based on trails that successfully combined anti-VEGF agents with immune checkpoint inhibitors in, for example, patients with renal cell carcinoma[128] and hepatocellular carcinoma[129], one might indeed argue that patients with liver metastases with a desmoplastic, angiogenic HGP would benefit more from such treatment regimens than patients with liver metastases with a replacement, vessel co-opting HGP. However, it is not obvious at this time that VEGF, given its multiple biological functions, would play a role only in the desmoplastic and not in the replacement HGP. It is indeed conceivable that in a nonangiogenic, replacement-type liver metastasis, VEGF still exerts its immunosuppressive and endothelial cell protective functions, while its angiogenic functions are locally counteracted by endogenous angiogenesis inhibitors. It is, with this in mind, also unclear whether the clinically relevant systemic immunosuppressive effects of the presence of liver metastases, leading to reduced benefit from immune checkpoint inhibitors, are growth pattern-dependent.[88] A better insight into the interaction of

liver-metastatic cancer cells with the complex (immune) environment of the liver will contribute to understanding the biology of the HGPs.[77]

In conclusion, we provide updated guidelines for scoring the histopathological growth patterns of liver metastases. These are of importance not only to implement the HGPs in the clinical care of patients with liver metastatic cancer, but also to properly conduct studies that seek to identify the biological basis for these growth patterns. The latter is important to better understand the heterogeneity of liver metastases, and thus perhaps also of tumour expansion in other organs where similar growth patterns have been described, such as in the lungs.[56,87]

References

1. van Dam PJ, van der Stok EP, Teuwen LA, et al. International consensus guidelines for scoring the histopathological growth patterns of liver metastasis. *Br J Cancer.* Nov 7 2017;117(10):1427-1441.
2. Stremitzer S, Vermeulen P, Graver S, et al. Immune phenotype and histopathological growth pattern in patients with colorectal liver metastases. *Br J Cancer.* May 2020;122(10):1518-1524.
3. Liang JY, Xi SY, Shao Q, et al. Histopathological growth patterns correlate with the immunoscore in colorectal cancer liver metastasis patients after hepatectomy. Cancer *Immunol Immunother.* Dec 2020;69(12):2623-2634.
4. Hoppener DJ, Nierop PMH, Hof J, et al. Enrichment of the tumour immune microenvironment in patients with desmoplastic colorectal liver metastasis. *Br J Cancer.* Jul 2020;123(2):196-206.
5. Watanabe K, Mitsunaga S, Kojima M, et al. The "histological replacement growth pattern" represents aggressive invasive behavior in liver metastasis from pancreatic cancer. *Cancer Med.* May 2020;9(9):3130-3141.
6. Messaoudi N, Henault D, Stephen D, et al. Prognostic implications of adaptive immune features in MMR-proficient colorectal liver metastases classified by histopathological growth patterns. *Br J Cancer.* Jan 3 2022.
7. Gulia S, Khurana S, Shet T, Gupta S. Radiographically occult intrasinusoidal liver metastases leading to hepatic failure in a case of breast cancer. *BMJ Case Rep.* Feb 15 2016;2016.
8. Cheng J, Wei J, Tong T, et al. Prediction of Histopathologic Growth Patterns of Colorectal Liver Metastases with a Noninvasive Imaging Method. *Ann Surg Oncol.* Dec 2019;26(13):4587-4598.
9. Han Y, Chai F, Wei J, et al. Identification of Predominant Histopathological Growth Patterns of Colorectal Liver Metastasis by Multi-Habitat and Multi-Sequence Based Radiomics Analysis. *Front Oncol.* 2020;10:1363.
10. Starmans MPA, Buisman FE, Renckens M, et al. Distinguishing pure histopathological growth patterns of colorectal liver metastases on CT using deep learning and radiomics: a pilot study. *Clin Exp Metastasis.* Oct 2021;38(5):483-494.
11. Alzubi MA, Sohal SS, Sriram M, et al. Quantitative assessment of breast cancer liver metastasis expansion with patient-derived xenografts. *Clin Exp Metastasis.* Jun 2019;36(3):257-269.
12. Piquet L, Dewit L, Schoonjans N, et al. Synergic Interactions Between Hepatic Stellate Cells and Uveal Melanoma in Metastatic Growth. *Cancers (Basel).* Jul 24 2019;11(8).
13. Vlachogiannis G, Hedayat S, Vatsiou A, et al. Patient-derived organoids model treatment response of metastatic gastrointestinal cancers. *Science.* Feb 23 2018;359(6378):920-926.
14. Ibrahim NS, Lazaris A, Rada M, et al. Angiopoietin1 Deficiency in Hepatocytes Affects the Growth of Colorectal Cancer Liver Metastases (CRCLM). *Cancers (Basel).* Dec 20 2019;12(1).
15. Masaki S, Hashimoto Y, Kunisho S, Kimoto A, Kitadai Y. Fatty change of the liver microenvironment influences the metastatic potential of colorectal cancer. *Int J Exp Pathol.* Oct 2020;101(5):162-170.
16. Tabaries S, Annis MG, Lazaris A, et al. Claudin-2 promotes colorectal cancer liver metastasis and is a biomarker of the replacement type growth pattern. *Commun Biol.* Jun 2 2021;4(1):657.
17. Bartlett AQ, Pennock ND, Klug A, Schedin P. Immune Milieu Established by Postpartum Liver Involution Promotes Breast Cancer Liver Metastasis. *Cancers (Basel).* Apr 3 2021;13(7).
18. Galjart B, Nierop PMH, van der Stok EP, et al. Angiogenic desmoplastic histopathological growth pattern as a prognostic marker of good outcome in patients with colorectal liver metastases. *Angiogenesis.* May 2019;22(2):355-368.
19. Hoppener DJ, Galjart B, Nierop PMH, et al. Histopathological Growth Patterns and Survival After Resection of Colorectal Liver Metastasis: An External Validation Study. *JNCI Cancer Spectr.* Jun 2021;5(3):pkab026.
20. Zhaoyang X, Carlos Fernádez M, Danyil K, Béla B, Le D, Qianni Z. Tissue Region Growing for Hispathology Image Segmentation. *Proceedings of the 2018 3rd International Conference on Biomedical Imaging, Signal Processing*; 2018; Italy.

21. Tellez D, Höppener D, Verhoef C, et al. Extending unsupervised neural image compression with supervised multitask learning. *Paper presented at: Medical Imaging with Deep Learning 2020.*
22. Tellez D, Litjens G, van der Laak J, Ciompi F. Neural Image Compression for Gigapixel Histopathology Image Analysis. *IEEE Trans Pattern Anal Mach Intell.* Feb 2021;43(2):567-578.
23. Nierop PMH, Galjart B, Hoppener DJ, et al. Salvage treatment for recurrences after first resection of colorectal liver metastases: the impact of histopathological growth patterns. *Clin Exp Metastasis.* Apr 2019;36(2):109-118.
24. Nierop PMH, Hoppener DJ, van der Stok EP, et al. Histopathological growth patterns and positive margins after resection of colorectal liver metastases. *HPB (Oxford).* Jun 2020;22(6):911-919.
25. Buisman FE, Van der Stok EP, Galjart B, et al. Histopathological growth patterns as biomarker for adjuvant systemic chemotherapy in patients with resected colorectal liver metastases. *Clin Exp Metastasis.* 2020.
26. Masson P. *Les tumeurs.* Traité De Pathologie Et Thérapie Appliquées. 1923;27(2):572-574.
27. Hamperl H. Die morphologie der tumoren. *Lehrbuch Der Allgemeinen Pathologie Und Der Pathologischen Anatomie.* 1956;6(3):243-244.
28. Elias H, Bouldin RF. Reaction of the normal liver parenchyma to metastatic carcinoma. *Acta Hepatosplenol.* 1962;9(6):357-386.
29. Elias H, Bierring F, Grunnet I. Cellular Changes in the Vicinity of Metastatic Carcinoma, Observed by Light and Electron Microscopy. *Oncologia.* 1964;210-224.
30. Vermeulen PB, Colpaert C, Salgado R, et al. Liver metastases from colorectal adenocarcinomas grow in three patterns with different angiogenesis and desmoplasia. *J Pathol.* Oct 2001;195(3):336-342.
31. Latacz E, Caspani E, Barnhill R, et al. Pathological features of vessel co-option versus sprouting angiogenesis. *Angiogenesis.* Feb 2020;23(1):43-54.
32. van Dam PJ, Daelemans S, Ross E, et al. Histopathological growth patterns as a candidate biomarker for immunomodulatory therapy. *Semin Cancer Biol.* Oct 2018;52(Pt 2):86-93.
33. Lugassy C, Kleinman HK, Vermeulen PB, Barnhill RL. Angiotropism, pericytic mimicry and extravascular migratory metastasis: an embryogenesis-derived program of tumor spread. *Angiogenesis.* Feb 2020;23(1):27-41.
34. Allison KH, Fligner CL, Parks WT. Radiographically occult, diffuse intrasinusoidal hepatic metastases from primary breast carcinomas: a clinicopathologic study of 3 autopsy cases. *Arch Pathol Lab Med.* Dec 2004;128(12):1418-1423.
35. Simone C, Murphy M, Shifrin R, Zuluaga Toro T, Reisman D. Rapid liver enlargement and hepatic failure secondary to radiographic occult tumor invasion: two case reports and review of the literature. *J Med Case Rep.* Nov 26 2012;6:402.
36. Watson AJ. Diffuse intra-sinusoidal metastatic carcinoma of the liver. *J Pathol Bacteriol.* Jan-Apr 1955;69(1-2):207-217.
37. Vaideeswar P, Munot S, Rojekar A, Deodhar K. Hepatic diffuse intra-sinusoidal metastases of pulmonary small-cell carcinoma. *J Postgrad Med.* Jul-Sep 2012;58(3):230-231.
38. Stessels F, Van den Eynden G, Van der Auwera I, et al. Breast adenocarcinoma liver metastases, in contrast to colorectal cancer liver metastases, display a non-angiogenic growth pattern that preserves the stroma and lacks hypoxia. *Br J Cancer.* Apr 5 2004;90(7):1429-1436.
39. Hoppener DJ, Nierop PMH, Herpel E, et al. Histopathological growth patterns of colorectal liver metastasis exhibit little heterogeneity and can be determined with a high diagnostic accuracy. *Clin Exp Metastasis.* Aug 2019;36(4):311-319.
40. Terayama N, Terada T, Nakanuma Y. Histologic growth patterns of metastatic carcinomas of the liver. *Jpn J Clin Oncol.* Feb 1996;26(1):24-29.
41. Frentzas S, Simoneau E, Bridgeman VL, et al. Vessel co-option mediates resistance to anti-angiogenic therapy in liver metastases. *Nat Med.* Nov 2016;22(11):1294-1302.
42. Bohlok A, Vermeulen P, Leduc S, et al. Association between the histopathological growth patterns of liver metastases and survival after hepatic surgery in breast cancer patients. *NPJ Breast Cancer.* Dec 18 2020;6(1):64.
43. Horn SR, Stoltzfus KC, Lehrer EJ, et al. Epidemiology of liver metastases.

Cancer Epidemiol. Aug 2020;67:101760.
44. Barnhill R, Vermeulen P, Daelemans S, et al. Replacement and desmoplastic histopathological growth patterns: A pilot study of prediction of outcome in patients with uveal melanoma liver metastases. *J Pathol Clin Res.* Oct 2018;4(4):227-240.
45. Barnhill R, van Dam PJ, Vermeulen P, et al. Replacement and desmoplastic histopathological growth patterns in cutaneous melanoma liver metastases: frequency, characteristics, and robust prognostic value. *J Pathol Clin Res.* Jul 2020;6(3):195-206.
46. Grossniklaus HE, Zhang Q, You S, McCarthy C, Heegaard S, Coupland SE. Metastatic ocular melanoma to the liver exhibits infiltrative and nodular growth patterns. *Hum Pathol.* Nov 2016;57:165-175.
47. Grossniklaus HE. Progression of ocular melanoma metastasis to the liver: the 2012 Zimmerman lecture. *JAMA Ophthalmol.* Apr 2013;131(4):462-469.
48. Meyer Y, Bohlok A, Hoppener D, et al. Histopathological growth patterns of resected non-colorectal, non-neuroendocrine liver metastases: a retrospective multicenter studyss. *Clin Exp Metastasis.* Feb 6 2022.
49. Fernandez Moro C, Bozoky B, Gerling M. Growth patterns of colorectal cancer liver metastases and their impact on prognosis: a systematic review. *BMJ Open Gastroenterol.* 2018;5(1):e000217.
50. Kwapisz D. Oligometastatic breast cancer. *Breast Cancer.* Mar 2019;26(2):138-146.
51. Tran CG, Sherman SK, Chandrasekharan C, Howe JR. Surgical Management of Neuroendocrine Tumor Liver Metastases. *Surg Oncol Clin N Am.* Jan 2021;30:39-55.
52. Teng S, Li YE, Yang M, et al. Tissue-specific transcription reprogramming promotes liver metastasis of colorectal cancer. *Cell Res.* Jan 2020;30(1):34-49.
53. Nielsen K, Rolff HC, Eefsen RL, Vainer B. The morphological growth patterns of colorectal liver metastases are prognostic for overall survival. *Mod Pathol.* Dec 2014;27(12):1641-1648.
54. Eefsen RL, Vermeulen PB, Christensen IJ, et al. Growth pattern of colorectal liver metastasis as a marker of recurrence risk. *Clin Exp Metastasis.* Apr 2015;32(4):369-381.
55. Kuczynski EA, Yin M, Bar-Zion A, et al. Co-option of Liver Vessels and Not Sprouting Angiogenesis Drives Acquired Sorafenib Resistance in Hepatocellular Carcinoma. *J Natl Cancer Inst.* Aug 2016;108(8).
56. Bridgeman VL, Vermeulen PB, Foo S, et al. Vessel co-option is common in human lung metastases and mediates resistance to anti-angiogenic therapy in preclinical lung metastasis models. *J Pathol.* Feb 2017;241(3):362-374.
57. Leenders WP, Kusters B, Verrijp K, et al. Antiangiogenic therapy of cerebral melanoma metastases results in sustained tumor progression via vessel co-option. *Clin Cancer Res.* Sep 15 2004;10(18 Pt 1):6222-6230.
58. Martens T, Laabs Y, Gunther HS, et al. Inhibition of glioblastoma growth in a highly invasive nude mouse model can be achieved by targeting epidermal growth factor receptor but not vascular endothelial growth factor receptor-2. *Clin Cancer Res.* Sep 1 2008;14(17):5447-5458.
59. Mentha G, Terraz S, Morel P, et al. Dangerous halo after neoadjuvant chemotherapy and two-step hepatectomy for colorectal liver metastases. *Br J Surg.* Jan 2009;96(1):95-103.
60. Rubbia-Brandt L, Giostra E, Brezault C, et al. Importance of histological tumor response assessment in predicting the outcome in patients with colorectal liver metastases treated with neo-adjuvant chemotherapy followed by liver surgery. *Ann Oncol.* Feb 2007;18(2):299-304.
61. Nierop PM, Hoppener DJ, Buisman FE, et al. Preoperative systemic chemotherapy alters the histopathological growth patterns of colorectal liver metastases. *J Pathol Clin Res.* Jan 2022;8(1):48-64.
62. Gomez Dorronsoro ML, Vera R, Ortega L, et al. Recommendations of a group of experts for the pathological assessment of tumour regression of liver metastases of colorectal cancer and damage of non-tumour liver tissue after neoadjuvant therapy. *Clin Transl Oncol.* Mar 2014;16(3):234-242.
63. Powley IR, Patel M, Miles G, et al. Patient-derived explants (PDEs) as a powerful preclinical platform for anti-cancer drug and biomarker discovery. *Br J Cancer.* Mar 2020;122(6):735-744.
64. Voabil P, de Bruijn M, Roelofsen LM, et al. An ex vivo tumor fragment platform to dissect response to PD-1 blockade in cancer. *Nat Med.* 2021;27(7):1250-1261.

65. Fornabaio G, Barnhill RL, Lugassy C, et al. Angiotropism and extravascular migratory metastasis in cutaneous and uveal melanoma progression in a zebrafish model. *Sci Rep.* Jul 11 2018;8(1):10448.
66. Latacz E, van Dam PJ, Vanhove C, et al. Can medical imaging identify the histopathological growth patterns of liver metastases? *Semin Cancer Biol.* Jun 2021;71:33-41.
67. Wei S, Han Y, Zeng H, et al. Radiomics diagnosed histopathological growth pattern in prediction of response and 1-year progression free survival for colorectal liver metastases patients treated with bevacizumab containing chemotherapy. *Eur J Radiol.* Sep 2021;142:109863.
68. Er EE, Valiente M, Ganesh K, et al. Pericyte-like spreading by disseminated cancer cells activates YAP and MRTF for metastatic colonization. *Nat Cell Biol.* Aug 2018;20(8):966-978.
69. Suzuki K, Tanaka M, Watanabe N, Saito S, Nonaka H, Miyajima A. p75 Neurotrophin receptor is a marker for precursors of stellate cells and portal fibroblasts in mouse fetal liver. *Gastroenterology.* Jul 2008;135(1):270-281 e273.
70. Wells RG. The portal fibroblast: not just a poor man's stellate cell. *Gastroenterology.* Jul 2014;147(1):41-47.
71. Trim N, Morgan S, Evans M, et al. Hepatic stellate cells express the low affinity nerve growth factor receptor p75 and undergo apoptosis in response to nerve growth factor stimulation. *Am J Pathol.* Apr 2000;156(4):1235-1243.
72. Passino MA, Adams RA, Sikorski SL, Akassoglou K. Regulation of hepatic stellate cell differentiation by the neurotrophin receptor p75NTR. *Science.* Mar 30 2007;315(5820):1853-1856.
73. Kendall TJ, Hennedige S, Aucott RL, et al. p75 Neurotrophin receptor signaling regulates hepatic myofibroblast proliferation and apoptosis in recovery from rodent liver fibrosis. *Hepatology.* Mar 2009;49(3):901-910.
74. Aimaiti Y, Jin X, Shao Y, Wang W, Li D. Hepatic stellate cells regulate hepatic progenitor cells differentiation via the TGF-beta1/Jagged1 signaling axis. *J Cell Physiol.* Jun 2019;234(6):9283-9296.
75. Cassiman D, Denef C, Desmet VJ, Roskams T. Human and rat hepatic stellate cells express neurotrophins and neurotrophin receptors. *Hepatology.* Jan 2001;33(1):148-158.
76. Vidal-Vanaclocha F, Crende O, Garcia de Durango C, et al. Liver prometastatic reaction: Stimulating factors and responsive cancer phenotypes. *Semin Cancer Biol.* Jun 2021;71:122-133.
77. Ciner AT, Jones K, Muschel RJ, Brodt P. The unique immune microenvironment of liver metastases: Challenges and opportunities. *Semin Cancer Biol.* Jun 2021;71:143-156.
78. Kurebayashi Y, Kubota N, Sakamoto M. Immune microenvironment of hepatocellular carcinoma, intrahepatic cholangiocarcinoma and liver metastasis of colorectal adenocarcinoma: Relationship with histopathological and molecular classifications. *Hepatol Res.* Jan 2021;51(1):5-18.
79. Bohlok A, Duran Derijckere I, Azema H, et al. Clinico-metabolic characterization improves the prognostic value of histological growth patterns in patients undergoing surgery for colorectal liver metastases. *J Surg Oncol.* May 2021;123(8):1773-1783.
80. Matsumoto K, Yoshitomi H, Rossant J, Zaret KS. Liver organogenesis promoted by endothelial cells prior to vascular function. *Science.* Oct 19 2001;294(5542):559-563.
81. Crivellato E, Nico B, Ribatti D. Contribution of endothelial cells to organogenesis: a modern reappraisal of an old Aristotelian concept. *J Anat.* Oct 2007;211(4):415-427.
82. Ding BS, Cao Z, Lis R, et al. Divergent angiocrine signals from vascular niche balance liver regeneration and fibrosis. *Nature.* Jan 2 2014;505(7481):97-102.
83. Daniel E, Cleaver O. Vascularizing organogenesis: Lessons from developmental biology and implications for regenerative medicine. *Curr Top Dev Biol.* 2019;132:177-220.
84. Muthuswamy SK. Self-organization in cancer: Implications for histopathology, cancer cell biology, and metastasis. *Cancer Cell.* Apr 12 2021;39(4):443-446.
85. Pezzella F, Di Bacco A, Andreola S, Nicholson AG, Pastorino U, Harris AL. Angiogenesis in primary lung cancer and lung secondaries. *Eur J Cancer.* Dec 1996;32A(14):2494-2500.

86. Evidence for novel non-angiogenic pathway in breast-cancer metastasis. Breast Cancer Progression Working Party. *Lancet.* May 20 2000;355(9217):1787-1788.
87. Teuwen LA, De Rooij L, Cuypers A, et al. Tumor vessel co-option probed by single-cell analysis. *Cell Rep.* Jun 15 2021;35(11):109253.
88. Lee JC, Green MD, Huppert LA, Chow C, Pierce RH, Daud AI. The Liver-Immunity Nexus and Cancer Immunotherapy. *Clin Cancer Res.* Jan 1 2022;28(1):5-12.
89. Garcia-Vicién G, Mezheyeuski A, Micke P, et al. Spatial Immunology in Liver Metastases from Colorectal Carcinoma according to the Histologic Growth Pattern. *Cancers.* 2022;14(3):689.
90. Szczepanski JM, Mendiratta-Lala M, Fang JM, Choi WT, Karamchandani DM, Westerhoff M. Sinusoidal Growth Pattern of Hepatic Melanoma Metastasis: Implications for Histopathologic Diagnosis. *Am J Surg Pathol.* Nov 18 2021.
91. Li WH, Wang S, Liu Y, Wang XF, Wang YF, Chai RM. Differentiation of histopathological growth patterns of colorectal liver metastases by MRI features. Quant *Imaging Med Surg.* Jan 2022;12(1):608-617.
92. de Ridder JA, Knijn N, Wiering B, de Wilt JH, Nagtegaal ID. Lymphatic Invasion is an Independent Adverse Prognostic Factor in Patients with Colorectal Liver Metastasis. *Ann Surg Oncol.* Dec 2015;22 Suppl 3:S638-645.
93. Serrablo A, Paliogiannis P, Pulighe F, et al. Impact of novel histopathological factors on the outcomes of liver surgery for colorectal cancer metastases. *Eur J Surg Oncol.* Sep 2016;42(9):1268-1277.
94. Fonseca GM, de Mello ES, Faraj SF, et al. Prognostic significance of poorly differentiated clusters and tumor budding in colorectal liver metastases. *J Surg Oncol.* Jun 2018;117(7):1364-1375.
95. Cremolini C, Milione M, Marmorino F, et al. Differential histopathologic parameters in colorectal cancer liver metastases resected after triplets plus bevacizumab or cetuximab: a pooled analysis of five prospective trials. *Br J Cancer.* Apr 2018;118(7):955-965.
96. Falcao D, Alexandrino H, Caetano Oliveira R, et al. Histopathologic patterns as markers of prognosis in patients undergoing hepatectomy for colorectal cancer liver metastases - Pushing growth as an independent risk factor for decreased survival. *Eur J Surg Oncol.* Aug 2018;44(8):1212-1219.
97. Ao T, Kajiwara Y, Yonemura K, et al. Prognostic significance of histological categorization of desmoplastic reaction in colorectal liver metastases. *Virchows Arch.* Sep 2019;475(3):341-348.
98. Zhang Y, Luo X, Lin J, et al. Gelsolin Promotes Cancer Progression by Regulating Epithelial-Mesenchymal Transition in Hepatocellular Carcinoma and Correlates with a Poor Prognosis. *J Oncol.* 2020;2020:1980368.
99. Baldin P, Van den Eynde M, Mlecnik B, et al. Prognostic assessment of resected colorectal liver metastases integrating pathological features, RAS mutation and Immunoscore. *J Pathol Clin Res.* Jan 2021;7(1):27-41.
100. Temido MJ, Caetano Oliveira R, Martins R, et al. Prognostic Factors After Hepatectomy for Gastric Adenocarcinoma Liver Metastases: Desmoplastic Growth Pattern as the Key to Improved Overall Survival. *Cancer Manag Res.* 2020;12:11689-11699.
101. Jayme VR, Fonseca GM, Amaral IMA, et al. Infiltrative Tumor Borders in Colorectal Liver Metastasis: Should We Enlarge Margin Size? *Ann Surg Oncol.* Nov 2021;28(12):7636-7646.
102. Zhang YL, He HJ, Cheng J, Shen DH. [Value of histopathological growth pattern in predicting 3-year progression free survival after operation in patients with liver metastasis of colorectal cancer]. *Zhonghua Bing Li Xue Za Zhi.* Jan 8 2021;50(1):26-31.
103. Meyer YM, Beumer BR, Hoppener DJ, et al. Histopathological growth patterns modify the prognostic impact of microvascular invasion in non-cirrhotic hepatocellular carcinoma. *HPB (Oxford).* Jul 30 2021.
104. Vles MD, Hoppener DJ, Galjart B, et al. Local tumour control after radiofrequency or microwave ablation for colorectal liver metastases in relation to histopathological growth patterns. *HPB (Oxford).* Jan 24 2022.
105. Ceausu AR, Ciolofan A, Cimpean AM, Magheti A, Mederle O, Raica M. The Mesenchymal-Epithelial and Epithelial-Mesenchymal Cellular Plasticity of Liver Metastases with Digestive Origin. *Anticancer Res.* Feb 2018;38(2):811-816.
106. Lazaris A, Amri A, Petrillo SK, et al. Vascularization of colorectal carcinoma liver metastasis: insight into stratification of patients for anti-angiogenic

therapies. *J Pathol Clin Res.* Jul 2018;4(3):184-192.
107. Wu JB, Sarmiento AL, Fiset PO, et al. Histologic features and genomic alterations of primary colorectal adenocarcinoma predict growth patterns of liver metastasis. *World J Gastroenterol.* Jul 14 2019;25(26):3408-3425.
108. Blank A, Schenker C, Dawson H, Beldi G, Zlobec I, Lugli A. Evaluation of Tumor Budding in Primary Colorectal Cancer and Corresponding Liver Metastases Based on H&E and Pancytokeratin Staining. *Front Med (Lausanne).* 2019;6:247.
109. Palmieri V, Lazaris A, Mayer TZ, et al. Neutrophils expressing lysyl oxidase-like 4 protein are present in colorectal cancer liver metastases resistant to anti-angiogenic therapy. *J Pathol.* Jun 2020;251(2):213-223.
110. Ao T, Kajiwara Y, Yonemura K, et al. Morphological consistency of desmoplastic reactions between the primary colorectal cancer lesion and associated metastatic lesions. *Virchows Arch.* 2020;477(1):47-55.
111. Rada M, Kapelanski-Lamoureux A, Petrillo S, et al. Runt related transcription factor-1 plays a central role in vessel co-option of colorectal cancer liver metastases. *Commun Biol.* Aug 10 2021;4(1):950.
112. Burren S, Reche K, Blank A, et al. RHAMM in liver metastases of stage IV colorectal cancer with mismatch-repair proficient status correlates with tumor budding, cytotoxic T-cells and PD-1/PD-L1. *Pathol Res Pract.* Jul 2021;223:153486.
113. Donnem T, Reynolds AR, Kuczynski EA, et al. Non-angiogenic tumours and their influence on cancer biology. *Nat Rev Cancer.* May 2018;18(5):323-336.
114. Baldin P, Van den Eynde M, Hubert C, Jouret-Mourin A, Komuta M. The role of the pathologist and clinical implications in colorectal liver metastasis. *Acta Gastroenterol Belg.* Jul-Sep 2018;81(3):419-426.
115. Kuczynski EA, Vermeulen PB, Pezzella F, Kerbel RS, Reynolds AR. Vessel co-option in cancer. *Nat Rev Clin Oncol.* Aug 2019;16(8):469-493.
116. Oliveira RC, Alexandrino H, Cipriano MA, Tralhao JG. Liver Metastases and Histological Growth Patterns: Biological Behavior and Potential Clinical Implications-Another Path to Individualized Medicine? *J Oncol.* 2019;2019:6280347.
117. Kuczynski EA, Reynolds AR. Vessel co-option and resistance to anti-angiogenic therapy. *Angiogenesis.* Feb 2020;23(1):55-74.
118. Oliveira RC, Alexandrino H, Cipriano MA, Alves FC, Tralhao JG. Predicting liver metastases growth patterns: Current status and future possibilities. *Semin Cancer Biol.* Jun 2021;71:42-51.
119. Rigamonti A, Feuerhake F, Donadon M, Locati M, Marchesi F. Histopathological and Immune Prognostic Factors in Colo-Rectal Liver Metastases. *Cancers.* 2021;13(5).
120. Garcia-Vicien G, Mezheyeuski A, Banuls M, Ruiz-Roig N, Mollevi DG. The Tumor Microenvironment in Liver Metastases from Colorectal Carcinoma in the Context of the Histologic Growth Patterns. *Int J Mol Sci.* Feb 3 2021;22(4).
121. Haas G, Fan S, Ghadimi M, De Oliveira T, Conradi LC. Different Forms of Tumor Vascularization and Their Clinical Implications Focusing on Vessel Co-option in Colorectal Cancer Liver Metastases. *Front Cell Dev Biol.* 2021;9:612774.
122. Rompianesi G, Pegoraro F, Ceresa CD, Montalti R, Troisi RI. Artificial intelligence in the diagnosis and management of colorectal cancer liver metastases. *World J Gastroenterol.* Jan 7 2022;28(1):108-122.
123. Paku S, Lapis K. Morphological aspects of angiogenesis in experimental liver metastases. *Am J Pathol.* Sep 1993;143(3):926-936.
124. Vidal-Vanaclocha F. The prometastatic microenvironment of the liver. *Cancer Microenviron.* 2008;1(1):113-129.
125. Barsky SH, Doberneck SA, Sternlicht MD, Grossman DA, Love SM. 'Revertant' DCIS in human axillary breast carcinoma metastases. *J Pathol.* 1997;183(2):188-194.
126. Schuppan D, Kim YO. Evolving therapies for liver fibrosis. *J Clin Invest.* May 2013;123(5):1887-1901.
127. Dezso K, Papp V, Bugyik E, et al. Structural analysis of oval-cell-mediated liver regeneration in rats. *Hepatology.* Oct 2012;56(4):1457-1467.
128. Chen YW, Rini BI. Approaches to First-Line Therapy for Metastatic Clear Cell Renal Cell Carcinoma. *Curr Oncol Rep* Online ahead of print 2022.
129. Sangro B, Sarobe P, Hervás-Stubbs S, Melero I. Advances in immunotherapy for hepatocellular carcinoma. *Nat Rev Gastroenterol Hepatol* 2021;18:525-543.

```
#------------------------------ Circleplots ------------------------------
#Legend
lgdi <- Legend(at = c("Classical", "Invasion", "Tumour interface",
                      "Immunological"), type = "grid",
               legend_gp =
                  gpar(fill = c("#7ec2e6", "#ffb657", "#9be05e", "#cfa3e6")),
                       title_position = "topleft", title = "Marker group")

#Export plot
pdf("Figures/CBplot.pdf", width = 10, height = 5, pointsize = 11)
layout(matrix(1:2, 1, 2))

#plot non-desmo
circos.par("start.degree" = 90, cell.padding = c(0, 0, 0, 0))
circos.initialize("a", xlim = c(0, 1))
circos.track(ylim = c(0.5, length(ndscore)+0.5), track.height = 0.8,
             bg.border = NA, panel.fun = function(x, y) {
               xlim = CELL_META$xlim
               circos.segments(rep(0, length(ndscore)), 1:length(ndscore),
                               rep(0.75, length(ndscore)),
                               1:length(ndscore), col = "#CCCCCC")
               circos.rect(rep(0, length(ndscore)),
                           1:length(ndscore) - 0.45, ndscore,
                           1:length(ndscore) + 0.45,
                           col = colors, border = "white")
               circos.text(rep(xlim[1], length(ndscore)),
                           1:length(ndscore), ndpctlbs,
                           facing = "downward", adj = c(1, 0.5), cex = 0.8)
               breaks = seq(0, 0.75, by = 0.25)
               circos.axis(h = "top", major.at = breaks,
                           labels = paste0(breaks*100, "%"),
                           labels.cex = 0.6)
             })
circos.clear()
title("Non-desmoplastic CRLM 152/183\n\n\n")

#plot desmo
circos.par("start.degree" = 90, cell.padding = c(0, 0, 0, 0))
circos.initialize("a", xlim = c(0, 1))
circos.track(ylim = c(0.5, length(dscore)+0.5), track.height = 0.8,
             bg.border = NA, panel.fun = function(x, y) {
               xlim = CELL_META$xlim
               circos.segments(rep(0, length(dscore)), 1:length(dscore),
               rep(0.75, length(dscore)), 1:length(dscore), col = "#CCCCCC")
               circos.rect(rep(0, length(dscore)),
                           1:length(dscore) - 0.45, dscore,
                           1:length(dscore) + 0.45,
                           col = colors, border = "white")
               circos.text(rep(xlim[1], length(dscore)),
                           1:length(dscore), dpctlbs,
                           facing = "downward", adj = c(1, 0.5), cex = 0.8)
               breaks = seq(0, 0.75, by = 0.25)
               circos.axis(h = "top", major.at = breaks,
                           labels = paste0(breaks*100, "%"),
                           labels.cex = 0.6)
```

Chapter V

The relationship between primary colorectal cancer histology and the histopathological growth patterns of corresponding liver metastases

-

BMC Cancer 2022

D.J. Höppener, J.P.L. Stook, B. Galjart, P.M.H. Nierop, I.D. Nagtegaal, P.B. Vermeulen, D.J. Grünhagen, C. Verhoef, M. Doukas.

Abstract

Background: The histopathological growth patterns (HGPs) are a prognostic and predictive biomarker in colorectal cancer liver metastasis (CRLM). This study evaluates the relationship between the HGP and primary colorectal cancer (CRC) histopathology.

Methods: A total of 183 treatment-naive patients with resected CRC and CRLM were included. Thirteen CRC histopathology markers were determined and compared between the desmoplastic and non-desmoplastic HGP; tumour sidedness, pT&pN stage, tumour grade, tumour deposits, perineural- (lympho-)vascular- and extramural venous invasion, peritumoural budding, stroma type, CRC growth pattern, Crohn's-like lymphoid reaction, and tumour-infiltrating lymphocyte (TIL) density. Logistic regression analysis was performed using both CRC and CRLM characteristics.

Results: Unfavourable CRC histopathology was more frequent in non-desmoplastic CRLM for all markers evaluated, and significantly so for a lower TIL density, absent Crohn's-like lymphoid reaction, and a "non-mature" stroma (all $p<0.03$). The cumulative prevalence of unfavourable CRC histopathology was significantly higher in patients with non-desmoplastic compared to desmoplastic CRLM, with a median (IQR) of 4 (3-6) vs 2 (1-3.5) unfavourable characteristics observed, respectively ($p<0.001$). Multivariable regression with 9 CRC histopathology markers and 2 CRLM characteristics achieved good discriminatory performance (AUC=0.83).

Conclusions: The results of this study associates primary CRC histopathology with the HGP of corresponding liver metastases.

Introduction

The management of colorectal cancer liver metastasis (CRLM) is clinically challenging and requires a multidisciplinary approach. This multidisciplinary need stems from the amenability of CRLM to local therapies such as surgical resection, ablation, and radiotherapy, which is dependent on hepatic tumour load and anatomical location, and the ability of systemic chemotherapy to act upon this through tumour load reduction.[1] Although up to half of all patients can be treated with curative intent, cancer recurrence after surgical treatment of CRLM still occurs in over two-thirds, with long-term cure achieved in approximately one fourth.[2-6] This illustrates a demand for reliable and discriminatory markers to guide clinical decision making, preferably within the pre-treatment setting.

Histopathology studies of CRLM have led to the discovery of distinct histopathological growth patterns (HGP) formed at the interface of liver metastases and the liver parenchyma.[7] A desmoplastic type is recognised in approximately one fifth of resected patients, characterised by the full encapsulation of all liver metastases by desmoplastic stroma (*figure 1A*).[8] Opposing is the non-desmoplastic type, which is primarily characterised by the complete or partial absence of tumour encapsulation, and secondarily by either invasion (*figure 1B*) or, rarely, compression (*figure 1C*) of the liver parenchyma.[8] The clinical importance of this histopathology marker has been established in multiple cohorts, which reported 5-year overall survival rates of up to 80% for desmoplastic and as low as 40% for non-desmoplastic[8,9], and have also suggested a benefit for adjuvant systemic chemotherapy for the treatment-naive non-desmoplastic patients only.[10] Since perioperative systemic chemotherapy is considered standard of care in most countries, and current HGP assessment requires a CRLM resection specimen, predicting

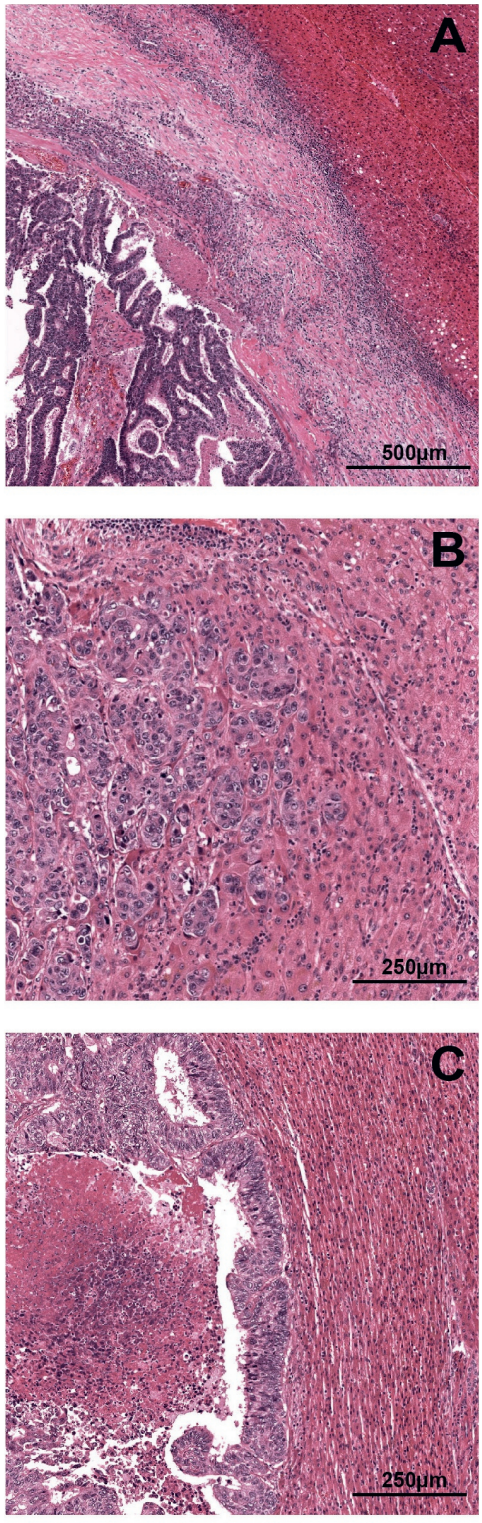

the HGP beforehand could help identify patients with favourable prognosis that do not require perioperative systemic chemotherapy, and could prevent unnecessary chemotherapy-associated morbidity.

As approximately half of all CRLM are metachronous, resection specimens of primary colorectal cancer are often available.[2-4] A possible clue to assess the

← *Figure 1. Haematoxylin and Eosin (H&E) stained examples of desmoplastic (A) and non-desmoplastic (B&C) histopathological growth patterns (HGP) of resected colorectal liver metastasis. A: H&E of the desmoplastic type HGP; note the broad band of desmoplastic stroma separating the tumour from the pre-existing liver parenchyma and the dense lymphocytic infiltrate. B: H&E of the replacement type HGP; note the infiltration of tumour cells into the pre-existing liver parenchyma with cell to cell contact between tumour cells and hepatocytes all the while retaining some of the liver cell plate architecture. C: H&E of the rare pushing type HGP; note the well circumscribed margin between the tumour cells and hepatocytes and the compression of the liver cell plates in the pre-existing liver parenchyma.*

HGP preoperatively might therefore lie in the primary CRC histopathology, especially given the number of available and established markers. In addition, associations could reveal underlying biological mechanisms of the distinct HGPs. This study therefore performs an exploratory analysis on the relationship between primary CRC histopathology and the HGP of corresponding CRLM.

Methods

Patient selection

A single centre retrospective cohort study was conducted in patients treated surgically with curative intent for CRLM at the Erasmus MC Cancer Institute (Rotterdam, the Netherlands) between January 2000 and February 2019. Eligible patients were those who had had resection of their primary CRC at either the Erasmus MC Cancer Institute or a referring centre affiliated with one of four regional Dutch pathology laboratories (Erasmus MC, Bravis hospital, Maasstad Hospital, or Pathan). Patients who received any preoperative radio- or systemic chemotherapy prior to CRC or CRLM surgery were excluded, as preoperative treatment may alter both CRC histopathology and the HGPs of CRLM.[11,12] In addition, patients with metachronous CRLM treated with adjuvant chemotherapy had to have had no systemic chemotherapy six months prior to CRLM diagnosis. Data on patient, CRLM, treatment characteristics, and overall survival (OS) was extracted from a prospectively maintained database. Institutional ethical review was obtained from the medical ethics committee of the Erasmus University Medical Center, Rotterdam, the Netherlands (MEC-2018-1743).

Colorectal liver metastasis HGP

Determination of the liver metastasis HGP was performed previously within the context of retrospective cohort

studies.[8,9] Assessment was at the time performed by at least two trained observers simultaneously on haematoxylin and eosin (H&E) stained tissue sections of resected CRLM, in accordance with international consensus guidelines, and blinded for all patient characteristics (including primary CRC) and survival.[7] In summary, assessment entails the systematic evaluation of the entire tumour liver interface using light microscopy to determine the relative proportion of each of three distinct HGPs (*figure 1*). In line with the upcoming updated consensus guidelines the Rotterdam cut-off was applied and patients were classified as desmoplastic if all metastases exclusively displayed a desmoplastic pattern (i.e. 100% desmoplastic, *figure 1A*), and as non-desmoplastic otherwise (i.e. <100% desmoplastic, *figures 1B* & *C*).

Primary CRC histopathology

For eligible patients all available H&E slides of resected CRC were requested from the respective pathology laboratories through the nationwide network and registry of histo- and cytopathology in the Netherlands (PALGA).[13] A literature study was conducted to identify CRC histopathology markers of interest, being those assessable on H&E stained slides, with clinical evidence suggesting a prognostic impact on (overall) survival following CRC resection, and with standardised guidelines and/or detailed methods of assessment. The literature study identified thirteen histopathology markers of interest, which were grouped in four categories. The *classical markers* comprised tumour sidedness, histologic grade, pT-stage, pN-stage, and tumour deposits. Under *invasion markers* were grouped lymphovascular invasion, extramural venous invasion, and perineural invasion. Amongst the *tumour interface markers* were peritumoural budding, CRC growth pattern, and fibrotic stroma type. Lastly, the *immunological markers* consisted of Crohn's-like lymphoid reaction, and tumour-infiltrating lymphocyte (TIL) density.

A scoring manual was drafted outlining the assessment, definitions, and classifications with corresponding H&E examples for each (novel) individual marker identified (histologic grade, pT&pN-stage, and tumour sidedness were not described). This scoring manual was reviewed by two expert pathologists (PBV and MD) to reach a final consensus (*supplementary file 1*; *available online*). A practice session was conducted using 64 digitalised H&E slides of resected CRC from 10 patients to reach agreement on the interpretation and application of the scoring manual. Hereafter the histopathology markers of interest were determined on all available H&E stained slides of included patients. Assessment was performed on a multi-head microscope by a gastro-intestinal pathologist (MD) and several PhD candidates, using the scoring manual as a reference, and blinded for patient characteristics, survival, and liver metastasis HGP. Scoring was done over the course of multiple (>20) brief morning sessions (1-2 hours) to prevent deterioration in assessment quality due to fatigue.

Classical markers

A right-sided tumour was defined as an anatomical CRC localisation proximal to the splenic flexure. The determination of histologic grade, pT&pN-stage, and tumour deposits was done in accordance with the 8th edition of the American Joint Committee on Cancer staging manual for CRC. [14] The 8th edition defines tumour deposits as discrete tumour nodules found within the lymph drainage area of CRC and containing no identifiable lymph node tissue or vascular/ neural structures (*figure 2A*).

Invasion markers

Lymphovascular invasion was defined as the presence of tumour cells within a definite endothelial-lined space (lymphatics or blood vessel) (*figure 2D*)[15], extramural venous invasion as

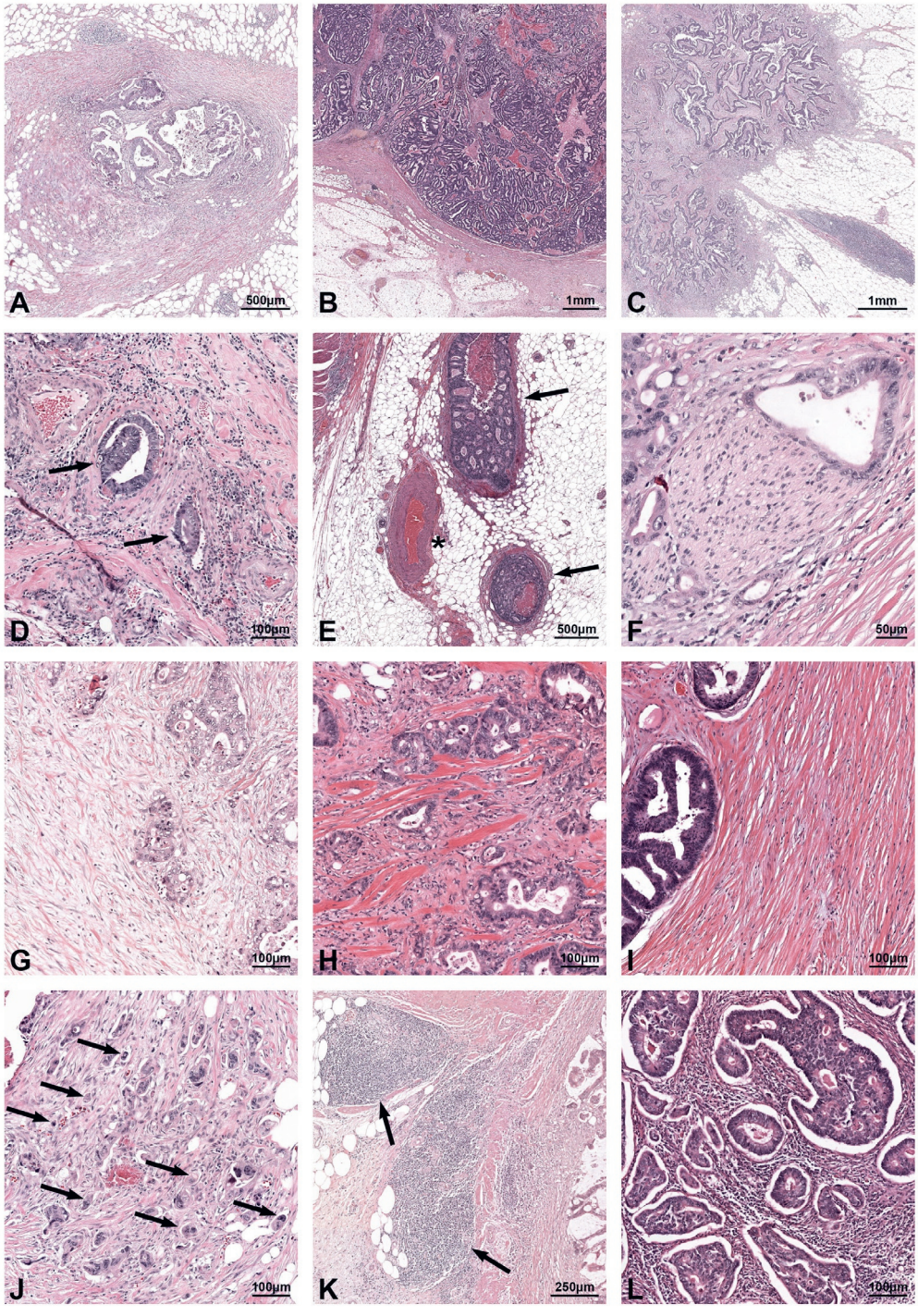
A
500µm
B
1mm
C
1mm
D
100µm
E
500µm
F
50µm
G
100µm
H
100µm
I
100µm
J
100µm
K
250µm
L
100µm

tumour invasion into large veins located in the subserosal or pericolic fat tissue (*figure 2E*)[16], and perineural (or intraneural) invasion as the presence of tumour cells inside the nerve sheath, or when at least one-third of the nerve circumference was encompassed by tumour cells (*figure 2F*)[17].

Tumour interface markers

Peritumoural budding was assessed in accordance with the 2016 International Tumor Budding Consensus Conference recommendations.[18] Peritumoural buds, defined as a single tumour cell or a cluster of up to four tumour cells without gland formation (*figure 2J*), were counted in a 20x magnification field at the invasive margin "hotspot" (field with the greatest density of buds in all available slides) and classified using a three-tier system;

← Figure 2. Haematoxylin and Eosin (H&E) stained examples of resected colorectal cancer (CRC) for individual markers. A: H&E example of a tumour deposit; note the absence of identifiable lymph node tissue and vascular or neural structures. B: H&E example of the expanding type growth pattern characterised by the pushing/well-circumscribed margin. C: H&E example of the infiltrating type growth pattern characterised by the diffuse and widespread invasion of normal tissue. D: H&E example of lymphovascular invasion; the arrows indicate tumour cells located within vascular structures, as can also be identified by the erythrocytes inside both respective lumen. E: H&E example of extramural venous invasion; the arrows indicate tumour growth into a large vein located in the subserosal fatty tissue and the asterisk indicates the accompanying artery. F: H&E example of perineural/ intraneural invasion of tumour cells inside the nerve sheath. G: H&E example of the immature fibrotic stroma type characterised by randomly oriented collagen bundles surrounded by myxoid stroma. H: H&E example of the intermediate fibrotic stroma type characterised by broad bands of brightly eosinophilic hyalinised collaen (ropy-like) intermingled with stroma. I: H&E example of the mature fibrotic stroma type characterised by multiple fine, mature, and stratiform fibres. J: H&E example of peritumoural budding; the arrows indicate examples of peritumoural buds located at the invasive margin (not all buds are indicated by arrows). K: H&E example of Chrohn's-like lymphoid reaction; the arrows indicate lymphoid aggregates of more than 300µm in diameter located in the advancing edge of the tumour. L: H&E example of a high density (50%) of tumour-infiltrating lymphocytes into the intratumoural stromal area at the invasive front.

Grade I (low) for 0-4 buds, Grade II (intermediate) for 5-9 buds, and Grade III (high) for ≥10 buds.[18] The CRC growth pattern was assessed according to Jass et al. and classified as either expanding or infiltrative based on a 50% predominance cut-off.[19] The expanding type is characterised by a pushing or well-circumscribed margin (*figure 2B*), whereas the infiltrative type invades diffusely with widespread penetration of normal tissue (*figure 2C*). The fibrotic stroma type according to Ueno et al. classifies the stroma beyond the muscularis propria (at least pT3 stage) into three distinct types based on morphology; immature in case randomly oriented collagen bundles are surrounded by myxoid stroma (*figure 2G*), intermediate when broad bands of brightly eosinophilic hyalinised collagen (ropy-like) are intermingled with stroma (*figure 2H*), and mature for a stroma composed of multiple fine, mature, and stratiform fibres (*figure 2I*).[20]

Immunological markers

Crohn's-Like lymphoid reaction is characterised by lymphoid aggregates of at least 300µm in diameter observed at the advancing edge of the tumour (*figure 2K*).[21] Crohn's-like lymphoid reaction was considered present in case at least one aggregate >300µm was observed in any slide. Tumour-infiltrating lymphocyte density was assessed by estimating the percentage of mononuclear inflammatory cells over the total intratumoural stromal area at the invasive front (*figure 2L*).[22]

Statistical analysis

Statistical comparisons between patients with a non-desmoplastic and desmoplastic phenotype were performed to compare baseline patient, CRLM, and treatment characteristics, and to test for associations between individual CRC histopathology markers and the HGP of corresponding CRLM. Nominal variables were compared

using the $\chi 2$ test and are reported as absolute counts with corresponding percentages. Non-parametric ordinal and numerical variables were compared using the Kruskall Wallis test and are reported as medians with corresponding interquartile ranges (IQR). The cumulative prevalence of unfavourable CRC histopathology was compared defined as the number of unfavourable characteristics observed per patient. For markers with more than two classes, a dichotomous classification was adapted, and for TIL density a percentage equal to or below the median was considered unfavourable. Uni- and multivariable binary logistic regression models were fitted with the HGP as dependent variable, and all CRC histopathology and any preoperatively available CRLM characteristics as candidate predictors. The prognostic impact of the HGP on OS following resection of CRLM was estimated by Kaplan-Meier survival analysis. Uni- and multivariable Cox regression analyses were additionally performed on OS following CRLM resection with all CRC histopathology and CRLM characteristics as candidate prognosticators. Given the large number of candidate predictors only those with a univariable p-value below 0.2 were entered into the multivariable models. Regression results are reported as multivariable odds ratios (OR) or hazard ratios (HR) with corresponding 95% confidence intervals (CI). Discriminatory capability of the multivariable logistic regression model to predict the HGP was assessed using the Area Under the Curve (AUC) metric of the receiver operating characteristic curve. The statistical significance level was set at a two-sided α of 0.05. All statistical analyses and data visualisation was performed using the R project for statistical computing version 4.1.1 (www.r-project.org), with packages rms (6.0-1), tableone (0.12.0), pROC (1.16.2), circlize (0.4.11)[23], and ggplot2 (3.3.2).

Results

Primary CRC slides were requested for a total of 196 eligible patients through PALGA and were available for 183 (93%). A desmoplastic HGP was observed in 31 (17%) out of the 183 patients included for analysis. Baseline patient, CRLM, and treatment characteristics stratified by HGP are reported in *table 1*. Patients with a non-desmoplastic HGP had a significantly larger CRLM diameter (median [IQR]: 3.2 [2.2, 4.1] vs 2.0 [1.3, 3.0] cm, p<0.001), a significantly higher preoperative serum carcinoembryonic antigen level (median [IQR]: 12.0 [5.0, 44.7] vs 5.7 [3.2, 10.6] µg/L, p=0.002), and more often had positive surgical margins upon CRLM resection (n=14 [9%] vs n=0 [0%], p=0.07) (*table 1*). Within the 119 patients with metachronous CRLM non-desmoplastic patients more often received adjuvant systemic chemotherapy (n=46 [45%] vs n=3 [19%], p=0.05, *table 1*).

Table 1. Baseline CRLM characteristics stratified by histopathological growth pattern

		missing (%)	Non-desmoplastic n = 152 (%)	Desmoplastic n = 31 (%)	p-value
Age at resection CRLM - *(median [IQR])*			67 [59, 74]	68 [62, 77]	0.26
Gender	Male		55 (36)	9 (29)	0.45
	Female		97 (64)	22 (71)	
Resection timing	Liver first		1 (1)	0 (0)	0.07
	Primary first		141 (93)	25 (81)	
	Synchronous		10 (7)	6 (19)	
Metastasis timing*	Metachronous		103 (68)	16 (52)	0.09
	Synchronous		49 (32)	15 (48)	
DFI in months* - *(median [IQR])*			12.0 [0.0, 24.2]	4.0 [0.0, 20.5]	0.11
Adjuvant CTx for CRC**	No		57 (55)	13 (81)	0.05
	Yes		46 (45)	3 (19)	
CRLM distribution	Unilobar		127 (84)	28 (90)	0.34
	Bilobar		25 (16)	3 (10)	
Number of CRLM - *(median [IQR])*		*1 (1)*	1.0 [1.0, 2.0]	1.0 [1.0, 2.0]	0.50
Largest CRLM in cm - *(median [IQR])*		*1 (1)*	3.2 [2.2, 4.1]	2.0 [1.3, 3.0]	<0.001
Preop. CEA in µg/L - *(median [IQR])*		*13 (7)*	12.0 [5.0, 44.7]	5.7 [3.2, 10.6]	0.002
Concomitant ablation	No		134 (88)	27 (87)	0.66
	RFA		15 (10)	4 (13)	
	MWA		3 (2)	0 (0)	
Resection margin involved	No	*4 (2)*	134 (91)	31 (100)	0.07
	Yes		14 (9)	0 (0)	
Extrahepatic disease	No		136 (89)	30 (97)	0.20
	Yes		16 (11)	1 (3)	

**Between resection of primary tumour and detection of CRLM. Synchronous is defined as CRLM diagnosed prior to or within 3 months following CRC resection.*
***Within the 119 patients with metachronous CRLM.*
CEA: carcinoembryonic antigen; CRLM: colorectal liver metastasis; CTx: chemotherapy; DFI: disease-free interval IQR: interquartile range; MWA: microwave ablation; RFA radiofrequency ablation.

Primary CRC histopathology

A total of 913 H&E slides of resected CRC were reviewed. The median number of tumour containing slides assessed per patient was 4 (IQR: 3-6) and did not differ between patients with corresponding non-desmoplastic (4 IQR [3-7]) and desmoplastic (4 IQR [3-5.5]) CRLM (p=0.27). The great majority were adenocarcinomas (n=179, 98%), with only 4 (2%) mucinous adenocarcinomas, which were equally distributed between non-desmoplastic (n=3, 2%) and desmoplastic (n=1, 3%) patients (p=0.66). Comparisons of all primary CRC histopathology markers stratified by corresponding liver metastasis HGP is reported in *table 2* and *figure 3A-C*.

Classical markers

Poorly differentiated (G3) tumours (5% vs 0%), right-sided tumours (30% vs 16%), pT4-stage (16% vs 6%), positive lymph nodes (62% vs 48%), and tumour deposits (21% vs 10%) were more common in patients with corresponding non-desmoplastic versus desmoplastic CRLM, but none of these differences reached statistical significance (p-values of 0.22, 0.11, 0.15, and 0.16, respectively, *table 2*).

Invasion markers

Invasion, either lymphovascular (41% vs 23%), extramural venous (41% vs 29%), or perineural (26% vs 13%), was more prevalent in patients with non-desmoplastic versus desmoplastic CRLM, but none of these differences reached formal statistical significance (p-values of 0.06, 0.22, and 0.13, respectively, *table 2*).

Tumour interface markers

Peritumoural budding (grade II/III vs I: 20% vs 10%) and an infiltrative CRC growth pattern (53% vs 42%) were also more common for patients with corresponding non-desmoplastic versus desmoplastic metastases, but again these differences

did not reach statistical significance (p=0.18 and p=0.28 respectively, *table 2*). Of the patients with non-desmoplastic CRLM, 18 (13%) had an immature, 33 (24%) an intermediate, and 87 (63%) a mature fibrotic stroma type, whereas this

Table 2. Primary CRC hisopathology compared for liver metastasis histopathological growth pattern

		missing (%)	Non-desmoplastic n = 152 (%)	Desmoplastic n = 31 (%)	p-value
Classical markers					
Primary tumour location	Rectum		17 (11)	3 (10)	0.23
	Left-sided		89 (59)	23 (74)	
	Right-sided		46 (30)	5 (16)	
Right-sided tumour	No		106 (70)	26 (84)	0.11
	Yes		46 (30)	5 (16)	
Differentiation grade	Well / moderate (G1/G2)		145 (95)	31 (100)	0.22
	Poor (G3)		7 (5)	0 (0)	
pT-stage	pT1		3 (2)	0 (0)	0.53
	pT2		15 (10)	3 (10)	
	pT3		109 (72)	26 (84)	
	pT4a		19 (12)	1 (3)	
	pT4b		6 (4)	1 (3)	
pT4-stage	No		127 (84)	29 (94)	0.15
	Yes		25 (16)	2 (6)	
pN-stage	N0		58 (38)	16 (52)	0.52
	N1a		28 (18)	6 (19)	
	N1b		30 (20)	3 (10)	
	N1c		4 (3)	0 (0)	
	N2a		15 (10)	4 (13)	
	N2b		17 (11)	2 (6)	
Positive lymph nodes	No		58 (38)	16 (52)	0.16
	Yes		94 (62)	15 (48)	
Tumour deposits	No		120 (79)	28 (90)	0.14
	Yes		32 (21)	3 (10)	
Invasion markers					
(lympho-)vascular invasion	No		90 (59)	24 (77)	0.06
	Yes		62 (41)	7 (23)	
Extramural vascular invasion	No		90 (59)	22 (71)	0.22
	Yes		62 (41)	9 (29)	
Perineural invasion	No		113 (74)	27 (87)	0.13
	Yes		39 (26)	4 (13)	
Tumour interface markers					
Peritumoural budding	Grade I		122 (80)	28 (90)	0.32
	Grade II		26 (17)	2 (6)	
	Grade III		4 (3)	1 (3)	
Peritumoural budding	No (Grade I)		122 (80)	28 (90)	0.18
	Yes (Grade II/III)		30 (20)	3 (10)	
Primary CRC growth pattern	Expanding		72 (47)	18 (58)	0.28
	Infiltrative		80 (53)	13 (42)	
Stroma type	Immature	*16 (9)**	18 (13)	2 (7)	0.02
	Intermediate		33 (24)	1 (3)	
	Mature		87 (63)	26 (90)	
Non-mature stroma	No		101 (66)	28 (90)	0.008
	Yes		51 (34)	3 (10)	
Immunological markers					
TIL density in % - *median [IQR]*			10 [5, 15]	15 [10, 20]	0.02
Median-to-low TIL density	No		47 (31)	18 (58)	0.004
	Yes		105 (69)	13 (42)	
Crohn's-like lymphoid reaction	No		21 (14)	0 (0)	0.03
	Yes		131 (86)	31 (100)	

**Only assessable in case of (near) extramural invasion (i.e., pT3-4)*
CRC: colorectal cancer; IQR: interquartile range; TIL: tumour-infiltrating lymphocyes.

was 2 (7%), 1 (3%), and 26 (90%) respectively for patients with desmoplastic CRLM, a difference that was statistically significant (p=0.02, *table 2*). Consequently, a non-mature

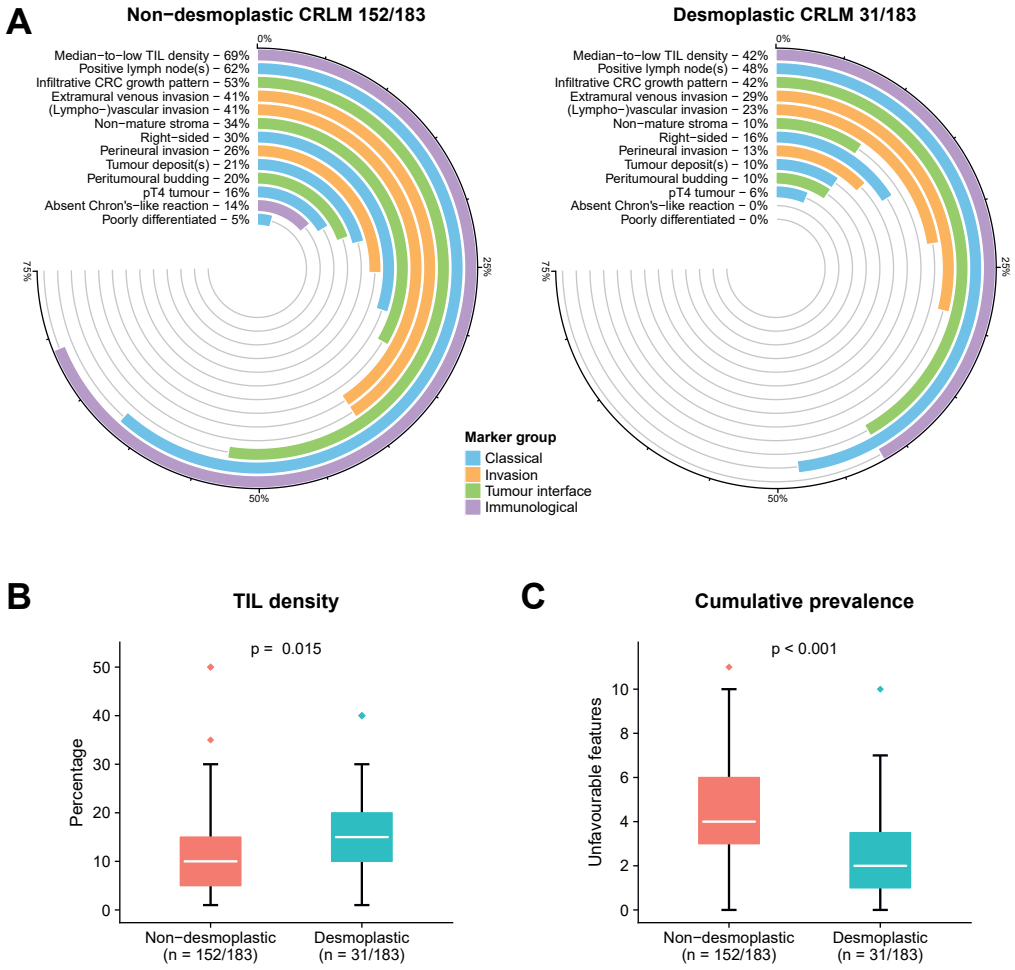

Figure 3. A: Graphical representation of the frequency of individual unfavourable histopathology features observed in the primary colorectal cancers (CRC) of patients with corresponding non-desmoplastic (left) and desmoplastic (right) liver metastases. B&C: Boxplots demonstrating the distribution of tumour-infiltrating lymphocyte (TIL) density (B) and the cumulative prevalence of unfavourable CRC histopathology characteristics (C) in patients with corresponding non-desmoplastic (red) and desmoplastic (blue) liver metastases. The p-value represents the result of the non-parametric Kruskall Wallis test.

(i.e., immature or intermediate) stroma was significantly more often observed in non-desmoplastic compared to desmoplastic patients (34% vs 10%, p=0.008, *table 2*).

Immunological markers

Crohn's-like lymphoid reaction was observed in 131 (86%) of the patients with non-desmoplastic CRLM versus in all 31 (100%) of the patients with desmoplastic CRLM (p=0.03, *table 2*). The TIL density (median [IQR]) was significantly lower for the non-desmoplastic (10% [5%-15%]) versus desmoplastic (15% [10%-20%]) patients (p=0.02, *figure 3B*). Consequently, a median-to-low (≤10%) TIL density was significantly more common in the non-desmoplastic (n=105 [69%]) compared to desmoplastic (n=13 [42%]) group (p=0.004, *table 2*).

Cumulative prevalence and HGP prediction

Overall, unfavourable CRC histopathology was significantly more prevalent in non-desmoplastic compared to desmoplastic patients with a median (IQR) of 4 (3-6) versus 2 (1-3.5) unfavourable features observed (p<0.001, *figure 3C*).

Table 3. Uni- and multivariable logistic regression analysis on the desmoplastic growth pattern

	Univariable		Multivariable (n=182)	
	OR [95%CI]	p-value	OR [95%CI]	p-value
CRLM characteristics				
Disease-free interval* (cont.) - *months*	0.98 [0.96-1.01]	0.18	0.99 [0.96-1.02]	0.54
Number of CRLM (cont.)	0.93 [0.72-1.21]	0.60	-	-
Diameter of largest CRLM (cont.) - *cm*	0.58 [0.41-0.81]	<0.01	0.55 [0.37-0.82]	<0.01
Preoperative CEA (cont.) - *100 µg/L*	0.42 [0.10-1.68]	0.22	-	-
Extrahepatic disease - *yes vs no*	0.28 [0.04-2.22]	0.23	-	-
Classical markers				
Right-sided tumour - *yes vs no*	0.44 [0.16-1.23]	0.12	0.50 [0.16-1.60]	0.24
pT4-stage - *yes vs no*	0.35 [0.08-1.56]	0.17	0.43 [0.08-2.26]	0.32
Positive lymph nodes - *yes vs no*	0.58 [0.27-1.26]	0.17	0.65 [0.25-1.69]	0.38
Tumour deposits - *yes vs no*	0.40 [0.11-1.41]	0.15	0.48 [0.08-2.95]	0.43
Invasion markers				
(lympho-)vascular invasion - *yes vs no*	0.42 [0.17-1.04]	0.06	0.68 [0.22-2.12]	0.51
Extramural vascular invasion - *yes vs no*	0.59 [0.26-1.38]	0.22	-	-
Perineural invasion - *yes vs no*	0.43 [0.14-1.30]	0.14	1.11 [0.28-4.46]	0.89
Tumour interface markers				
Peritumoural budding - *Grade II/III vs I*	0.44 [0.12-1.53]	0.19	0.51 [0.13-2.02]	0.34
CRC growth pattern - *Infiltrative vs expanding*	0.65 [0.30-1.42]	0.28	-	-
Non-mature stroma - *yes vs no*	0.21 [0.06-0.73]	0.01	0.29 [0.07-1.25]	0.10
Immunological markers				
TIL density (cont.) - *10%*	1.69 [1.15-2.47]	<0.01	1.60 [1.01-2.54]	0.05

**Between resection of primary tumour and detection of CRLM*

Abbreviations in alphabetical order: Cont.: entered as continous variable; CEA: carcinoembryonic antigen; CI: confidence interval; CRC: colorectal cancer; CRLM: colorectal liver metastasis; OR: odds ratio; TIL: tumour-infiltrating lymfocyte.

The results of the uni- and multivariable binary logistic regression analyses to predict the HGP are reported in *table 3*. Differentiation grade and Crohn's-like lymphoid reaction could not be analysed using logistic regression given absent cases in the desmoplastic group. Upon univariable analysis the CRLM characteristics disease-free interval and diameter, and all primary CRC histopathology features except extramural vascular invasion and CRC growth pattern had a p-value below 0.2 and were considered for multivariable analysis (*table 3*). Of all 11 predictors in the multivariable model, only the diameter of the largest CRLM and TIL density proved independent predictors for a desmoplastic HGP, with an OR (95%CI) of 0.55 (0.37-0.82) for each additional cm and 1.60 (1.01-2.54) per 10% increase in TIL density, respectively (*table 3*). The multivariable logistic regression model achieved an AUC of 0.83 to predict the HGP.

Survival

Patients with a desmoplastic HGP had a significantly longer OS following resection of CRLM with an estimated 5-year (95%CI) survival of 77% (64-94%) compared to 39% (31-48%) for non-desmoplastic (p=0.003, *figure 4*). Univariable OS regression analysis revealed four CRLM characteristics (age at resection, number of CRLM, extrahepatic disease, and the HGP) and nine CRC histopathology features (right-sided, differentiation grade, pT4-stage, positive lymph nodes, tumour deposits, [lympho]-vascular, extramural vascular and perineural invasion, and the CRC growth pattern) with a p-value below 0.2 and were considered for multivariable analysis (*supplementary table 1*). Of these, only age at resection, the HGP, and right-sided CRC proved independent predictors for survival, with adjusted HRs (95%CI) of 1.33 [1.10-1.62] per 10-year age increase, 1.97 [1.10-3.53] for a non-desmoplastic HGP, and 1.86 [1.23-2.83] for right-sided tumours, respectively (*supplementary table 1*).

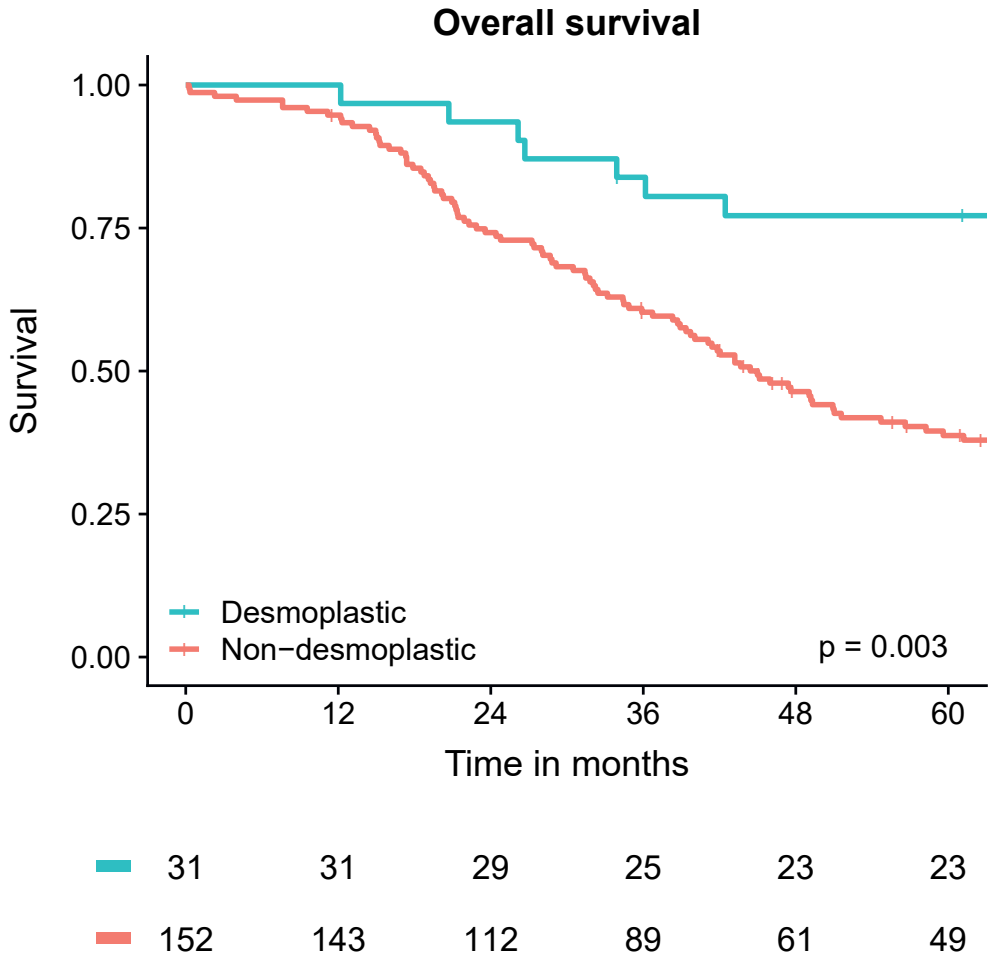

Figure 4. Kaplan-Meier analysis on overall survival following resection of colorectal liver metastasis stratified by histopathological growth pattern. The p-value represents the results of the overall log-rank test.

Discussion

The present study evaluated the relationship between thirteen established CRC histopathology markers and the HGPs of corresponding CRLM in a cohort of 183 resected patients. For all markers, unfavourable CRC histopathology was more frequent for patients with corresponding non-desmoplastic CRLM. While many of these individual marker differences did not reach statistical significance, the cumulative prevalence

of unfavourable CRC histopathology was significantly higher in the non-desmoplastic patients.

At least two other studies have previously evaluated CRC histopathology in relation to the CRLM growth pattern phenotype. The more recent study by Wu et al. evaluated 29 patients and compared primary CRC histopathology between 15 patients with a predominant (i.e. >50%) desmoplastic versus 14 with a predominant replacement pattern.[24] The study significantly associated the predominant replacement group (i.e. non-desmoplastic) with higher peritumoural budding grades, an infiltrative CRC growth pattern, and absent Crohn's disease-like response. Rajaganeshan and colleagues evaluated in 55 patients the relationships between primary CRC growth pattern and CRLM encapsulation, the latter defined as >50% fibrous capsule formation separating tumour from stroma (i.e. >50% desmoplastic), and also significantly associated an infiltrative CRC growth pattern with corresponding non-encapsulated (i.e. non-desmoplastic) CRLM.[25] An important distinction with these studies lies in the classification of the HGP, as both applied a 50% predominance cut-off as opposed to the newly recommended Rotterdam criteria of entirely desmoplastic versus otherwise. There is compelling evidence from both a prognostic[8,9] and immunologic[26] standpoint that it is this distinction between desmoplastic and non-desmoplastic that delineates clinical relevance. Results of studies applying predominance cut-offs are therefore difficult to extrapolate in light of this new classification, as the predominant desmoplastic groups (i.e. >50%) are by definition, and based on previous studies on HGP distribution[8,9], actually for more than half composed of non-desmoplastic cases. Nevertheless, taking all current evidence as a whole, non-desmoplastic CRLM have repeatedly been associated with unfavourable CRC histopathology, something also evident from the relationship with lymph

node positivity observed in multiple large cohort studies evaluating the HGPs.[8,9] The current study confirms these associations and adds further compelling evidence of the relationship between CRC histopathology and the HGPs of corresponding CRLM.

While not all individual marker differences demonstrated a statistically significant association, both the immunology markers TIL-density and Crohn's-like lymphoid reaction did, with higher TIL-densities and increased Crohn's-like lymphoid reaction observed in the patients with desmoplastic CRLM. Both markers have been associated with a survival benefit after resection of primary CRC and are thought to reflect anti-tumour (host) immunity, with increased TIL-densities and Crohn's-like reaction indicative of a more effective antitumour host-response.[27] The cellular composition and structure of these Crohn's-like lymphoid aggregates is similar to secondary lymphoid organs, and studies have linked these structures with increased TIL infiltration[27] and cytotoxic gene expression signatures[28], indicating that these lymphoid aggregates are functional components of the adaptive anticancer immune response in CRC.[29] These results therefore suggest an increased adaptive immune response in the originating primary colorectal cancers of patients who develop corresponding desmoplastic liver metastasis. Evaluations of the immune microenvironment of CRLM have revealed similar results, that is an increased and distinctly cytotoxic immune response observed in the desmoplastic HGP.[26,30] This now associates the desmoplastic phenotype with increased antitumour immunity in both the originating primary colorectal tumour, as well as the localised liver metastasis microenvironment, hinting at a degree of systemic anti-tumour response in these patients. Taken together with recent associations between microsatellite instability-high colorectal cancers, an actionable target for immunotherapy

in stage I-III[31] and IV[32] CRC, and desmoplastic CRLM[9], there is growing evidence to suggest that (systemic) anticancer immunity plays an important role in the underlying biology of the HGPs. While this infers causality, the fact that patient-derived xenografts in SCID-beige mouse with defective T- B- and NK-cell activity have been successful in producing liver lesions with an identical HGP as the donor patient metastasis following intrahepatic transplantation however argues against the HGPs as a solely immunologically driven process.[33] In addition, liver metastases appear to suppress systemic immunity in general, with immunotherapies appearing less effective in the presence of hepatic dissemination.[34] Whether the HGP of a liver metastasis influences the degree of systemic immunosuppression remains to be explored.

Of the other markers evaluated the extramural fibrotic stroma type was also significantly associated with the corresponding liver metastasis HGP. The prognostic impact of the extramural stroma type after resection of primary CRC has been demonstrated in multiple retrospective series, and more recently within a prospective phase III trial.[20,35,36] In addition, characterisation of the extramural stroma type of primary CRC also proved prognostic for survival following resection of corresponding CRLM.[37] Although this could not be validated in the current study, which found a univariable HR (95%CI) of 1.06 (0.72-1.57) for a non-mature stroma type (supplementary file 2). Of the three types recognised, the immature type has the worst prognosis, followed by the intermediate type, and with the most favourable prognosis observed in the mature type. There are several arguments to indicate that the non-mature stroma types (i.e., immature and intermediate) reflect a state of activated epithelial-mesenchymal transition (EMT) promoting invasive and migratory cancer properties. Both have for instance been associated

with higher degrees of tumour budding[38], a known phenotype of EMT-related gene expression[39], which was also true in this study cohort (data not shown). The non-mature stroma's, and notably the characterising myxoid stroma of the immature type, also exhibit increased extracellular matrix component depositions amongst which fibronectin[40], a known activator of EMT.[41] In addition, the defining eosinophilic collagen bundles of the intermediate type are similarly observed in keloids, a microenvironment characterised by overexpression of fibroblast associated growth factors including transforming growth factor β (TGF-β).[42] Taking the position that these are alike, TGF-β, a well-recognised EMT stimulating factor, is likely to be upregulated in the intermediate type.[43] The association between non-desmoplastic CRLM and these non-mature stroma types suggests increased EMT activation in the primary tumours of these patients. Indeed, other histomorphological signs of invasive and migratory growth potential such as vessel invasion and peritumoural budding were also exclusively more frequent in the primary tumours of corresponding non-desmoplastic metastases, albeit not statistically significantly so.

Besides the association with individual histopathology markers, this study found that overall, unfavourable CRC histopathology was associated with non-desmoplastic CRLM given the significantly higher cumulative prevalence of unfavourable charactheristics observed in these patients. This suggests that the information contained in primary CRC histology may be exploited to predict the HGP. And indeed, a multivariable model containing 9 primary CRC characteristics and 2 CRLM characteristics achieved good performance (AUC=0.83) to predict the HGP. Of all CRC markers included only TIL density proved an independent predictor, with all other characteristics failing to reach statistical significance. When interpreting these results it is important

to consider that almost all markers had an estimated odds-ratio around the 0.5 mark, but were insignificant as a result of a large uncertainty of this estimate, i.e. wide confidence intervals. The model therefore predominantly demonstrates that prediction of the HGP using both CRLM and CRC histopathology characteristics could be feasible, but that the current sample-size is insufficient to properly assess the individual predictive properties of all included markers. Something also highlighted by the fact that not all markers could be included in these regression analyses given absent cases in the desmoplastic group. As such, the results of this study should serve more as a stepping stone for a deep-learning digital-pathology approach in a larger cohort. Several deep-learning models already exist for the automated detection and classification of individual markers, for instance peritumoural budding[44], TIL density[45], and the fibrotic stroma type[46]. Additionally, studies have shown deep-learning on histopathology capable of predicting relevant outcomes in a hypothesis-free manner, i.e., not training the model to predict specific markers but instead let the model identify relevant features itself for accurate prediction of the outcome of interest. Examples are the prediction of survival after resection of both primary CRC[47] and CRLM[48], and such a hypothesis-free approach could also be considered to predict the HGP of CRLM on digitalised slides of the corresponding primary CRC tumour. Such a study would require a large number of digitalised slides of resected CRC and corresponding CRLM from multiple independent cohorts. Collection of such datasets may therefore be worthwhile to pursue.

The survival analysis in light of the HGP, other CRLM and patient characteristics, and all included CRC histopathology markers demonstrated the HGP as one of three independent predictors for overall survival upon multivariable analysis.

But again, the lack of statistical power was evident, as multiple markers – including established prognosticators such as lymph-node positivity – demonstrated clinically relevant estimates but failed to reach statistical significance based on the estimate uncertainty (supplementary file 2). Nevertheless, these results support the clinical relevance of this biomarker, similarly to the two previous retrospective series on which this cohort is partly based.[8,9] In addition, a recent study of over 4000 patients evaluating survival after CRLM surgery in light of new biomarkers including the HGP found it to be amongst the independent prognosticators with the largest impact on survival, only being equalled by KRAS and BRAF mutational status, respectively.[6]

The results of this study have to be considered in light of its limitations. Most importantly the inadequate sample-size to detect small to moderate individual marker differences, increasing the likelihood of type 2 statistical errors and not allowing for sufficiently powered multivariable regression analysis increasing the risk for overfitted models. For example, as a general rule of thumb it is advised that the number of variables in a multivariable regression model should not exceed 10% of the total number of events. In our study this relates to the 31 patients with a desmoplastic HGP, and therefore the multivariable model should preferably be limited to less than 4 predictors instead of the 11 actually included. The results should therefore be interpreted with caution and serve more as a proof of concept for a future validation or follow-up study. In addition, this study only included patients who did not receive any chemo- or radiotherapy prior to both CRC and CRLM surgery. While this is from an analysis standpoint not a limitation per se, the applicability of the results is lessened as most patients who undergo surgical resection of CRLM are generally

treated with preoperative systemic chemotherapy which can alter the HGP, with higher rates of the desmoplastic HGP found after chemotherapy.[12] Interestingly, within the 119 patients with metachronous CRLM, those who received adjuvant systemic chemotherapy following CRC resection more often had a non-desmoplastic HGP. This is likely the result of confounding by indication, as both node-positivity and pT4 stage were more common in the patients with a non-desmoplastic HGP. Moreover, all patients in the current study did not receive any chemotherapy in the six months prior to CRLM diagnosis. Another limitation is the lack of data on molecular characteristics such as KRAS and BRAF mutational status. Unfortunately, many of the patients in this study were operated on before the implementation of these genetic markers into routine clinical practice, and data on these markers was consequently only available for less than one-fifth. Previous studies however did not find an association between these markers and the HGP of CRLM[9], and found the prognostic impact independent of these genetic alterations[6,9], but in-depth genetic association studies remain lacking. Lastly, all histopathological assessment was observer-based, while an increasing number of automated assessments are available for more reproducible and precise estimations. These limitations underscore the need for external validation not limited to treatment-naive patients, and ideally with observer-independent methods of assessment.

In conclusion, our results associate primary colorectal cancer histopathology with the histopathological growth patterns of corresponding colorectal liver metastases, and may aid in their preoperative determination. In addition, it associates the desmoplastic phenotype with an increased host-immune response, and the non-desmoplastic type with histomorphological evidence of epithelial-mesenchymal transition at the primary tumour microenvironment level.

References

1. Primrose JN. Surgery for colorectal liver metastases. *Br J Cancer.* Apr 27 2010;102(9):1313-1318.
2. Elferink MA, de Jong KP, Klaase JM, Siemerink EJ, de Wilt JH. Metachronous metastases from colorectal cancer: a population-based study in North-East Netherlands. *Int J Colorectal Dis.* Feb 2015;30(2):205-212.
3. van der Geest LG, Lam-Boer J, Koopman M, Verhoef C, Elferink MA, de Wilt JH. Nationwide trends in incidence, treatment and survival of colorectal cancer patients with synchronous metastases. *Clin Exp Metastasis.* Jun 2015;32(5):457-465.
4. Manfredi S, Lepage C, Hatem C, Coatmeur O, Faivre J, Bouvier AM. Epidemiology and management of liver metastases from colorectal cancer. *Ann Surg.* Aug 2006;244(2):254-259.
5. Tomlinson JS, Jarnagin WR, DeMatteo RP, et al. Actual 10-year survival after resection of colorectal liver metastases defines cure. *J Clin Oncol.* Oct 10 2007;25(29):4575-4580.
6. Buisman FE, Giardiello D, Kemeny NE, et al. Predicting 10-year survival after resection of colorectal liver metastases; an international study including biomarkers and perioperative treatment. *Eur J Cancer.* Jun 2022;168:25-33.
7. van Dam PJ, van der Stok EP, Teuwen LA, et al. International consensus guidelines for scoring the histopathological growth patterns of liver metastasis. *Br J Cancer.* Nov 7 2017;117(10):1427-1441.
8. Galjart B, Nierop PMH, van der Stok EP, et al. Angiogenic desmoplastic histopathological growth pattern as a prognostic marker of good outcome in patients with colorectal liver metastases. *Angiogenesis.* May 2019;22(2):355-368.
9. Hoppener DJ, Galjart B, Nierop PMH, et al. Histopathological Growth Patterns and Survival After Resection of Colorectal Liver Metastasis: An External Validation Study. *JNCI Cancer Spectr.* Jun 2021;5(3):pkab026.
10. Buisman FE, Van der Stok EP, Galjart B, et al. Histopathological growth patterns as biomarker for adjuvant systemic chemotherapy in patients with resected colorectal liver metastases. *Clin Exp Metastasis.* 2020.
11. Nagtegaal ID, Glynne-Jones R. How to measure tumour response in rectal cancer? An explanation of discrepancies and suggestions for improvement. *Cancer Treat Rev.* Mar 2020;84:101964.
12. Nierop PM, Hoppener DJ, Buisman FE, et al. Preoperative systemic chemotherapy alters the histopathological growth patterns of colorectal liver metastases. *J Pathol Clin Res.* Jan 2022;8(1):48-64.
13. Casparie M, Tiebosch ATMG, Burger G, et al. Pathology databanking and biobanking in The Netherlands, a central role for PALGA, the nationwide histopathology and cytopathology data network and archive. *Analytical Cellular Pathology.* 2007;29(1):19-24.
14. Weiser MR. AJCC 8th Edition: Colorectal Cancer. *Ann Surg Oncol.* Jun 2018;25(6):1454-1455.
15. Compton CC, Fielding LP, Burgart LJ, et al. Prognostic factors in colorectal cancer. College of American Pathologists Consensus Statement 1999. *Arch Pathol Lab Med.* Jul 2000;124(7):979-994.
16. Leijssen LGJ, Dinaux AM, Amri R, et al. Impact of intramural and extramural vascular invasion on stage II-III colon cancer outcomes. *J Surg Oncol.* May 2019;119(6):749-757.
17. Liebig C, Ayala G, Wilks JA, Berger DH, Albo D. Perineural invasion in cancer: a review of the literature. *Cancer.* Aug 1 2009;115(15):3379-3391.
18. Lugli A, Kirsch R, Ajioka Y, et al. Recommendations for reporting tumor budding in colorectal cancer based on the International Tumor Budding Consensus Conference (ITBCC) 2016. *Mod Pathol.* Sep 2017;30(9):1299-1311.
19. Jass JR, Love SB, Northover JM. A new prognostic classification of rectal cancer. *Lancet.* Jun 6 1987;1(8545):1303-1306.
20. Ueno H, Ishiguro M, Nakatani E, et al. Prognostic value of desmoplastic reaction characterisation in stage II colon cancer: prospective validation in a Phase 3 study (SACURA Trial). *Br J Cancer.* Mar 2021;124(6):1088-1097.
21. Ueno H, Hashiguchi Y, Shimazaki H, et al. Objective criteria for crohn-like lymphoid reaction in colorectal cancer. *Am J Clin Pathol.* Apr 2013;139(4):434-441.

22. Iseki Y, Shibutani M, Maeda K, et al. A new method for evaluating tumor-infiltrating lymphocytes (TILs) in colorectal cancer using hematoxylin and eosin (H-E)-stained tumor sections. *PLoS One.* 2018;13(4):e0192744.
23. Gu Z, Gu L, Eils R, Schlesner M, Brors B. circlize implements and enhances circular visualization in R. *Bioinformatics.* 2014;30(19):2811-2812.
24. Wu JB, Sarmiento AL, Fiset PO, et al. Histologic features and genomic alterations of primary colorectal adenocarcinoma predict growth patterns of liver metastasis. *World J Gastroenterol.* Jul 14 2019;25(26):3408-3425.
25. Rajaganeshan R, Prasad R, Guillou PJ, et al. The influence of invasive growth pattern and microvessel density on prognosis in colorectal cancer and colorectal liver metastases. *Br J Cancer.* Apr 10 2007;96(7):1112-1117.
26. Hoppener DJ, Nierop PMH, Hof J, et al. Enrichment of the tumour immune microenvironment in patients with desmoplastic colorectal liver metastasis. *Br J Cancer.* Jul 2020;123(2):196-206.
27. Rozek LS, Schmit SL, Greenson JK, et al. Tumor-Infiltrating Lymphocytes, Crohn's-Like Lymphoid Reaction, and Survival From Colorectal Cancer. *JNCI: Journal of the National Cancer Institute.* 2016;108(8).
28. Coppola D, Nebozhyn M, Khalil F, et al. Unique ectopic lymph node-like structures present in human primary colorectal carcinoma are identified by immune gene array profiling. *The American journal of pathology.* 2011;179(1):37-45.
29. Maoz A, Dennis M, Greenson JK. The Crohn's-Like Lymphoid Reaction to Colorectal Cancer-Tertiary Lymphoid Structures With Immunologic and Potentially Therapeutic Relevance in Colorectal Cancer. *Frontiers in Immunology.* 2019-August-22 2019;10(1884).
30. Brunner SM, Kesselring R, Rubner C, et al. Prognosis according to histochemical analysis of liver metastases removed at liver resection. *Br J Surg.* Dec 2014;101(13):1681-1691.
31. Chalabi M, Fanchi LF, Dijkstra KK, et al. Neoadjuvant immunotherapy leads to pathological responses in MMR-proficient and MMR-deficient early-stage colon cancers. *Nature Medicine.* 2020/04/01 2020;26(4):566-576.
32. André T, Shiu K-K, Kim TW, et al. Pembrolizumab in Microsatellite-Instability–High Advanced Colorectal Cancer. *New England Journal of Medicine.* 2020/12/03 2020;383(23):2207-2218.
33. Tabaries S, Annis MG, Lazaris A, et al. Claudin-2 promotes colorectal cancer liver metastasis and is a biomarker of the replacement type growth pattern. *Commun Biol.* Jun 2 2021;4(1):657.
34. Lee JC, Green MD, Huppert LA, Chow C, Pierce RH, Daud AI. The Liver-Immunity Nexus and Cancer Immunotherapy. *Clin Cancer Res.* Jan 1 2022;28(1):5-12.
35. Ueno H, Shinto E, Shimazaki H, et al. Histologic Categorization of Desmoplastic Reaction: Its Relevance to the Colorectal Cancer Microenvironment and Prognosis. *Annals of Surgical Oncology.* 2015/05/01 2015;22(5):1504-1512.
36. Ueno H, Kanemitsu Y, Sekine S, et al. A Multicenter Study of the Prognostic Value of Desmoplastic Reaction Categorization in Stage II Colorectal Cancer. *Am J Surg Pathol.* Aug 2019;43(8):1015-1022.
37. Ueno H, Konishi T, Ishikawa Y, et al. Histologic Categorization of Fibrotic Cancer Stroma in the Primary Tumor Is an Independent Prognostic Index in Resectable Colorectal Liver Metastasis. *The American Journal of Surgical Pathology.* 2014;38(10).
38. Ueno H, Kanemitsu Y, Sekine S, et al. Desmoplastic Pattern at the Tumor Front Defines Poor-prognosis Subtypes of Colorectal Cancer. *The American Journal of Surgical Pathology.* 2017;41(11):1506-1512.
39. De Smedt L, Palmans S, Andel D, et al. Expression profiling of budding cells in colorectal cancer reveals an EMT-like phenotype and molecular subtype switching. *British journal of cancer.* 2017;116(1):58-65.
40. Ueno H, Shinto E, Shimazaki H, et al. Histologic categorization of desmoplastic reaction: its relevance to the colorectal cancer microenvironment and prognosis. *Ann Surg Oncol.* May 2015;22(5):1504-1512.
41. Tzanakakis G, Kavasi RM, Voudouri K, et al. Role of the extracellular matrix in cancer-associated epithelial to mesenchymal transition phenomenon. *Dev Dyn.* Mar 2018;247(3):368-381.
42. Bran GM, Goessler UR, Hormann K, Riedel F, Sadick H. Keloids: current concepts of pathogenesis (review). *Int J Mol Med.* Sep 2009;24(3):283-293.
43. Lamouille S, Xu J, Derynck R. Molecular mechanisms of epithelial–mesenchymal

transition. *Nature Reviews Molecular Cell Biology.* 2014/03/01 2014;15(3):178-196.
44. Fisher NC, Loughrey MB, Coleman HG, Gelbard MD, Bankhead P, Dunne PD. Development of a semi-automated method for tumor budding assessment in colorectal cancer and comparison with manual methods. *bioRxiv.* 2021:2021.2006.2017.448482.
45. Saltz J, Gupta R, Hou L, et al. Spatial Organization and Molecular Correlation of Tumor-Infiltrating Lymphocytes Using Deep Learning on Pathology Images. *Cell Reports.* 2018/04/03/ 2018;23(1):181-193.e187.
46. Nearchou IP, Ueno H, Kajiwara Y, et al. Automated Detection and Classification of Desmoplastic Reaction at the Colorectal Tumour Front Using Deep Learning. *Cancers.* 2021;13(7):1615.
47. Skrede O-J, De Raedt S, Kleppe A, et al. Deep learning for prediction of colorectal cancer outcome: a discovery and validation study. *The Lancet.* 2020;395(10221):350-360.
48. Tellez D, Höppener D, Verhoef C, et al. Extending unsupervised neural image compression with supervised multitask learning. *Paper presented at: Medical Imaging with Deep Learning2020.*

Supplementary material

Supplementary Table 1. Uni- and multivariable Cox regression analysis for overall survival

	Univariable		Multivariable (n=182)	
	HR [95%CI]	p-value	HR [95%CI]	p-value
CRLM characteristics				
Age at CRLM resection (cont.) - *10 years*	1.25 [1.05-1.51]	0.01	1.33 [1.10-1.62]	<0.01
Disease-free interval* (cont.) - *months*	1.00 [0.99-1.01]	0.56	-	-
Number of CRLM (cont.)	1.10 [1.00-1.21]	0.04	1.04 [0.94-1.15]	0.49
Diameter of largest CRLM (cont.) - *cm*	1.04 [0.96-1.13]	0.31	-	-
Preoperative CEA (cont.) - *100 µg/L*	1.02 [0.92-1.13]	0.73	-	-
Extrahepatic disease - *yes vs no*	1.70 [0.95-3.04]	0.07	1.61 [0.88-2.96]	0.12
Resection margin - *R1 vs R0*	0.95 [0.49-1.81]	0.87	-	-
HGP - *non-desmoplastic vs desmoplastic*	2.28 [1.31-3.99]	<0.01	1.97 [1.10-3.53]	0.02
Classical markers				
Right-sided tumour - *yes vs no*	1.86 [1.27-2.73]	<0.01	1.86 [1.23-2.83]	<0.01
Differentiation grade - *poor vs well/moderate*	2.75 [1.20-6.30]	0.02	1.49 [0.60-3.70]	0.39
pT4-stage - *yes vs no*	1.75 [1.10-2.78]	0.02	1.68 [0.94-2.98]	0.08
Positive lymph nodes - *yes vs no*	1.72 [1.19-2.49]	<0.01	1.47 [0.96-2.23]	0.07
Tumour deposits - *yes vs no*	1.37 [0.88-2.11]	0.16	1.34 [0.76-2.35]	0.31
Invasion markers				
(lympho-)vascular invasion - *yes vs no*	1.45 [1.01-2.08]	0.04	1.13 [0.75-1.71]	0.55
Extramural vascular invasion - *yes vs no*	1.33 [0.93-1.92]	0.12	0.97 [0.62-1.50]	0.88
Perineural invasion - *yes vs no*	1.35 [0.90-2.02]	0.15	1.01 [0.61-1.67]	0.97
Tumour interface markers				
Peritumoural budding - *Grade II/III vs I*	1.21 [0.77-1.91]	0.41	-	-
CRC growth pattern - *Infiltrative vs expanding*	1.39 [0.97-1.98]	0.07	1.03 [0.68-1.57]	0.88
Non-mature stroma - *yes vs no*	1.06 [0.72-1.57]	0.75	-	-
Immunological markers				
Crohn's-like lymphoid reaction - *no vs yes*	1.35 [0.80-2.28]	0.26	-	-
TIL density (cont.) - *10%*	0.92 [0.75-1.12]	0.39	-	-

**Between resection of primary tumour and detection of CRLM*

Abbreviations in alphabetical order: Cont.: entered as continous variable; CEA: carcinoembryonic antigen; CI: confidence interval; CRC: colorectal cancer; CRLM: colorectal liver metastasis; HGP: histopathological grwoth pattern; HR: hazard ratio; TIL: tumour-infiltrating lymfocyte.

```
#---------------------- FlowCyt CTx- tumour boxfigure ----------------------
#Make plots in combined plotlist
pltlst = list()
for (i in 1:length(varlst)) {
  #Creating data frame
  nprdfr <- tbl_df(cbind(pltdat[varlst[i]], idpvar))
  colnames(nprdfr) <- c("idp", "dep")
  nprdfr <- na.omit(nprdfr)
  varnam <- titles[varlst[i]]

  #Nonparametric test
  nprres <- kruskal.test(nprdfr$idp~nprdfr$dep)
  nprpvl <- nprres$p.value

  #Nonparametric table
  dfdep1 <- nprdfr %>% filter(dep==levels(nprdfr$dep)[1])
  dfdep2 <- nprdfr %>% filter(dep==levels(nprdfr$dep)[2])
  nprtbl <- rbind(quantile(dfdep1$idp, probs=c(0.25, 0.5, 0.75)),
                  quantile(dfdep2$idp, probs=c(0.25, 0.5, 0.75)))
  nprtbl <- cbind(nprtbl, rbind(count(dfdep1), count(dfdep2)),
                  levels(nprdfr$dep))
  colnames(nprtbl) <- c("LQ", "M", "UQ", "N", "DEP")

  #Plot
  p <- ggplot(nprdfr, aes(x=dep, y=idp)) +
    geom_boxplot(color=clrs_2, size=0, width=0, outlier.shape=18,
                 outlier.size=2) +
    stat_boxplot(geom="errorbar", width=0.1, size=0.75, color="black") +
    geom_boxplot(color=clrs_2, fill=clrs_2, size=0, coef=0, width=0.40,
                 outlier.shape=NA) +
    stat_summary(geom="crossbar", width=0.35, size=0.30, color="white",
                 fun.data=function(x){return(c(y=median(x),
                                               ymin=median(x),
                                               ymax=median(x)))}) +
    ylim(0,(max(nprdfr$idp)*1.05)) +
    scale_x_discrete(labels=c((paste(levels(nprdfr$dep)[1], "\n(n = ",
                                     count(dfdep1), "/",
                                     count(nprdfr), ")", sep="")),
                              (paste(levels(nprdfr$dep)[2], "\n(n = ",
                                     count(dfdep2), "/",
                                     count(nprdfr), ")", sep="")))) +
    labs(title=paste(varnam[1,1]), x=element_blank(), y=ylabls[i]) +
    theme(plot.title = element_text(size=14, face="bold", hjust=0.5),
          axis.text = element_text(size=11, color="black"),
          axis.title = element_text(size=12, color="black"),
          panel.grid.major=element_blank(),
          panel.grid.minor=element_blank(),
          panel.background=element_blank(),
          axis.line.x=element_line(colour="black", size=0.25),
          axis.line.y=element_line(colour="black", size=0.25),
          axis.ticks=element_line(colour="black", size=0.25),
          legend.position="none")

  #Plotlist
  pltlst[[i]] <- eval(parse(text=ifelse(ltrans[i]=="log10",
```

Chapter VII

Enrichment of the tumour immune microenvironment in patients with desmoplastic colorectal liver metastasis

-

British Journal of Cancer 2020

D.J. Höppener, P.M.H. Nierop, J. Hof, K. Sideras, G. Zhou, L. Visser, A.S.H. Gouw, K.P. de Jong, D. Sprengers, J. Kwekkeboom, P.B. Vermeulen, D.J. Grünhagen, C. Verhoef.

Abstract

Background: Patients with resected colorectal liver metastasis (CRLM) that display only the desmoplastic histopathological growth pattern (dHGP) exhibit superior survival compared to patients with any non-desmoplastic growth (non-dHGP). The aim of this study was to compare the tumour microenvironment between dHGP and non-dHGP.

Methods: the tumour microenvironment was investigated in three cohorts of chemo-naive patients surgically treated for CRLM. In cohort A semi-quantitative immunohistochemistry was performed, in cohort B intra- and peritumoural T-cells were counted using immunohistochemistry and digital image analysis, and in cohort C the relative proportions of individual T-cell subsets were determined by flow-cytometry.

Results: 117, 34 and 79 patients were included in cohorts A, B, and C, with dHGP being observed in 27%, 29% and 15% of patients, respectively. Cohorts A&B independently demonstrated peri- and intratumoural enrichment of cytotoxic CD8+ T-cells in dHGP, as well as a higher CD8+/CD4+ ratio (cohort A). Flowcytometric analysis of fresh tumour tissues in cohort C confirmed these results; dHGP was associated with higher CD8+ and lower CD4+ T-cell subsets, resulting in a higher CD8+/CD4+ ratio.

Conclusion: The tumour microenvironment of patients with dHGP is characterised by an increased and distinctly cytotoxic immune infiltrate, providing a potential explanation for their superior survival.

Introduction

Colorectal cancer (CRC) represents one of the most common solid malignancies.[1] Metastatic spread occurs in roughly half of all patients during the course of the disease, with colorectal liver metastasis (CRLM) presenting as the most frequent distant metastasis.[2-5] Depending on the hepatic tumour load and vessel involvement, local therapies, often in conjunction with systemic therapy, selectively allow for curatively intended treatment strategies, even in the case of limited extrahepatic metastatic disease.[6] Herein surgical resection is often considered the mainstay treatment modality.[7] Reported 5-year overall survival (OS) rates after curatively intended surgical treatment for CRLM generally range from 40-60%.[8,9]

Prognostication and prediction of treatment effect after surgical treatment of CRLM has changed little over time and is based mainly on clinicopathological factors, most notably the nodal status of the primary tumour, the number and size of hepatic metastases, and RAS mutational status.[10-16] Only in mismatch repair deficient tumours, which account for roughly 3% of patients with CRLM[17], has a clear therapeutic indication been demonstrated for immune checkpoint inhibitors.[18,19] This clearly emphasises the need for additional, clinically relevant biomarkers. To this end, recent efforts have focussed on the quantification and classification of immune cells present within the tumour microenvironment (TME) of CRC and/or CRLM.[20-26] Results have been promising, with favourable prognosis demonstrated in patients with increased and activated (i.e. cytotoxic) immune infiltrates in the TME.[20-26]

Another emerging biomarker encompassing the TME is the histopathological growth pattern (HGP) of CRLM. The HGPs describe the morphology and interaction between tumour

and liver cells at the tumour-liver interface.[27] Histomorphologically, three phenotypes are distinguished: the replacement (rHGP) type, where the tumour-cells "replace" liver cells while the sinusoidal architecture is maintained at the tumour-liver interface (*figure 1A*), the rare pushing (pHGP) type, where the tumour cells "push" against the liver cell-plates (*figure 1B*), and the desmoplastic type (dHGP), where a band of desmoplastic stroma separates the tumour from the liver parenchyma (*figure 1C*). Apart from these apparent differences upon histomorphological examination, the desmoplastic and pushing types have angiogenic ways of vascularisation, while the replacement type relies on vessel co-option.[27-31] For all that, clinical relevance seems determined by two classes; either patients where tumours are fully enclosed by a desmoplastic rim (i.e. 100% dHGP), or patients where any non-desmoplastic (i.e. <100% dHGP; non-dHGP) pattern is observed, as multiple HGPs can appear in conjunction.[32] Especially in chemo-naive subjects (i.e. not treated with systemic chemotherapy within 6 months prior to resection of CRLM), patients with dHGP exhibit superior survival compared to their non-dHGP counterparts, with reported 5-year OS rates of nearly 80% in dHGP and as low as 40% in (any) non-dHGP.[32]

Upon histomorphological examination, dHGP is often characterised by a distinct immune infiltrate surrounding the desmoplastic stroma (*figure 1C*), although this has never been quantified, classified, or been compared to the non-dHGP counterparts.[32] The aim of this study was therefore to quantify, classify, and compare the TME of CRLM between patients with dHGP and non-dHGP. Given there is evidence to suggest that systemic therapy not only affects the immune infiltrate in the TME[26,33], but also the proportional distribution and possibly the prognostic value of the HGPs[32], our study focussed on chemo-naive subjects only.

→ *Figure 1. The histopathological growth patterns (HGP) of colorectal liver metastasis on Hematoxylin & Eosin stained tissue sections. (A) The replacement HGP, (B) the pushing HGP (pHGP), and (C) the desmoplastic HGP.*

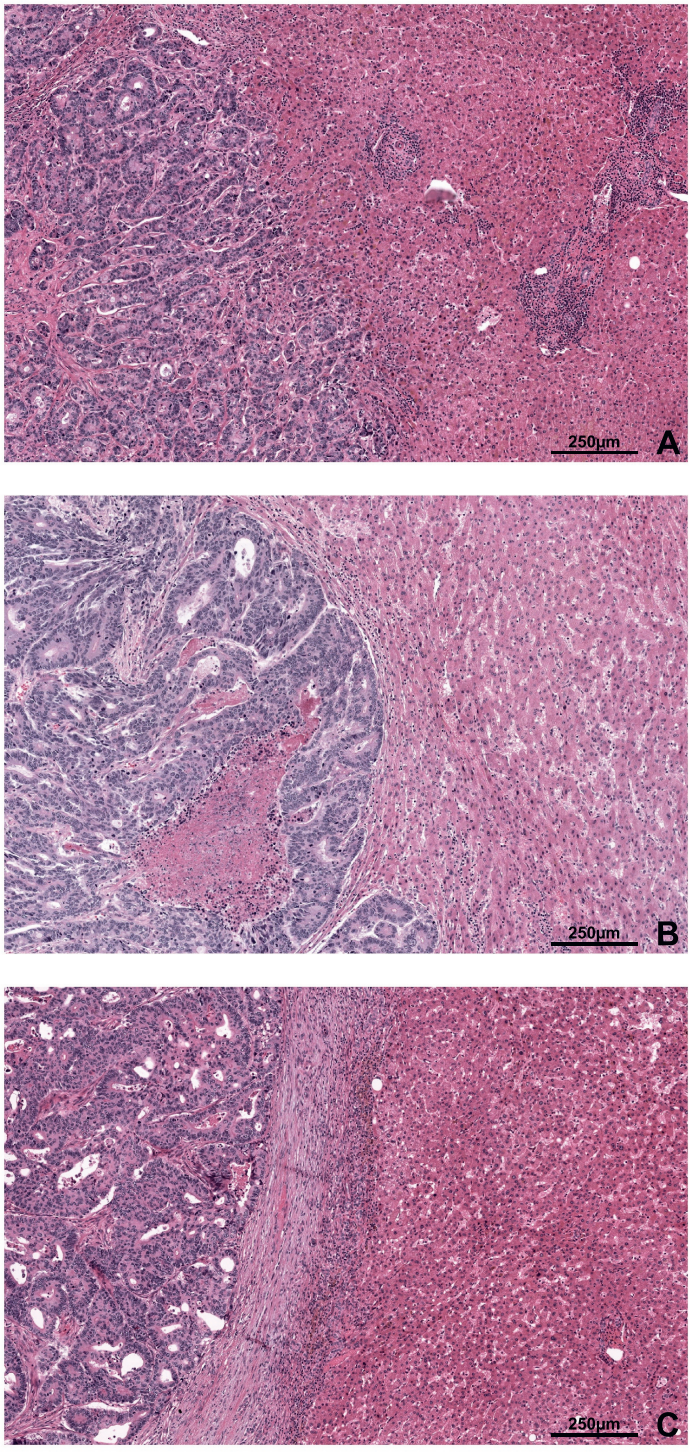

Methods

Investigation of the TME of CRLM was performed in three cohorts, each analysed using distinct methods. Scoring of the HGPs of CRLM was performed similarly across all cohorts and according to international consensus guidelines.[27] The current study was approved by the medical ethics committee of the Erasmus University Medical Center (MEC-2018-1743).

Scoring of the HGP of CRLM

In each of the three cohorts, all available H&E stained slides of Formalin-Fixed Paraffin-Embedded tissue blocks of resected CRLM specimens were retrieved from the archives of the respective pathology departments. Scoring of the HGP was performed retrospectively using either light-microscopy or digitalised slide images. All available and eligible (digitalised) tissue sections were reviewed by simultaneous assessment of at least two trained observers. For all tissue sections subjected to review, the relative percentage of each distinct HGP (i.e. pushing, desmoplastic and replacement type) was determined at the tumour-liver interface. Given recent findings by Galjart et al[32], patients were classified as dHGP if only the desmoplastic type was observed in all reviewed sections (i.e. 100% dHGP, *figure 1C*), and as non-dHGP if any pushing and/or replacement type was observed in any of the reviewed sections (i.e. <100% dHGP, *figure 1A*&*B*).

Cohort A: semi-quantitative Immunohistochemistry

In the first cohort, analysis of the TME of CRLM was performed using semi-quantitative immunohistochemistry (IHC) in patients who underwent partial hepatectomy with curative intent at either the Erasmus MC Cancer Institute, Rotterdam, the Netherlands, or the University Medical Centre Groningen (UMCG), Groningen, the Netherlands. Patients eligible for inclusion were those with complete metastasectomy (defined as resection margin >0mm), who did not receive any pre-

and/or postoperative chemotherapy in addition to partial hepatectomy, a Clinical Risk Score[10] (CRS) of 3 or lower, no extrahepatic disease at time of surgery, and no known medical history of secondary malignancy. Data on this cohort, together with RNA sequencing experiments performed in the UMCG cohort only, has previously been submitted for publication (submitted manuscript). Immunohistochemistry staining was performed on 4µm thick tissue sections cut from Formalin-Fixed Paraffin-Embedded samples of resected CRLM (*supplementary figure 1*). For each Formalin-Fixed Paraffin-Embedded sample, a control slide was stained for H&E to confirm the presence of tumorous and adjacent liver tissue. Immunohistochemistry staining for CD4 (SP35), CD8 (SP57), CD45 (RP2/18), CD79A (SP18) and Kappa/Lambda (double polyclonal staining) was done using the Ventana automated staining system (Roche, Basel, Switzerland). Manual staining was performed with the primary antibodies FoxP3 (236A/E7, 1/100 dilution) and SLAMF7 (HPA055945, 1/200 dilution). Positive and negative controls were implemented. All IHC stained tissue sections were assessed by two trained observers. Expression was graded semi-quantitatively ranging from 1 to 3, and was determined for peritumoural and intratumoural regions separately. Peritumoural was defined as expression observed at the tumour-liver interface, and intratumoural was defined as expression observed in the stroma surrounding the tumour cells, or immunopositive intraepithelial lymphocytes. After consensus was reached by both observers, expression of each marker was classified into “low” and “high” using the cut-off value resulting in the most even distribution (1 vs ≥2 or ≤2 vs 3). In addition, the CD8 to CD4 ratio was calculated by dividing their respective semi-quantitative scores (i.e. grade 1 to 3) for the peritumoural and intratumoural regions seperately. A “high” CD8 to CD4 ratio was defined as a ratio greater or equal to the median.

Cohort B: quantitative IHC by digital image analysis
Analysis of the TME in the second cohort consisted of quantitative IHC using digital image analysis. Patients were eligible if they underwent partial hepatectomy with curative intent at the Erasmus MC Cancer Institute, Rotterdam, the Netherlands, and if they did not receive any systemic chemotherapy treatment in the six months prior to resection. This cohort represents a subset of a larger cohort that has previously been published.[25] Immunohistochemistry staining for CD8 (SP57) and FoxP3 (236A/E7, 1/100 dilution) was performed on 4µm thick tissue sections using the Ventana Benchmark Ultra automated staining system (Roche, Basel, Switzerland). Stained tissue sections were digitalised at 40x using the NanoZoomer 2.0HT system (Hamamatsu Photonic, Shizuoka, Japan). Peri- and intratumoural cell densities of CD8+ and FoxP3+ were measured in cells/mm^2 using the Visiopharm Integrator System (version 4.2.2.0, Visiopharm, Hoersholm, Denmark). Peritumoural cell densities were determined in four high-power fields (0.54mm in diameter) at the tumour-liver interface (*supplementary figure 2*). The intratumoural cell densities were determined in several (4-6) large circular areas containing viable tumorous tissue (*supplementary figure 2*). In addition, the CD8+/FoxP3+ ratio was determined for peri- and intratumoural densities separately.

Cohort C: flow cytometry
In the third cohort the TME was analysed using flow cytometry. Patients eligible for inclusion were those who underwent partial hepatectomy at the Erasmus MC Cancer Institute, Rotterdam, the Netherlands, and if they did not receive any systemic chemotherapy treatment in the six months prior to resection. Data on (part of) this cohort has previously been published.[22,23,25] The relative proportions of CD4+ T-cells, CD4+FoxP3- T-helper cells, CD4+FoxP3+ T-regulatory

cells, and CD8+ cytotoxic T-cells within live CD3+ T-cells were determined by flowcytometry in mononuclear cells (MNCs) isolated from fresh tumour tissue, tumour-free liver (obtained as distant as possibly from the tumour; minimum 1 cm distance), and in peripheral blood mononuclear cells (PMBCs) isolated from peripheral blood collected prior to surgery. Ficoll density gradient centrifugation was used for PBMC isolation. Single cell suspensions from tumour and tumour-free liver were obtained by tissue digestion. Fresh tissue was cut into small pieces and digested for 30 minutes at 37˚C with interrupted gentle swirling either in PRMI 1640 medium (Lonza, Breda, the Netherlands) with 0.5 mg/ml collagenase IV (Sigma-Aldrich, St. Louis, MO, USA) and 0.1 mg/ml DNase I (Roche, Basel, Switzerland), or in Hanks' Balanced Salt solution with Ca2+ and Mg2+ (Sigma, Zwijndrecht, the Netherlands) with 0.125 mg/ml collagenase IV and 0.2 mg/ml DNase I.[22,23] Filtration of cell suspensions was done through 100µm pore cell strainers (BD Biosciences, Franklin Lakes, NJ, USA). Ficoll density gradient centrifugation was used to obtain MNCs. Viability was determined by trypan blue exclusion. Cells were surface-labelled with fluorochrome-conjugated antibodies against CD45 (optional), CD3, CD4, and CD8. Intracellular FoxP3 was stained using FoxP3-specific antibody (clone 236A/E7; eBioscience, San Diego, CA, USA) after fixation and permeabilisation using the FoxP3 staining buffer set of eBioscience (San Diego, CA, USA). Subsequent flow cytometric analysis was performed using a FACS Canto II flow cytometer (BD Biosciences, Franklin Lakes, NJ, USA) and FlowJo software (version 10.0, BD, Franklin Lakes, NJ, USA) as described previously.[22,23] Viable (aqua LIVE/DEAD fluorescent dye-negative) leukocytes were gated in single cells using either CD45 or FSC/SSC. Live T-cells were defined based on CD3 expression. Within live CD3+ T-cells, the relative proportions of CD8+ and CD4+ T-cell subsets were determined.

Within the CD4+ T-cells, the T-regulatory subset was defined as CD4+FoxP3+ while the T-helper subset was defined as CD4+FoxP3-. In addition to these subsets, the ratio between CD8+/CD4+ T-cells and the ratio between CD4+FoxP3-/CD4+FoxP3+ T-cells was calculated. A representative example of the flow cytometry gating strategy is provided in *supplementary figure 3*. The study was approved by the medical ethics committee of the Erasmus University Medical Center (MEC-2012-331) and signed informed consent was obtained from all patients prior to tissue and blood donation.

Survival

The overall survival (OS), defined as the time in months from resection of CRLM till death, was compared between patients with dHGP and non-dHGP in all three cohorts combined.[32] Overall survival was estimated by Kaplan-Meier method and reported as five year OS rate with corresponding 95% confidence interval (CI). Survival curves were compared using the log-rank test.

Statistical analysis

The TME was compared in each cohort between patients who exhibited only dHGP (i.e. 100% dHGP) and patients in whom any non-dHGP was observed (i.e. <100% dHGP). Categorical data were compared using the chi-squared test and non-parametric continuous data using the Kruskal Wallis test. In addition, linear regression was performed to study possible relations between the observed percentage of dHGP at the tumour-liver interface and the TME. Herein the total proportion of dHGP observed at the tumour-liver interface represented the independent variable, and continuous data observed in the TME the dependent outcome variable. In order to test if the HGP and the TME were independent of clinical risk, the CRS was determined.[10] Patients were classified as either low (CRS 0-2) or high (CRS 3-5) risk. Independency of the HGP

with CRS was tested for all cohorts combined and for each cohort separately. Independency with CRS was also tested for CD8, CD4 and FoxP3 within each cohort. Categorical data are reported as frequency and/or percentage, and plotted using bar-charts with binomial 95% CI. When plotted, binomial 95% CI for proportions were calculated using the Clopper-Pearson method. Non-parametric continuous data are reported as median with corresponding 25th (Q1) and 75th (Q3) percentile (i.e. inter-quartile range (IQR)), and plotted using boxplots. Outliers in boxplots were defined according to the 1.5 rule (i.e. outside [Q1-1.5*IQR; Q3+1.5*IQR]). Statistical significance was defined as an $\alpha<0.05$. All statistical analyses were performed using R version 3.5.3 (http://www.r-project.org).

Results

Data on 198 individual patients were collected, 160 of whom received treatment at the Erasmus MC Cancer Institute, and the remaining 38 at the University Medical Centre Groningen. Of the 160 patients of the Erasmus MC one was included in all three cohorts, two were included in both cohorts A and C, and twenty-eight were included in both cohorts B and C. Upon histopathological examination dHGP was observed in 46 patients (23%). The CRS was available for 191 patients (98%) and was independent of the HGP (p=0.089, *supplementary table 1*). Clinicopathological patient characteristics stratified by cohort are reported in *table 1*.

Cohort A: semi-quantitative IHC

A total of 117 patients were included in the first cohort, 79 of whom underwent resection of CRLM at the Erasmus MC Cancer Institute between March 2000 and February 2015, and 38 of whom underwent resection of CRLM at the University Medical Centre Groningen between January 1994 and June 2013.

Clinicopathological patient characteristics are reported in *table 1*. Thirty-two patients exhibited dHGP (27%), and eighty-five non-dHGP (73%). The results of peritumoural and intratumoural IHC expression stratified by HGP are reported in *figure 2* and *figure 3*, respectively. All intratumoural expression was scored based on stromal expression, with the exception of CD8, which was determined on both stromal and intraepithelial lymphocyte expression. The cut-off to determine "high" expression was grade 3 for CD4 and CD45, and grade ≥2 for all other markers. The TME of dHGP patients more often displayed high peritumoural CD8, CD45, CD79A, Kappa/Lambda and SLAMF7 expression, all p≤0.001 (*figure 2*). Similarly, high intratumoural CD8 (intraepithelial), CD79A, FoxP3 and Kappa/Lambda were more frequently observed in the TME of patients with dHGP, all p<0.05 (*figure 3*).

Table 1. Baseline characteristics stratified by cohort

		Cohort A Semi-quantitative IHC n = 117 (%)	Cohort B Quantitative IHC n = 34 (%)	Cohort C Flow cytometry n = 79 (%)
Centre	Erasmus MC	79 (68)	34 (100)	79 (100)
	UMCG	38 (32)	0 (0)	0 (0)
Age at resection of CRLM - *(median [IQR])*		67 [61, 73]	65 [57, 72]	67 [59, 75]
Gender	Female	50 (43)	11 (32)	29 (37)
	Male	67 (57)	23 (68)	50 (63)
Primary tumour location	Left-sided	48 (41)	17 (50)	40 (51)
	Right-sided	48 (41)	11 (32)	25 (32)
	Rectal	21 (18)	5 (15)	11 (14)
	Missing	0 (0)	1 (3)	3 (4)
Adjuvant CTx for CRC	No	85 (73)	31 (91)	63 (80)
	Yes	30 (26)	3 (9)	15 (19)
	Missing	2 (2)	0 (0)	1 (1)
Nodal status of primary CRC	N0	59 (50)	18 (53)	39 (49)
	N+	58 (50)	14 (41)	39 (49)
	Missing	0 (0)	2 (6)	1 (1)
DFI in months* - *(median [IQR])*		15.0 [4.0, 25.0]	7.0 [0.0, 17.5]	8.0 [0.0, 18.5]
Preop. CEA in µg/L - *(median [IQR])*		16.1 [4.6, 50.5]	6.0 [3.9, 17.0]	13.0 [5.6, 29.1]
Number of CRLM - *(median [IQR])*		1.0 [1.0, 2.0]	2.0 [1.0, 2.0]	1.0 [1.0, 2.0]
Largest CRLM in cm - *(median [IQR])*		3.4 [2.5, 4.5]	2.4 [1.5, 3.5]	3.0 [2.0, 3.8]
Clinical risk score	Low risk (0-2)	101 (86)	22 (65)	57 (72)
	High risk (3-5)	16 (14)	8 (24)	17 (22)
	Missing	0 (0)	4 (12)	5 (6)
HGP	dHGP	32 (27)	10 (29)	12 (15)
	non-dHGP	85 (73)	24 (71)	67 (85)

**Between resection of primary CRC and detection of CRLM*
Abbreviations in alphabetical order: CEA: carcinoembryonic antigen; CRC: colorectal cancer; CRLM: colorectal liver metastasis; DFI: disease-free interval; dHGP: desmoplastic type histopathological growth pattern; IHC: immunohistochemistry; IQR: interquartile range; non-dHGP: non-desmoplastic type histopathological growth pattern; UMCG: University Medical Centre Groningen.

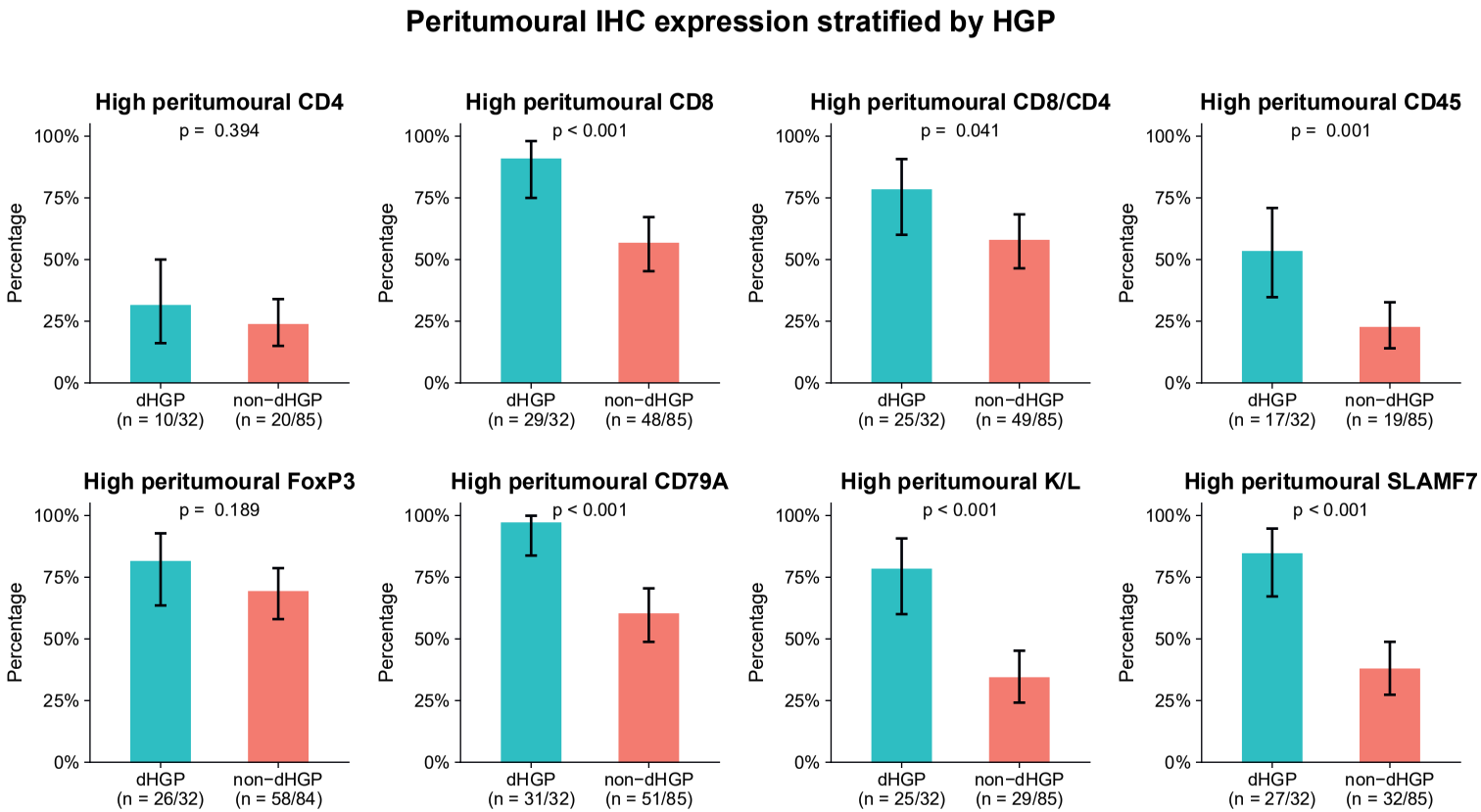

Figure 2. Results of semi-quantitative immunohistochemistry (IHC) in cohort A: bar charts representing the proportion of patients with high peritumoural expression of individual markers stratified by histopathological growth pattern (HGP). The black lines represent the binomial 95% confidence interval (Clopper-Pearson). K/L: Kappa/Lambda

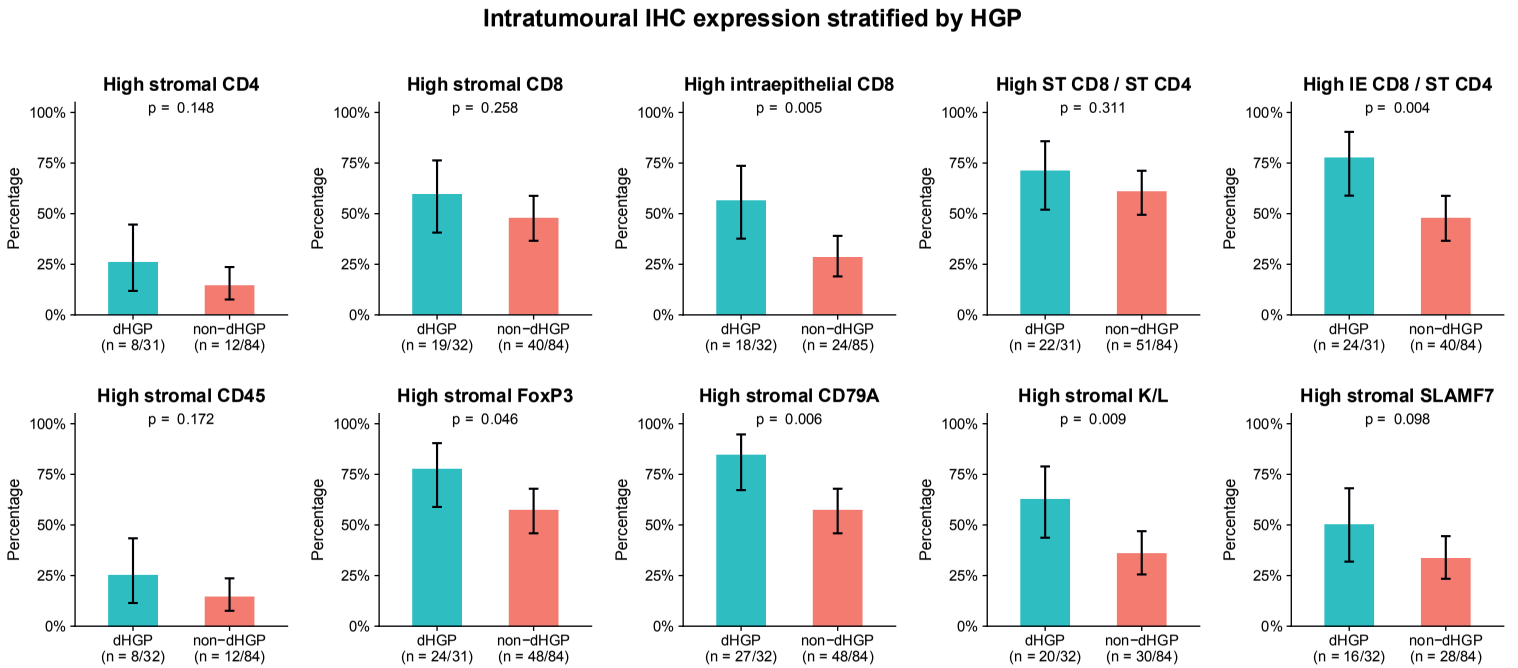

Figure 3. Results of semi-quantitative immunohistochemistry (IHC) in cohort A: bar charts representing the proportion of patients with high intratumoural expression of individual markers stratified by histopathological growth pattern (HGP). The black lines represent the binomial 95% confidence interval (Clopper-Pearson). ST: stromal; IE: intraepithelial; K/L: Kappa/Lambda.

Concerning the CD8 to CD4 ratio, patients with dHGP more often displayed a high peritumoural CD8/CD4 (p=0.041, *figure 2*), as well as a high intraepithelial CD8 to stromal CD4 (p=0.004, *figure 3*). No difference was found in the stromal CD8 to stromal CD4 ratio (p=0.311, *figure 3*). Peri- and intratumoural CD8, CD4, and FoxP3 expression were all independent of CRS (all p>0.10, *supplementary table 1*).

Cohort B: quantitative IHC by digital image analysis

Quantitative IHC by digital image analysis was performed in 34 patients who underwent partial hepatectomy at the Erasmus MC Cancer Institute between October 2009 and October 2011. Clinicopathological patient characteristics are reported in *table 1*. Out of 34, dHGP was observed in 10 (29%), and non-dHGP in 24 (71%) patients. *Figure 4A* reports the peri- and intratumoural CD8 and FoxP3 counts stratified by HGP using boxplots. The TME of dHGP patients was associated with significantly higher peri- and intratumoural CD8 (p=0.002 and p=0.014, respectively), and peritumoural FoxP3 counts (p=0.026). No significant difference was observed concerning intratumoural FoxP3 counts, or the peri- and intratumoural CD8/FoxP3 ratios. *Figure 4B* displays the linear regression models investigating the peri- and intratumoural CD8 and FoxP3 counts and the total percentage of dHGP at the tumour-liver interface. The percentage of dHGP at the tumour-liver interface proved a significant positive predictor for both peritumoural (β=4.261, p<0.001) and intratumoural (β=1.99, p=0.002) CD8 counts. No such associations were found for peri- and intratumoural FoxP3 counts, or the peri- and intratumoural CD8/FoxP3 ratios (all p>0.10, *figure 4B*). Peri- and intratumoural CD8 and FoxP3 counts were all independent of CRS (all p>0.15, *supplementary table 1*).

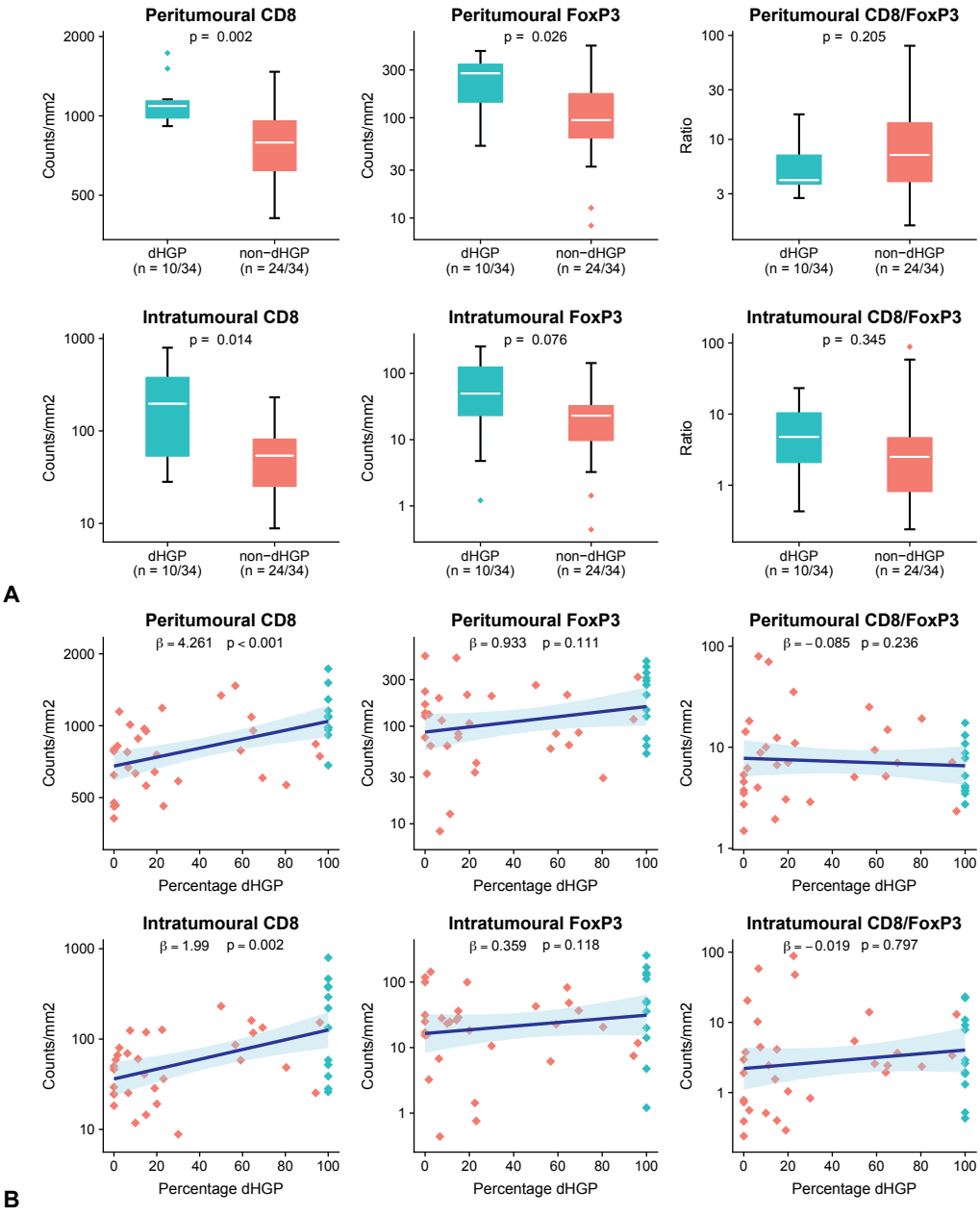

*Figure 4. Results of quantitative immunohistochemistry in cohort B. (A) Box and whiskerplots of intra- and peritumoural counts/mm² stratified by histopathological growth pattern (HGP) and displayed on a logarithmic scale. The white line represents the median, the box represents the inter-quartile rage (IQR), and the whiskers represents the range. Outliers are defined according to the 1.5 rule (i.e. outside [Q1-1.5*IQR; Q3+1.5*IQR]).*

← Figure 4 continued. (B) Linear regression models of intra- and peritumoural counts/mm² (y-axis, logarithmic scale) and the percentage of the desmoplastic type histopathological growth pattern (dHGP) scored at the tumour-liver interface (x-axis). The blue line represents the regression coefficient, the lightblue ribbon represents the corresponding 95% confidence interval. Measurements of individual patients are displayed using dots. Red dots represent patients with non-dHGP (i.e. < 100% dHGP) and blue dots represent patients with dHGP (i.e. 100% dHGP).

Cohort C: flow cytometry

Viable MNCs were successfully isolated from tumour tissue of 79 patients who underwent partial hepatectomy at the Erasmus MC Cancer Institute between October 2009 and August of 2018. Viable MNCs from tumour-free liver tissue were successfully isolated in 73, and viable PBMCs from peripheral blood samples in 55 of the 79 patients. Clinicopathological patient characteristics are reported in *table 1*. Twelve (15%) patients were found to have dHGP; non-dHGP was seen in 67 patients (85%). *Figure 5A* reports the relative proportions of T-cell subsets within CD3+ T cells isolated from tumour tissue stratified by HGP using boxplots. The relative proportion of CD8+ T-cells was significantly higher in patients with dHGP (p=0.015), while the relative proportion of CD4+ T-cells was significantly higher in patients with non-dHGP (p=0.004). Congruently, the CD8/CD4 ratio was significantly higher in dHGP patients (p=0.001). This difference in CD4+ T-cells was due to a higher relative CD4+FoxP3- T-helper subset in non-dHGP only (p=0.006), as no difference was observed for the CD4+FoxP3+ regulatory T-cell subset (p=0.551). Concerning the CD4+FoxP3-/CD4+FoxP3+ ratio, no difference was observed (p=0.566). Similar results were seen in the linear regression models investigating T-cell subsets in tumour tissue and the percentage of dHGP at the tumour-liver interface, reported in *figure 5B*. A positive linear association was found for the percentage of dHGP and the CD8+ T-cell subset (β=0.094, p=0.007), while a negative

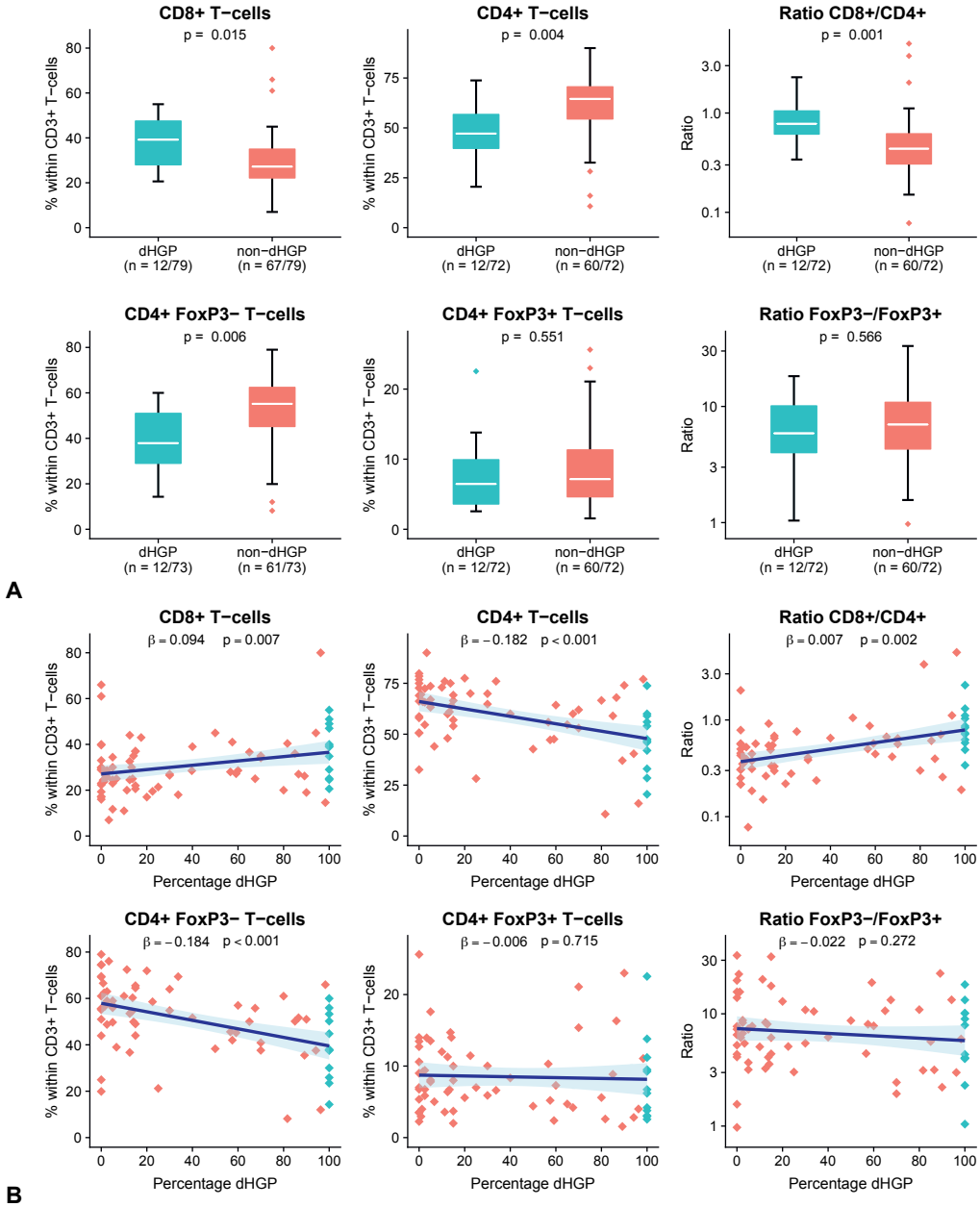

*Figure 5. Results of flow cytometry of fresh tumour samples in cohort C. (A) Box and whiskerplots of the relative proportion of individual T-cell subsets stratified by histopathological growth pattern (HGP). Ratio's are displayed on a logarithmic scale. The white line represents the median, the box represents the inter-quartile rage (IQR), and the whiskers represents the range. Outliers are defined according to the 1.5 rule (i.e. outside [Q1-1.5*IQR; Q3+1.5*IQR]).*

← Figure 5 continued. (B) Linear regression models of the relative proportion of individual T-cell subsets (y-axis) and the percentage of the desmoplastic type histopathological growth pattern (dHGP) scored at the tumour-liver interface (x-axis). Ratio's are displayed on a logarithmic scale. The blue line represents the regression coefficient, the light blue ribbon represents the corresponding 95% confidence interval. Measurements of individual patients are displayed using dots. Red dots represent patients with non-dHGP (i.e. < 100% dHGP) and blue dots represent patients with dHGP (i.e. 100% dHGP).

linear association was seen for the CD4+ T-cell subset (β=-0.182, p<0.001). Correspondingly, the percentage of dHGP was positively associated with the CD8+/CD4+ ratio (β=0.007, p=0.002). Within the CD4+ subsets, the percentage of dHGP was only negatively associated with the CD4+FoxP3- subset (β=-0.184, p<0.001), as no association was found between dHGP and the CD4+FoxP3+ subset (p=0.715). No linear association was found for the CD4+FoxP3-/CD4+FoxP3+ ratio (p=0.272). The relative proportions of CD8+, CD4+, CD4+FoxP3-, and CD4+FoxP3+ T-cells in fresh tumour tissues were all independent of CRS (all p>0.30, *supplementary table 1*).

The relative proportions of T-cell subsets within CD3+ T-cells in tumour-free liver tissues and peripheral blood stratified by HGP, as well as the linear regression models investigating T-cell subsets in tumour-free liver or peripheral blood and the percentage of dHGP at the tumour-liver interface, are reported in the supporting documentation (*supplementary figures 4A*, *5A*, *4B*, and *5B*, respectively). When stratifying for HGP, no differences existed in the relative proportions of T-cell subsets in either tumour-free liver tissues (all p>0.30, *supplementary figure 4A*), or peripheral blood samples (all p>0.50, *supplementary figure 5A*). Interestingly, the percentage of dHGP at the tumour-liver interface was negatively associated with the relative proportion of CD4+ T-cells in tumour-free liver samples (β=-0.103, p=0.021, *supplementary figure 4B*), and

positively associated with the CD8+/CD4+ ratio (β=0.022, p=0.026, *supplementary figure 4B*). Again, this association was owing to the CD4+FoxP3- T-helper subset (β=-0.099, p=0.018, *supplementary figure 4B*), as no association existed for the CD4+FoxP3+ regulatory T-cell subset (β=-0.003, p=0.371, *supplementary figure 4B*). No association was found for the CD8+ subset, or the CD4+FoxP3-/CD4+FoxP3+ ratio (both p>0.10, *supplementary figure 4B*). Concerning possible associations between T-cell subsets in blood samples and the percentage of dHGP at the tumour-liver interface, no relationships were found (all p>0.20, *supplementary figure 5B*).

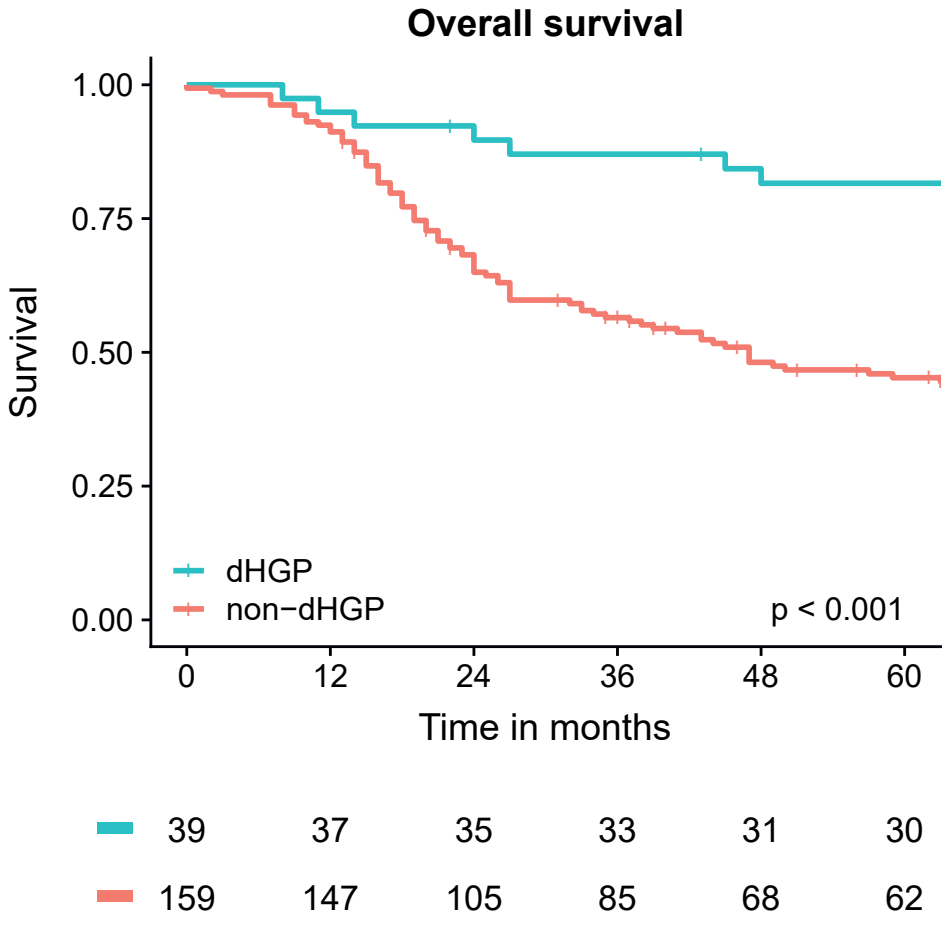

Figure 6. Kaplan-Meier overall survival estimates stratified by histopathological growth pattern (HGP) in all three cohorts combined.

Survival

Survival data was available for all 198 patients. The Kaplan-Meier estimates for OS stratified by HGP are reported in *figure 6*. The five year OS (95% CI) rate for patients with dHGP was 82% (70-95) compared to 45% (38-54) for non-dHGP (overall log-rank: p<0.001).

Discussion

The current study aimed to quantify, classify and compare the tumour microenvironment (TME) of patients with dHGP and non-dHGP. Three distinct analytic methods were applied, in three cohorts of chemo-naive patients undergoing resection of CRLM (with one patient included in all three cohorts, two included in both cohorts A&C, and twenty-eight in both cohorts B&C). In order to correctly interpret the results, it is important to recognise the difference in outcome measures of each analytical method.

In the first cohort (A) semi-quantitative IHC scoring was applied. High peritumoural expression of CD8, CD45, CD79A, Kappa/Lambda and SLAMF7, and intratumoural CD8 (intraepithelial), CD79A, Kappa/Lambda and FoxP3 were significantly more often seen in patients with dHGP. In addition, dHGP was associated with a high peritumoural CD8/CD4 ratio, as well as a high intraepithelial CD8 to stromal CD4 ratio. These differences suggest a general increased immune infiltrate in dHGP, both in the peritumoural and the intratumoural TME. In cohort A, intratumoural CD8 was determined for both stromal and intraepithelial expression. Interestingly, high intraepithelial CD8 expression was more often seen in dHGP patients (p=0.005), whereas no significant difference was found for stromal CD8 expression (p=0.258). Intraepithelial CD8+ lymphocytes have been linked to favourable prognosis in colorectal cancer, and are

associated with antitumour immunity.[34] Furthermore, it has been postulated that intraepithelial CD8+ lymphocytes play an important role in the suppression of micrometastasis, and hence are associated with a decrease in distant metastasis.[34] The higher expression of intraepithelial CD8+ lymphocytes in patients with dHGP therefore corroborates the recent findings that patients with non-dHGP are at higher risk for extrahepatic and multi-organ recurrences following first surgical treatment of CRLM.[35]

This general increased immune infiltrate in patients with dHGP seen in cohort A is supported by cohort B, where CD8 and FoxP3 expressions were quantified both peri- and intratumourally using digital image analysis. Median counts/ mm^2 of peritumoural CD8 and FoxP3, and intratumoural CD8 were significantly higher in dHGP patients. Previously published results describing a cohort that consisted of the same patients plus patients treated with preoperative chemotherapy suggested that the CD8/FoxP3 ratio was prognostic for survival after resection of CRLM.[25] Given the superior survival observed in chemo-naive dHGP patients[32], one would expect dHGP to be associated with a high CD8/FoxP3 ratio. Contrastingly, no relationship between the HGP and the CD8/ FoxP3 ratio was found.

Assuming a general increased immune infiltrate is present in dHGP, interpretation of individual markers from cohorts A and B is somewhat difficult due to the non-relative nature of their outcome. Relative increases in the TME of non-dHGP patients could exist but – given the absence of normalisation methods for individual IHC markers – are potentially missed when analysing just expression grades or absolute cell counts. Furthermore, IHC analysis does not always allow for adequate discrimination between individual cell populations. For instance concerning CD4, which is expressed on both

CD4+FoxP3- T-helper cells, as CD4+FoxP3+ T-regulatory cells. In the third cohort, analysis was performed using flow-cytometry, which incorporates a relative outcome measure (i.e. proportion within live CD3+ T-cells), and allows for discrimination of T-helper and T-regulatory cell populations.

Flow cytometry in fresh tumour tissues showed a relative increase in CD8+ T-cells within infiltrated CD3+ T-cells in the TME of patients with dHGP. Contrastingly, the TME of non-dHGP patients was associated with a relative increase in CD4+ T-cells within infiltrating CD3+ T-cells. These results are in-line with cohort A, considering the semi-quantitative nature of the outcome measure and that CD4 was the only marker in which no significant difference in either intra- or peritumoural expression existed between dHGP and non-dHGP. The relative increase in CD8 and relative decrease in CD4 in the TME of dHGP patients was consistent with the CD8/CD4 ratio, which was significantly higher in patients with dHGP in both cohorts A and C. The relative increase of CD4+ T-cells in the TME of non-dHGP patients appeared only due to an increased CD4+FoxP3- T-helper subset, as no difference was found for the T-regulatory subset. This is especially interesting considering the previously demonstrated immunosuppressive effect of CD4+FoxP3+ T-regulatory cells on anti-tumour immunity.[22,36] The absence of a difference in relative numbers of T-regulatory cells within CD3+ T-cells in the TME between dHGP and non-dHGP patients suggests that the detrimental prognosis observed in non-dHGP patients may not be mediated by T-regulatory cells (or at least T-regulatory cell numbers, since functionality was not studied). The flowcytometric data show that the observed increases in absolute numbers of FoxP3+ cells observed in cohorts A and B are probably due to increased absolute number of T-cells in the TME of dHGP patients, and not to selective enrichment of the regulatory T-cell subset within infiltrating CD3+ T-cells.

While the T-cell immune infiltrate was investigated in all three cohorts, B and plasma cells were only investigated in the first. Herein CD79A, a double polyclonal Kappa/Lambda, and SLAMF7 staining were used to identify B-lineage and plasma cells. As stated before, interpretation of these individual markers should be done with caution due to absent normalisation. Nevertheless some of the most striking differences in both the peri- and intratumoural TME in cohort A were observed in the expression of these B/plasma cell markers. For instance high peritumoural CD79A was observed in all but one (97%) of the patients with dHGP versus 60% in non-dHGP, and high intratumoural CD79A in more than 80% versus less than 60%. Similarly large differences were seen for intra- and peritumoural Kappa/Lambda and peritumoural SLAMF7. While T-cells in CRC (metastases) have been studied extensively, less is known about the prognostic impact of B and plasma cells. A recent review identified five studies investigating the prognostic impact of CD20+ B-cell tumour infiltration within CRC (metastases).[37] Three of these studies demonstrated a positive,[38-40] one demonstrated a negative,[41] and one failed to demonstrate any prognostic effect of tumour-infiltrating CD20+ B-cells.[42] The majority of studies in other cancer types also report positive prognostic effects of tumour-infiltrating B-cells.[37] It is thought that B-cell production of stimulatory cytokines can enhance the T-cell anti-tumour response.[37] In addition the production of tumour antigen-specific antibodies by plasma cells could trigger antibody-dependent cellular cytotoxicity and enhance antigen presentation to T-cells through Fc receptors on dendritic cells.[37] It has however also been suggested that B and plasma cell infiltration is the result of IFNγ production and might therefore be more a reflection of the T-cell anti-tumour response rather than a mediating factor.[43] Although only demonstrated in a single cohort by a single method, these results suggest that the TME of

dHGP could also be characterised by B-cell and plasma cell enrichment. Further research should aim at validating these findings and to determine underlying mechanisms.

Assimilation of all three cohorts demonstrates an increased absolute and relative infiltration of CD8+ cytotoxic T-cells in the TME of patients with dHGP. This provides a potential explanation to the superior survival previously observed in patients with dHGP,[32] and also within the current study. All the more because the HGP and the immune infiltrate at the TME were found to be independent of clinical risk. Not only has increased infiltration of CD8+ cytotoxic T-cells been linked to prognosis in primary CRC[44] and metastatic CRC patients[24,40,45], but Katz and colleagues have specifically correlated increased CD8+ T-cell infiltration to prolonged survival following resection of CRLM.[21] Brunner et al. also found that high CD8+ infiltration was linked to favourable prognosis in patients with CRLM.[46] Moreover, Brunner et al. specifically correlated fibrotic capsule formation (which likely represents the 100% dHGP population of our study) with high CD8+, CD45+ and CD4+ infiltration on IHC, suggesting a general increased immune infiltrate in those patients.[46] This is similar to our results from cohorts A and B of the current study, where a general increased immune infiltrate in dHGP was found. This general increased immune infiltrate further adds to the possible explanation for the superior survival observed in dHGP, since Brunner et al. specifically reported that an increased immune infiltrate, especially in combination with fibrotic capsule formation, was strongly related to favourable prognosis.[46] Likewise, Katz et al. reported a general increased infiltration of CD3 T-cells to be prognostic following surgical treatment of CRLM.[21] More recently, the internationally validated immunoscore for stage I-III CRC proposed by Galon et al.[20,47], derived from intra- and peritumoural densities of CD3+ and CD8+ T-cells,

was also found to be positively correlated with favourable prognosis in patients with CRLM.[26]

The question then arises whether the immune response seen in the TME drives the HGP phenotype (i.e. HGPs are host-determined), or that intrinsic tumour characteristics determine the HGP, in turn driving the immune phenotype (i.e. HGPs are tumour-driven). Linear regression analysis in cohorts B and C demonstrated a positive linear relationship between the percentage of dHGP scored at the tumour-liver interface and CD8+ T-cells, as well as the CD8/CD4 ratio. In addition, a negative linear association for CD4+ T-cells existed, which was explained by a negative linear association in the CD4+ FoxP3- T-helper cell subset only. These linear relationships indicate a level of interactivity between the immune infiltrate and the HGP phenotype. Considering that flow cytometry of distant tumour-free liver samples demonstrated similar linear relationships between CD4+ T-cells, CD4+FoxP3- T-helper cells, the CD8/CD4 ratio, and the percentage of dHGP scored at the tumour-liver interface, HGPs could, in part, be host-determined. Linear regression analysis of peripheral blood samples and the percentage of dHGP showed no such linear correlations, suggesting that the HGP phenotype may be more influenced by the local immunologic environment of the liver than by systemic immunity.

The strength of our study is that three cohorts were independently studied using distinct analytic methods. However, some limitations have to be noted. Firstly, data on intrinsic tumour characteristics such as mismatch repair status and RAS/RAF mutational status were unavailable in all three cohorts. It would have been especially valuable to include mismatch repair status since it is currently the only indication for checkpoint inhibitors within metastatic CRC. Consequently mismatch repair status is thought to be a main

driving force of the immune infiltrate.[18,19] Mismatch repair deficiency is however only present in 3% of the patients with CRLM.[17] As such mismatch repair deficiency alone could never account for the entire dHGP phenotype, which is present in roughly 20% of chemo-naive CRLM patients[32], suggesting (at least partial) independency. Secondly, although HGP evaluation was performed according to international consensus guidelines[27], assessment was done by several observers and both light-microscopy and digitalised slide images were used. This is likely of little relevance though, as interobserver reliability for HGP assessment (even for trained observers with limited histopathological experience) was found to be excellent.[48] Furthermore, within- and between metastasis concordance of HGPs is especially high in chemo-naive patients.[48] Thirdly, the semi-quantitative IHC assessment in cohort A only incorporated grading of antibody expression and not antibody intensity compared to positive control. Previous studies have incorporated methods for scoring both antibody expression and antibody intensity.[49] Such methods would have likely added discriminatory power in cohort A and is something that should be considered for similar future investigations. Finally, flow cytometry could only be performed in samples from which sufficient viable MNCs for flowcytometric analysis could successfully be isolated. Thus patients with a desert immune-phenotype are not included in the analyses. No data was available on the frequency of unsuccessful isolation of viable MNC's from tumour, tumour-free liver, or peripheral blood samples. In addition, CD45 was not always included in the flow cytometry panel due to limited channels. It would be interesting to compare CD3+ T-cells (and its subsets) based on the CD45+ population.

In conclusion, the current study demonstrates that the tumour microenvironment of chemo-naive patients with a purely angiogenic desmoplastic growth pattern is characterised by a

general increased and distinctly cytotoxic immune infiltrate compared to patients with any observed non-desmoplastic growth. These findings provide a potential explanation for the superior survival observed in chemo-naive patients with purely desmoplastic colorectal liver metastases.

References

1. Brenner H, Kloor M, Pox CP. Colorectal cancer. *Lancet.* Apr 26 2014;383(9927):1490-1502.
2. Hackl C, Neumann P, Gerken M, Loss M, Klinkhammer-Schalke M, Schlitt HJ. Treatment of colorectal liver metastases in Germany: a ten-year population-based analysis of 5772 cases of primary colorectal adenocarcinoma. *BMC Cancer.* Nov 4 2014;14:810.
3. Engstrand J, Nilsson H, Stromberg C, Jonas E, Freedman J. Colorectal cancer liver metastases - a population-based study on incidence, management and survival. *BMC Cancer.* Jan 15 2018;18(1):78.
4. van der Geest LG, Lam-Boer J, Koopman M, Verhoef C, Elferink MA, de Wilt JH. Nationwide trends in incidence, treatment and survival of colorectal cancer patients with synchronous metastases. *Clin Exp Metastasis.* Jun 2015;32(5):457-465.
5. Elferink MA, de Jong KP, Klaase JM, Siemerink EJ, de Wilt JH. Metachronous metastases from colorectal cancer: a population-based study in North-East Netherlands. *Int J Colorectal Dis.* Feb 2015;30(2):205-212.
6. Pawlik TM, Schulick RD, Choti MA. Expanding criteria for resectability of colorectal liver metastases. *Oncologist.* Jan 2008;13(1):51-64.
7. de Ridder JAM, van der Stok EP, Mekenkamp LJ, et al. Management of liver metastases in colorectal cancer patients: A retrospective case-control study of systemic therapy versus liver resection. *Eur J Cancer.* May 2016;59:13-21.
8. Tomlinson JS, Jarnagin WR, DeMatteo RP, et al. Actual 10-year survival after resection of colorectal liver metastases defines cure. *J Clin Oncol.* Oct 10 2007;25(29):4575-4580.
9. Jones RP, Jackson R, Dunne DF, et al. Systematic review and meta-analysis of follow-up after hepatectomy for colorectal liver metastases. *Br J Surg.* Apr 2012;99(4):477-486.
10. Fong Y, Fortner J, Sun RL, Brennan MF, Blumgart LH. Clinical score for predicting recurrence after hepatic resection for metastatic colorectal cancer: analysis of 1001 consecutive cases. *Ann Surg.* Sep 1999;230(3):309-318; discussion 318-321.
11. Konopke R, Kersting S, Distler M, et al. Prognostic factors and evaluation of a clinical score for predicting survival after resection of colorectal liver metastases. *Liver Int.* Jan 2009;29(1):89-102.
12. Nagashima I, Takada T, Matsuda K, et al. A new scoring system to classify patients with colorectal liver metastases: proposal of criteria to select candidates for hepatic resection. *J Hepatobiliary Pancreat Surg.* 2004;11(2):79-83.
13. Nordlinger B, Guiguet M, Vaillant JC, et al. Surgical resection of colorectal carcinoma metastases to the liver. A prognostic scoring system to improve case selection, based on 1568 patients. Association Francaise de Chirurgie. *Cancer.* Apr 1 1996;77(7):1254-1262.
14. Rees M, Tekkis PP, Welsh FK, O'Rourke T, John TG. Evaluation of long-term survival after hepatic resection for metastatic colorectal cancer: a multifactorial model of 929 patients. *Ann Surg.* Jan 2008;247(1):125-135.
15. Hoppener DJ, Nierop PMH, van Amerongen MJ, et al. The Disease-Free Interval Between Resection of Primary Colorectal Malignancy and the Detection of Hepatic Metastases Predicts Disease Recurrence But Not Overall Survival. *Ann Surg Oncol.* Sep 2019;26(9):2812-2820.

16. Brudvik KW, Jones RP, Giuliante F, et al. RAS Mutation Clinical Risk Score to Predict Survival After Resection of Colorectal Liver Metastases. *Ann Surg.* Jan 2019;269(1):120-126.
17. Haddad R, Ogilvie RT, Croitoru M, et al. Microsatellite Instability as a Prognostic Factor in Resected Colorectal Cancer Liver Metastases. *Annals of Surgical Oncology.* 2004/11/01 2004;11(11):977-982.
18. Kalyan A, Kircher S, Shah H, Mulcahy M, Benson A. Updates on immunotherapy for colorectal cancer. *J Gastrointest Oncol.* Feb 2018;9(1):160-169.
19. Le DT, Uram JN, Wang H, et al. PD-1 Blockade in Tumors with Mismatch-Repair Deficiency. *N Engl J Med.* Jun 25 2015;372(26):2509-2520.
20. Pagès F, Mlecnik B, Marliot F, et al. International validation of the consensus Immunoscore for the classification of colon cancer: a prognostic and accuracy study. *The Lancet.* 2018/05/26/ 2018;391(10135):2128-2139.
21. Katz SC, Pillarisetty V, Bamboat ZM, et al. T Cell Infiltrate Predicts Long-Term Survival Following Resection of Colorectal Cancer Liver Metastases. *Annals of Surgical Oncology.* September 01 2009;16(9):2524-2530.
22. Pedroza-Gonzalez A, Verhoef C, Ijzermans JN, et al. Activated tumor-infiltrating CD4+ regulatory T cells restrain antitumor immunity in patients with primary or metastatic liver cancer. *Hepatology.* Jan 2013;57(1):183-194.
23. Zhou G, Noordam L, Sprengers D, et al. Blockade of LAG3 enhances responses of tumor-infiltrating T cells in mismatch repair-proficient liver metastases of colorectal cancer. *Oncoimmunology.* 2018;7(7):e1448332.
24. Lazarus J, Oneka MD, Barua S, et al. Mathematical Modeling of the Metastatic Colorectal Cancer Microenvironment Defines the Importance of Cytotoxic Lymphocyte Infiltration and Presence of PD-L1 on Antigen Presenting Cells. *Annals of Surgical Oncology.* September 01 2019;26(9):2821-2830.
25. Sideras K, Galjart B, Vasaturo A, et al. Prognostic value of intra-tumoral CD8(+) /FoxP3(+) lymphocyte ratio in patients with resected colorectal cancer liver metastasis. *J Surg Oncol.* Jul 2018;118(1):68-76.
26. Van den Eynde M, Mlecnik B, Bindea G, et al. The Link between the Multiverse of Immune Microenvironments in Metastases and the Survival of Colorectal Cancer Patients. *Cancer Cell.* Dec 10 2018;34(6):1012-1026 e1013.
27. van Dam PJ, van der Stok EP, Teuwen LA, et al. International consensus guidelines for scoring the histopathological growth patterns of liver metastasis. *Br J Cancer.* Nov 7 2017;117(10):1427-1441.
28. Vermeulen PB, Colpaert C, Salgado R, et al. Liver metastases from colorectal adenocarcinomas grow in three patterns with different angiogenesis and desmoplasia. *J Pathol.* Oct 2001;195(3):336-342.
29. Eefsen RL, Van den Eynden GG, Hoyer-Hansen G, et al. Histopathological growth pattern, proteolysis and angiogenesis in chemonaive patients resected for multiple colorectal liver metastases. *J Oncol.* 2012;2012:907971.
30. Van den Eynden GG, Bird NC, Majeed AW, Van Laere S, Dirix LY, Vermeulen PB. The histological growth pattern of colorectal cancer liver metastases has prognostic value. *Clin Exp Metastasis.* Aug 2012;29(6):541-549.
31. Frentzas S, Simoneau E, Bridgeman VL, et al. Vessel co-option mediates resistance to anti-angiogenic therapy in liver metastases. *Nat Med.* Nov 2016;22(11):1294-1302.
32. Galjart B, Nierop PMH, van der Stok EP, et al. Angiogenic desmoplastic histopathological growth pattern as a prognostic marker of good outcome in patients with colorectal liver metastases. *Angiogenesis.* May 2019;22(2):355-368.
33. Tanis E, Julie C, Emile JF, et al. Prognostic impact of immune response in resectable colorectal liver metastases treated by surgery alone or surgery with perioperative FOLFOX in the randomised EORTC study 40983. *Eur J Cancer.* Nov 2015;51(17):2708-2717.
34. Ohtani H. Focus on TILs: prognostic significance of tumor infiltrating lymphocytes in human colorectal cancer. *Cancer Immun.* Feb 21 2007;7:4.
35. Nierop PMH, Galjart B, Hoppener DJ, et al. Salvage treatment for recurrences after first resection of colorectal liver metastases: the impact of histopathological growth patterns. *Clin Exp Metastasis.* Apr 2019;36(2):109-118.
36. Zou W. Regulatory T cells, tumour immunity and immunotherapy. *Nature Reviews Immunology.* 2006/04/01 2006;6(4):295-307.
37. Wouters MCA, Nelson BH. Prognostic Significance of Tumor-Infiltrating B Cells and Plasma Cells in Human Cancer. *Clin Cancer Res.* Dec 15 2018;24(24):6125-6135.

38. Meshcheryakova A, Tamandl D, Bajna E, et al. B cells and ectopic follicular structures: novel players in anti-tumor programming with prognostic power for patients with metastatic colorectal cancer. *PLoS One.* 2014;9(6):e99008.
39. Berntsson J, Nodin B, Eberhard J, Micke P, Jirstrom K. Prognostic impact of tumour-infiltrating B cells and plasma cells in colorectal cancer. *Int J Cancer.* Sep 1 2016;139(5):1129-1139.
40. Mlecnik B, Van den Eynde M, Bindea G, et al. Comprehensive Intrametastatic Immune Quantification and Major Impact of Immunoscore on Survival. *J Natl Cancer Inst.* Jan 1 2018;110(1).
41. Kasajima A, Sers C, Sasano H, et al. Down-regulation of the antigen processing machinery is linked to a loss of inflammatory response in colorectal cancer. *Hum Pathol.* Dec 2010;41(12):1758-1769.
42. Baeten CI, Castermans K, Hillen HF, Griffioen AW. Proliferating endothelial cells and leukocyte infiltration as prognostic markers in colorectal cancer. *Clin Gastroenterol Hepatol.* Nov 2006;4(11):1351-1357.
43. Guy TV, Terry AM, Bolton HA, Hancock DG, Shklovskaya E, Fazekas de St. Groth B. Pro- and anti-tumour effects of B cells and antibodies in cancer: a comparison of clinical studies and preclinical models. *Cancer Immunol Immunother.* Aug 2016;65(8):885-896.
44. Diederichsen ACP, v. B. Hjelmborg J, Christensen PB, Zeuthen J, Fenger C. Prognostic value of the CD4+/CD8+ ratio of tumour infiltrating lymphocytes in colorectal cancer and HLA-DR expression on tumour cells. Cancer Immunology, *Immunotherapy.* July 01 2003;52(7):423-428.
45. Glaire MA, Domingo E, Sveen A, et al. Tumour-infiltrating CD8+ lymphocytes and colorectal cancer recurrence by tumour and nodal stage. *British Journal of Cancer.* 2019/09/01 2019;121(6):474-482.
46. Brunner SM, Kesselring R, Rubner C, et al. Prognosis according to histochemical analysis of liver metastases removed at liver resection. *Br J Surg.* Dec 2014;101(13):1681-1691.
47. Galon J, Costes A, Sanchez-Cabo F, et al. Type, density, and location of immune cells within human colorectal tumors predict clinical outcome. *Science.* Sep 29 2006;313(5795):1960-1964.
48. Hoppener DJ, Nierop PMH, Herpel E, et al. Histopathological growth patterns of colorectal liver metastasis exhibit little heterogeneity and can be determined with a high diagnostic accuracy. *Clin Exp Metastasis.* Aug 2019;36(4):311-319.
49. Milione M, Miceli R, Barretta F, et al. Microenvironment and tumor inflammatory features improve prognostic prediction in gastro-entero-pancreatic neuroendocrine neoplasms. *J Pathol Clin Res.* Oct 2019;5(4):217-226.

Supplementary materials

Supplementary table 1. Comparison of the HGP and the TME by clinical risk score.

		Clinical risk score		
		Low risk (CRS 0-2)	High risk (CRS 3-5)	
All patients		n = 158 (%)	n = 33 (%)	p-value
HGP	dHGP	41 (26)	4 (12)	0.089
	non-dHGP	117 (74)	29 (88)	
Cohort A: semi-quantitative IHC		n = 101 (%)	n = 16 (%)	p-value
HGP	dHGP	30 (30)	2 (12)	0.151
	non-dHGP	71 (70)	14 (88)	
CD8 - high peritumoural		67 (66)	10 (62)	0.764
CD8 - high stromal		48 (48)	11 (69)	0.123
CD8 - high intratumoural		36 (36)	6 (38)	0.886
CD4 - high peritumoural		28 (28)	2 (12)	0.195
CD4 - high stromal		17 (17)	3 (19)	0.877
FoxP3 - high peritumoural		73 (73)	11 (69)	0.724
FoxP3 - high stromal		63 (64)	9 (56)	0.571
Cohort B: quantitative IHC		n = 22 (%)	n = 8 (%)	p-value
HGP	dHGP	7 (32)	2 (25)	0.719
	non-dHGP	15 (68)	6 (75)	
CD8 - intratumoural counts/mm^2 - *(median [IQR])*		50.9 [26.1, 77.4]	76.4 [55.8, 168.0]	0.159
CD8 - peritumoural counts/mm^2 - *(median [IQR])*		918.2 [694.6, 1093.3]	892.0 [702.7, 1257.4]	0.851
FoxP3 - intratumoural counts/mm^2 - *(median [IQR])*		24.1 [11.8, 46.8]	32.0 [5.4, 103.0]	0.888
FoxP3 - peritumoural counts/mm^2 - *(median [IQR])*		126.5 [75.1, 254.4]	150.2 [52.5, 366.2]	0.851
Cohort C: flow cytometry (fresh tumour tissues)		n = 57 (%)	n = 17 (%)	p-value
HGP	dHGP	10 (18)	2 (12)	0.570
	non-dHGP	47 (82)	15 (88)	
% CD8+ T-cells* - *(median [IQR])*		27.2 [22.3, 37.0]	28.5 [24.5, 34.4]	0.928
% CD4+ T-cells* - *(median [IQR])*		62.0 [47.2, 69.2]	60.5 [56.7, 69.9]	0.363
% CD4+ FoxP3- T-cells* - *(median [IQR])*		51.3 [38.5, 61.0]	54.7 [50.6, 59.9]	0.317
% CD4+ FoxP3+ T-cells* - *(median [IQR])*		6.7 [4.0, 10.0]	8.8 [5.6, 11.4]	0.371

**Expressed as percentage of CD3+ T-cells gate*

Abbreviations in alphabetical order: CRS: clinical risk score; dHGP: desmoplastic type histopathological growth pattern; HGP: histopathological growth pattern; IHC: immunohistochemistry; IQR: interquartile range; non-dHGP: non-desmoplastic type histopathological growth pattern; TME: tumour microenvironment.

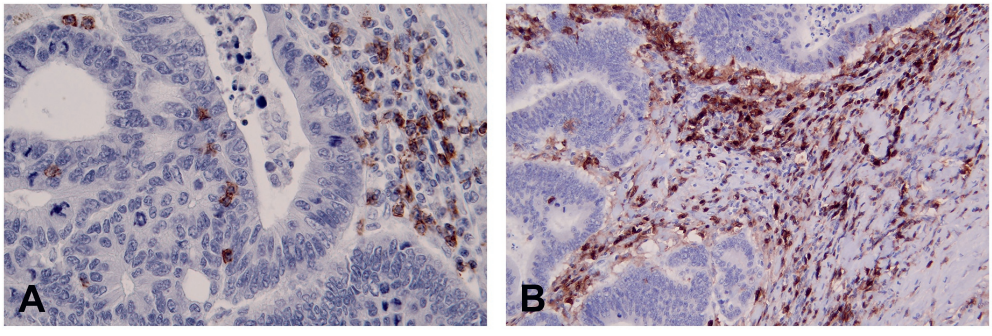

Supplementary figure 1. Examples of immunohistochemistry (IHC) staining used in cohort A.(A) CD8 IHC staining.(B) CD4 IHC staining.

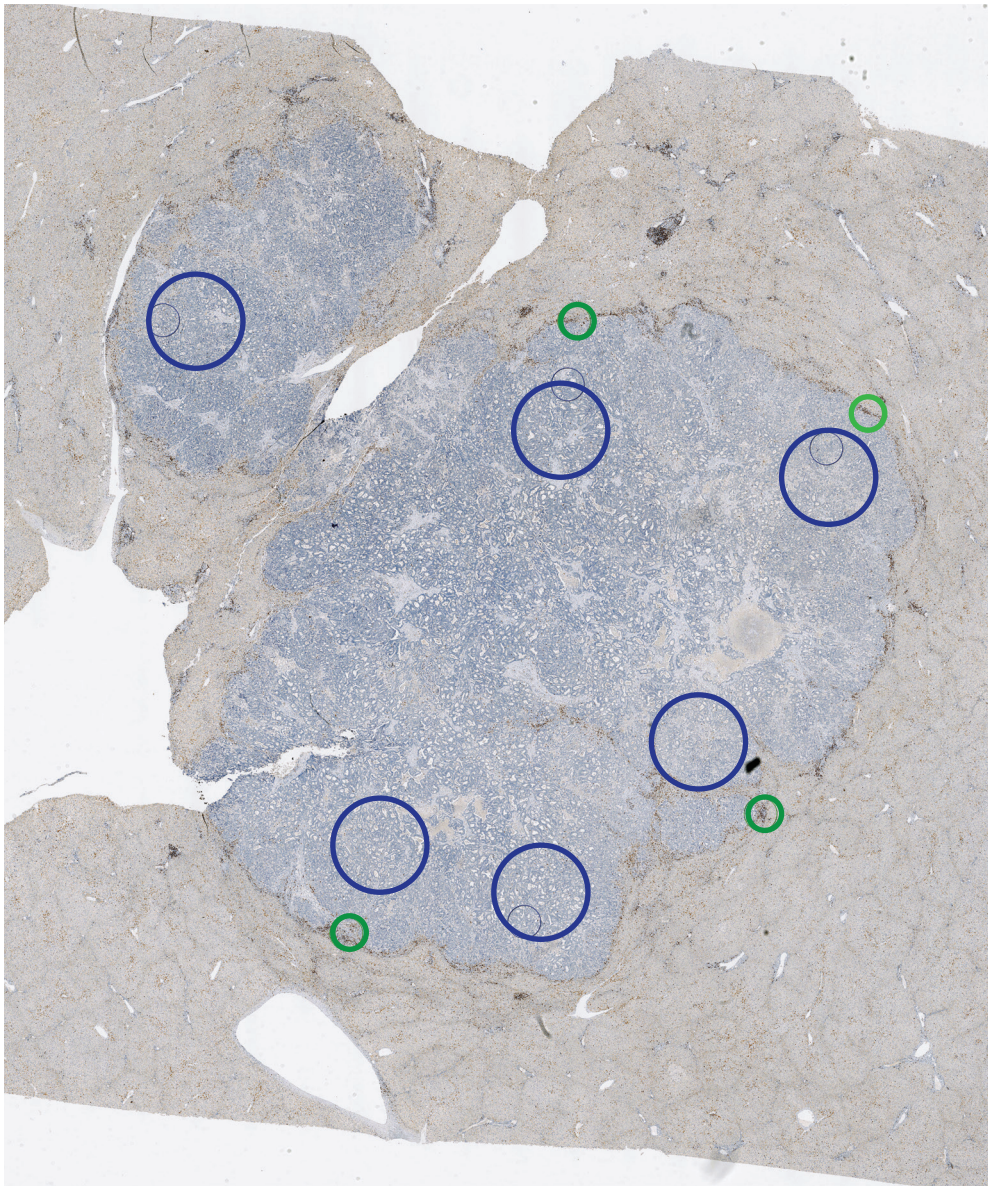

Supplementary figure 2. Quantitative immunohistochemistry using digital image analysis in cohort B. Intratumoural celdensities were determined in several (4-6) large circular areas containing viable tumorous tissue (blue circles). The peritumoural celdensities were determined in four high-power fields (0.54mm in diameter) at the tumour-liver interface (greencircles).

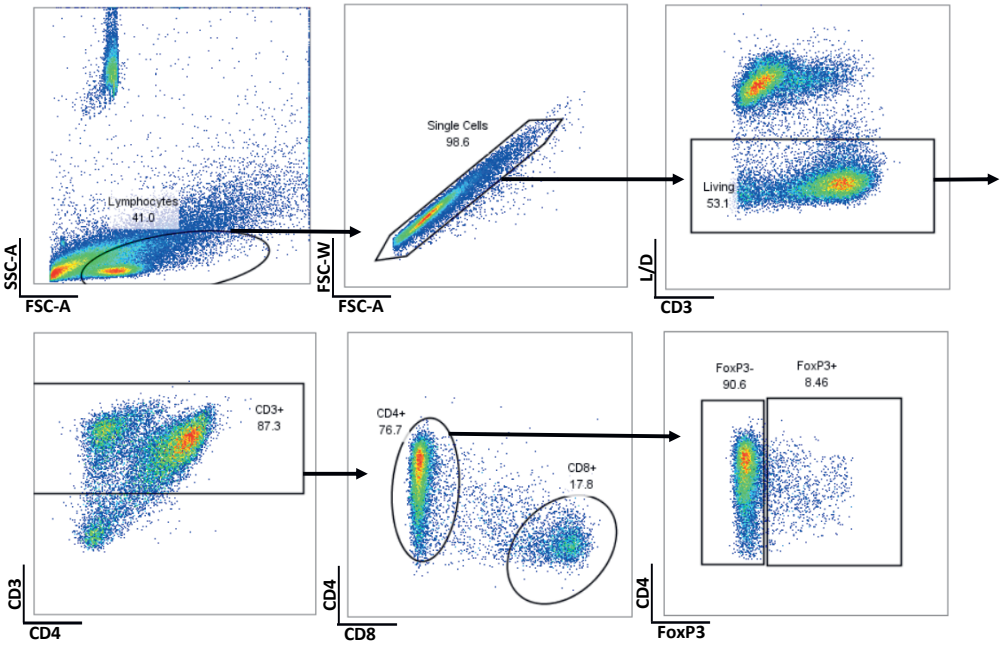

Supplementary figure 3. Representative example of the flow cytometry gating strategy (top-left to bottom-right) in cohort C. Flow cytometric analysis was performed using a FACS Canto II flow cytometer and FlowJo software. Viable (aqua LIVE/DEAD [L/D] fluorescent dye-negative) leukocytes were gated in single cells using FSC and SSC. Live T-cells were defined based on CD3 expression. Within live CD3+ T-cells, the relative proportions of CD8+ and CD4+ T-cell subsets were determined. Within the CD4+ T-cells, the T-regulatory subset was defined as CD4+FoxP3+ while the T-helper subset was defined as CD4+FoxP3-. SSC-A: side scatter area; FSC-A: forward scatter area; FSC-W: forward scatter width.

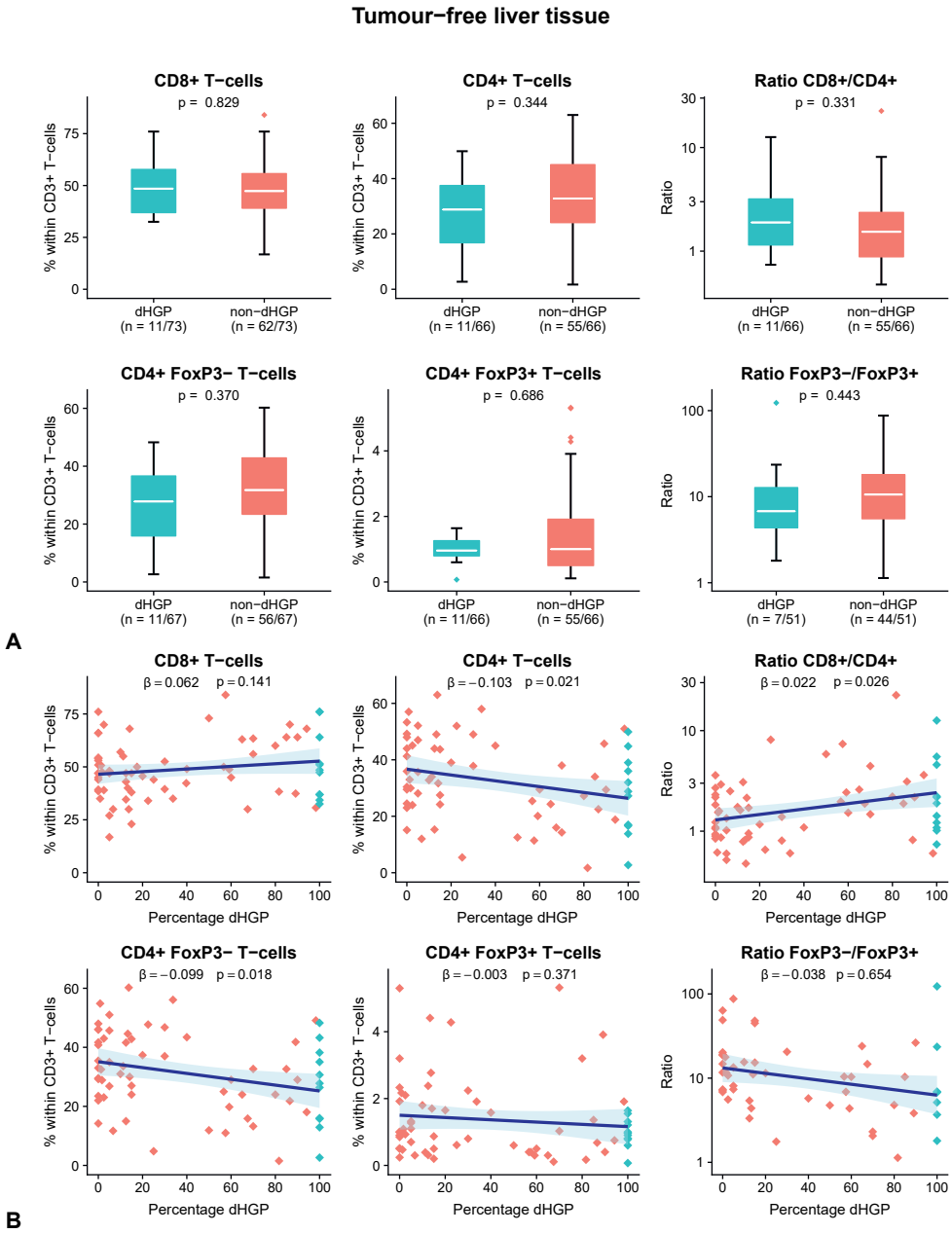

*Supplementary figure 4. Results of flow cytometry of fresh tumour-free liver samples in cohort C. (A) Box and whiskerplots of the relative proportion of individual T-cell subsets stratified by histopathological growth pattern (HGP). Ratio's are displayed on a logarithmic scale. The white line represents the median, the box represents the inter-quartile rage (IQR), and the whiskers represents the range. Outliers are defined according to the 1.5 rule (i.e. outside [Q1-1.5*IQR; Q3+1.5*IQR]). (B) Linear regression models of the relative proportion of individual T-cell subsets (y-axis) and the percentage of the desmoplastic type histopathological growth pattern (dHGP) scored at the tumour-liver interface (x-axis). Ratio's are displayed on a logarithmic scale. The blue line represents the regression coefficient, the lightblue ribbon represents the corresponding 95% confidence interval. Measurements of individual patients are displayed using dots. Red dots represent patients with non-dHGP (i.e. < 100% dHGP) and blue dots represent patients with dHGP (i.e. 100% dHGP).*

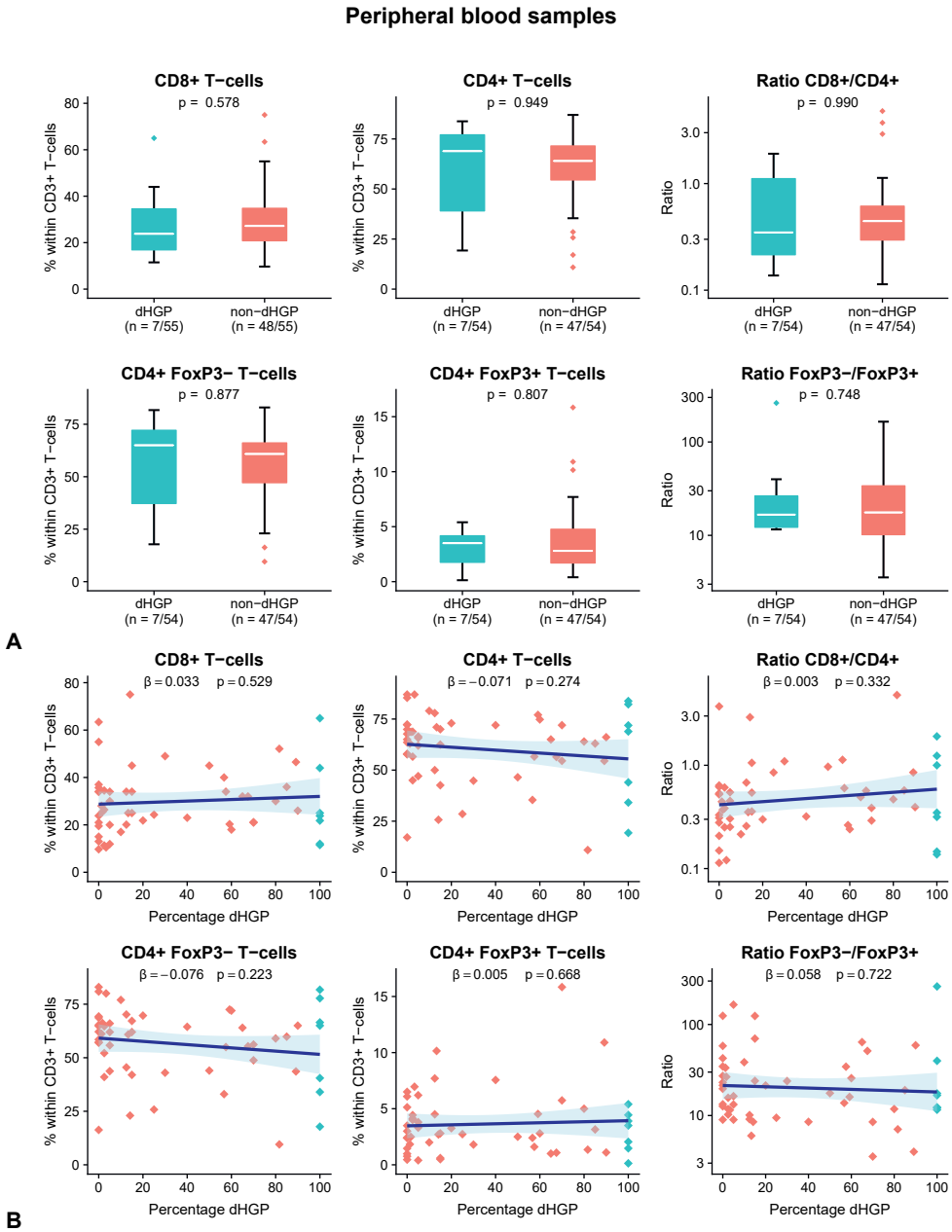

*Supplementary figure 5. Results of flow cytometry of peripheral blood samples in cohort C. (A) Box and whiskerplots of the relative proportion of individual T-cell subsets stratified by histopathological growth pattern (HGP). Ratio's are displayed on a logarithmic scale. The white line represents the median, the box represents the inter-quartile rage (IQR), and the whiskers represents the range. Outliers are defined according to the 1.5 rule (i.e. outside [Q1-1.5*IQR; Q3+1.5*IQR]). (B) Linear regression models of the relative proportion of individual T-cell subsets (y-axis) and the percentage of the desmoplastic type histopathological growth pattern (dHGP) scored at the tumour-liver interface (x-axis). Ratio's are displayed on a logarithmic scale. The blue line represents the regression coefficient, the lightblue ribbon represents the corre-sponding 95% confidence interval. Measurements of individual patients are displayed using dots. Red dots represent patients with non-dHGP (i.e. < 100% dHGP) and blue dots represent patients with dHGP (i.e. 100% dHGP).*

```r
#----------------------------- Summary table -----------------------------
#Variable selection
tdat <- PhD
gvar <- c("HGP")
vars <- c("Cohort", "Age_At_Resection_CRLM", "Gender", "ASA_cat",
          "Left_right_sided", "pT_cat", "N_CRC", "Total_leasions_treated",
          "Diam_CRLM", "DFI_CRLM", "CEA_preop", "Neo_CTx_CRLM", "R0_R1",
          "EHD", "KRAS", "BRAF", "MSI")
npar <- c("Age_At_Resection_CRLM", "Total_leasions_treated", "Diam_CRLM",
          "DFI_CRLM", "CEA_preop")
flnm <- c("PhD/Chapter 9 - Summary/Summary_table.csv")

#Baseline table
T1 <- CreateTableOne(vars = vars, strata = gvar,
                     argsApprox = list(correct=FALSE),
                     includeNA=FALSE, data = tdat)
pT1 <- print(T1, nonnormal = npar, explain = TRUE,
             showAllLevels = TRUE, catDigits = 1, format = "fp",
             contDigits = 1, missing = TRUE, noSpaces = TRUE)

#Exporting table
write.csv2(pT1, file = flnm)
```

Chapter IX

Summary

Summary

Here the contents of this thesis are summarised in a chapter by chapter fashion outlining the study design, methodologies, and results of each. This thesis concerns the histopathological growth patterns (HGP) of resected colorectal cancer liver metastasis. The HGPs are defined as three separate phenotypes of the tumour-liver interface as recognised on haematoxylin and eosin stained tissue slides; the desmoplastic, replacement, and pushing type. Besides this phenotypical distinction, patients can be classified into those with only demoplastic type growth observed, i.e. desmoplastic, and opposing non-desmoplastic cases, hence recognised by any pushing and/or replacement growth. This latter classification finds its basis in prognosis, with superior survival observed for desmoplastic patients.

Chapter 2 focussed on the reliability and replicability of the HGP. Classification of which is performed on a two-dimensional representation of a three dimensional liver metastasis. This study sought to assess the reliability of this two-dimensional representation by appraising the within metastasis concordance in resected colorectal liver metastases with two or more distinct samples, and the between metastasis concordance in the case of two or more resected colorectal liver metastasis within the same patient. The learning curve of assessment was additionally investigated. Two novice assessors – one without pathology experience and a gastro-intestinal pathologist – received two training sessions of 50 slides followed by a test session in which they had to determine the HGP in 50 slides individually. Both the within at 95% and between metastasis concordance at 90% proved to be high, also upon external validation. After two training sessions both observers achieved excellent agreement (Cohen's kappa >0.95) with the gold standard. These results strengthen the HGPs as a reliable and replicable biomarker.

Equally important as reliability is clinical relevance. In *chapter 3* external validation of the prognostic impact of the HGP on survival following resection of colorectal liver metastasis was pursued. To this end a multicentre retrospective cohort study was performed in 780 patients treated with curative intent for colorectal liver metastasis in either the Memorial Sloan Kettering Cancer Center (New York, USA), the Radboud UMC (Nijmegen, the Netherlands), and the Erasmus MC Cancer Institute (Rotterdam, the Netherlands). Survival was compared between patients classified as desmoplastic versus non-desmoplastic. In addition a cut-off analysis was performed based on the extent of desmoplastic growth at the tumour-liver interface. Analogous results were obtained, with the desmoplastic phenotype associated with a more than two-fold reduction in mortality and cancer-recurrence risk. The extent of non-desmoplastic growth observed did not impact prognosis. These results confirmed the desmoplastic versus non-desmoplastic distinction as the clinically relevant classification in patients undergoing resection of colorectal liver metastasis.

These results were incorporated in the updated consensus guidelines to score the histopathological growth patterns, as presented in *chapter 4*. The chapter is the result of an international group of collaborators involved in HGP research, and provides an overview of studies concerning the HGPs since the publication of the previous guidelines edition. Novel strategies to predict the HGP are discussed, as well as animal models that successfully replicate the donor patient HGP. In these guidelines the use of the desmoplastic versus non-desmoplastic cut-off in patients with colorectal liver metastasis is advocated based on the results from previous studies such as *chapter 3*, but also on a presented pooled analysis in a large international multicentre cohort of 1931 patients, demonstrating analogous

results. Lastly, several hypotheses are proposed on the cellular and molecular mechanisms that drive the biology of the different HGPs allowing for future pre-clinical and clinical research opportunities.

Chapter 5 evaluated the relationship between the HGP and the histopathology of the originating colorectal tumour. For 183 treatment-naive patients with resected colorectal liver metastasis the histopathology slides of the corresponding and resected primary tumour were collected. Thirteen established colorectal cancer histopathology features were determined and compared between the corresponding liver metastasis HGP. Unfavourable colorectal cancer histopathology was more frequent in non-desmoplastic cases for all markers evaluated, and significantly so for three of the evaluated markers. Not surprisingly, unfavourable colorectal cancer histopathology was significantly more prevalent in patients with non-desmoplastic liver metastasis, with a median of 4 versus 2 unfavourable characteristics observed in desmoplastic patients, respectively. Multivariable logistic regression analysis based on 9 primary colorectal cancer markers and 2 liver metastasis characteristics achieved good performance to predict the HGP. These study results associate primary colorectal cancer histopathology with the HGP of corresponding liver metastasis and opens up opportunities for the preoperative determination of the HGP.

In *chapter 6* the automated classification of the HGP was evaluated. In collaboration with the Digital Pathology Group of the Radboud UMC (Nijmegen, the Netherlands) a multitask neural image compression pipeline to classify the HGP on gigapixel histopathology images of resected liver metastasis was developed. The pipeline consists of two steps. First, the entire gigapixel image is compressed into a low-dimensional embedding vector using a neural network, the

encoder, maintaining the spatial arrangement of the original slide. Second, convolutional neural networks are trained on the entire compressed slide as input to predict the image level label of interest, the HGP. A supervised multitask learning architecture to train the encoder was developed which optimised the compression for several different histopathology tasks simultaneously based on existing datasets. The classifier was trained on 941 whole-slide images from 237 patients and achieved good classification performance (area under the curve 0.89). External validation was performed in 2787 previously unseen whole-slide images from 741 patients and identical results were obtained (0.88). The prognostic impact of the classified HGP was similar to the ground-truth across all patients, but outperformed in patients pre-treated with chemotherapy. These experimental results suggest that automated HGP classification is reliable and may improve prognostication of patients pre-treated with chemotherapy.

The last two studies of this thesis focussed on the underlying biology of the HGPs, where in *chapter 7* the immune microenvironment was characterised in three separate cohorts, employing different methods in each. In 117 patients semi-quantative immunohistochemistry analysis was performed, in 34 immunohistochemistry followed by digital image analysis, and lastly in 79 patients live cell populations were quantified by flow-cytometric analysis of fresh tumour tissues. In all three cohorts the desmoplastic HGP was characterised by a enriched and distinctly cytotoxic immune microenvironment. In addition, linear regression analyses found evidence for some linearity between the degree of immune infiltration and the proportion of the desmoplastic HGP along the tumour-liver interface. The study results suggest that localised immune infiltration and the HGP are interrelated, and may represent an underlying biological mechanism to these phenotypes.

IX

In the final study of this thesis, *Chapter 8*, the relationship with the HGP phenotype and the DNA genotype was interrogated. In collaboration with the Memorial Sloan Kettering Cancer Center (New York, USA) and the S:CORT consortium (United Kingdom) next generation sequencing data was compared between 104 patients with a desmoplastic versus 357 patients with a non-desmoplastic HGP, respectively. Nineteen putative colorectal cancer driver genes, microsatellite instability and POLE mutant hypermutation, and tumour mutational burden were compared. The results in and across both cohorts do not find evidence for a major difference in tumorigenesis on a DNA level, and consequently point to other biological mechanisms than oncogenetics underlying the prognostic impact of these histologic phenotypes. While associations between genetic drivers of adaptive anti-cancer immunity (i.e. hypermutation) and the desmoplastic phenotype were observed and could potentially explain a minority of these inflamed tumours, results were conflicting between cohorts. Multivariable overall survival analysis corrected for genetic and patient factors confirmed the desmoplastic phenotype as an independent prognostic factor. The study therefore demonstrates that the HGP phenotype is (largely) independent of DNA genotype.

Nederlandse samenvatting

Het onderwerp van dit proefschrift betreft de histopathologische groeipatronen (HGPs) van gereseceerde colorectale levermetastasen. De groeipatronen zijn gedefinieerd als drie verschillende fenotypen van de tumor-lever overgang. Deze drie fenotypen worden herkend op hematoxyline en eosine gekleurde microscopiepreparaten en betreffen respectievelijk het desmoplastische, vervangende, en duwende groeipatroon. Behalve dit fenotypische onderscheid is er een tweede classificatie aan de hand van prognose, waarbij patiënten met een volledig desmoplastisch groeipatroon een langere algehele overleving vertonen ten opzichte van patiënten met ook maar enig niet-desmoplastisch groeipatroon (vervangend en/of duwend), ongeacht de uitgebreidheid hiervan.

Hoofdstuk 2 richt zich op de betrouwbaarheid en reproduceerbaarheid van deze histopathologische biomarker. De heterogeniteit van het groeipatroon indien geclassificeerd als desmoplastisch versus niet-desmoplastisch werd bepaald tussen verschillende microscopiepreparaten van dezelfde tumor, en tussen verschillende metastasen van dezelfde patiënt. Daarnaast werd de leerbaarheid van het classificeren onderzocht. Hiervoor ondergingen twee onervaren beoordelaars – een met minimale pathologie ervaring en een ervaren gastro-intestinaal patholoog – twee training sessies bestaande uit het gezamenlijk bepalen van het groeipatroon in 50 afzonderlijke preparaten. Iedere training sessie werd gevolgd door een evaluatie sessie waarin de beoordelaars afzonderlijk het groeipatroon in 50 ongeziene preparaten moesten bepalen. Het onderzoek toonde aan dat de overeenkomst van het groeipatroon uitermate hoog is. Een gemiddelde overeenkomst van 95% werd gevonden tussen verschillende preparaten van dezelfde uitzaaiing, en 90% tussen uitzaaiingen van dezelfde patiënt. Na twee training sessies behaalde beide beoordelaars

een nagenoeg perfecte overeenkomst (Cohen's kappa >0.95) met de gouden standaard. Deze studieresultaten tonen aan dat de betrouwbaarheid en reproduceerbaarheid van het groeipatroon uitermate hoog is.

Om de klinische relevantie van het groeipatroon te onderschrijven werd in *hoofdstuk 3* een externe validatie studie naar prognose verricht. Dit werd bewerkstelligd middels een internationale multicenter retrospectieve cohortstudie van 780 patiënten die resectie van colorectale levermetastasen ondergingen in het Memorial Sloan Kettering Cancer Center in New York (Verenigde Staten), het Radboud UMC in Nijmegen (Nederland), of het Erasmus MC Kanker Instituut in Rotterdam (Nederland). De algehele overleving na resectie werd vergeleken tussen patiënten met een desmoplastisch en een niet-desmoplastisch groeipatroon. Daarnaast werden additionele analyses verricht naar de prognostische waarde van verschillende hoeveelheden van het niet-desmoplastisch groeipatroon. De studie bevestigd de eerder behaalde resultaten, namelijk dat patiënten met een desmoplastisch groeipatroon een twee keer zo lange algehele overleving hebben vergeleken met patiënten met een niet-desmoplastisch groeipatroon. Ook hebben desmoplastische patiënten een twee keer zo kleine kans op het ontwikkelen van een recidief na chirurgie. Daarnaast is het niet de hoeveelheid maar de aanwezigheid van niet-desmoplastische groei die de prognose lijkt te bepalen.

De tweede versie van de internationale richtlijnen voor het scoren van de groeipatronen worden gepresenteerd in *hoofdstuk 4* van dit proefschrift. Dit hoofdstuk is het resultaat van een internationaal samenwerkingsverband van groeipatroon onderzoekers. Naast het beschrijven van alle nieuwe studies sinds de publicatie van de vorige editie van deze richtlijn, worden ook veelbelovende methoden om het

groeipatroon preoperatief te voorspellen en proefdiermodellen uiteengezet. Daarnaast adviseert de richtlijn het gebruik van de desmoplastische versus niet-desmoplastische classificatie, onder andere gebaseerd op resultaten van eerdere studies zoals *hoofdstuk 3*, maar ook aan de hand van een gepoolde analyse in een groot internationaal multicenter cohort van 1931 individuele patiënten met vergelijkbare resultaten. Tot slot worden in deze nieuwe richtlijn meerdere hypothesen geponeerd naar de onderliggende biologie van de verschillende groeipatronen.

De relatie tussen de histopathologie van de primaire tumor en het groeipatroon werd onderzocht in *hoofdstuk 5*. In totaal werden van 183 patiënten zowel de microscopiepreparaten van de gereseceerde primaire tumor als ook de bijbehorende levermetastasen verzameld. Dertien verschillende histopathologische kenmerken werden bepaald in de preparaten van de primaire tumor en vervolgens vergeleken tussen de verschillende groeipatronen van de bijbehorende levermetastasen. Hieruit bleek dat van alle dertien kenmerken de ongunstige variant altijd vaker voorkwam in patiënten met een niet-desmoplastisch groeipatroon, en voor drie van deze kenmerken was dit verschil ook statistisch significant. Het mediane aantal ongunstige kenmerken was dan ook 4 in patiënten met een niet-desmoplastisch groeipatroon versus 2 in patiënten met een desmoplastisch groeipatroon. De resultaten van deze studie tonen een associatie aan tussen de histopathologie van de primaire tumor en het groeipatroon van de bijbehorende levermetastasen. Deze associatie kan hoogstwaarschijnlijk gebruikt worden om het groeipatroon preoperatief te voorspellen.

In samenwerking met de Digitale Pathologie van het Radboud UMC te Nijmegen werd in *hoofdstuk 6* een meertaaks neuraal netwerk ontwikkeld en geëvalueerd voor de automatische classificatie van het groeipatroon op gigapixel afbeeldingen van gereseceerde colorectale levermetastasen. Dit classificatie algoritme bestaat uit twee afzonderlijke stappen. Allereerst wordt de gehele gigapixel afbeelding gecomprimeerd tot een laag dimensionale representatie met gebruik van een neuraal netwerk, de encoder. Vervolgens wordt deze gecomprimeerde representatie als input gebruikt om het groeipatroon te voorspellen met convolutionele neurale netwerken. Voor het trainen van de encoder werd een gesuperviseerde meertaaks leerarchitectuur ontwikkeld welke de compressie optimaliseert aan de hand van vier verschillende histopathologie classificatie taken. Het ontwikkelde model werd getraind op 941 gedigitaliseerde preparaten van 237 patiënten en behaalde een goed discriminatoir vermogen (AUC 0.89). Vergelijkbare resultaten werden behaald met de externe validatie in 2787 digitale preparaten van 741 patiënten (0.88). Over de gehele groep gezien was de prognostische waarde van het door het model geclassificeerde groeipatroon vergelijkbaar met die van het handmatig geclassificeerde groeipatroon. Echter specifiek in de patiënten die voorbehandeling met chemotherapie ondergingen was het automatisch geclassificeerde groeipatroon beter in staat om prognose te voorspellen dan het handmatig geclassificeerde groeipatroon. De behaalde experimentele resultaten suggereren dan ook dat automatische classificatie van het groeipatroon haalbaar is, en dat het mogelijk tot betere prognosticatie kan leiden in patiënten voorbehandeld met chemotherapie.

In de laatste twee studies van dit proefschrift werd de onderliggende biologie van het groeipatroon onderzocht. Zo werd in *hoofdstuk 7* het lokale immunologische klimaat

op metastaseniveau gekarakteriseerd aan de hand van drie afzonderlijke methodes. In 117 patiënten werd gebruik gemaakt van semi-kwantitatieve immunohistochemie, in 34 kwantitatieve immunohistochemie aan de hand van digitale beeldanalyse, en tot slot in 79 patiënten werden levende cel populaties gekwantificeerd met flow-cytometrie van vers gereseceerd tumor- en leverweefsel. In alle drie de cohorten kwam naar voren dat het lokale immunologische klimaat van metastasen met een desmoplastisch groeipatroon gekenmerkt wordt door een verrijkt en specifiek cytotoxisch immuun infiltraat. Aan de hand van regressieanalyses werd de uitgebreidheid van het lokale immuun infiltraat geassocieerd met de hoeveelheid van het desmoplastische groeipatroon. De studie toont aan dat het lokale immunologische klimaat en het groeipatroon aan elkaar gerelateerd zijn. Of dit ook een causaal verband betreft zal uit aanvullend onderzoek moeten blijken.

De laatste studie, *hoofdstuk 8*, richt zich op de relatie tussen het HGP fenotype en het DNA genotype. In samenwerking met het Memorial Sloan Kettering Cancer Center in New York (Verenigde Staten) en het S:CORT consortium uit het Verenigd Koningrijk werd next generation sequencing data vergeleken tussen 104 patiënten met een desmoplastisch en 357 met een niet-desmoplastisch groeipatroon. Negentien colorectaal carcinoom gerelateerde genen, microsatelliet instabiliteit en POLE gerelateerde hypermutatie, en de tumor mutatie graad werden vergeleken. De resultaten in zowel de gepoolde als cohort afzonderlijke analyses geven geen aanwijzingen voor een onderliggend verschil in tumorigenese op DNA niveau, en suggereren derhalve dat oncogenetica geen onderliggend biologisch mechanisme is van de verschillende groeipatronen. Wel waren er aanwijzingen dat genetische afwijkingen gerelateerd aan de anti-kanker immuunrespons vaker voorkomen in patiënten met een desmoplastisch groeipatroon, al waren deze associaties inconsequent en derhalve onzeker.

```r
#Loading required packages
library(shiny)
library(ggplot2)
library(gridExtra)

# Define UI ----
ui <- fluidPage(
  titlePanel("Prediction model"),

  #Side bar input variables ----
  sidebarLayout(
    sidebarPanel(width=3,

      #Patient characteristics ----
      helpText("Patient characteristics"),

      radioButtons("Gender", "Gender",
                   choices = list("Female" = "Female",
                                  "Male" = "Male"),
                   selected = "Male", inline=TRUE),

      sliderInput("age_60_l", p("Age at CRLM resection",
                  em("(if <60 enter 60)")),
                  min = 60, max = 100, value = c(61)),

      #Primary tumour parameters ----
      br(),

      helpText("Primary tumor characteristics"),

      selectInput("Left_right_sided", "Primary tumor location",
                  choices = list("Right sided" = "Right-sided",
                                 "Left sided" = "Left-sided",
                                 "Rectal" = "Rectum"),
                  selected = "Left-sided"),

      radioButtons("pT_cat", "(y)pT stage",
                  choices = list("(y)pT0-2" = "pT 0-2",
                                 "(y)pT3-4" = "pT 3-4"),
                  selected = "pT 3-4", inline=TRUE),

      radioButtons("N_CRC", "(y)pN stage",
                  choices = list("(y)pN0" = "N0",
                                 "(y)pN1-2" = "N+"),
                  selected = "N0", inline=TRUE),

     #CRLM parameters ----
      br(),

      helpText("CRLM characteristics"),

      sliderInput("DFI_w", p("Disease-free interval in months",
                  em("(if >48 enter 48)")),
                  min = 0, max = 48, value = c(0)),
```

Chapter X

General discussion and future perspectives

X

This thesis aimed to validate and establish the histopathological growth patterns (HGPs) of colorectal cancer liver metastasis as a relevant biomarker, and to assess the role of immunology and genetics as underlying biological mechanisms. Here, we evaluate this thesis in relation to this aim by considering its contents, the current knowledgebase, and future perspectives with regard to several aspects. To appraise the relevance of the HGPs as a biomarker we need to first consider the validity of its measurement. Besides validity, the utility of this measurement needs to be established to determine clinical relevance. Depending on this validity and utility, appropriate implementation of this biomarker into clinical care can be weighed. In addition, critical appraisal of the biological aspects of the growth patterns is required to better understand and improve upon these applied aspects. Lastly, it is important to reflect on the histopathological growth patterns within the larger context of liver metastasis and colorectal cancer treatment.

Validity

The definition of a biomarker is a measurable indicator of some biological state or condition. This requires that this indicator can indeed be measured validly. The HGPs are obtained from the visual study by light microscopy or digital equivalents of haematoxylin and eosin (H&E) stained tissue sections of resected colorectal liver metastasis.[1] Such histological markers are by design prone to particular shortcomings. The H&E stained tissue sections obtained by the pathological sampling process represent two-dimensional representations of a three-dimensional structure, introducing potential within sample heterogeneity. Within the context of the surgical treatment of liver metastatic tumours this is further amplified by between sample heterogeneity in case of two or more metastases, which is true for the majority of patients with colorectal liver metastasis.[2] Second to the

sampling-related heterogeneity there is the inter-observer variability of the measurement to which all observer-dependent measurements are subjected.[3]

In *chapter 2* of this thesis the validity of the HGPs as a biomarker was evaluated by determining the within and between metastasis heterogeneity. A high within (94%) and between (90%) metastasis HGP concordance was demonstrated, although this was affected by preoperative systemic chemotherapy, which doubled the odds for within sample heterogeneity, and reduced between metastasis concordance with 6%.[4] In addition to quantifying sample-related heterogeneity, the learning curve of two novice assessors – including a gastro-intestinal pathologist – was evaluated. Following two supervised training sessions, both achieved near perfect agreement with the gold standard (Cohen's kappa > 0.95). These results bolster the validity of the HGP as a biomarker, as such high rates of concordance are similar to clinically applied genetic tests[5], and the inter observer agreement supersedes that of other histological markers[6]. But importantly, this only applies to the HGP when classified according to the Rotterdam cut-off as proposed in *chapter 4*. This cut-off markedly simplifies HGP classification as it considers only the presence and absence of the particular HGP phenotypes rather than their relative extent. This is relevant as the validity when considering the individual phenotype extent may be markedly less; the previous version of the consensus guidelines reported on the intraclass correlation coefficient between 12 independent observers and found it to be somewhere between 0.4 and 0.9 for the common replacement and desmoplastic phenotypes, and seldom above 0.5 for the rare pushing HGP.[1] Besides a clear prognostic difference, the simplification and increased validity therefore provide additional arguments to support the Rotterdam cut-off criteria. Since the Rotterdam criteria are

now advocated in the updated guidelines presented in *chapter 4*, future HGP research will most likely increase in validity as it adopts this cut-off.

A future step in the HGP as a biomarker will be achieved by the introduction of observer-independent methods of HGP classification. The newly developed neural image compression (NIC) with multitask learning classification pipeline presented in *chapter 6* of this thesis comes close to achieving this goal. In both the training and validation cohorts, excellent classification performance with an area under the curve greater or equal to 0.88 was reached. With several computational advancements available to improve on the classifier itself, and an at least four times as large dataset available for training, the next iteration may achieve performance equalling or even surpassing that of dedicated pathologists, as also seen in other deep learning approaches applied to several histologic classification tasks. [7-14] This will however require a large study on the inter-observer agreement of the HGP, as the data presented in *chapter 2* is limited to three observers and a relatively small amount of samples. Such a study will provide the necessary reference data, for the classification performance of an AI model can hardly be improved beyond the disagreement that already exists amongst the ground-truth on which it is trained, i.e. the pathologist based determination.

It is concerning this HGP "ground-truth" that in *chapter 6* an interesting observation was made; upon external validation this early stage NIC classifier already outperformed the observer-based classification in terms of prognosis in the patients pre-treated with systemic chemotherapy. In other words, the NIC classifier was worse at distinguishing the labels it was aimed to predict than it was at distinguish that which those labels were supposed to reflect; prognosis.

This was exemplified by the analysis of the true/false positive/negative classified patients. In chemo-naive patients this analysis was as expected, as superior survival was only "captured" in the true cases according to the observer-based classification, but remarkably in the pre-treated patients superior survival was only seen in those cases that the NIC model classified as true cases, i.e. the true and false positive patients. This implies that the "ground-truth" HGP as determined by the current assessment methods in pre-treated patients may be incorrect.

Besides the findings put forward in *chapters 2* & *6*, there are multiple other arguments to question the validity of the HGP after systemic chemotherapy when determined by the current assessment methods. First, the prognostic impact may be reduced[15], although results are equivocal.[16] Second, there is ample evidence that systemic chemotherapy induces histopathological changes that "alter" the HGP, leading to an increase of the desmoplastic type.[17] It is reasonable to consider this increase as potential evidence of biological change. Studies have for instance suggested that the response to chemotherapy is dependent on the HGP, as higher degrees of pathological response to systemic chemotherapy were significantly more common to patients with a predominantly desmoplastic HGP.[18] However, this reasoning may be seriously flawed. Histopathological response to chemotherapy is defined by fibrosis.[19] Similarly, the single defining feature of the desmoplastic HGP is fibrosis separating tumour and liver cells.[1] Therefore, chemotherapy induced regression of any hepatic tumour with peripheral fibronisation will by default be classified as desmoplastic, regardless of the morphology present prior to chemotherapy. From a more fundamental point of view, how can one possibly assess the manner in which a tumour "grows" within the liver parenchyma when one only observes it after it has "shrunk"

through therapy? While this of course does not apply to all liver metastasis, as not all respond and some even progress during chemotherapy, the concept should not be abandoned. The evidence put forward by this thesis and that of others provides strong arguments that the validity of the HGP is less after systemic chemotherapy. Fortunately, deep learning models such as the one presented in *chapter 6* may overcome this limitation and may still allow for valid HGP classification after chemotherapy.

Utility

In the case of biomarkers utility is synonymous with clinical relevance; can we guide treatment or make medical decision based on the biological state or condition that is measured. Early on, studies on the HGPs found an association with survival, suggesting it may be a useful biomarker to determine patient prognosis. These early reports considered the relative presence of the different HGP phenotypes to classify patients and found that those with a predominantly desmoplastic HGP had better overall and recurrence-free survival following surgical treatment of colorectal liver metastasis.[1,20-23] With the first large scale retrospective study by our group formal assessment of the optimal patient classification cut-off was possible. This study revealed a remarkable association; superior overall survival was exclusive to those patients with a completely desmoplastic phenotype across all resected metastases, and any observed non-desmoplastic phenotype – no matter the quantity – was associated with a more conventional prognosis.[15] In *chapter 3* of this thesis external validation of this finding was successfully achieved with near identical results.[16] These studies have proven instrumental in defining the HGP utility, and have resulted in revised cut-off criteria as advocated in the updated consensus guidelines for the assessment of the

HGP, as presented in *chapter 4*.[24] Ultimately, with this new classification the HGP biomarker allows us to identify a one-fifth minority of patients undergoing surgical resection of colorectal cancer liver metastasis with an approximate two-fold reduction in mortality and recurrence risk.[15,16] In reality this patient group exhibits survival characteristics more comparable to the non-metastatic setting, underscoring the prognostic impact of this biomarker.[25] When compared to other biomarkers within colorectal cancer liver metastasis surgery, the HGP sits amongst those with the highest prognostic impact, only being equalled by KRAS and BRAF mutational status.[2,26] These results substantiate the utility of the HGP as a biomarker to determine patient prognosis after resection of colorectal liver metastasis.

Although useful, clinical relevance extends beyond assessing prognosis. It is those markers which can predict specific therapeutic effectiveness that achieve a lasting and considerable change in actual clinical care, and are therefore held in high regard. There are several preliminary results to suggest that the HGP could be amongst these so-called predictive biomarkers. For instance, patients with a desmoplastic HGP experience mostly liver limited recurrences as opposed to the multi-organ and frequently extra-hepatic recurrence patterns seen in non-desmoplastic patients.[27] This ultimately translates into a higher degree of salvageable recurrences seen in patients with a desmoplastic HGP and, coupled with the higher possibility of achieving radical resection margins for metastases with a desmoplastic phenotype[28], these results suggest that the HGP is predictive for lasting local treatment control following surgical resection of colorectal liver metastasis. Besides recurrence patterns, there is evidence that hints at a difference in chemotherapy efficacy as well. A large retrospective study found that in preoperatively chemo-naive

patients adjuvant systemic chemotherapy improved overall survival in patients with a non-desmopalstic HGP only, suggesting that the HGP may be predictive for chemotherapy sensitivity.[29] This predictive impact was not seen in patients already pre-treated with chemotherapy. As however eluded to before, the validity of the HGP measurement may be compromised following pre-operative systemic chemotherapy. Fortunately, automated methods of assessment as outlined in *chapter 6* might successfully mitigate this limitation in the near future. Besides systemic chemotherapy, the recent interest in hepatic arterial infusion pump chemotherapy for the treatment of colorectal cancer liver metastasis has led to multiple clinical trials currently underway in the Netherlands.[30,31] This treatment is unique in that its effect is localised to the liver. It is therefore hypothesised that patients at high risk of extrahepatic recurrence, for which the HGP is a strong biomarker, may benefit less – or not at all – from this specialised localised treatment. And indeed, a recent study which modelled the risk of extrahepatic recurrence at two years to predict systemic and hepatic arterial chemotherapy treatment effect found that liver-directed regional chemotherapy did not improve survival in patients at very high risk of extrahepatic recurrence when compared to systemic chemotherapy only.[26] Again, the HGP proved amongst the strongest predictors for extrahepatic recurrence risk, and manifested as the strongest liver-metastasis specific marker in this study.[26]
It therefore seems likely that the utility of the HGP extends beyond prognosis into the prediction of systemic and localised chemotherapeutic effectiveness, making this marker a promising candidate for personalised treatment in the surgical management of colorectal cancer liver metastasis.

In recent years oncological practice has experienced a paradigm shift with the introduction and evolution of immune

checkpoint inhibitors, more commonly known as immunotherapy. These novel treatments have radically altered the life expectancy of previously terminally ill patients with cancers such as melanoma and lung.[32,33] The colorectal cancer field was slow to adopt these therapeutics, as initial effectiveness seemed limited.[34] It was however discovered that the highly mutated microsatellite instable colorectal cancers do respond well to these novel treatments, with results from phase III clinical trials in microsatellite instable stage IV colorectal cancer demonstrating a hazard ratio of 0.6 for progression-free survival when compared to conventional systemic chemotherapy.[35] It therefore seems clear that there are specific subgroups of colorectal cancer patients that benefit from immunotherapy, and current evidence suggests that they can be identified by a state of hypermutation as present in microsatellite instability and POLE proofreading domain mutated forms of colorectal cancer.[36] In *chapters 3* & *8* of this thesis an association with these hypermutated forms of colorectal cancer (i.e., microsatellite instable and POLE mutant) and the desmoplastic HGP was demonstrated. These results provide evidence to support the HGP as a candidate biomarker for immunotherapy in liver-metastatic colorectal cancer. The risk of conjecture should however also be recognised, as these findings still require formal validation. For instance, in *chapter 3* there was a high degree of missing data and a higher than expected prevalence of microsatellite instable tumours, suggesting some form of selection bias, and in *chapter 8* results were equivocal between both cohorts evaluated. Given the ease of HGP determination and the high validity of the measurement, it nevertheless seems worthwhile to elaborate on the potential utility of the HGP to guide immunotherapy use.[37]

Implementation

When considering the implementation of the HGP into clinical practice based on its validity and utility, it becomes evident that so far the HGP is only applicable as a biomarker for prognosis and potentially adjuvant chemotherapy in chemonaive patients undergoing resection of colorectal liver metastasis. Given there are real-world examples of pathology-based biomarkers that guide adjuvant treatment, for instance TNM-stage in non-metastatic colorectal cancer, clinical implementation could be feasible. Realistically however, the current applicability of the HGPs is considerably restricted as in the majority of countries perioperative chemotherapy is considered the standard of care in the surgical management of colorectal liver metastasis[38,39], although this could very well change based on recent insights.[40] For the future development and implementation of the HGP into clinical practice preoperative determination will therefore be essential.

It is partly to this end that in *chapter 5* of this thesis the relationship between primary colorectal cancer histology and the HGP of corresponding liver metastases was investigated.[41] In this relatively small study it was found that amongst the thirteen colorectal cancer markers determined, unfavourable characteristics were unilaterally more common in the primary tumours of patients with corresponding non-desmoplastic liver metastases. Quantitatively, based on combined-marker analysis the median number of unfavourable primary colorectal cancer histopathology features was 4 in patients with corresponding non-desmoplastic liver metastases compared to 1 in patients with desmoplastic liver metastases. These results provide evidence that there is a relationship between the histopathology of the primary colorectal tumour and the HGP of the corresponding liver metastases. Most of all, they serve as a proof of concept for

an artificial intelligence approach. If a sufficiently large dataset of matching primary and metastatic colorectal cancer resection specimens is collected and digitalised, automatic determination of the liver metastasis HGP on slides of the resected primary tumour may be achievable in the near-future, especially when employing deep-learning techniques as those developed in *chapter 6*.

Besides considering the histology of the primary tumour, deep-learning models applied to preoperative computed tomography or magnetic resonance imaging, so called radiomics, is another promising approach for the preoperative determination of the HGP. Several models have been published achieving varying degrees of performance.[42–45] Importantly, not all of these studies considered the revised cut-off criteria to classify the HGP as advocated in the updated guidelines presented in *chapter 4*.[24] Since clinical relevance seems dictated by this new cut-off, the development of additional models that take this revised classification into account are required. Furthermore, formal external validation of these developed models is essential, as often such models prove highly tuned to the dataset on which they are built and rarely achieve comparable performance when applied to previously unseen datasets.[46] Preliminary results are nevertheless promising, and with an ever increasing level of detail captured in medical imaging it seems plausible that preoperative determination of the HGP can, in time, be achieved through radiomics.

In addition to artificial intelligence approaches, the introduction of novel diagnostic tests also provides opportunities for the preoperative determination of the HGP. So called liquid biopsies have emerged that can detect circulating tumour cells as well as tumour DNA, and results seem promising that these measurements are sensitive for

residual disease following resection, but also provide longitudinal measurements of chemotherapy response.[47] With results awaited for a large cohort study of 240 patients undergoing surgical resection of colorectal liver metastasis in which these liquid biopsies have been determined perioperatively, investigational opportunities into their utility to determine the HGP will become available.

Ultimately, for the HGP to be implemented into clinical care will also require inclusion in standard pathology reporting guidelines as well as national and international clinical guidelines for the treatment of colorectal cancer liver metastasis. For this to be achieved will no doubt necessitate additional clinical research, but most importantly prospective clinical trials. The development of the HGP as a biomarker therefore presently sits at a critical stage; there is sufficient evidence to suggest clinical validity and utility, but ultimately unless a research group or collaboration with sufficient funding supports a prospective clinical trial, actual implementation remains uncertain. Consequently, the design of such a prospective clinical trial deserves due consideration.

The simplest design is that of a randomised controlled trial administering adjuvant systemic chemotherapy in preoperatively chemonaive patients stratified by the HGP. Such a trial would provide the necessary evidence to advocate adjuvant systemic chemotherapy in patients with a non-desmoplastic HGP, or negate it in the case of the desmoplastic HGP, depending on perspective. With a negative randomised controlled trial on adjuvant systemic chemotherapy recently performed and published in colorectal liver metastasis, such a trial design should be considered cautiously.[40] First of all because determination of the HGP in the previously performed trial is a far more cost-

effective way to address the research question at hand. And secondly, taking the position that 80% of patients are non-desmoplastic, and an effect of adjuvant systemic chemotherapy is expected in these patients, one would expect to find at least some benefit on a population level. Instead the trial reported a longer disease-free survival for the non-chemotherapy group at interim analysis.[40] Rather one could consider a more extensive study design, which may additionally incorporate immunotherapy and hepatic arterial infusion pump (HAIP) chemotherapy, or base chemotherapy allocation on a patient-level risk estimate calculated using real-world data.[26] For such studies to realistically be considered however results of the currently ongoing PUMP-trial[31] have to be awaited (and also analysed in light of the HGP). In addition, more definitive evidence on the link between the desmoplastic HGP and hypermutated forms of colorectal cancer seems required, potentially followed by a phase-I or phase-II trial of immunotherapy in patients with the desmoplastic HGP. Lastly, sample size requirements would be considerable and raises feasibility concerns. Nevertheless, opportunities seem plentiful for a future trial to achieve personalised care in this patient group.

Biology

Following all of the above it can be stated that the HGP as a biomarker can be measured validly and appears to indicate a biological state or condition with sufficient clinical implications to investigate implementation into clinical care. The logical question than emerges as to what exactly is this biological state or condition that is measured.

In *chapter 7* of this thesis, the relationship between immune enrichment in the tumour microenvironment and the HGP was evaluated.[48] By studying three cohorts of patients in which

the tumour immune microenvironment was assessed by separate methodologies this study puts forward evidence to suggest that the desmoplastic HGP is characterised by an enriched and distinctly cytotoxic immune infiltrate when compared to the non-desmoplastic HGP. Furthermore, linear regression analyses revealed some linearity between the degree of immune infiltration and the proportion of the desmoplastic HGP along the tumour-liver interface. The latter suggests some form of interactivity between the HGP phenotype and the degree of immune infiltration. One could therefore hypothesise that only in the complete desmoplastic phenotype a state of near-equilibrium between immune response and cancer-progression has been reached, and that any non-desmoplastic HGP may be indicative of an increased cancer-progression imbalance. This hypothesis also implies that there are states of imbalance where the anticancer immune response prevails. Such cases most likely do not or seldom develop metastases, and as such are not represented in any studies and may be impossible to identify. The extremely rare but widely recognised phenomenon of spontaneous regression of advanced metastatic cancer may still provide some evidence to support such states, especially since they have been associated with acute infections and fever.[49,50] This immune-derived hypothesis suggests that the HGPs may, in part, be a liver-specific representation of the systemic anticancer immune response. Results from *chapter 5* do lend support to this, given the significantly higher percentage of tumour-infiltrating lymphocytes that was observed in the primary resection specimens of patients with corresponding desmoplastic liver metastases when compared to patients with a non-desmoplastic HGP.[41] Besides the results presented in *chapter 7*, several other reports are available that have linked the desmoplastic HGP to an increased local immune infiltration and provide additional evidence for this hypothesis.[51-53] The recent emergence of patient-derived

xenograft models where the patient HGP can be replicated by the transplantation of tumour cells into the livers of mice with a knocked-out immune system may however advocate against it.[54] Nonetheless, replicating the patient donor HGP in an environment devoid of any recipient host-immune system is not identical to proving that the donor HGP is independent of the human donor host-immune response. It could still be that immunoselective pressure in the human host has a lasting effect on the biological behaviour of the transplanted tumours, or at least lasting for remaining life-span of the recipient mice. Furthermore, if cancer cells can successfully be transplanted, so can the associated immune-cells which could potentially undergo some form of clonal expansion within the recipient mice-liver. And indeed, figure 5A of *chapter 4* paradoxically demonstrates a distinct immune infiltrate surrounding a transplanted colorectal liver metastasis with a desmoplastic HGP in the host-liver of an immunologically knocked-out mouse.[24] Whether there is actually any concurrent transplantation of an ongoing immune response can easily be investigated by immunohistochemical analyses of these patient-derived xenograft models and may provide additional data to either support or oppose the hypothesis that the HGPs are primarily a phenotypical expression of the anticancer host-immune response.

The relationship between the HGP phenotype and corresponding DNA genotype was investigated in *chapter 8* of this thesis. By studying the mutation rates of 19 (metastatic) colorectal cancer putative driver genes in two cohorts with a combined total of over 450 patients the study found convincing evidence that for the most part, the HGP phenotype is independent of the DNA genotype. For 17 of the 19 genes including KRAS, NRAS, and BRAF, no associations with the HGP could be demonstrated. Neither in the combined cohort nor in the stratified analyses. Moreover, the impact of the

HGP on overall survival was independent of these and other colorectal cancer hallmark genes. Regarding KRAS en BRAF status, similar results were found in *chapter 3*.[16] These results therefore clearly demonstrate that the prognostic impact of the HGP is not dependent on underlying genetics, at least not on a DNA level. The study did however reveal an association between the desmoplastic HGP and a higher prevalence of hypermutated forms of colorectal cancer, as identified by microsatellite instability and POLE proofreading domain mutations. Additionally, mutations in PTEN and B2M were also associated with the desmoplastic phenotype. Notably though, these results were equivocal between both cohorts, which complicates the interpretation of these results. Separately, analysis in *chapter 3* did also demonstrate an association between microsatellite instability and the desmoplastic HGP.[16] With no other data currently available other than that presented in *chapters 3* & *8*, a possible relationship between the HGP and these hypermutated forms of cancer remains plausible yet elusive, and will require additional clarification. Especially since these hypermutated forms of colorectal cancer are known drivers of anticancer immunity in colorectal cancer[36], and have proven responders to immunotherapy.[35] A definitive study associating these forms of cancer with the desmoplastic HGP could therefore lend additional support to the hypothesis that the HGPs are primarily an expression of the anticancer immune response.

The results of this thesis shed light on immunology and the DNA genotype as potential underlying mechanisms to the HGPs. Besides these, many other hypotheses and future research opportunities have been put forward by the international collaboration of researchers involved in HGP research as outlined in *chapter 4*.

The bigger picture

Partly based on the results put forward in this thesis, one may conclude that the HGP is a biomarker for prognosis and possibly treatment effect in patients undergoing resection of colorectal cancer liver metastasis, and that this biomarker can easily and reliably be determined using light microscopy. Several strong arguments have been provided in favour of the continued development and implementation of this biomarker into clinical practice. The argument may however also be raised that the HGP is ultimately irrelevant.

For if colorectal cancer can be detected and treated before metastatic spread can occur, there would be no need for metastatic colorectal cancer biomarkers. Recently, the introduction of a nationwide colorectal cancer screening program has indeed brought reality closer to this ideal, as screening reduces the incidence of stage IV disease and cancer associated mortality.[55,56] This of course does not negate clinical research in advanced stages of colorectal cancer, or any cancer for that matter, since it is unlikely that this ideal can actually be achieved. Nevertheless the goal of prevention and earlier detection should not be ignored, and warrants allocation of significant resources. This must however not be confused with the earlier detection of recurrences after curative treatment of cancer, as there is ample evidence that this does not improve survival outcomes, not in colorectal cancer cancer[57,58], nor in other common cancer types for that matter.[59]

Besides this fundamental argument, the HGP could be regarded as a single data point captured on H&E stained slides of resected liver metastasis. In addition to the HGP, there are currently multiple other known data points that can be extracted from these slides, and potentially an infinite number of yet unknown ones. Recent developments in medical

research have shown the limits of observer-dependent methods of assessment, and preliminary results show that artificial intelligence, or deep-learning, is capable of directly predicting prognosis (and possibly treatment effect) in an unsupervised fashion from digitalised slides of resection specimens.[14,60] In that sense, the continued development of such models may ultimately achieve unparalleled levels of prediction, as it will automatically consider and extract a plethora of data-points from a single digitalised image, including the HGP. Nevertheless, markers such as the HGP will prove instrumental for the supervised training and hypothesis-based deep-learning approaches that are required to develop and optimise such future models.

So while the HGP may ultimately become irrelevant as a biomarker, luckily for this thesis, this is not yet the case. Given the prognostic impact and potential to guide clinical treatment, the continued development of this marker seems worthwhile, especially since the HGPs expand to other primary and secondary liver metastatic tumours.[61-65] This strongly suggests that this histology marker is the phenotypical expression of a pan-cancer biological mechanism. The continued development of this and other markers has the potential to personalise cancer treatment. And therein lies the crux of the current era of clinical cancer research. Ultimately the goal must be to combine all knowledge and markers including the HGP, and to continually expand upon this developed knowledgebase. Herein the collection of large-scale biobanks with high-quality clinical, molecular, imaging, and pathological data will prove instrumental and should be pursued through international collaborative efforts.

References

1. van Dam PJ, van der Stok EP, Teuwen LA, et al. International consensus guidelines for scoring the histopathological growth patterns of liver metastasis. *Br J Cancer*. Nov 7 2017;117(10):1427-1441.
2. Buisman FE, Giardiello D, Kemeny NE, et al. Predicting 10-year survival after resection of colorectal liver metastases; an international study including biomarkers and periop-erative treatment. *Eur J Cancer*. Jun 2022;168:25-33.
3. Cross SS. Grading and scoring in histopathology. *Histopathology*. Aug 1998;33(2):99-106.
4. Hoppener DJ, Nierop PMH, Herpel E, et al. Histopathological growth patterns of colorec-tal liver metastasis exhibit little heterogeneity and can be determined with a high diag-nostic accuracy. *Clin Exp Metastasis*. Aug 2019;36(4):311-319.
5. Bhullar DS, Barriuso J, Mullamitha S, Saunders MP, O'Dwyer ST, Aziz O. Biomarker con-cordance between primary colorectal cancer and its metastases. *EBioMedicine*. Feb 2019;40:363-374.
6. Chetty R, Gill P, Govender D, et al. International study group on rectal cancer regression grading: interobserver variability with commonly used regression grading systems. *Hum Pathol*. Nov 2012;43(11):1917-1923.
7. Bulten W, Pinckaers H, van Boven H, et al. Automated deep-learning system for Gleason grading of prostate cancer using biopsies: a diagnostic study. *Lancet Oncol*. Feb 2020;21(2):233-241.
8. Nagpal K, Foote D, Tan F, et al. Development and Validation of a Deep Learning Algo-rithm for Gleason Grading of Prostate Cancer From Biopsy Specimens. *JAMA Oncol*. Sep 1 2020;6(9):1372-1380.
9. Coudray N, Ocampo PS, Sakellaropoulos T, et al. Classification and mutation prediction from non-small cell lung cancer histopathology images using deep learning. *Nat Med*. Oct 2018;24(10):1559-1567.
10. Ehteshami Bejnordi B, Mullooly M, Pfeiffer RM, et al. Using deep convolutional neural networks to identify and classify tumor-associated stroma in diagnostic breast biopsies. *Mod Pathol*. Oct 2018;31(10):1502-1512.
11. Mercan E, Mehta S, Bartlett J, Shapiro LG, Weaver DL, Elmore JG. Assessment of Ma-chine Learning of Breast Pathology Structures for Automated Differentiation of Breast Cancer and High-Risk Proliferative Lesions. *JAMA Netw Open*. Aug 2 2019;2(8):e198777.
12. Wu M, Yan C, Liu H, Liu Q. Automatic classification of ovarian cancer types from cyto-logical images using deep convolutional neural networks. *Biosci Rep*. Jun 29 2018;38(3).
13. Hekler A, Utikal JS, Enk AH, et al. Deep learning outperformed 11 pathologists in the classification of histopathological melanoma images. *Eur J Cancer*. Sep 2019;118:91-96.
14. Skrede O-J, De Raedt S, Kleppe A, et al. Deep learning for prediction of colorectal cancer outcome: a discovery and validation study. *The Lancet*. 2020;395(10221):350-360.
15. Galjart B, Nierop PMH, van der Stok EP, et al. Angiogenic desmoplastic histopathologi-cal growth pattern as a prognostic marker of good outcome in patients with colorectal liver metastases. *Angiogenesis*. May 2019;22(2):355-368.
16. Hoppener DJ, Galjart B, Nierop PMH, et al. Histopathological Growth Patterns and Sur-vival After Resection of Colorectal Liver Metastasis: An External Validation Study. *JNCI Cancer Spectr*. Jun 2021;5(3):pkab026.
17. Nierop PM, Hoppener DJ, Buisman FE, et al. Preoperative systemic chemotherapy alters the histopathological growth patterns of colorectal liver metastases. *J Pathol Clin Res*. Jan 2022;8(1):48-64.
18. Frentzas S, Simoneau E, Bridgeman VL, et al. Vessel co-option mediates resistance to anti-angiogenic therapy in liver metastases. *Nat Med*. Nov 2016;22(11):1294-1302.
19. Mandard AM, Dalibard F, Mandard JC, et al. Pathologic assessment of tumor regression after preoperative chemoradiotherapy of esophageal carcinoma. Clinicopathologic cor-relations. *Cancer*. Jun 1 1994;73(11):2680-2686.
20. Vermeulen PB, Colpaert C, Salgado R, et al. Liver metastases from colorectal adenocar-cinomas grow in three patterns with different angiogenesis and desmoplasia. *J Pathol*. Oct 2001;195(3):336-342.
21. Eefsen RL, Vermeulen PB, Christensen IJ, et al. Growth pattern of colorectal

liver metas-tasis as a marker of recurrence risk. *Clin Exp Metastasis*. Apr 2015;32(4):369-381.
22. Nielsen K, Rolff HC, Eefsen RL, Vainer B. The morphological growth patterns of colorec-tal liver metastases are prognostic for overall survival. *Mod Pathol*. Dec 2014;27(12):1641-1648.
23. Van den Eynden GG, Bird NC, Majeed AW, Van Laere S, Dirix LY, Vermeulen PB. The his-tological growth pattern of colorectal cancer liver metastases has prognostic value. *Clin Exp Metastasis*. Aug 2012;29(6):541-549.
24. Latacz E, Höppener D, Bohlok A, et al. Histopathological growth patterns of liver metas-tasis: updated consensus guidelines for pattern scoring, perspectives and recent mecha-nistic insights. *British Journal of Cancer*. 2022/06/01 2022.
25. Brouwer NPM, Bos A, Lemmens V, et al. An overview of 25 years of incidence, treat-ment and outcome of colorectal cancer patients. *Int J Cancer*. Dec 1 2018;143(11):2758-2766.
26. Galjart B, Buisman FE, Höppener DJ, et al. Extrahepatic disease recurrence risk modu-lates the effectiveness of (neo)adjuvant therapy in patients with resected colorectal liv-er metastasis. *Manuscript in preparation*.
27. Nierop PMH, Galjart B, Hoppener DJ, et al. Salvage treatment for recurrences after first resection of colorectal liver metastases: the impact of histopathological growth pat-terns. *Clin Exp Metastasis*. Apr 2019;36(2):109-118.
28. Nierop PMH, Hoppener DJ, van der Stok EP, et al. Histopathological growth patterns and positive margins after resection of colorectal liver metastases. *HPB (Oxford)*. Jun 2020;22(6):911-919.
29. Buisman FE, Van der Stok EP, Galjart B, et al. Histopathological growth patterns as bi-omarker for adjuvant systemic chemotherapy in patients with resected colorectal liver metastases. *Clin Exp Metastasis*. 2020.
30. Buisman FE, Grünhagen DJ, Homs MYV, et al. Adjuvant Hepatic Arterial Infusion Pump Chemotherapy After Resection of Colorectal Liver Metastases: Results of a Safety and Feasibility Study in The Netherlands. *Ann Surg Oncol*. Dec 2019;26(13):4599-4607.
31. Buisman FE, Homs MYV, Grünhagen DJ, et al. Adjuvant hepatic arterial infusion pump chemotherapy and resection versus resection alone in patients with low-risk resectable colorectal liver metastases - the multicenter randomized controlled PUMP trial. *BMC Cancer*. Apr 5 2019;19(1):327.
32. Hodi FS, O'Day SJ, McDermott DF, et al. Improved Survival with Ipilimumab in Patients with Metastatic Melanoma. *New England Journal of Medicine*. 2010/08/19 2010;363(8):711-723.
33. Borghaei H, Paz-Ares L, Horn L, et al. Nivolumab versus Docetaxel in Advanced Nonsquamous Non–Small-Cell Lung Cancer. *New England Journal of Medicine*. 2015/10/22 2015;373(17):1627-1639.
34. Ganesh K, Stadler ZK, Cercek A, et al. Immunotherapy in colorectal cancer: rationale, challenges and potential. *Nature Reviews Gastroenterology & Hepatology*. 2019/06/01 2019;16(6):361-375.
35. André T, Shiu K-K, Kim TW, et al. Pembrolizumab in Microsatellite-Instability–High Ad-vanced Colorectal Cancer. *New England Journal of Medicine*. 2020/12/03 2020;383(23):2207-2218.
36. Domingo E, Freeman-Mills L, Rayner E, et al. Somatic POLE proofreading domain muta-tion, immune response, and prognosis in colorectal cancer: a retrospective, pooled bi-omarker study. *The Lancet Gastroenterology & Hepatology*. 2016/11/01/ 2016;1(3):207-216.
37. van Dam PJ, Daelemans S, Ross E, et al. Histopathological growth patterns as a candi-date biomarker for immunomodulatory therapy. *Semin Cancer Biol*. Oct 2018;52(Pt 2):86-93.
38. Nordlinger B, Sorbye H, Glimelius B, et al. Perioperative chemotherapy with FOLFOX4 and surgery versus surgery alone for resectable liver metastases from colorectal cancer (EORTC Intergroup trial 40983): a randomised controlled trial. *Lancet*. Mar 22 2008;371(9617):1007-1016.
39. Nordlinger B, Sorbye H, Glimelius B, et al. Perioperative FOLFOX4 chemotherapy and surgery versus surgery alone for resectable liver metastases from colorectal cancer (EORTC 40983): long-term results of a randomised, controlled, phase 3 trial. *Lancet Oncol*. Nov 2013;14(12):1208-1215.
40. Kanemitsu Y, Shimizu Y, Mizusawa J, et al. Hepatectomy Followed by mFOLFOX6

Ver-sus Hepatectomy Alone for Liver-Only Metastatic Colorectal Cancer (JCOG0603): A Phase II or III Randomized Controlled Trial. *J Clin Oncol*. Dec 1 2021;39(34):3789-3799.
41. Höppener DJ, Stook JPL, Galjart B, et al. The relationship between primary colorectal cancer histology and the histopathological growth patterns of corresponding liver me-tastases. *BMC Cancer*. 2022.
42. Cheng J, Wei J, Tong T, et al. Prediction of Histopathologic Growth Patterns of Colorec-tal Liver Metastases with a Noninvasive Imaging Method. *Ann Surg Oncol*. Dec 2019;26(13):4587-4598.
43. Han Y, Chai F, Wei J, et al. Identification of Predominant Histopathological Growth Pat-terns of Colorectal Liver Metastasis by Multi-Habitat and Multi-Sequence Based Radi-omics Analysis. *Front Oncol*. 2020;10:1363.
44. Starmans MPA, Buisman FE, Renckens M, et al. Distinguishing pure histopathological growth patterns of colorectal liver metastases on CT using deep learning and radiomics: a pilot study. *Clin Exp Metastasis*. Oct 2021;38(5):483-494.
45. Li WH, Wang S, Liu Y, Wang XF, Wang YF, Chai RM. Differentiation of histopathological growth patterns of colorectal liver metastases by MRI features. *Quant Imaging Med Surg*. Jan 2022;12(1):608-617.
46. Lambin P, Leijenaar RTH, Deist TM, et al. Radiomics: the bridge between medical imag-ing and personalized medicine. *Nature Reviews Clinical Oncology*. 2017/12/01 2017;14(12):749-762.
47. Heitzer E, Haque IS, Roberts CES, Speicher MR. Current and future perspectives of liquid biopsies in genomics-driven oncology. *Nature Reviews Genetics*. 2019/02/01 2019;20(2):71-88.
48. Hoppener DJ, Nierop PMH, Hof J, et al. Enrichment of the tumour immune microenvi-ronment in patients with desmoplastic colorectal liver metastasis. *Br J Cancer*. Jul 2020;123(2):196-206.
49. Jessy T. Immunity over inability: The spontaneous regression of cancer. *J Nat Sci Biol Med*. Jan 2011;2(1):43-49.
50. Abdelrazeq AS. Spontaneous regression of colorectal cancer: a review of cases from 1900 to 2005. *International Journal of Colorectal Disease*. 2007/07/01 2007;22(7):727-736.
51. Stremitzer S, Vermeulen P, Graver S, et al. Immune phenotype and histopathological growth pattern in patients with colorectal liver metastases. *Br J Cancer*. May 2020;122(10):1518-1524.
52. Brunner SM, Kesselring R, Rubner C, et al. Prognosis according to histochemical analysis of liver metastases removed at liver resection. *Br J Surg*. Dec 2014;101(13):1681-1691.
53. Liang JY, Xi SY, Shao Q, et al. Histopathological growth patterns correlate with the im-munoscore in colorectal cancer liver metastasis patients after hepatectomy. *Cancer Immunol Immunother*. Dec 2020;69(12):2623-2634.
54. Tabaries S, Annis MG, Lazaris A, et al. Claudin-2 promotes colorectal cancer liver metas-tasis and is a biomarker of the replacement type growth pattern. *Commun Biol*. Jun 2 2021;4(1):657.
55. Toes-Zoutendijk E, Kooyker AI, Elferink MA, et al. Stage distribution of screen-detected colorectal cancers in the Netherlands. *Gut*. 2018;67(9):1745-1746.
56. Greuter MJ, Demirel E, Lew JB, et al. Long-Term Impact of the Dutch Colorectal Cancer Screening Program on Cancer Incidence and Mortality-Model-Based Exploration of the Serrated Pathway. *Cancer Epidemiol Biomarkers Prev*. Jan 2016;25(1):135-144.
57. Primrose JN, Perera R, Gray A, et al. Effect of 3 to 5 years of scheduled CEA and CT fol-low-up to detect recurrence of colorectal cancer: the FACS randomized clinical trial. *JAMA*. Jan 15 2014;311(3):263-270.
58. Wille-Jorgensen P, Syk I, Smedh K, et al. Effect of More vs Less Frequent Follow-up Testing on Overall and Colorectal Cancer-Specific Mortality in Patients With Stage II or III Colorectal Cancer: The COLOFOL Randomized Clinical Trial. *JAMA*. May 22 2018;319(20):2095-2103.
59. Galjart B, Höppener DJ, Aerts JGJV, Bangma CH, Verhoef C, Grünhagen DJ. Follow-up strategy and survival for five common cancers: a meta-analysis. *European Journal of Cancer*. 2022.
60. Tellez D, Höppener D, Verhoef C, et al. Extending unsupervised neural image compres-sion with supervised multitask learning. Paper presented at: *Medical*

Imaging with Deep Learning2020.
61. Meyer Y, Bohlok A, Hoppener D, et al. Histopathological growth patterns of resected non-colorectal, non-neuroendocrine liver metastases: a retrospective multicenter studyss. *Clin Exp Metastasis*. Feb 6 2022.
62. Meyer YM, Beumer BR, Hoppener DJ, et al. Histopathological growth patterns modify the prognostic impact of microvascular invasion in non-cirrhotic hepatocellular carcino-ma. *HPB (Oxford)*. Jul 30 2021.
63. Barnhill R, van Dam PJ, Vermeulen P, et al. Replacement and desmoplastic histopatho-logical growth patterns in cutaneous melanoma liver metastases: frequency, character-istics, and robust prognostic value. *J Pathol Clin Res*. Jul 2020;6(3):195-206.
64. Barnhill R, Vermeulen P, Daelemans S, et al. Replacement and desmoplastic histo-pathological growth patterns: A pilot study of prediction of outcome in patients with uveal melanoma liver metastases. *J Pathol Clin Res*. Oct 2018;4(4):227-240.
65. Bohlok A, Vermeulen P, Leduc S, et al. Association between the histopathological growth patterns of liver metastases and survival after hepatic surgery in breast cancer patients. *NPJ Breast Cancer*. Dec 18 2020;6(1):64.

X

```r
#Set working directory
setwd("V:/USERS/038931/Research/PhD/Appendices")

#Loading packages
library(dplyr)
library(tidyr)
library(ggplot2)
library(cowplot)
library(DescTools)
library(gridExtra)
library(grid)
library(survival)
library(survminer)
library(rms)
library(tableone)
library(scales)
library(reshape2)
library(ggpubr)
library(RColorBrewer)
library(circlize)
library(ComplexHeatmap)

#Appendix I - list of publications
https://pubmed.ncbi.nlm.nih.gov/?term=Höppener+DJ

#Appendix II - Contributing authors
Authors <- read.csv("Contributing_authors.csv",
                    header = F, sep = ";", dec = ".",
                    stringsAsFactors = FALSE)
print(Authors)

#Appendix III - PhD Portfolio
ects <- c(0.3, 0.5, 0.6, 0.9, 1, 1.2, 1.5, 2, 5.7)

ECTS <- c()
for (i in 1:100) {
  ECTS <- c(ECTS, sample(ects, 1))
  if (sum(ECTS)>=30) {
    break
  }
}

print(ECTS)

#Appendix IV - About the author
Life <- read.csv("Life.csv",
                 header = T, sep = ";", dec = ".",
                 stringsAsFactors = TRUE)
print(Life)

#Appendix V - Dankwoord
print("Dankjewel")
print("Thank you")
print("Merci beaucoup")
print("Dankeschöhn")
```

Appendices

Appendix I - List of publications

This thesis

- Höppener DJ*, Nierop PMH*, Herpel E, Rahbari NN, Doukas M, Vermeulen PB, Grunhagen DJ, Verhoef C. Histopathological growth patterns of colorectal liver metastasis exhibit little heterogeneity and can be determined with a high diagnostic accuracy. *Clin Exp Metastasis.* Aug 2019.

- Höppener DJ, Galjart B, Nierop PMH, Buisman FE, van der Stok EP, Coebergh van den Braak RRJ, van Amerongen MJ, Balachandran VP, Jarnagin WR, Kingham TP, Doukas M, Shia J, Nagtegaal ID, Vermeulen PB, Koerkamp BG, Grunhagen DJ, de Wilt JHW, D'Angelica MI, Verhoef C. Histopathological Growth Patterns and Survival After Resection of Colorectal Liver Metastasis: An External Validation Study. *JNCI Cancer Spectr.* Jun 2021.

- Latacz E*, Höppener DJ*, Bohlok A*, Leduc S, Tabariès S, Fernández Moro C, Lugassy C, Nyström H, Bozóky B, Floris G, Geyer N, Brodt P, Llado L, Van Mileghem L, De Schepper M, Majeed AW, Lazaris A, Dirix P, Zhang Q, Petrillo SK, Vankerckhove S, Joye I, Meyer Y, Gregorieff A, Roig NR, Vidal-Vanaclocha F, Denis L, Oliveira RC, Metrakos P, Grünhagen DJ, Nagtegaal ID, Mollevi DG, Jarnagin WR, D'Angelica MI, Reynolds AR, Doukas M, Desmedt C, Dirix L, Donckier V, Siegel PM, Barnhill R, Gerling M, Verhoef C, Vermeulen PB. Histopathological growth patterns of liver metastasis: updated consensus guidelines for pattern scoring, perspectives and recent mechanistic insights. *British Journal of Cancer.* 2022.

- Höppener DJ, Stook JPL, Galjart B, Nierop PMH, Nagtegaal ID, Vermeulen PB, Grünhagen DJ, Verhoef C, Doukas M. The relationship between primary colorectal cancer histology and the histopathological growth patterns of corresponding liver metastases. *BMC Cancer.* 2022.

- Höppener DJ, W. A, Tellez D, Nierop PMH, Nagtegaal ID, Doukas M, de Wilt JHW, Grünhagen DJ, van der Laak JAWM, Ciompi F, Verhoef C. Development and Validation of a Neural Image Compression Pipeline to Classify the Colorectal Liver Metastasis Growth Pattern on Gigapixel Histopathology Images.

  Adapted from: Tellez D, Höppener DJ, Verhoef C, Grünhagen D, Nierop P, Drozdzal M, Laak J, Ciompi F. Extending unsupervised neural image compression with supervised

multitask learning. Paper presented at: *Medical Imaging with Deep Learning 2020.*

◇ Höppener DJ, Nierop PMH, Hof J, Sideras K, Zhou G, Visser L, Gouw ASH, de Jong KP, Sprengers D, Kwekkeboom J, Vermeulen PB, Grunhagen DJ, Verhoef C. Enrichment of the tumour immune microenvironment in patients with desmoplastic colorectal liver metastasis. *British journal of Cancer.* Jul 2020.

◇ Höppener DJ, Nierop PMH, Buisman FE, Galjart B, Wilting SM, Smid M, Pugh SA, Richman SD, Balachandran VP, Jarnagin WR, Kingham TP, Vermeulen PB, Shia J, Quirke P, Bridgewater JA, Maughan TS, Groot Koerkamp B, Grünhagen DJ, Verhoef C, Primrose JN, D'Angelica MI. The colorectal liver metastasis growth pattern phenotype is not dependent on DNA genotype. *Manuscript in preparation.*

Other

◇ Galjart B, Höppener DJ, Aerts JGJV, Bangma CH, Verhoef C, Grünhagen DJ. Follow-up strategy and survival for five common cancers: a meta-analysis. *European Journal of Cancer.* 2022.

◇ Buisman FE, Giardiello D, Kemeny NE, Steyerberg EW, Höppener DJ, Galjart B, Nierop PMH, Balachandran VP, Cercek A, Drebin JA, Gönen M, Jarnagin WR, Kingham TP, Vermeulen PB, Wei AC, Grünhagen DJ, Verhoef C, D'Angelica MI, Koerkamp BG. Predicting 10-year survival after resection of colorectal liver metastases; an international study including biomarkers and perioperative treatment. *European Journal of Cancer*. Jun 2022.

◇ Nierop PMH*, Höppener DJ*, Buisman FE, van der Stok EP, Galjart B, Balachandran VP, Jarnagin WR, Kingham TP, Shia J, Mauer M, Nordlinger B, Julie C, Groot Koerkamp B, Doukas M, Vermeulen PB, Grunhagen DJ, D'Angelica MI, Verhoef C. Preoperative systemic chemotherapy alters the histopathological growth patterns of colorectal liver metastases. *J Pathol Clin Res*. Jan 2022.

◇ Vles MD, Höppener DJ, Galjart B, Moelker A, Vermeulen PB, Grunhagen DJ, Verhoef C. Local tumour control after radiofrequency or microwave ablation for colorectal liver metastases in relation to histopathological growth patterns. *HPB (Oxford)*. Jan 2022.

- de Geest TW, van Amerongen MJ, Nierop PMH, Höppener DJ, Grünhagen DJ, Moelker A, Fütterer JJ, Verhoef C, de Wilt JHW. Propensity score matching demonstrates similar results for radiofrequency ablation compared to surgical resection in colorectal liver metastases. *Eur J Surg Oncol*. Jan 2022.

- Meyer Y, Bohlok A, Höppener DJ, Galjart B, Doukas M, Grunhagen DJ, Labar A, Lucidi V, Vermeulen PB, Verhoef C, Donckier V. Histopathological growth patterns of resected non-colorectal, non-neuroendocrine liver metastases: a retrospective multicenter studyss. *Clin Exp Metastasis*. Feb 2022.

- van Rees JM, Höppener DJ, Hagemans JAW, Rothbarth J, Grünhagen DJ, Nuyttens J, van Meerten E, de Vries M, Verhoef C. The clinical relevance of indeterminate lung nodules in patients with locally recurrent rectal cancer. *Eur J Surg Oncol*. Jan 2021.

- Meyer YM, Beumer BR, Höppener DJ, Nierop PMH, Doukas M, de Wilde RF, Sprengers D, Vermeulen PB, Verhoef C, JNM IJ. Histopathological growth patterns modify the prognostic impact of microvascular invasion in non-cirrhotic hepatocellular carcinoma. *HPB (Oxford)*. Jul 2021.

- Höppener DJ, Grünhagen DJ, Eggermont AMM, van der Veldt AAM, Verhoef C. An Overview of Liver Directed Locoregional Therapies. *Surg Oncol Clin N Am*. Jan 2021.

- Nierop PMH, Höppener DJ, van der Stok EP, Galjart B, Buisman FE, Balachandran VP, Jarnagin WR, Kingham TP, Allen PJ, Shia J, Vermeulen PB, Groot Koerkamp B, Grunhagen DJ, Verhoef C, D'Angelica MI. Histopathological growth patterns and positive margins after resection of colorectal liver metastases. *HPB (Oxford)*. Jun 2020.

- Hof J, Visser L, Höppener DJ, Nierop PMH, Terpstra MM, Gouw ASH, Grünhagen DJ, Verhoef C, Sijmons RH, de Jong KP, Kok K. B Cells as Prognostic Biomarker After Surgery for Colorectal Liver Metastases. *Front Oncol*. 2020.

- Buisman FE, Van der Stok EP, Galjart B, Vermeulen PB, Balachandran VP, Coebergh van den Braak RRJ, Creasy JM, Höppener DJ, Jarnagin WR, Kingham TP, Nierop PMH, Sadot E, Shia J, Groot Koerkamp B, D'Angelica MI, Verhoef C. Histopathological growth patterns as biomarker for

adjuvant systemic chemotherapy in patients with resected colorectal liver metastases. *Clin Exp Metastasis*. 2020.

◇ Nierop PMH, Galjart B, Höppener DJ, van der Stok EP, Coebergh van den Braak RRJ, Vermeulen PB, Grunhagen DJ, Verhoef C. Salvage treatment for recurrences after first resection of colorectal liver metastases: the impact of histopathological growth patterns. *Clin Exp Metastasis*. Apr 2019.

◇ Höppener DJ, Verhoef C. ASO Author Reflections: The Prognostic Value of Time to Metastasis in Colorectal Liver Metastasis. *Ann Surg Oncol*. Dec 2019.

◇ Höppener DJ, Nierop PMH, van Amerongen MJ, Olthof PB, Galjart B, van Gulik TM, de Wilt JHW, Grunhagen DJ, Rahbari NN, Verhoef C. The Disease-Free Interval Between Resection of Primary Colorectal Malignancy and the Detection of Hepatic Metastases Predicts Disease Recurrence But Not Overall Survival. Ann Surg Oncol. Sep 2019.

◇ Galjart B, Nierop PMH, van der Stok EP, van den Braak R, Höppener DJ, Daelemans S, Dirix LY, Verhoef C, Vermeulen PB, Grunhagen DJ. Angiogenic desmoplastic histopathological growth pattern as a prognostic marker of good outcome in patients with colorectal liver metastases. *Angiogenesis*. May 2019.

◇ Hoogstins CE, Weixler B, Boogerd LS, Höppener DJ, Prevoo HA, Sier CF, Burger JW, Verhoef C, Bhairosingh S, Farina Sarasqueta A, Burggraaf J, Vahrmeijer AL. In Search for Optimal Targets for Intraoperative Fluorescence Imaging of Peritoneal Metastasis From Colorectal Cancer. *Biomark Cancer*. 2017.

◇ Handgraaf HJM, Boogerd LSF, Höppener DJ, Peloso A, Sibinga Mulder BG, Hoogstins CES, Hartgrink HH, van de Velde CJH, Mieog JSD, Swijnenburg RJ, Putter H, Maestri M, Braat AE, Frangioni JV, Vahrmeijer AL. Long-term follow-up after near-infrared fluorescence-guided resection of colorectal liver metastases: A retrospective multicenter analysis. *Eur J Surg Oncol*. Aug 2017.

** Shared first authorship*

Appendix II - Contributing authors

W. Aswolinskiy
V.P. Balachandran
R. Barnhill
A. Bohlok
B. Bozóky
J.A. Bridgewater
Pnina Brodt
F.E. Buisman
R. Caetano Oliveira
F. Ciompi
R.R.J. Coebergh van den Braak
M.I. D'Angelica
K.P. de Jong
M. de Schepper
J.H.W. de Wilt
L. Denis
C. Desmedt
P. Dirix
L. Dirix
V. Donckier
M. Doukas
C. Fernández Moro
G. Floris
B. Galjart
M. Gerling
N. Geyer
A.S.H. Gouw
A. Gregorieff
B. Groot Koerkamp
D.J. Grünhagen
E. Herpel
J. Hof
W.R. Jarnagin
I. Joye
T.P. Kingham
J. Kwekkeboom
E. Latacz
A. Lazaris
S. Leduc
L. Llado
C. Lugassy
A.W. Majeed
T.S. Maughan
P. Metrakos
Y. Meyer
D.G. Mollevi
I.D. Nagtegaal
P.M.H. Nierop
H. Nyström
S.K. Petrillo
J.N. Primrose
S.A. Pugh
P. Quirke
N.N. Rahbari
A.R. Reynolds
S.D. Richman
N. Ruiz Roig
J. Shia
K. Sideras
P.M. Siegel
M. Smid
D. Sprengers
J.P.L. Stook
S. Tabariès
David Tellez
M.J. van Amerongen
J.A.W.M. van der Laak
E.P. van der Stok
L. van Mileghem
S. Vankerckhove
C. Verhoef
P.B. Vermeulen
F. Vidal-Vanaclocha
L. Visser
S.M. Wilting
Q. Zhang
G. Zhou

Appendix III - PhD Portfolio

PhD Candidate: Diederik Jacobus Höppener
Period: August 2017 - December 2021
Erasmu MC department: Surgery
Promotor: prof. dr. C. Verhoef | Copromotor: dr. D.J. Grünhagen

Academic & Research Skills	Year	ECTS
Scientific Integrity	2020	0.3
BROK 'Basiscursus Regelgeving Klinisch Onderzoek'	2019	1.5
Biostatistical Methods I: Basic Principles	2017	5.7

Oral Presentations	Year	ECTS
Hepatocellular Carcinomas Display Histopathological Growth Patterns in Non-cirrhotic Patients That Mediate the Prognostic Effect of Microvascular Invasion. *73rd SSO virtual meeting.*	2020	1
The Disease-Free Interval Between Resection of Primary Colorectal Malignancy and the Detection of Hepatic Metastasis is of Limited Prognostic Value Following Surgical Treatment for Colorectal Liver Metastasis. *72nd SSO, San Diego, United States of America.*	2019	1
De prognostische waarde van het ziektevrije interval na chirurgische behandeling van colorectale levermetastasen. *NVvH Chirurgendagen, Veldhoven, the Netherlands.*	2019	1
The Immune Signature of the Desmoplastic Type Histopathological Growth Pattern. *Annual Liver Metastasis Research Network, Valencia, Spain.*	2019	1
Observed differences in the tumour microenvironment provide a potential explanation for the superior survival of patients with desmoplastic colorectal liver metastasis. *39th ESSO, Rotterdam, the Netherlands.*	2019	1
Validation and correlation of the HGP as biomarker. *Annual Liver Metastasis Research Network, Montreal, Canada.*	2018	1
Intra-metastases and Intra-patient Single Time-frame Histopathological Growth Patterns Concordance of Resected Colorectal Liver Metastases. *13th IHPBA, Geneva, Switzerland*	2018	1

Poster Presentations	Year	ECTS
The Relationship between Circulating Tumour Cells and the Histopathological Growth Pattern of Resectable Colorectal Liver Metastasis. *13th IHPBA, Geneva, Switzerland.*	2018	0.5

Teaching	Year	ECTS
Supervising internship & master thesis Erasmus MC - J.P.L. Stook	2021	2
Supervising internship & master thesis Erasmus MC - M.J. Vles	2021	2
Supervising internship & master thesis Erasmus MC - J.M. van Rees	2019	2
Supervising internship & master thesis Erasmus MC - S. Hazen	2018	2
Basic Life Support examinator medical students	2018	0.5

(Inter)national conferences	Year	ECTS
73rd SSO virtual meeting	2020	0.6
NVvH Chirurgendagen, Veldhoven, the Netherlands.	2019	0.6
Annual Liver Metastasis Research Network, Valencia, Spain.	2019	0.6
72nd SSO Congess, San Diego, United States of America.	2019	1.2
39th ESSO Congress, Rotterdam, the Netherlands.	2019	0.9
NVvH Chirurgendagen, Veldhoven, the Netherlands.	2018	0.6
Annual Liver Metastasis Research Network, Montreal, Canada.	2018	0.6
38th ESSO Congress, Budapest, Hungary.	2018	0.9
13th IHPBA Congress, Geneva, Switzerland.	2018	1.2

Appendix IV - About the author

Diederik Jacobus Höppener (*figuur 1*) werd geboren op 28 juli 1992 in Deventer als tweede in een gezin van vier. Hij behaalde in 2010 zijn Gymnasiumdiploma aan het Beekdal Lyceum te Arnhem.

Met een N&T en N&G profiel, een affiniteit voor technische vakken, en een profielwerkstuk over tweetakt expansieuitlaten leek het overduidelijk dat Diederik zijn oudere broer naar Delft zou volgen. Geheel onverwacht besloot hij om Geneeskunde te gaan studeren in Leiden. In zijn studententijd was hij naast de studie veel bezig met het verenigingsleven en muziek; zo speelde hij viool en was hij actief betrokken bij het oudste studenten muziekgezelschap van Nederland. De eerste ervaring tijdens de studie met de Chirurgie was wat onconventioneel, hij belandde namelijk in jaar 1 op de operatietafel met een acute appendicitis.

Tijdens de coschappen raakte Diederik ondanks zijn eerdere ervaring toch geïnteresseerd in de Chirurgie. Hij begon zijn wetenschappelijke carrière dan ook bij de Image-Guided Surgery groep in het LUMC, waar hij betrokken was bij een onderzoek naar het effect van indocyanine groen bij resectie van colorectale levermetastasen. Na een semi-arts stage bij de Chirurgie behaalde hij zijn artsendiploma in 2017. Hij besloot om door te gaan met wetenschappelijk onderzoek, en via het Leidse kreeg hij de mogelijkheid om te solliciteren voor een PhD positie bij professor Verhoef in het Daniel den Hoed ziekenhuis te Rotterdam (wat helaas nu niet meer bestaat).

Het bleek een goede zet. Hij mocht zich storten op de histopathologische groeipatronen van colorectale levermetastasen en, onder leiding van prof. dr. C. Verhoef en dr. D.J. Grünhagen, resulteerde dat in dit proefschrift.

Appendix IV

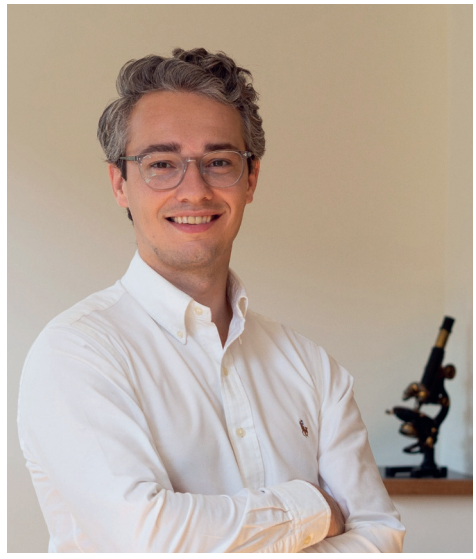

Figuur 1. *Diederik Jacobus Höppener*

Enigszins verrassend hield dit in dat hij veelvuldig pathologiepreparaten moest bekijken met een microscoop, zowel in Nederland, als in Duitsland, maar ook in New York, iets wat hij dacht dat hij na zijn studie Geneeskunde nooit meer zou doen. Zijn technische affiniteit heeft hij gelukkig niet verloren, zo leerde hij zichzelf met plezier maar toch ook frustratie de programmeertaal R voor statistische analyses.

Het was ook tijdens zijn promotietijd dat Diederik zijn huidige passie heeft ontdekt; kitesurfen. Hij is momenteel de trotse recordhouder van het WOO hoogterecord op de Na21. De eerlijkheid gebiedt wel te zeggen dat hij ook de enige is met een WOO.

Na zijn promotietraject vervolgde Diederik zijn chirurgische carrière als ANIOS in het IJsselland Ziekenhuis te Capelle aan den IJssel. Dit werk heeft zijn interesse in de Chirurgie alleen maar doen vergroten, en hij hoopt dan ook zijn chirurgische ambities verder te mogen ontwikkelen.

Appendix V - Dankwoord

In de woorden van mijn promotor: “De meeste mensen lezen alleen het dankwoord, en misschien de introductie en de discussie als je geluk hebt.” Wat dat betreft is dit dus echt *last but not least*. Tijdens mijn promotie heb ik het genoegen gehad om met velen samen te werken. Dit heeft mij veel meer opgeleverd dan alleen een proefschrift en een reeks publicaties. Dit dankwoord is gericht aan allen die mij op welke manier dan ook geholpen hebben om dit proefschrift tot stand te brengen.

Geachte promotor, prof. dr. C. Verhoef, beste Kees. Mijn eerste kennismaking met het Rotterdamse was tijdens ons sollicitatiegesprek in de Daniël den Hoed, wat op zichzelf al een unieke ervaring was. Maar het echte unieke kwam in die jaren daarna. Het vertrouwen wat je geeft om eigen ideeën en interesses uit te werken is exceptioneel. Er wordt altijd op gelijke hoogte overlegd, waarbij je ook daadwerkelijk luistert naar wat de ander zegt. Op zich is dat al bijzonder genoeg, maar wat het uniek maakt is de humor, het karakter, en de betrokkenheid die hierbij komt kijken. Het is gewoon abnormaal geestig en plezierig om bij je te werken. Ik ken dan ook geen andere groep waar de onderzoekers *en plein public* belachelijk gemaakt worden, ze dit vervolgens alleen maar grappig (en normaal) vinden, en waarbij de professor hen appt om te vragen hoe hun vakantie was. Kees, heel veel dank.

Geachte copromotor, dr. D.J. Grünhagen, beste Dirk. Het is moeilijk om niet in herhaling te vallen, want het is grotendeels ook de inbreng en begeleiding vanuit jou die de afgelopen jaren zo uitdagend en plezierig hebben gemaakt. Het blijft indrukwekkend hoe analytisch en doordringend je commentaar tijdens menig overleg en op menig artikel is. Je hebt altijd tijd om te sparren, en staat open voor andere invalshoeken en nieuwe ideeën. Maar buiten dit breng je ook

plezier in het werk en ben je buitengewoon betrokken. De combinatie van Kees als promotor en jij als copromotor is een unieke, en ik had me werkelijk geen beter team kunnen voorstellen. Het was me meer dan een genoegen, en laten we hopen dat het hier niet bij blijft.

Geachte leden van de promotiecommissie, ik wil u allen hartelijk danken voor het beoordelen van mijn proefschrift en de bereidheid hierover van gedachten te wisselen. Met enkelen van u heb ik ook het voorrecht gehad om te mogen samenwerken aan de inhoud ervan, waarvoor veel dank.

Beste Chirurgen van de Daniel den Hoed, en later van de OGC in de Nieuwbouw; dank voor alle steun en bijdragen aan dit proefschrift, de skireizen, het karten en curlen, en uiteraard de gezelligheid. Ik ben blij dat ik “de Daniel” nog heb mogen meemaken.

Geachte dr. P.B. Vermeulen, beste Peter. Dit proefschrift is grotendeels te danken aan u. Het is uw vastberadenheid en energie die de groeipatronen hebben gebracht tot waar ze nu staan. Uw toewijding is uniek en aanstekelijk, en ik heb dan ook enorm genoten van onze samenwerking. Van het scoren van dozen en dozen coupes in afgelegen kamertjes in het Erasmus MC, tot aan de jaarlijkse bijeenkomsten van het LMRN, we konden altijd op u rekenen. Het is mede dankzij u dat ik nu zelfs enthousiast kan worden van een “mooie” coupe. Ik weet dat de samenwerking tussen Antwerpen en Rotterdam nog lang niet klaar is.

Geachte dr. M. Doukas, beste Michail. Ik denk dat ik niemand anders ken die met zoveel energie, enthousiasme, en vriendelijkheid te werk gaat in het Erasmus MC als u (excuses, jij). De tijd die jij naast je al zeer drukke en intensieve klinische taken vrijmaakt om onderzoekers zoals ik

te helpen met het scoren van coupes is echt buitengewoon. De ochtendsessies waarbij we om 7 uur begonnen met koffie zullen me lang bijblijven. Deze waren zeer leerzaam en interessant, maar vooral ook gezellig door de verhalen over Griekenland, de vele grapjes, en uw bodemloze energie. Jij hebt voor mij de pathologie als vakgebied wezenlijk doen veranderen.

Beste dr. Groot Koerkamp, beste Bas, ik wil je bedanken voor de mogelijkheid om onderzoek te doen in samenwerking met, en op locatie in New York. Daarnaast heb ik buitengewoon veel respect en waardering voor de energie, het enthousiasme, en de wetenschappelijke drive die je bewerkstelligd binnen de Heelkunde in het Erasmus MC, en daarbuiten.

Dear dr. D'Angelica, thank you for the continued collaboration and the opportunity to perform research at your department. Your contributions and insights to the field of Surgical Oncology are inspiring.

Dear prof. Primrose, it has been an absolute pleasure to work with you and your team. Your willingness for collaboration is remarkable and admirable, as is your enthusiasm. My hope is that the meeting in Rotterdam will happen sooner than later, and preferably prior to the next pandemic.

Beste onderzoekers van het Radboud UMC, prof. dr. De Wilt, en prof. dr. Nagtegaal, veel dank voor alle samenwerking op chirurgisch en pathologisch niveau. My thanks also to the Digital Pathology Group of dr. van der Laak and dr. Ciompi. Your work in digital pathology is truly inspiring and groundbreaking. It has been a pleasure to collaborate.

Sandra, zonder jou was het onderzoek een stuk moeilijker en saaier geweest. Dank voor alle hulp en gezelligheid. Naast je eigen boot, houd je ook het schip genaamd de OGC varende!

Appendix V

Boris, de belangrijkste bijdrage die jij aan mijn promotietijd hebt gedaan staat niet in dit boek, niet op pubmed, en heeft niks te maken met promoveren, maar vinden we op de Brouwersdam. De vele kitesessies behoren tot de leukste (en pijnlijkste) momenten van de afgelopen jaren. Maar naast de vele kite sessies waren er ook de R sessies, internationale sessies, HGP sessies, review sessies, dumpert sessies, KWF sessies, Sranang sessies, en lockdown sessies, die het onderzoek toch echt een stuk plezieriger hebben gemaakt. Ik ben blij dat je als paranimf naast me zal staan, zolang je maar niet 10 minuten voor aanvang van de verdediging komt met: “moeten we niet gewoon …”.

Maarten, wat hebben wij samen veel coupes bekeken. Gelukkig hebben we deze op zich monotone taak toch plezierig kunnen invullen. Zonder jou was dit proefschrift zeker niet tot stand gekomen, en was menig internationaal avontuur een stuk minder avontuurlijk geweest. Ontzettend bedankt voor het samenwerken en de goede tijd, had het niet willen missen!

Florian, het is echt een plezier om met jou samen te werken, of dit nou het onderzoek of de kliniek betreft. Je staat altijd voor anderen klaar, werkt ontzettend hard, maar bent vooral ook uitermate grappig. Daarnaast was New York natuurlijk nooit gelukt zonder jouw hulp! Ik ben je dan ook erg dankbaar voor alles en de goede tijd samen. Ik kijk uit naar de volgende rondjes op de racefiets, kitesessies op de brouwersdam, of gewoon een borrel.

Wills, de eerste keer dat wij samen een borrel hadden vroeg je om 5 euro om sambal te kopen van de sambal man en kocht je de meest pittige. Enkele dagen later had je het zwaar en vertelde je dat die sambal zo pittig was dat je hem niet kon eten. Ik wist daarna dat we een goede tijd met elkaar gingen hebben. Het hoogtepunt (of dieptepunt?) was toch echt het

diner bij jou thuis. Namens Galjart, nogmaals sorry. Ik kijk uit naar het samenwerken in de kliniek!

Kelly, een betere “opvolger” voor alle Future studies had er denk ik niet kunnen zijn. Dank voor het managen en succesvol runnen van deze leuke maar ingewikkelde projecten, de koffiemomenten in het IJsselland, en mijn whatsapp stickercollectie. Ik vind het jammer dat we maar een relatief korte tijd collega’s zijn geweest, ook al voelt het langer.

Yannick, als volgende dedicated groeipatroon onderzoeker hebben we de nodige scoorsessies en coupeperikelen meegemaakt. Geheel in stijl hebben we daar gelukkig de nodige kitesessies aan kunnen toevoegen!

Hakan, gebaseerd op je kiteskills is de database in meer dan goede handen.

Alle onderzoekers van de Daniël en later de OGC; Mirelle, Jan, Daniëlle, Pien, Nadine, Milea, Melissa, Janine, Ivona, Job, Ben, Berend, Stijn, Elisabeth, Hidde, Evalyn, Jan van R, Robert, Sam, Chris, Michelle, Anne-Rose, Lissa, Ibtissam, Enrico, en alle anderen, het was altijd lachen op de A-gang en later de Na. Tijdens het onderzoeksleven moet je het vooral hebben van je collega’s, en met jullie zat het dus zeker meer dan goed. Ik denk met plezier terug aan alle (internationale) avonturen en borrels, en kijk uit naar het volgende moment dat ik weer op mijn handen ga staan.

Jean-Luc en Mark-Jan, het was een plezier om jullie te begeleiden. Dank voor jullie inzet en werk, en hopelijk pakken jullie het onderzoek verder op!

Aan alle chirurgen en collega’s van het IJsselland Ziekenhuis; ik had me geen beter vervolg kunnen wensen.

Appendix V

Clef en Sophie, en later Mees en Mariëlle, Rotterdam is voor mij synoniem aan jullie, en onze vriendschap. Ik had op geen betere plek dan de ML kunnen landen toen ik begon aan dit proefschrift. Het vervolg op de Proveniers zal ik jullie altijd dankbaar voor zijn. Ik weet dat er nog veel gaat komen, of dat nou hier, in België, of elders is.

Bob, Joost, en Bart, of eigenlijk Zwerver, OV boy, en Harde lach, een PhD geldt als verdubbelaar hè. Binnenkort is het wellicht dr. Vane. Ik kijk uit naar de volgende epische skireizen en meer.

Stan, dank voor de vriendschap, alle reizen, en andere avonturen sinds we elkaar hebben leren kennen in Leiden. Ik ben blij dat ook jij als paranimf naast me staat.

Préfaillanen, op naar de volgende editie.

Oma Conny en Opa Jacques, jullie zijn een inspiratie.

Cynthia, Fabian, Stephanie, Gio, John, en Maria, van je schoonfamilie moet je het hebben! Ik hoop op zon bij de volgende vakantie.

Daan & Nienke, Elena & Luc, en Susanna & Stijn, ik ben gelukkig om onderdeel van ons gezin te zijn met alle steun en toeverlaat die we aan elkaar hebben. Plus het is gezellig.

Pap en Mam, dank voor alles.

Ellis, je bent de enige met wie ik een samenlevingscontract wil aangaan. Nu is het mijn beurt; vampire principles.

```
#Circleplot random ----
circos.par("start.degree" = 90, clock.wise = FALSE, gap.degree = 15,
           track.margin = c(0,0), cell.padding = c(0,0,0,0))
circos.initialize(sectors = grps, xlim = xlim)
#Survival time
circos.track(ylim = c(0, max(dat$OS)), bg.border = NA, track.height = 0.655,
             panel.fun = function(x, y) {
  sect <- CELL_META$sector.index
  dframe <- dat[dat$HGP == sect, ]
  value = as.matrix(dframe[c("DFS1", "DFS2", "DFS3", "DFS4", "DFS5", "DFS6",
                             "PallSurv")])
  value[is.na(value)] <- 0
  circos.barplot(value, 1:nrow(dframe) - 0.5, col = survcol, bar_width = 1)
})
#Survival status
set_track_gap(0.012)
circos.track(ylim = c(0, 1), track.height=0.04, panel.fun = function(x, y) {
  sect <- CELL_META$sector.index
  dframe <- dat[dat$HGP == sect, ]
  value = model.matrix(~dframe$AWD_NED - 1)
  value[is.na(value)] <- 0
  circos.barplot(value, 1:nrow(dframe) - 0.5, col = statcol, bar_width = 1)
})
#HGP distribution
set_track_gap(0.015)
circos.track(ylim = c(0, 100), track.height=0.11, panel.fun=function(x, y) {
  sect <- CELL_META$sector.index
  dframe <- dat[dat$HGP == sect, ]
  value = as.matrix(dframe[c("dHGP", "pHGP", "rHGP")])
  circos.barplot(value, 1:nrow(dframe) - 0.5, col = hgpcol, bar_width = 1)
})
#CEA
set_track_gap(0.02)
circos.track(ylim = c(0, 1), track.height=0.015, panel.fun = function(x, y) {
<->})
#Numb CRLM
set_track_gap(0)
circos.track(ylim = c(0, 1), track.height=0.015, panel.fun = function(x, y) {
<->})
#Diam CRLM
set_track_gap(0)
circos.track(ylim = c(0, 1), track.height=0.015, panel.fun = function(x, y) {
<->})
#pN stage
set_track_gap(0)
circos.track(ylim = c(0, 1), track.height=0.015, panel.fun = function(x, y) {
<->})
#pT stage
set_track_gap(0)
circos.track(ylim = c(0, 1), track.height=0.015, panel.fun = function(x, y) {
<->})
#EHD
set_track_gap(0)
circos.track(ylim = c(0, 1), track.height=0.015, panel.fun = function(x, y) {
<->})
```